Influence de la matière organique naturelle et des surfaces minérales sur la spéciation des radionucléides en contexte environnemental

Noémie Janot

▶ **To cite this version:**

Noémie Janot. Influence de la matière organique naturelle et des surfaces minérales sur la spéciation des radionucléides en contexte environnemental. Géochimie. Institut de physique du globe de paris - IPGP, 2011. Français. NNT : . tel-00643374v1

HAL Id: tel-00643374

https://theses.hal.science/tel-00643374v1

Submitted on 21 Nov 2011 (v1), last revised 23 Jan 2012 (v3)

HAL is a multi-disciplinary open access archive for the deposit and dissemination of scientific research documents, whether they are published or not. The documents may come from teaching and research institutions in France or abroad, or from public or private research centers.

L'archive ouverte pluridisciplinaire **HAL**, est destinée au dépôt et à la diffusion de documents scientifiques de niveau recherche, publiés ou non, émanant des établissements d'enseignement et de recherche français ou étrangers, des laboratoires publics ou privés.

Institut de Physique du Globe de Paris

Université Denis Diderot

Ecole Doctorale des Sciences de la Terre

****

Doctorat en Géochimie Fondamentale et Appliquée

Influence de la matière organique naturelle et des surfaces minérales sur la spéciation des radionucléides en contexte environnemental

Noémie Janot

Thèse dirigée par Marc Benedetti et Pascal Reiller

Soutenue le 31 mai 2011

Membre du Jury :

Aline Dia	Rapporteur
Michael Kumke	Rapporteur
François Guyot	Président
Jamie Lead	Examinateur
Marc Benedetti	Co-directeur de thèse
Pascal Reiller	Co-directeur de thèse

Sommaire

CHAPITRE 1 – INTRODUCTION

INFLUENCE DES COLLOÏDES ORGANIQUES ET MINÉRAUX SUR LA SPÉCIATION DES RADIONUCLÉIDES

1 Introduction générale

Les activités anthropiques peuvent entraîner la pollution des sols ou des eaux par rejet de contaminants. La mise au point de techniques de remédiation des milieux naturels impactés passe par la compréhension des mécanismes contrôlant la mobilité de ces contaminants, quelle que soit leur nature (métaux lourds, pesticides, hydrocarbures…). En particulier, l'utilisation de l'énergie nucléaire pour la production d'électricité pose la question de la prise en compte des radionucléides, dont il convient de connaître et de comprendre les conditions de mobilité et de biodisponibilité afin de mieux appréhender les risques sanitaires et environnementaux qui y sont associés sur tout le cycle du combustible.

Les colloïdes présents dans les milieux naturels, qu'ils soient minéraux – argiles ou (hydr)oxydes métalliques principalement – ou organiques – matière organique naturelle –, jouent un rôle important dans les processus de contrôle du transport des contaminants (des radionucléides dans le cas étudié). En effet, les propriétés de complexation et d'adsorption des colloïdes vont influer sur la spéciation des polluants, c'est-à-dire la répartition de leurs différentes espèces chimiques. Ces interactions peuvent, selon les conditions physico-chimiques du milieu, favoriser le transport des radionucléides par complexation avec les colloïdes mobiles (McCarthy et al. 1998; Santschi et al. 2002) ou au contraire avantager leur fixation par adsorption sur les surfaces minérales ou sédimentation (Crançon 2001; Crançon and van der Lee 2003; Crançon et al. 2010).

L'obtention de données en laboratoire, sur des systèmes contrôlés, peut permettre de mieux appréhender et prédire le comportement des radionucléides dans un milieu naturel. Dans la littérature, de nombreuses études abordent cette problématique de façon limitée et s'intéressent uniquement à des systèmes binaires: radionucléide/matière organique et radionucléide/minéral. En effet, l'étude du comportement d'un polluant dans un système réel où coexistent matière organique et surface minérale nécessite en premier lieu de comprendre les interactions des composés deux à deux : contaminant/matière organique et contaminant/minéral, mais aussi matière organique/minéral. Ces interactions ne couvrent cependant pas tous les processus gouvernant la migration du contaminant d'intérêt dans un système ternaire contaminant/matière organique naturelle/surface minérale.

L'étude des systèmes binaires et ternaire dans différentes conditions de pH, de force ionique et de concentration en matière organique pourra permettre de décrire les mécanismes contrôlant la spéciation du radionucléide dans le système dans une large gamme de paramètres. De cette

manière, des modèles pourront être calibrés, permettant de prédire la spéciation des radionucléides dans des conditions environnementales variées.

2 Réactivité des colloïdes naturels

Les eaux naturelles sont riches en objets de taille variable, d'origine organique ou minérale. Parmi eux, les colloïdes sont définis comme des molécules ou des objets polymoléculaires ayant, au moins dans une direction, une dimension comprise entre 1 nm et 1 µm (IUPAC) : cette classe comprend notamment les argiles, les oxydes métalliques et les substances humiques (Figure 1).

Les colloïdes peuvent être considérés comme des particules restant en suspension sous l'effet de leur mouvement Brownien. Ce sont des entités supramoléculaires, qui lorsqu'elles sont chargées développent un champ électrique de surface, et dont la réactivité dépend des paramètres physico-chimiques du milieu.

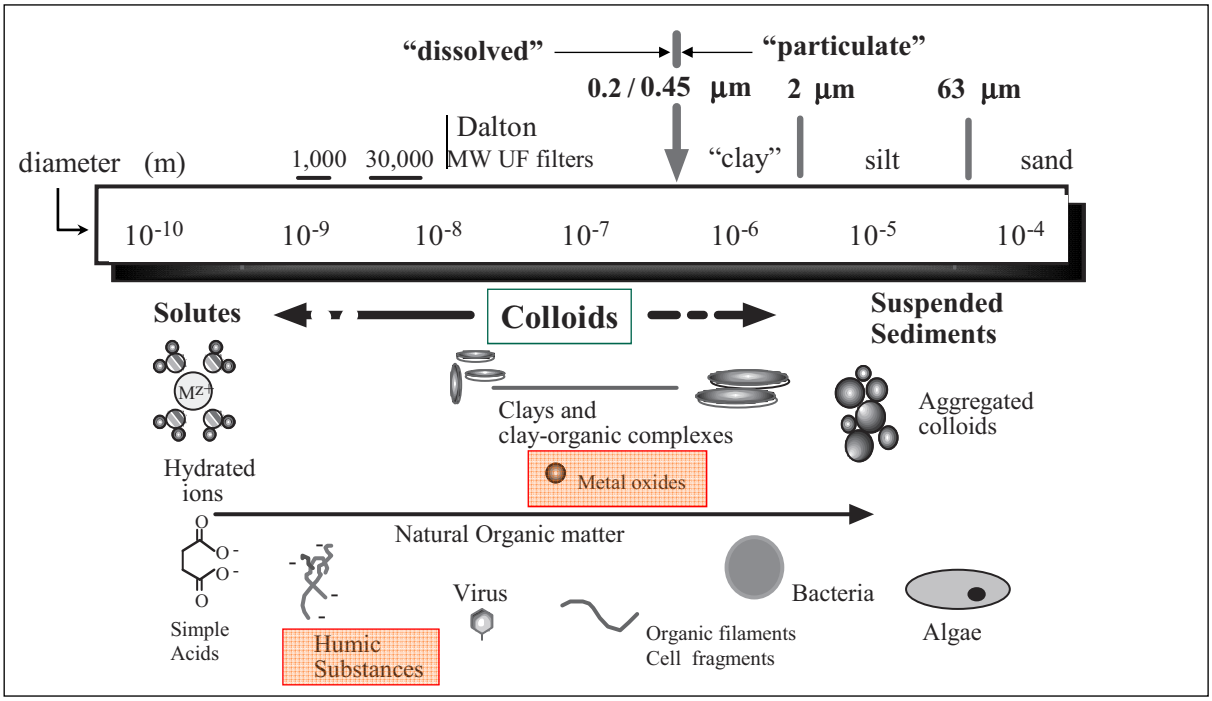

Figure 1. Classification des composants d'un milieu aqueux, en fonction de la taille (d'après Ranville and Schmiermund 1999).

2.1 Réactivité des surfaces minérales

2.1.1 Description de la charge de surface

Les surfaces minérales présentent une charge naturelle qui influence leur réactivité vis-à-vis des métaux ou de la matière organique. Cette charge dépend de l'arrangement structural des atomes en surface, et dans le cas des phyllosilicates de l'existence de charges permanentes. Dans le cas des oxydes métalliques, la surface est composée d'atomes métalliques liés à des atomes d'oxygène présentant un déficit de coordination. En solution, les molécules d'eau se dissocient et des protons viennent compléter cette lacune de coordination. La charge de surface résultante peut être estimée par mesure de la mobilité électrophorétique ou quantifiée par titrages potentiométriques (Figure 2).

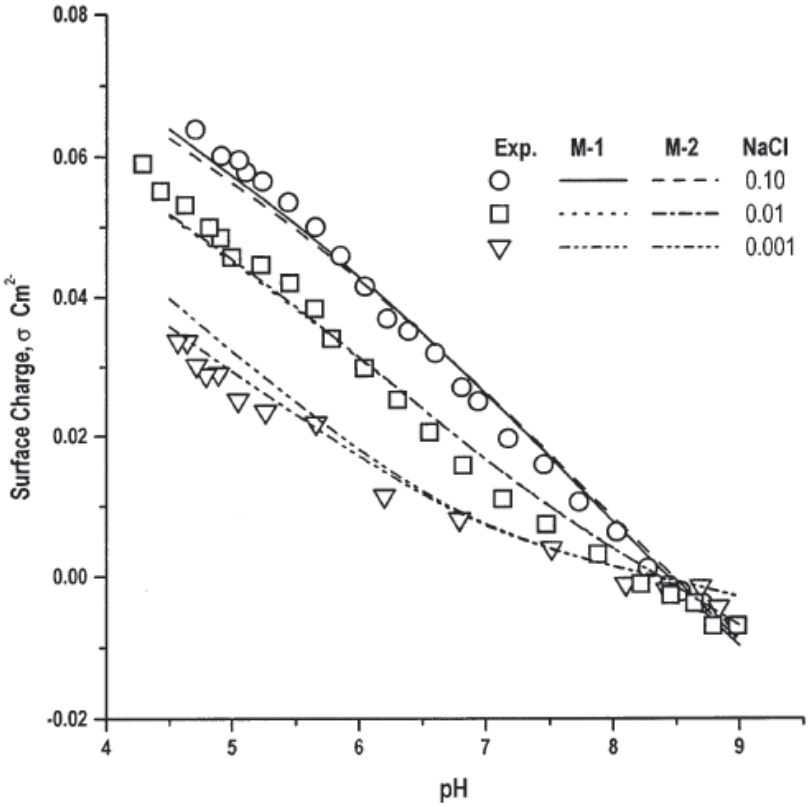

Figure 2. Titrage potentiométrique d'une suspension de gibbsite (Weerasooriya et al. 2001).

Cette charge est issue de réactions entre les groupes fonctionnels de la surface minérale notés $\equiv S_xOH^n$ et les ions de la solution, aussi bien des réactions acido-basiques que des réactions d'adsorption. Elle est ainsi fonction du pH, selon le type de réaction suivant :

$$\equiv S_xOH^n + H^+ \rightleftarrows \equiv S_xOH_2^{n+1}$$

La charge de surface diminue donc lorsque le pH augmente. Le point où la charge de surface est nulle, c'est-à-dire pour lequel il y a autant de charges positives que de charges négatives est le point de charge nulle, pour lequel le pH est noté pH_{pzc} (point of zero charge). Il est propre à chaque minéral (Figure 3).

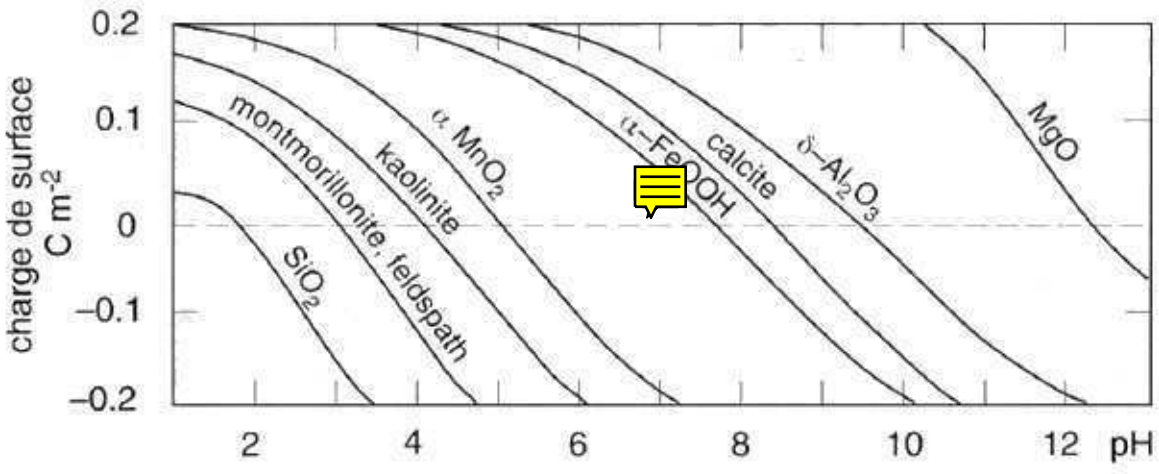

Figure 3. Influence du pH sur la charge de surface de quelques colloïdes minéraux (Stumm and Morgan 1996, p. 539).

La charge électrique de la surface est compensée par une charge opposée en solution, selon une distribution diffuse d'ions de charge opposée dans une double couche (DDL, Diffuse Double Layer). Il existe plusieurs modèles de représentation de l'interface solution – solide. Celui utilisé dans ce travail est le modèle double-couche de Stern (Basic Stern Model, ou BSM), qui considère une couche dite de Stern, entre la surface minérale et la double-couche diffuse (cf. Figure 4). Les contre-ions sont situés à l'extérieur de la couche de Stern, contrairement aux ions spécifiquement adsorbés. La charge de surface totale σ_0 (exprimée en C m^{-2}) est alors égale à :

$$\sigma_0 = -(\sigma_s + \sigma_d)$$

où σ_s est la charge dans la couche de Stern et σ_d la charge dans la DDL, avec :

$$\sigma_s = \frac{N_i Z e}{1 + \frac{N_A w}{Mc} \exp\left(\frac{-(Ze\psi_d + \varphi)}{kT}\right)}$$

où N_i est le nombre de sites d'adsorption par m² de surface, Z la charge de l'ion, e la charge élémentaire ($1{,}602 \cdot 10^{-19}$ C), N_A la constante d'Avogadro ($6{,}02 \cdot 10^{23}$ ions mol^{-1}), w la densité du solvant (kg m^{-3}), M le poids moléculaire du solvant (g mol^{-1}), c la concentration molaire d'électrolyte (M), ψ_d le potentiel de Stern (V), φ le potentiel d'adsorption spécifique dans la

couche de Stern (J), k la constante de Boltzmann ($1{,}38 \cdot 10^{-23}$ J K^{-1}), et T la température absolue (K).

D'après le modèle de Gouy-Chapman, la densité de charge dans la DDL σ_d est liée au potentiel de Stern ψ_d (en V) selon la relation suivante :

$$\sigma_d = \sqrt{\frac{2c\varepsilon kT}{\pi}} \sinh\left(\frac{Ze\psi_d}{2kT}\right)$$

où, ε est la constante diélectrique de l'eau (78,5 à 25 °C).

A 25 °C, on obtient la relation simplifiée :

$$\sigma_d = 0{,}1174\ c^{1/2} \sinh(Z\ \psi_d \times 19{,}46)$$

ou encore :

$$\sigma_d = 2{,}3\ I^{1/2}\ \psi_d$$

où I est la force ionique de la solution (M).

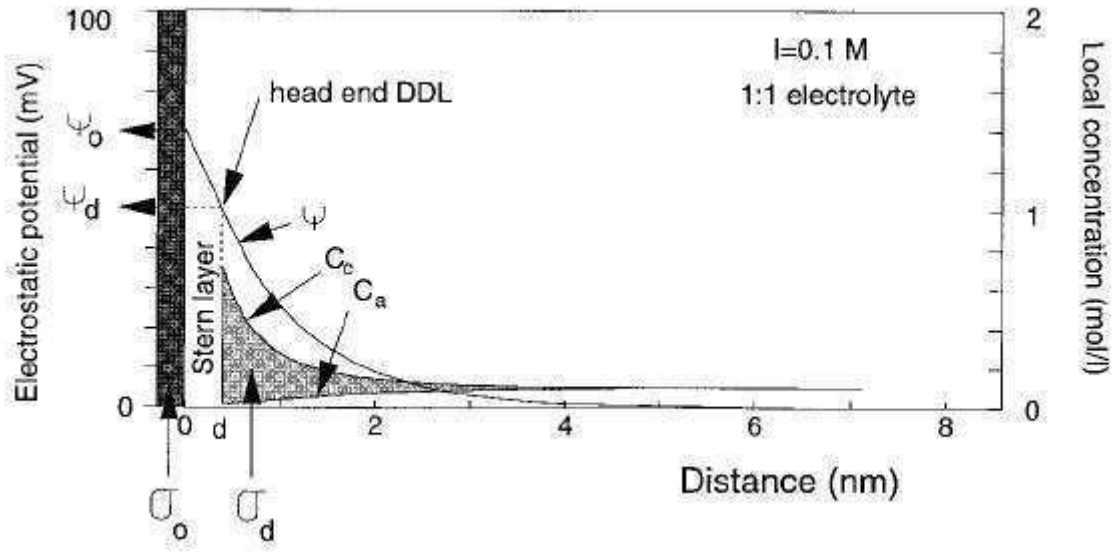

Figure 4. Représentation schématique du modèle de Stern (Hiemstra and van Riemsdijk 1996).

Le potentiel électrique ψ diminue lorsque la distance à la surface x (en m) augmente selon la relation suivante :

$$\tanh\left(\frac{ZF\psi}{4RT}\right) = \tanh\left[\left(\frac{ZF\psi_d}{4RT}\right)\exp(-\kappa\, x)\right]$$

Cette diminution est exponentielle lorsque $\psi < 25$ mV, selon la relation suivante :

$$\psi = \psi_d \exp(-\kappa\, x)$$

où κ est le paramètre de Debye (en m^{-1}), correspondant à l'inverse de l'épaisseur de la DDL. Cette épaisseur diminue lorsque la charge de l'électrolyte ou sa concentration augmentent.

Avec cette représentation, la distance minimale d'approche des ions de l'électrolyte correspond à l'extérieur de la couche de Stern, soit la distance d sur la Figure 4. La concentration en contre-ions C_c augmente à l'approche de la surface, au contraire de la concentration en co-ions C_a selon les relations suivantes :

$$C_c = C_{x=\infty} \exp\left(\frac{-ZF\psi}{RT}\right)$$

$$C_a = C_{x=\infty} \exp\left(\frac{ZF\psi}{RT}\right)$$

2.1.2 Modélisation de la charge de surface des (hydr)oxydes métalliques

Le modèle CD-MUSIC (Hiemstra and van Riemsdijk 1996) est un modèle couramment utilisé pour décrire l'adsorption des ions sur les (hydr)oxydes métalliques. Il est constitué de 2 parties :

- Le modèle de distribution de charge (CD) qui décrit les interactions électrostatiques ;
- Le modèle de complexation de surface (MUlti-SIte Complexation).

Le modèle de distribution de charge choisi considère la répartition des charges à l'interface selon les principes suivants :

- Les protons sont placés sur la surface (le plan 0 sur la Figure 4) ;
- Les ions électrolytiques sont positionnés sur le plan 1 (extérieur de la couche de Stern, soit le début de la DDL, situé à la distance d sur la Figure 4) ;
- La charge des ions adsorbés spécifiquement sur la surface est répartie entre les plans 0 et 1.

Le concept de distribution de la charge permet la définition de groupes de surface et de leur charge correspondante.

L'approche CD-MUSIC est basée sur la structure cristallographique du minéral et sur le principe de distribution de charge de Pauling (1929), qui implique que la charge d'un cation soit compensée par les oxygènes voisins. On définit alors la valeur de la valence d'une liaison ν de la façon suivante :

$$\nu = z / CN$$

où z est la charge du cation et CN son nombre de coordination. Dans le cas d'Al_2O_3, le minéral utilisé par la suite dans ce travail, les ions Al^{3+} (z = 3) répartissent leurs charges entre les 6 atomes d'oxygène voisins (CN = 6), d'où ν = ½. Les groupes de surface ≡AlOH présentent donc une charge de -½. Ils peuvent se protoner selon la réaction suivante :

$$\equiv AlOH^{½-} + H_3O^+ \rightleftarrows \equiv AlOH_2^{½+} + H_2O \qquad \log K \approx 10$$

Il existe également la surface des oxydes d'aluminium des groupes doublement coordinés, qui sont alors non chargés $\equiv Al_2OH^0$. La charge de l'oxygène étant neutralisée, ils ne peuvent se protoner qu'à des très faibles valeurs de pH, ou dissocier un proton qu'aux pH élevés (Hiemstra et al. 1999), selon les réactions suivantes :

$$\equiv Al_2O^- + H_3O^+ \rightleftarrows \equiv Al_2OH^0 + H_2O \qquad \log K = 11.9$$

$$\equiv Al_2OH^0 + H_3O^+ \rightleftarrows \equiv Al_2OH_2^+ + H_2O \qquad \log K = 0$$

Dans la gamme de pH étudiée généralement (entre 3 et 12), ces groupes sont donc neutres et ne sont pas pris en compte dans la modélisation de la charge de surface du minéral.

2.2 Réactivité de la matière organique naturelle

2.2.1 Définition des substances humiques

La matière organique naturelle est issue de la décomposition du vivant : résidus de plantes, biomasse du sol, humus stable. Ce dernier correspond aux substances humiques et non humiques (acides aminés, résines, molécules organiques). Les substances humiques (SH) sont définies de manière opérationnelle, en fonction de leur procédure d'extraction. Elles sont séparées en trois fractions, selon leurs conditions de précipitation :

- Les Acides Fulviques (AF) sont solubles quel que soit le pH ;
- Les Acides Humiques (AH) précipitent à pH < 3 ;
- L'humine est insoluble quel que soit le pH.

Les SH constituent la majorité du carbone organique (40 à 60 %) et sont considérées comme représentatives de la matière organique naturelle. Les gammes de concentrations en substances humiques dans divers milieux aquatiques sont données dans le Tableau 1, adapté de Thurman (1985).

Tableau 1. Concentrations en substances humiques dans les eaux naturelles (Thurman 1985; Tipping 2002).

Type d'eau	Concentrations en SH (mg/L)	Carbone organique dissous (mg/L)
Eau souterraine	0,05 – 0,10	0,5 – 1,5
Eau de mer	0,10 – 0,25	0,5 – 1,0
Lac	1 – 4	2 – 10
Rivière	1 – 4	1 – 10
Zone humide	10 – 30	10 – 50

2.2.2 Composition et structure des substances humiques

Les substances humiques sont composées majoritairement d'atomes de carbone (40 à 60 %), d'oxygène (35 à 45 %), d'hydrogène (≈ 5 %), mais aussi d'azote (1 à 5 %) et de soufre (moins de 2 %). Les rapports élémentaires permettent d'estimer l'origine et l'aromaticité des substances humiques (Rice and ~~Maccarthy~~ Λ 1991).

Les substances humiques sont des mélanges composites, constitués de composants aromatiques et aliphatiques multifonctionnels. Elles présentent plusieurs groupes fonctionnels caractéristiques polaires : -COOH, -OH, -C=O, -NH_2. Du fait de leur hétérogénéité et de leur complexité, la plupart des données sur les SH correspondent donc à des propriétés moyennes d'un ensemble de molécules diverses.

Les tailles des substances humiques sont fonction de leur origine (SH des sols ou aquatiques) ainsi que des conditions physico-chimiques du milieu. Les poids moléculaires des SH sont ainsi compris entre 500 et 2000 Da pour les AF de 1000 à plus de 10000 Da pour les AH (Thurman et al. 1982).

Il semblerait qu'il y ait plusieurs niveaux d'agrégation et d'interactions des SH. Des travaux en diffusion de rayons X ou de neutrons aux petits angles semblent montrer que les SH sont composées d'agrégats de type fractal, de taille comprise entre 1 et 200 nm (Österberg et al. 1995; Rice et al. 1999; Reiller et al. en écriture). Le niveau nanométrique a aussi été observé en microscopie à force atomique (AFM) (Baalousha and Lead 2007), en fractionnement par couplage flux-force (FFF) (Bouby et al. 2002), ou en analyse de dispersion de Taylor-Aris (d'Orlyé and Reiller soumise). Des objets de 60-500 nm ont eux été observés en diffusion

dynamique de la lumière (Caceci and Moulin 1991; Reid et al. 1991; Pinheiro et al. 1996; Rice et al. 1999; Manning and Bennett 2000).

Les agrégats humiques sont ainsi de plus en plus considérés comme des associations supramoléculaires de plus petites molécules, de poids moléculaire inférieur à 2000 Da (Moulin et al. 2001; These et al. 2004) dont la cohésion serait assurée par des liaisons hydrogène ou hydrophobes (Wershaw 1993; Conte and Piccolo 1999; Wershaw 1999; Piccolo 2001; Simpson et al. 2002), ce qui est en accord avec les résultats obtenus en diffusion de rayonnement aux petits angles.

Les conditions physico-chimiques de la solution ont une influence sur la conformation des SH. En effet, du fait de leurs nombreuses fonctions ionisables, les SH sont sensibles aux variations de force ionique : quand la concentration en électrolyte augmente, la taille des agrégats humiques observables en diffusion dynamique de la lumière diminue (1999) : il y a compression de la structure de ces agrégats du fait de l'écrantage de la répulsion entre charges. En revanche, il semble que la taille des plus petits objets ne soit pas affectée par une variation de force ionique (d'Orlyé and Reiller soumise).

2.2.3 Propriétés optiques des substances humiques

Les spectres d'absorption UV-Visible des SH sont relativement monotones, décroissants quand la longueur d'onde augmente et ne montrent aucune bande caractéristique. L'augmentation d'absorbance dans l'UV proche (< 400nm) traduit la présence de structures aromatiques mais aucun chromophore particulier ne peut être clairement mis en évidence. Étant donné la complexité des mélanges humiques, ces spectres peuvent être dus à la superposition des influences de tous les chromophores présents, ainsi qu'à des effets de chromisme (Vekshin 1999), un phénomène qui exalte ou inhibe l'absorption lorsque les chromophores interagissent dans le mélange.

Il est courant d'utiliser l'absorption des SH pour déterminer leur concentration en solution, notamment vers 250 nm, représentatif des chromophores aromatiques. Cette propriété a également été utilisée pour déterminer leur taille (Reid et al. 1990). Cependant, l'absorption d'une suspension de SH est modifiée par les conditions physico chimiques comme le pH et la force ionique (Dryer et al. 2008). Ces propriétés seront discutées plus en détail dans le Chapitre 2.

2.2.4 Propriétés acido-basiques et charge des substances humiques

Les SH sont riches en groupes fonctionnels oxygénés – carboxyl, phénol, alcool – qui dominent leurs propriétés chimiques. Leur réactivité est généralement associée à deux grands groupes de ~~groupes~~ fonctionnels, carboxyliques et phénoliques. Du fait de la dissociation de ces groupements fonctionnels ~~neutres~~, la charge de surface des SH est toujours négative, et son intensité est fonction à la fois du pH et de la force ionique. De la même manière que pour les surfaces minérales, cette charge est généralement étudiée par titrages potentiométriques. La Figure 5 présente une compilation de plusieurs données de la littérature proposée par Milne et al. (2001). Elle illustre la charge de ces composés ainsi que leur hétérogénéité.

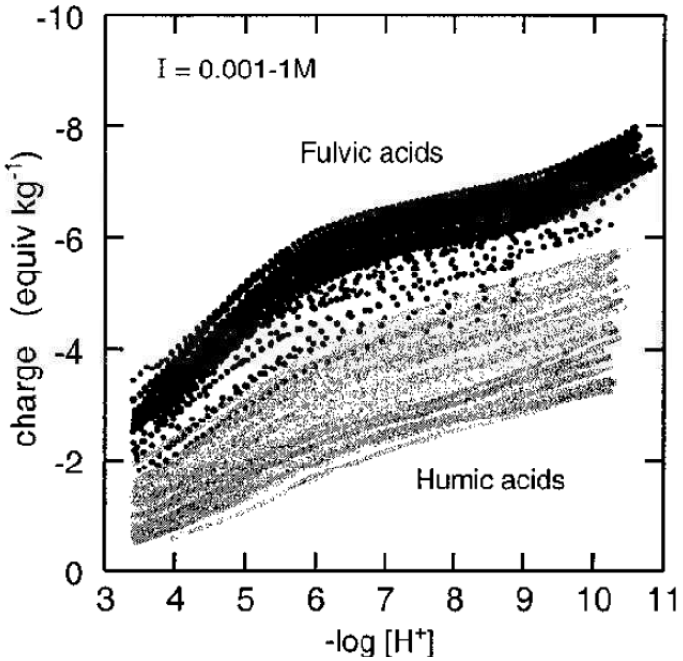

Figure 5. Variation de la charge de plusieurs acides fulviques et humiques en fonction du pH de la solution, à différentes forces ioniques (Milne et al. 2001).

Le caractère variable de la charge des acides humiques et fulviques induit une dépendance de la protonation à la force ionique, surtout pour les acides humiques (Figure 5). Les ions métalliques M^{n+} peuvent être liés comme contre-ions ou liés spécifiquement à des groupes réactifs, et la compétition entre ions M^{n+} peut être influencée par la nature chimique des ions liés (Marang et al. 2008; Marang et al. 2009).

La répulsion intra ou inter-moléculaire des acides humiques diminue lorsque le pH diminue (les groupes fonctionnels captent des protons et les molécules sont moins chargées négativement), et lorsque la force ionique augmente (écrantage des charges).

2.2.5 Modélisation des réactions aux interfaces

Du fait de la grande hétérogénéité des substances humiques, il existe de nombreux modèles de complexation des ions par les SH. Dans cette étude, nous avons utilisé le modèle NICA-Donnan (Kinniburgh et al. 1996), le seul qui sera défini ici ; concernant les autres modèles, le lecteur pourra se référer aux ouvrages de référence (Tipping 2002; Reiller 2010). Il combine le modèle NICA (Non-Ideal Competitive Adsorption) (Benedetti et al. 1995), qui décrit les interactions entre les ions et les SH ainsi que les effets de compétition entre les différents ions, et le modèle de Donnan (Benedetti et al. 1996), utilisé pour rendre compte des interactions électrostatiques.

2.2.5.1 Prise en compte de l'électrostatique : le modèle de Donnan

Dans ce modèle, les substances humiques sont considérées comme un gel de volume variable, électriquement neutre, dans lequel les ions peuvent pénétrer (Benedetti et al. 1996; Kinniburgh et al. 1996; Avena et al. 1999; Saito et al. 2005). Ce volume de Donnan V_D dépend essentiellement de la force ionique de la solution. La charge Q_{tot} est répartie uniformément dans l'ensemble du gel, et est neutralisée par les contre-ions à l'intérieur du volume de Donnan V_D selon l'équation suivante :

$$\frac{Q_{tot}}{V_D} = \sum z_i \, (c_i - c_{Di})$$

où c_i est la concentration de l'espèce i en solution, c_{Di} la concentration de l'espèce i dans le gel de Donnan et z_i la charge de l'ion. Ces deux concentrations sont reliées par un facteur de Boltzmann χ, avec son potentiel de Donnan implicite ψ_D :

$$c_{D_i} = \chi^{z_i} \, c_i$$

où

$$\chi = \exp\left(\frac{-e\psi_D}{kT}\right)$$

Dans le modèle de Donnan, le potentiel ψ_D est constant à l'intérieur du volume de Donnan (Figure 6). Il n'y a aucune hypothèse particulière concernant la géométrie des substances humiques, contrairement au modèle de la double couche diffuse dans lequel le potentiel varie avec la distance à l'interface, et est donc dépendant de la géométrie de l'objet étudié.

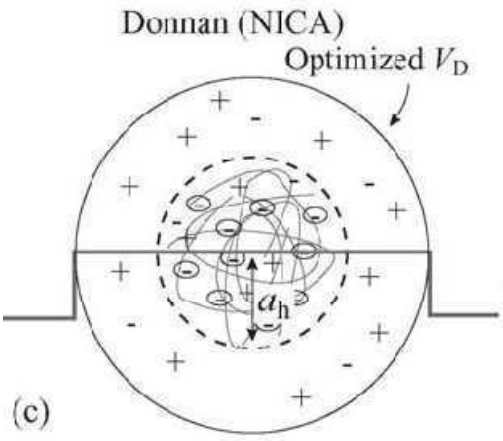

Figure 6. Représentation électrostatique du modèle de Donnan. La ligne représente le profil du potentiel électrique (issu de Saito et al. 2005).

Cette approche nécessite la connaissance du volume de Donnan V_D sur toute la gamme des conditions de la solution. Sa mesure directe est impossible, mais Benedetti et al. (1996) ont montré que le volume de Donnan apparent diminue lorsque la force ionique I augmente selon la relation empirique suivante :

$$\log V_D = b\,(1 - \log I) - 1$$

où b est un paramètre empirique donc la valeur est généralement comprise entre 0.3 et 0.5 pour les AH, et entre 0.7 et 0.9 pour les AF.

Il y a une relation étroite entre le volume de Donnan et le potentiel de Donnan : pour une charge donnée, un plus petit volume de Donnan implique une plus forte concentration de contre-ions dans la phase de Donnan, un plus grand facteur de Boltzmann et donc une valeur absolue du potentiel de Donnan plus élevée.

La représentation de la charge des SH en fonction de la concentration en protons dans le volume de Donnan permet de corriger les données des effets électrostatiques. De cette manière, les différentes courbes obtenues à plusieurs forces ioniques se confondent en une « Courbe Maîtresse » (Master Curve), illustrée sur la Figure 7.

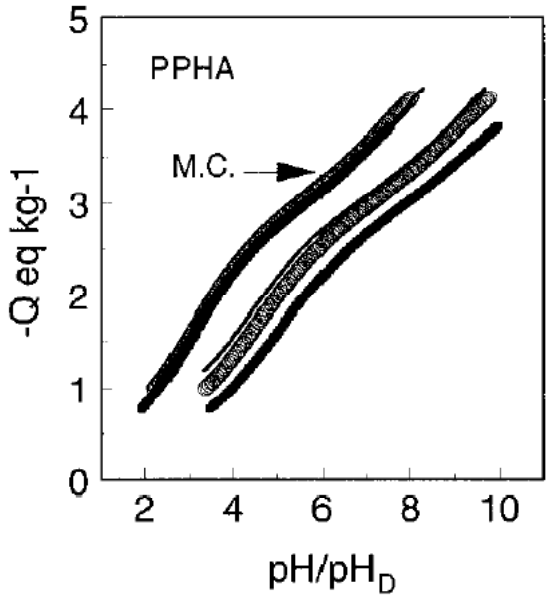

Figure 7. Courbes de titrages d'un acide humique à (■) 0.01 M; (○) 0.1 M; (-) 0.33 M en fonction du pH. Les symboles fléchés en tant que M.C. (Master Curve) correspondent aux données après correction des effets électrostatiques par le modèle de Donnan et sont donnés en fonction du pH_D (pH dans le gel de Donnan) (Benedetti et al. 1996).

Le calcul de concentrations des différents composants dans la phase de Donnan c_{D_i} , permet de déterminer des paramètres de liaison spécifique intrinsèques, c'est-à-dire indépendants des effets électrostatiques du milieu.

2.2.5.2 Le modèle NICA

Le modèle NICA est fondé sur une approche continue de la distribution des sites de liaison des substances humiques. Dans cette approche, la quantité d'ions i complexés à une substance humique Q_i est donnée par l'équation suivante :

$$Q_i = \frac{n_{i,1}}{n_{H,1}} Q_{max,1} \frac{(\widetilde{K}_{i,1} c_i)^{n_{i,1}}}{1 + \sum_i (\widetilde{K}_{i,1} c_i)^{n_{i,1}}} \times \frac{\left[\sum_i (\widetilde{K}_{i,1} c_i)^{n_{i,1}}\right]^{p_1}}{1 + \left[\sum_i (\widetilde{K}_{i,1} c_i)^{n_{i,1}}\right]^{p_1}} + \frac{n_{i,2}}{n_{H,2}} Q_{max,2} \frac{(\widetilde{K}_{i,2} c_i)^{n_{i,2}}}{1 + \sum_i (\widetilde{K}_{i,2} c_i)^{n_{i,2}}} \times \frac{\left[\sum_i (\widetilde{K}_{i,2} c_i)^{n_{i,2}}\right]^{p_2}}{1 + \left[\sum_i (\widetilde{K}_{i,2} c_i)^{n_{i,2}}\right]^{p_2}}$$

Deux types de sites réactionnels (notés 1 et 2 dans l'équation précédente) sont pris en compte. Ils sont assimilés à des groupes fonctionnels de type carboxylique (dits de faible affinité pour les protons) et phénolique (dits de forte affinité pour les protons).

Q_{max} correspond à la capacité maximale d'adsorption d'un site, n_i reflète la non-idéalité du système liée aux interactions latérales et/ou aux effets stœchiométriques – il est spécifique à

chaque ion ($0 < n < 1$, où 1 est le cas idéal) –, c_i correspond à la concentration de l'espèce i en solution, p est la largeur de la distribution pour chaque type de site, et $\tilde{K}_i$ est la valeur médiane de la distribution pour chaque type de sites et pour l'ion i. Milne et al. (2001) ont déterminé les paramètres NICA-Donnan intrinsèques génériques pour la protonation d'acides fulviques et humiques à partir d'un large jeu de données. Les valeurs sont rappelées dans le Tableau 2.

Tableau 2. Paramètres NICA-Donnan génériques intrinsèques pour la protonation des acides fulviques et humiques (d'après Milne et al. 2001).

	b	$Q_{max1,H}$	$\log\tilde{K}_{H1}$	m_1	$Q_{max2,H}$	$\log\tilde{K}_{H2}$	m_2
Acides fulviques	0.57	5.88	2.34	0.38	1.86	8.60	0.53
Acides humiques	0.49	3.15	2.93	0.50	2.55	8.00	0.26

Ces paramètres génériques donnent lieu à la distribution de sites illustrée par la Figure 8. Cette distribution correspond aux valeurs de constantes d'affinités intrinsèques, c'est-à-dire corrigées des effets électrostatiques par le modèle de Donnan.

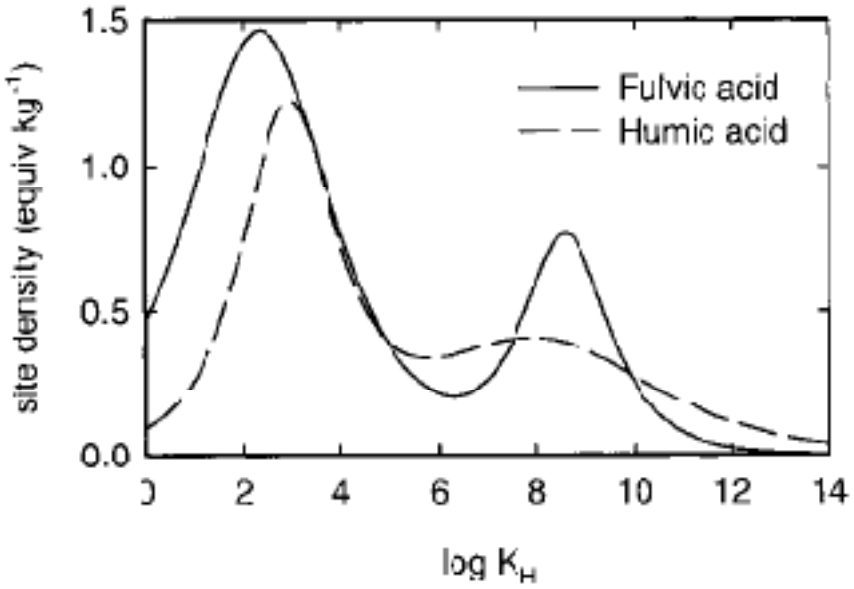

Figure 8. Distribution des constantes d'affinité intrinsèques pour le proton obtenue en utilisant les paramètres NICA-Donnan génériques (d'après Milne et al. 2001).

3 Interactions entre colloïdes organiques et minéraux

La matière organique naturelle présente une grande affinité pour les surfaces minérales. Les substances humiques, chargées négativement, s'adsorbent facilement sur les solides. De nombreuses études portent sur les interactions entre différentes substances humiques et différentes phases minérales

- Oxydes de fer (Gu et al. 1994; Avena and Koopal 1998; Reiller et al. 2002; Saito et al. 2004; Reiller et al. 2006) ;
- Oxydes d'aluminium (Ochs et al. 1994; Schlautman and Morgan 1994; Buleva and Petkanchin 1999; Tombacz et al. 2000; Claret et al. 2008; Ghosh et al. 2010) ;
- Argiles (Meier et al. 1999; Hur and Schlautman 2003; Ghosh et al. 2009).

Notre système d'étude comprenant un oxyde d'aluminium comme surface minérale, par la suite, nous nous sommes focalisés sur l'étude des SH en contact avec les oxydes.

3.1 Nature des interactions

L'adsorption des substances humiques sur une surface minérale met en jeu plusieurs processus (Ochs et al. 1994; Schlautman and Morgan 1994):

- Échange de ligands, qui provoque la formation de complexes de sphère interne entre les fonctions carboxyliques et phénoliques des substances humiques et les sites de surface des oxydes, d'où une variation de l'adsorption en fonction du pH ;
- Échange d'anions ou de cations selon le pH de la solution et le point de charge nulle de la surface. L'échange d'anions correspond à l'interaction électrostatique entre les minéraux chargés positivement et les échantillons humiques chargés négativement ;
- Interactions hydrophobes ou latérales, lorsque la force ionique est suffisamment importante pour écranter les charges négatives des molécules organiques, ou lorsque le pH neutralise ces charges (aux faibles valeurs de pH).

Lors de l'adsorption de SH sur un minéral, il y a fractionnement de l'agrégat humique, créant ainsi deux compartiments organiques, l'un en solution et l'autre à la surface. Ces deux fractions présentent des propriétés physico-chimiques différentes ainsi qu'une affinité différente pour les ions. Ce fractionnement dépend des paramètres physico-chimiques de la solution, notamment pH et force ionique, mais également de la SH et du minéral, ainsi que du

ratio organique/minéral. Il est donc difficile de comparer les données de la littérature, du fait de l'hétérogénéité des conditions utilisées.

L'adsorption de SH sur les oxydes modifie les charges des composés. Plus la quantité d'acide humique dans le système augmente, plus le point isoélectrique des suspensions organo-minérales diminue (Fairhurst et al. 1995b). Saito et al. (2004) ont réalisé des titrages potentiométriques de suspensions de goethite et d'AH. Les résultats diffèrent de la somme de la charge des deux composés pris séparément, signe d'un ajustement de charge des colloïdes (cf. Figure 9).

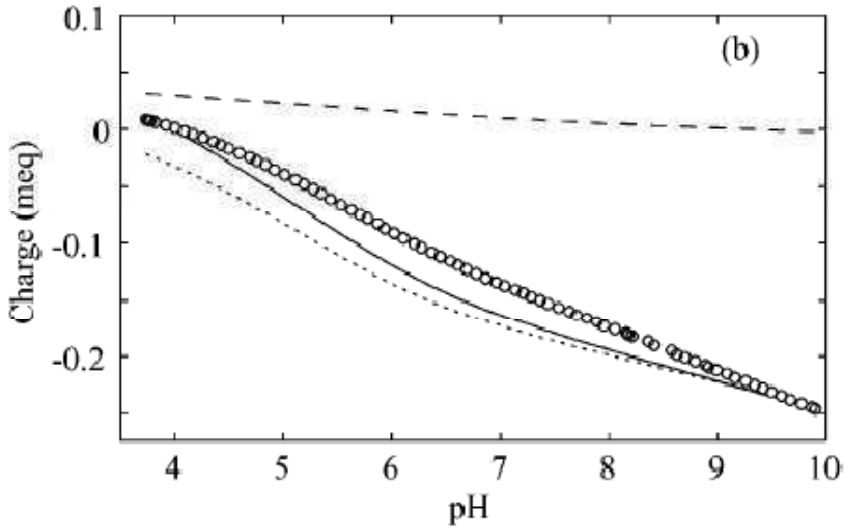

Figure 9. Charge d'une suspension d'acide humique et de goethite en fonction du pH (*I* = 0.01 M KNO_3). Les cercles correspondent aux résultats obtenus pour le mélange (0.22 $g_{HA}/g_{goethite}$), les tirets à ceux de la goethite, les pointillés à ceux de l'AH, et la ligne pleine à ceux d'un mélange sans interaction (Saito et al. 2004).

3.2 Effet des conditions de la solution

L'adsorption des substances humiques est fortement dépendante du pH (Figure 10), du fait de l'échange de ligands et des interactions électrostatiques. En effet, lorsque le pH diminue, la charge de surface positive de l'oxyde minéral est plus importante et, suite à la neutralisation des fonctions oxygénées, la matière organique est moins négativement chargée. La répulsion électrostatique est donc moins forte. De plus, la quantité de SH adsorbée par complexation de sphère interne augmente, comme attendu par analogie avec les acides organiques simples (Gu et al. 1995). La quantité de SH adsorbée diminue donc lorsque le pH augmente (Figure 10).

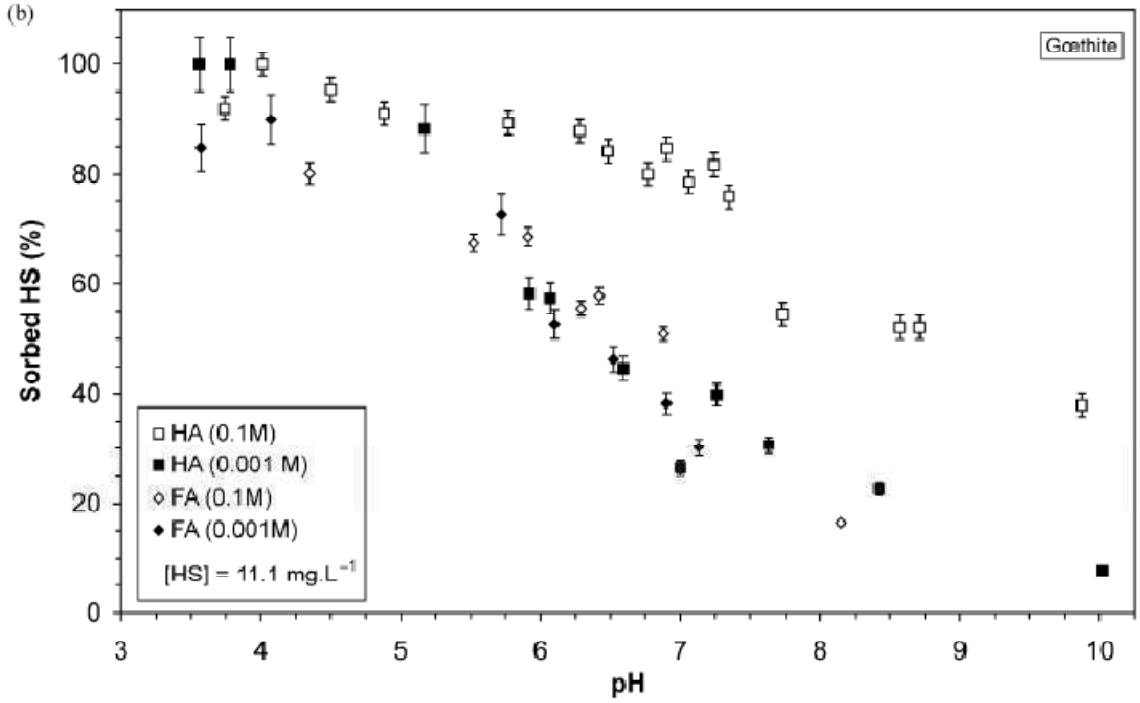

Figure 10. Adsorption de SH sur de la goethite (Reiller et al. 2002).

En revanche, l'effet de la force ionique sur la rétention de substances humiques est différent du cas des acides organiques simples, parfois utilisés comme analogues des SH, et dont l'adsorption augmente lorsque la force ionique diminue (Ali and Dzombak 1996). La force ionique a moins d'influence sur l'adsorption des AF (Filius et al. 2000; Christl and Kretzschmar 2001; Reiller et al. 2002), alors qu'elle a un impact important sur l'adsorption des AH. Les acides fulviques, de plus petite taille, sont adsorbés à proximité de la surface minérale, contrairement aux AH dont une grande partie des agrégats est située dans la solution, donc plus sensibles à l'électrostatique (Figure 11). De manière générale, comme illustré par la Figure 10, l'adsorption augmente avec la force ionique pour les AH (Reiller et al. 2002; Weng et al. 2006a). A force ionique élevée, les charges négatives des molécules d'AH sont écrantées par les ions électrolytiques. La répulsion est moindre, autorisant une plus grande quantité d'AH à s'adsorber à la surface minérale.

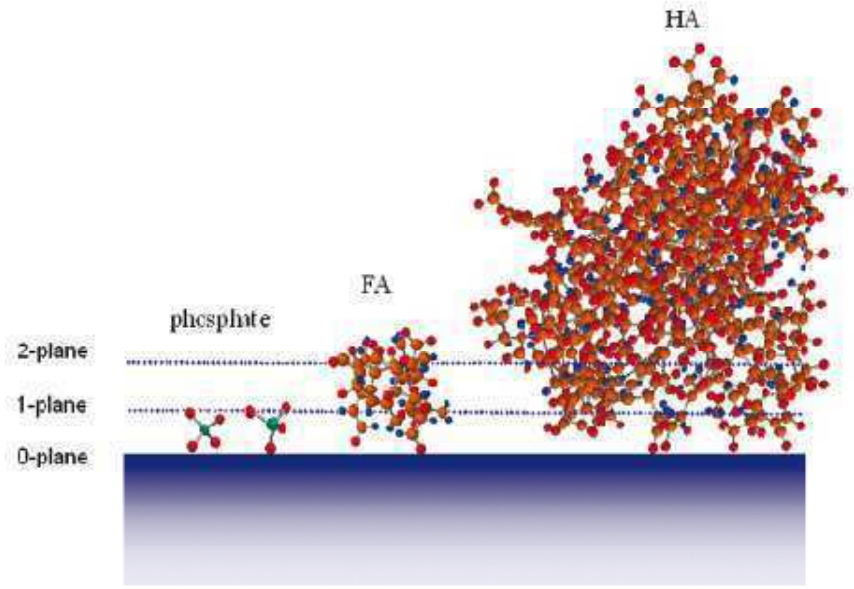

Figure 11. Représentation schématique d'un ion phosphate, un acide fulvique et un acide humique sur une surface (Weng et al. 2008b).

3.3 Caractérisation du fractionnement

Le fractionnement dû à l'adsorption des SH sur des surfaces minérales provoque une modification de leur structure. Il peut être caractérisé par analyse des spectres d'absorbance UV/Visible – qui renseignent sur l'aromaticité des SH – par chromatographie d'exclusion stérique (SEC) ou en spectrométrie de masse électrospray (ESI-MS) – qui renseignent sur la distribution en taille des échantillons, en général corrélée à leur poids moléculaire (MW).

Toutes les études présentant des résultats spectrophotométriques (calcul de paramètres d'absorbance spécifique SUVA, de ratios d'absorbances E_2/E_3, ou encore d'absorptivité molaire ε_{280}) montrent une diminution de l'aromaticité dans le surnageant lorsque le fractionnement est important (quand il y a peu de SH dans le système) : il y a adsorption préférentielle des fractions les plus aromatiques (Gu et al. 1995; Meier et al. 1999; Chorover and Amistadi 2001; Zhou et al. 2001; Reiller et al. 2006; Claret et al. 2008).

Les résultats des études SEC sont plus variables. En effet, la plupart des études montrent une adsorption préférentielle des fractions de poids moléculaire plus élevé pour différents extraits de matière organique sur de la goethite, pour des valeurs de pH comprises entre 4 et 7.5 (Meier et al. 1999; Chorover and Amistadi 2001; Zhou et al. 2001). Cependant, Hur & Schlautman (2004) ont montré que le poids moléculaire apparent de la fraction non adsorbée d'AH Aldrich purifié (PAHA) sur de l'hématite dépendait du pH : en dessous du point de

charge nulle de l'oxyde (pH 8) le poids moléculaire en solution est supérieur à l'original, alors qu'à pH plus élevé le poids moléculaire apparent de la solution est plus faible, traduisant une adsorption préférentielle des fractions à poids moléculaire plus important. Ces observations sont en accord avec celles de Reiller et al. (2006) qui ont étudié l'adsorption de PAHA sur de l'hématite à pH 7 par ESI-MS et ont noté la sorption préférentielle de la fraction de faible poids moléculaire ($m/z < 600$ Da). En revanche, Zhou et al. (2001) ont observé la tendance inverse pour un système AF aquatique/goethite, avec une adsorption préférentielle des composants à fort poids moléculaire à faible pH et poids moléculaire intermédiaire à haut pH. Ces derniers résultats sont en accord avec ceux de Meier et al (1999) ont remarqué par SEC une absorption préférentielle des fractions à poids moléculaire élevé de SH naturelles sur de la goethite et de la kaolinite à pH 4.

Il semble donc difficile de conclure quant à une tendance générale de la modification en taille des SH sur les surfaces minérales. Il y a certainement une influence de l'origine de la matière organique (aquatique ou terrestre notamment), ainsi que de la surface, car Hur & Schlautman (2003) ont observé des comportements différents entre l'hématite et la kaolinite. L'influence du pH a un rôle majeur, encore mal défini à ce jour. Il semble également y avoir une évolution cinétique, avec l'adsorption en premier lieu de fractions de faible poids moléculaire remplacées avec le temps par de plus grosses fractions (Ochs et al. 1994; Gu et al. 1995).

Le plus souvent, la concentration des SH en solution est mesurée par spectrophotométrie UV/Visible. Cependant, en dessous d'une certaine concentration initiale en SH, cette méthode induit un biais par rapport à une mesure de carbone organique dissous (DOC), du fait du fractionnement des molécules organiques et de la modification des proportions de chromophores (Gu et al. 1996; Zhou et al. 2001; Claret et al. 2008).

Certaines études faites sur la fraction solide par résonance magnétique nucléaire du ^{13}C ou en spectroscopie infrarouge ont montré la présence de nombreux groupes carboxyliques complexés avec les surfaces d'oxyde (Chorover and Amistadi 2001; Kang and Xing 2008; Ghosh et al. 2009).

4 Géochimie de l'europium(III)

4.1 Choix du radionucléide d'étude

Dans le cadre de la maîtrise des risques liés à l'utilisation de l'énergie nucléaire, il est nécessaire de mieux connaître le comportement des produits issus du cycle nucléaire dans l'environnement, notamment vis-à-vis de la matière organique naturelle. Parmi eux, les actinides trivalents tels que l'américium(III) et le curium(III) sont importants de par leur toxicité radiologique et chimique. Dans la série des lanthanides, l'europium(III) est un relativement bon analogue chimique des actinides trivalents, présentant l'avantage d'être non radioactif, d'où une plus grande facilité de manipulation. Les fonctions complexantes des SH étant principalement oxygénées, l'analogie entre Eu(III) et les actinides(III) est très importante (Reiller 2010).

En solution, l'europium(III) s'hydrolyse à partir de pH 6 et précipite selon sa concentration. La Figure 12 montre la spéciation de l'europium(III) en solution en fonction du pH en absence de carbonates.

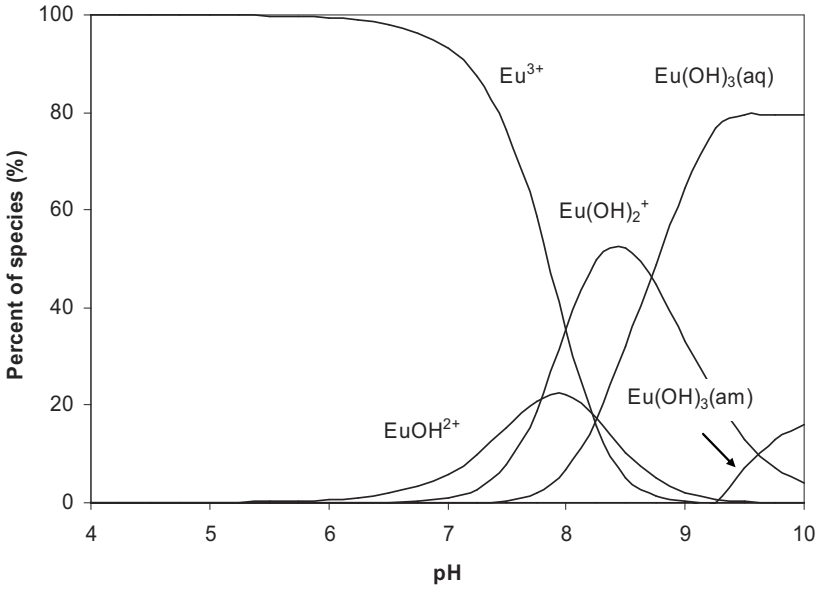

Figure 12. Spéciation de l'Europium en solution en fonction du pH, dans le cas d'une absence de carbonates. [Eu(III)] = 10^{-6} mol/L, I = 0.1 mol/L NaClO4. Calcul à partir des données de Hummel et al. (2002).

4.2 Étude de la spéciation de Eu(III) en solution : La spectrofluorimétrie laser à résolution temporelle

4.2.1 Principe de la spectrofluorimétrie laser à résolution temporelle

La Spectrofluorimétrie Laser à Résolution Temporelle (SLRT) permet d'analyser la spéciation de certains métaux fluorescents en solution tels que certains actinides (UO_2^{2+}, Cm^{3+}, Am^{3+}) et lanthanides (Eu^{3+}, Tb^{3+}, Sm^{3+}, Dy^{3+}, Ce^{3+}, Gd^{3+}, Tm^{3+}). Elle est fondée sur l'analyse de l'émission lumineuse de composés suite à leur excitation par une onde laser pulsée suivie de la résolution temporelle (positionnement d'une porte de mesure après l'impulsion laser) du signal de fluorescence permettant l'élimination des fluorescences parasites à temps de vie courts (organique, Raman, Rayleigh) (Berthoud et al. 1989).

La durée de l'impulsion laser (de l'ordre de la ns) est courte devant la durée de vie de la fluorescence de l'élément étudié (plusieurs dizaines de µs dans le cas des éléments f). La fluorescence peut être mesurée à partir de la fin de l'impulsion laser t_0 (Figure 13). Elle est mesurée à partir d'un certain délai *D*, correspondant au retard par rapport à t_0, et pendant une durée *L* (la largeur de la porte de mesure).

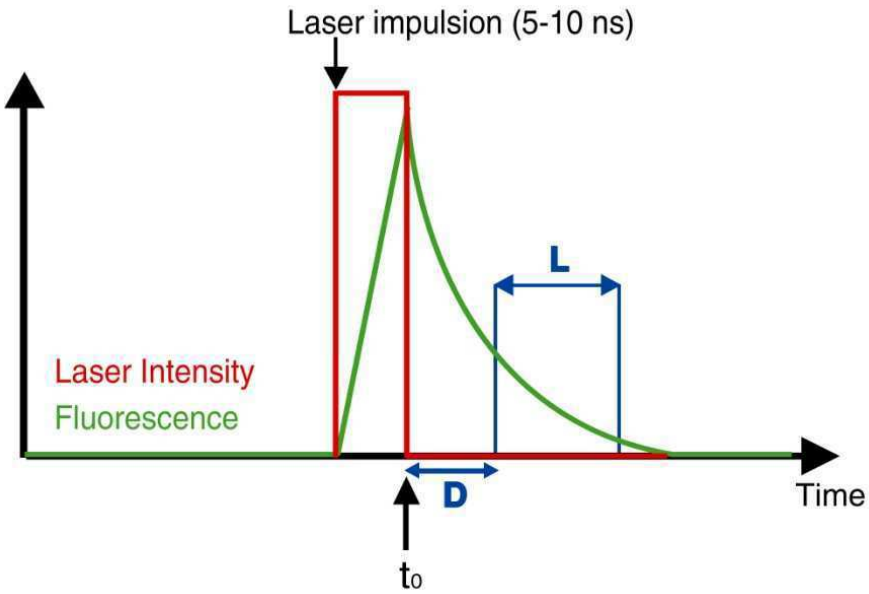

Figure 13. Principe de la résolution temporelle.

La caractérisation spécifique d'un élément ou d'une forme chimique particulière de celui-ci est rendue possible par les trois niveaux de sélectivité de la SLRT :

- *La longueur d'onde d'excitation* : la source d'excitation laser est choisie à une longueur d'onde correspondant à une bande d'absorption spécifique du composé.
- *Les spectres et temps de vie de luminescence* : les spectres de luminescence d'un élément sont composés de bandes plus ou moins sensibles à sa spéciation. Le temps de décroissance de la luminescence τ varie avec l'environnement chimique, en raison des couplages vibrationnels avec les ligands qui affectent la vitesse de désexcitation.
- *La résolution temporelle* : lorsque les caractéristiques spectroscopiques sont suffisamment distinctes, la discrimination des espèces en solution est permise par le choix des paramètres d'analyse (*D* et *L* notamment). Le spectre de luminescence d'une espèce, en mélange avec d'autres, peut ainsi être obtenu. Notamment, la résolution temporelle permet de séparer la luminescence de l'Eu(III) de la fluorescence des substances humiques, du fait de temps de vie très différents (de l'ordre de la nanoseconde pour les SH) (Dobbs et al. 1989b).

4.2.2 Luminescence de l'europium(III)

La configuration de l'europium(III) à l'état fondamental est [Xe] $6s^2$ $4f^7$. Cet état fondamental, du fait du couplage spin-orbite, est dégénéré en 7 niveaux ^7F_j, avec $0 \leq j \leq 6$ (Bünzli 1989). Les principaux pics couramment observés sur les spectres de luminescence de l'europium(III) correspondent à la désexcitation radiative de l'état excité $^5D_0$ (υ = 17 257 cm^{-1}) vers les niveaux $^7F_1$ ($\lambda_{max} \approx 593$ nm), $^7F_2$ ($\lambda_{max} \approx 618$ nm) et $^7F_4$ ($\lambda_{max} \approx 700$ nm). La Figure 14 (issue de Plancque et al. 2003) montre le spectre de l'ion libre Eu^{3+} et les transitions électroniques correspondantes. En milieu complexant, l'influence du champ de ligands sur les niveaux électroniques modifie l'intensité des pics de luminescence, et particulièrement celle de la transition dite hypersensible $^5D_0 \rightarrow {}^7F_2$ (Jorgensen and Judd 1964), qui est un dipôle électrique. En général, la formation de complexes provoque peu de déplacement des maxima des pics en longueur d'onde, mais peut induire des variations de la forme du pic du fait du champ de ligand (dégénérescence 2j+1 pour chaque niveau j). La transition $^5D_0 \rightarrow {}^7F_0$ ($\lambda_{max} \approx 580$ nm) est interdite pour des raisons électriques et magnétiques (Judd 1962; Ofelt 1962), mais elle apparaît lorsque l'environnement de l'europium(III) n'est pas centro-symétrique.

La transition $^5D_0 \rightarrow {}^7F_1$, qui est un dipôle magnétique, est la plus indépendante à la spéciation de l'Eu(III). Les variations du ratio d'asymétrie, correspondant au rapport des intégrales des transitions $^5D_0 \rightarrow {}^7F_2/{}^5D_0 \rightarrow {}^7F_1$, renseignent ainsi sur des modifications dans la symétrie de

l'environnement chimique de Eu(III). Ce paramètre dépend également de la polarité des ligands, du rapport de concentration entre le ligand et l'ion, ainsi que de la constante diélectrique du solvant (Marmodée et al. 2009).

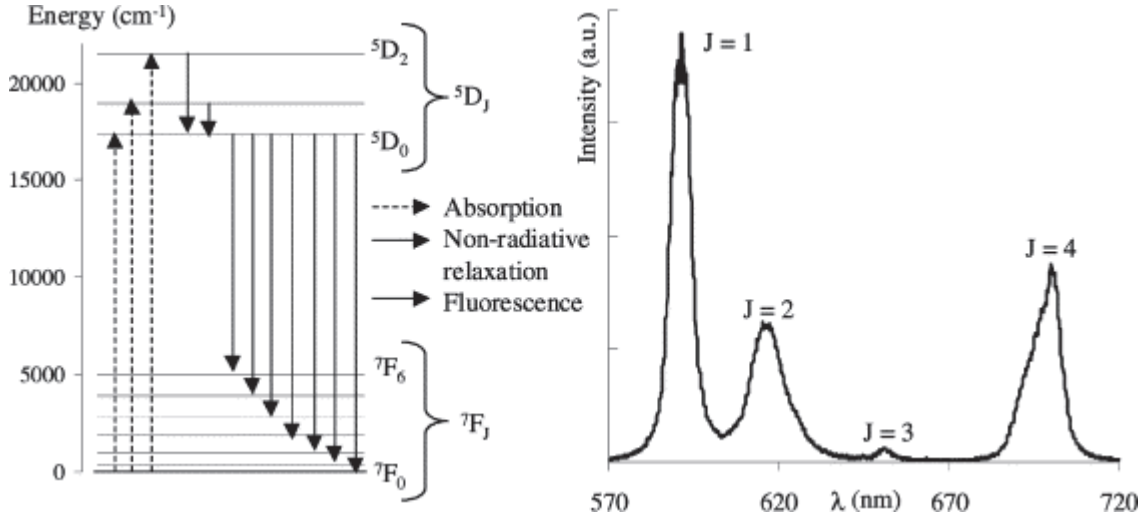

Figure 14. Diagramme des niveaux d'énergie et spectre de luminescence de l'Eu(III). Les pics sont issus des transitions $^5D_0 \rightarrow {}^7F_J$ (valeurs de J sur le spectre) (Plancque et al., 2003)

La luminescence de Eu(III) est enregistrée à différents délais. La décroissance de chaque état excité est décrite par une exponentielle, et le temps de décroissance de la luminescence est calculé à partir de l'équation suivante, pour un cas à *n* niveaux excités:

$$F_i = \int_D^{D+L} F_i^o \exp\left(-\frac{t}{\tau_i}\right) dt = F_i^o \, \tau_i \exp\left(-\frac{D}{\tau_i}\right)\left(1 - \exp\left(-\frac{L}{\tau_i}\right)\right)$$

$$F = F° \sum_{i=1}^{n} \left[x_i \, \tau_i \exp\left(-\frac{D}{\tau_i}\right)\left(1 - \exp\left(-\frac{L}{\tau_i}\right)\right)\right]$$

où F est l'intensité mesurée au maximum d'un pic ou son aire calculée, x_i est la proportion de chaque décroissance, *D* est le délai par rapport au début de la luminescence, et *L* la largeur de la porte de mesure. L'intensité initiale F° et le temps de décroissance τ de l'espèce *i* sont ajustés par la méthode des moindres carrés. Les incertitudes sur ces valeurs et les matrices de corrélation peuvent être calculées à l'aide de la macro Excel SolverAid (de Levie 2005).

La désexcitation d'un ion est due à une somme de contributions radiatives et non radiatives. Parmi les processus non radiatifs, le couplage entre l'état excité d'un élément et les niveaux vibroniques des molécules d'eau contribue à l'extinction de sa luminescence en solution. Cette

inhibition est particulièrement importante dans le cas des lanthanides et des actinides (III) (Horrocks and Sudnick 1979; Kimura and Choppin 1994). Les variations de temps de décroissance de luminescence sont donc interprétées comme des substitutions de molécules d'eau dans la première sphère de coordination de l'ion : le temps de décroissance de $Eu(H_2O)_9^{3+}$ est d'environ 100-110 µs, et croît si le nombre de molécules d'eau diminue. Kimura et al. (1998) ont déterminé une relation entre le temps de décroissance de la luminescence de l'europium(III) τ_{Eu} et le nombre de molécules d'eau présentes dans la première sphère d'hydratation de l'ion n :

$$n = \frac{1.07}{\tau_{Eu}} - 0.62$$

Cependant, Takahashi et al. (2000) ont montré que cette relation était dépendante du système et n'était donc pas applicable de manière générale. Il existe des relations plus complètes qui relient n à ~~(~~$1/\tau(H_2O) - 1/\tau(D_2O)$~~)~~, et nécessitent donc la mesure des temps de décroissance dans H_2O et D_2O pour chaque système (Horrocks and Sudnick 1979; Supkowski and Horrocks 2002).

4.3 Complexation avec les substances humiques

La complexation d'un cation métallique avec des SH influence la conformation des molécules organiques. En présence de cations, même à l'état de trace, l'agglomération des molécules humiques a été observée par technique de fractionnement par couplage flux-force ou « flow-field flow fractionation » (FFFF) (Suteerapataranon et al. 2006). Des analyses d'agrégats Eu(III)~~-~~/HA par microscopies en transmission de rayons X (STXM) et à balayage laser (LSLM) ont montré que les zones d'enrichissement en Eu(III) dans ces agrégats à pH 5 correspondaient également à des zones d'enrichissement local en groupes carboxyliques (Naber et al. 2006) ou au moins complexants (Plaschke et al. 2009).

La complexation de l'europium(III) avec des SH a déjà été étudiée notamment par des méthodes d'échange d'ions (Fairhurst et al. 1995b; Lead et al. 1998), ultrafiltration (Caceci 1985) ou SLRT (Dobbs et al. 1989a; Marang et al. 2008), qui ont permis de proposer des paramètres de complexation, fonctions du pH expérimental et du modèle utilisé. Milne et al. (2003) ont utilisé ~~des~~ jeux de données préexistants pour déterminer des paramètres de complexation intrinsèques Eu(III)~~-~~/AH et Eu(III)~~-~~/AF génériques dans le cadre du modèle NICA-Donnan. Ces paramètres sont donnés dans le Tableau 3. Notons un bon accord entre ces données et celles plus récentes de Marang et al. (2008) pour le site 1.

Tableau 3. Paramètres génériques de complexation de l'Eu(III) avec des acides humiques ou fulviques déterminés par Milne et al. (2003)

	$\log \tilde{K}_1$	n_1	$\log \tilde{K}_2$	n_2
Eu/AH	1.92	0.57	3.43	0.36
Eu/AF	-1.92	0.47	5.87	0.45

Avec ces paramètres génériques, il est possible de calculer la spéciation de l'Eu(III) en présence de 10 mg/L d'AH en utilisant le logiciel de spéciation ECOSAT (Keizer and van Riemsdijk 1994). Le résultat est représenté dans la Figure 15. Les espèces hydrolysées sont en proportions trop faibles pour être visibles sur une représentation en pourcentage. L'Eu(III) est en grande majorité complexé à l'AH entre pH 4 et pH 10. Au-delà, la précipitation de l'hydroxyde d'europium $Eu(OH)_3(s)$ peut intervenir.

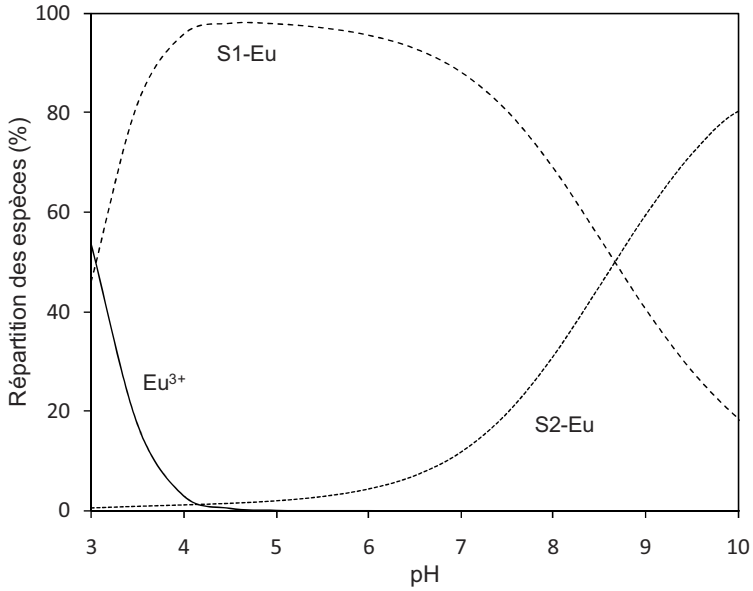

Figure 15. Spéciation d'une solution d'Eu(III) (10^{-6} mol/L) en présence de 10 mg/L d'AH en fonction du pH (*I* = 0.1 M).

La spéciation de l'europium en présence de matière organique a beaucoup été étudiée par SLRT, mais la plupart des auteurs ont étudié le système à un seul pH :

- pH 9 pour Moulin et al. (1999) ;
- pH 6.3 pour Tan et al. (2008) ;
- pH 6.5 pour Jain et al. (2009) ;
- pH 5 pour Brevet et al. (2009) et Reiller & Brevet (2010).

La Figure 16 présente le spectre SLRT de l'europium(III) en présence d'AH (trait noir) et d'AF (trait rouge pointillé) à pH 6.3 (Tan et al. 2008). Lorsque l'europium est complexé, la bande correspondant à la transition hypersensible $^5D_0 \rightarrow {}^7F_2$ devient plus importante que celle correspondant à la transition $^5D_0 \rightarrow {}^7F_1$.

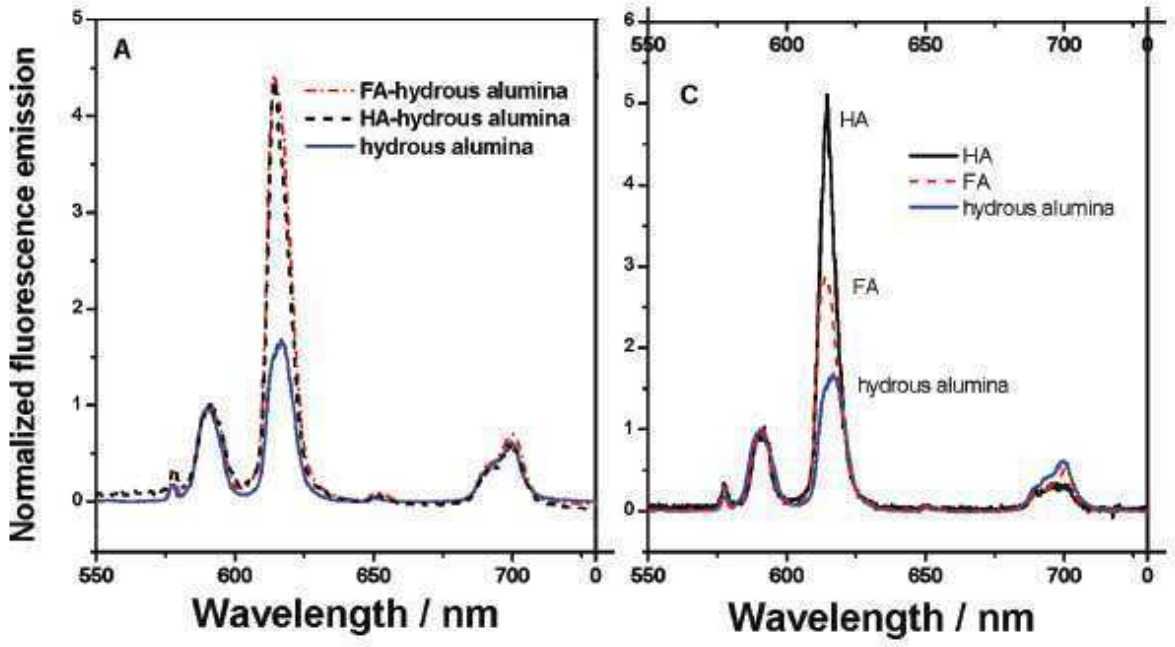

Figure 16. Spectre de luminescence de l'europium en présence d'alumine, d'acide humique ou fulvique ou dans un système ternaire à pH 6.3 (Tan et al. 2008).

Le spectre de luminescence de l'europium(III) est donc très différent en milieux aqueux non complexant et en présence de ligands humiques. La présence de SH a également un impact sur la décroissance de la luminescence de l'Eu(III). En effet, en présence de substances humiques, quelle que soit leur origine, la luminescence de Eu(III) présente une décroissance bi-exponentielle (Chung et al. 2005; Marang 2007; Brevet et al. 2009; Marang et al. 2009; Reiller and Brevet 2010). Le premier temps de décroissance τ_1 est toujours plus court que le temps de décroissance de l'ion aqueux Eu^{3+} – $\tau \approx 100\text{-}110$ µs (Horrocks and Sudnick 1979), cf. § 4.2.2 – et est généralement assimilé à un échange rapide d'énergie entre l'ion et les ~~groupes~~ fonctionnels organiques auxquels il est complexé. Cette décroissance rapide n'apparaît pas dans toutes les études, notamment du fait d'un trop grand pas de déplacement dans la porte de mesure utilisé par certains auteurs : lorsque le délai entre deux mesures est trop important, cette première composante peut ne pas être mise en évidence. Cette décroissance bi-exponentielle a également été observée pour les systèmes Tb(III)/AH (Kumke et al. 2005) et Cm(III)/AH (Panak et al. 1996; Morgenstern et al. 2000; Chung et al. 2005;

Freyer et al. 2009). La durée de la seconde décroissance τ_2 augmente avec le pH, traduisant un changement continu dans l'environnement de l'ion lors de la complexation avec l'AH (Morgenstern et al. 2000).

4.4 Interactions avec les surfaces minérales

L'adsorption de l'europium(III) a été étudiée sur de nombreux oxydes et hydroxydes métalliques

- Hématite (Fairhurst et al. 1995b; Sakuragi et al. 2004) ;
- Goethite (Fairhurst and Warwick 1998) ;
- Alumine (Rabung et al. 2000; Wang et al. 2006; Tan et al. 2008) ;
- Dioxyde de titane (Tan et al. 2009).

Les résultats de la littérature montrent une forte adsorption de l'Eu(III) sur ces surfaces en fonction du pH. L'adsorption augmente avec le pH, présentant un front de sorption, ou « pH-edge », compris entre 4 et 6 selon le type d'oxyde métallique et la concentration en europium(III) dans le système (cf. Figure 17). Certains auteurs ont en effet remarqué que le pH-edge augmente avec la concentration en Eu(III) : Rabung et al. (2000) sur γ-Al_2O_3, Tan et al. (2009) sur TiO_2.

L'influence du potentiel de surface sur la réaction de sorption a un faible impact sur les métaux de forte charge. Le pH-edge se situe à un pH < pH_{PZC} pour les oxydes d'aluminium et de fer. L'adsorption a donc lieu même lorsque la surface minérale est chargée positivement : il y a formation de complexes de sphère interne entre Eu(III) et les sites de surface. Dans l'intervalle des incertitudes expérimentales, les auteurs observent que la sorption est peu dépendante de la force ionique, ce qui confirme la formation de complexes de sphère interne stables. A pH ≤ 6, la forme prédominante de Eu(III) est le complexe aqueux $Eu(H_2O)_9^{3+}$ (peu de complexe carbonate ou d'hydrolyse, d'après Hummel et al. 2002) : seule la complexation de Eu^{3+} est observée.

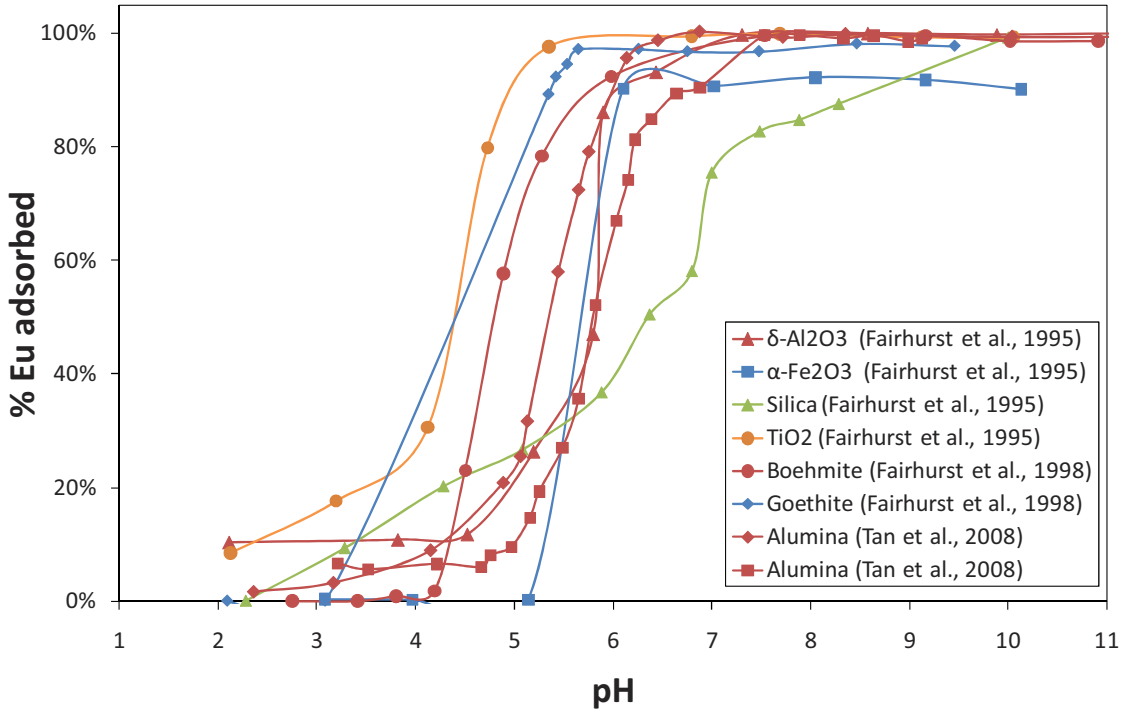

Figure 17. Influence du pH sur l'adsorption d'Eu(III) sur divers oxydes (Fairhurst et al. 1995b; Fairhurst and Warwick 1998; Tan et al. 2008). Les lignes ont été ajoutées pour faciliter la lecture.

Quelques travaux ont déjà porté sur l'adsorption de l'europium(III) sur des oxydes d'aluminium en utilisant la SLRT. Le spectre de luminescence de l'Eu(III) en présence d'alumine à pH 6,3 est représenté sur la Figure 16. A pH 6,3, Tan et al. (2008) ont trouvé un temps de décroissance de luminescence de l'europium(III) de 219 ± 5 µs, et un ratio $^7F_1/^7F_2$ égal à 0,51. Rabung et al. (2000) ont étudié un système Eu(III)/γ-Al_2O_3 à différents pH. Les résultats de leur étude SLRT sont reportés dans le Tableau 4.

Tableau 4. Résultats de l'étude SLRT d'un système Eu(III)/γ-Al_2O_3 en fonction du pH (Rabung et al. 2000)

pH	4	5	6	7	8
τ (µs)	114	105	183	239	235
$^7F_1/^7F_2$	2.4	1.6	0.9	0.4	0.3
$^7F_2/^7F_1$	0.4	0.6	1.1	2.5	3.3

Les résultats de ces deux études sont cohérents et montrent que lorsque le pH augmente, le temps de décroissance de la luminescence de Eu(III) augmente également. Au fur et à mesure de l'adsorption d'Eu(III) sur la surface et la formation de complexes de sphère interne, des molécules d'eau sont expulsées de la première sphère d'hydratation de l'ion (cf. § 4.2.2). L'évolution du ratio avec le pH montre une évolution de la symétrie de l'environnement de l'europium(III) avec la complexation.

5 Étude des systèmes ternaires

Dans le cas des systèmes ternaire métal/SH/surface minérale, il est difficile de comparer entre elles les données de la littérature, tant les composants étudiés sont variés, de même que leurs concentrations respectives (qui ne sont pas toujours représentatives de conditions environnementales). Cependant, certaines tendances se retrouvent pour différents systèmes.

Le protocole expérimental est souvent comparable, avec des expériences en flacons fermés dites « en batch » et l'analyse du système après un temps d'équilibre donné (généralement entre 24 et 72 heures). Si certaines études ont mis en évidence une influence de l'ordre d'ajout des composés dans le système sur la rétention d'ions trivalents à des temps courts (sur de la silice, Kar et al. 2011), celle-ci n'est plus vue lorsque le temps d'équilibre dépasse 3 jours (sur de la kaolinite ou de la silice, Takahashi et al. 1999; sur de l'alumine, Wang et al. 2006).

5.1 Influence des conditions de la solution

A l'échelle macroscopique, la présence d'acide humique modifie l'adsorption d'europium(III) sur les oxydes métalliques (Fairhurst et al. 1995b; Tan et al. 2008; Kaplan et al. 2010) ou les argiles (Samadfam et al. 1998). A faible pH, l'adsorption d'europium(III) augmente fortement en présence de SH, du fait de la sorption des molécules organiques qui complexent l'europium(III) et l'entraînent sur la surface. En fonction de la concentration en SH dans le système, à pH intermédiaire (entre 5 et 8), la quantité d'europium adsorbée peut diminuer du fait de la diminution de la sorption des SH (cf. Figure 18). Enfin, à pH élevé (pH > 8), en fonction du système, on peut observer une ré-augmentation de la sorption de l'europium(III) (Fairhurst et al. 1995b; Fairhurst et al. 1995a; Fairhurst and Warwick 1998) du fait de la compétition de Eu(III) entre les SH qui se désorbent et les sites de surface du minéral.

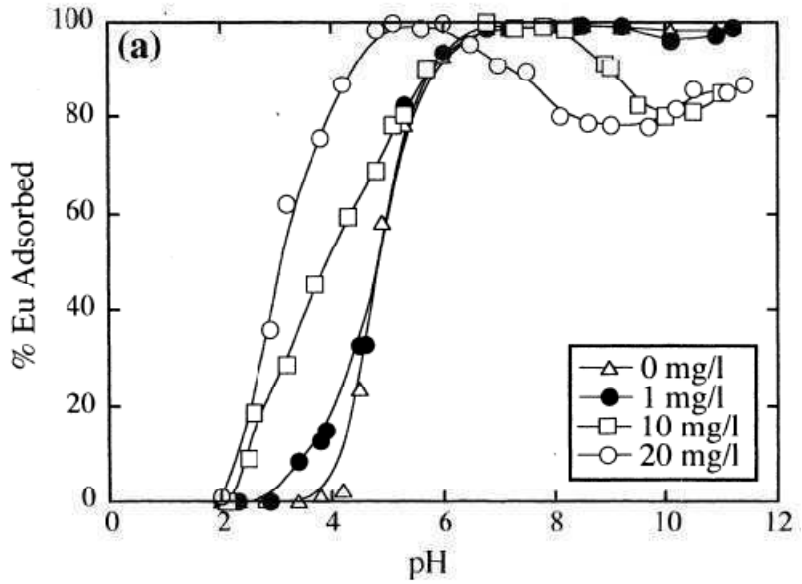

Figure 18. Influence de la concentration en AH (mg/l) sur la rétention d'Eu(III) sur de la boehmite (Fairhurst and Warwick 1998).

La force ionique semble également avoir une influence sur le comportement des métaux dans un système ternaire (Christl and Kretzschmar 2001; Sakuragi et al. 2004). Plus elle augmente, plus l'adsorption du métal (Cu(II), Eu(III), ou Am(III)) augmente, notamment du fait de l'augmentation de la quantité de SH adsorbée sur la surface.

D'un point de vue spectroscopique, Tan et al. (2008) ont montré une différence dans les spectres des systèmes binaire et ternaire, notamment le ratio d'asymétrie $^7F_2/^7F_1$ (cf. Figure 16). Ces auteurs n'ont pas mis en évidence la double décroissance de luminescence de l'europium(III), en raison d'un pas trop grand entre leurs mesures, et n'ont déterminé qu'un temps de décroissance global, différent entre les systèmes binaires et le système ternaire à pH 6,3. L'environnement de l'europium(III) semble différent dans les deux systèmes étudiés.

En revanche, dans le cas des études de systèmes ternaires, peu se sont intéressées à l'influence des ions multivalents sur l'adsorption des SH sur les surfaces (Boily and Fein 2000). Ces auteurs ont montré une augmentation de l'adsorption des AH sur de l'alumine avec la concentration en calcium. Afin d'interpréter les variations d'adsorption de l'ion étudié, il semble donc nécessaire de quantifier également les variations d'adsorption des SH.

5.2 Modélisation des interactions

En dépit du nombre d'études portant sur ces systèmes ternaires, leur modélisation pose toujours des problèmes. En effet, il n'y a pas d'additivité des systèmes binaires métal/surface et métal/SH, comme montré par Vermeer et al. (1999) pour un système Cd/PAHA/hématite ou Christl & Kretzschmar (2001) pour un système Cu/AF/hématite (cf. Figure 19).

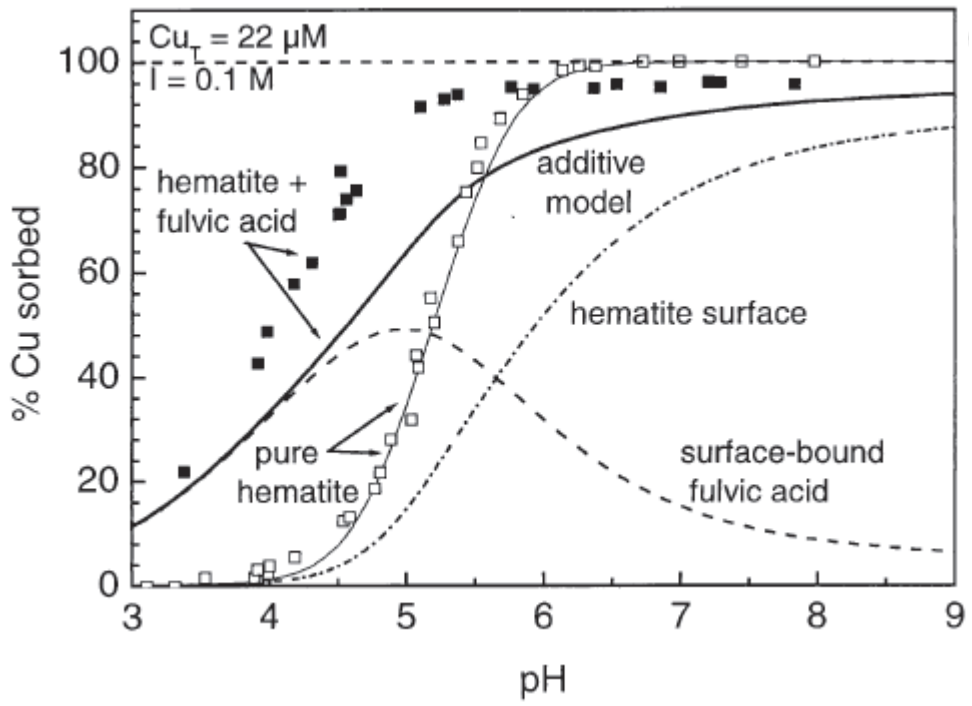

Figure 19. Comparaison entre les résultats expérimentaux (carrés noirs) et la somme des modèles binaires (ligne pleine) pour l'adsorption du cuivre sur de l'hématite en présence d'acide fulvique (Christl and Kretzschmar 2001).

Cette non-additivité linéaire est due aux interactions entre la matière organique naturelle et les surfaces minérales, qui modifient leurs propriétés de surface, d'aggrégation et de complexation vis-à-vis des métaux. Récemment, Weng et al. (2008a) ont proposé une stratégie de modélisation de l'adsorption du cuivre(II) sur de la goethite en présence d'acide fulvique à différents pH et concentrations en métal et AF en utilisant le modèle Ligand and Charge Distribution (LCD) qui décrit l'adsorption de SH sur des surfaces minérales (Filius et al. 2001; Weng et al. 2006b). Heidman et al. (2005) ont quant à eux utilisé un modèle linéaire additif (LAM) pour modéliser l'adsorption du cuivre(II) et du plomb(II) sur de la kaolinite en présence d'AF. Ces exemples de modélisation de répartition d'un métal concernent des systèmes ternaires comprenant des acides fulviques. Cependant, l'utilisation d'acides humiques apporte des difficultés supplémentaires à la modélisation. En effet, leur adsorption

est plus fortement dépendante de la force ionique que dans le cas des AF {Reiller, 2002 #149}(Weng et al. 2007), ce qui complique la description de ces systèmes dans une large gamme de paramètres. Weng et al (2009) sont cependant parvenus à une modélisation du système arséniate/AH,AF/goethite à différents pH, en utilisant le modèle LCD.

Kaplan et al. (2010) ont étudié un système Eu(III)/MON/sédiment (kaolinite, goethite, hématite) et ont essayé de le modéliser en définissant un compartiment supplémentaire correspondant à la matière organique adsorbée sur le solide. De cette manière, les auteurs ont utilisé des constantes de complexation différentes pour les deux compartiments de matière organique ainsi définis. Les résultats nécessitent des ajustements, mais les auteurs sont parvenus à décrire les tendances de comportement de l'europium en fonction de la concentration en matière organique à différents pH (3,9, 5,3 et 6,7).

Afin de modéliser un système ternaire, il semble donc nécessaire de prendre en compte de manière différente les deux compartiments organiques (en solution et à la surface), mais aussi les effets électrostatiques.

6 Objectifs de la thèse et présentation du manuscrit

L'objectif de ce travail de thèse est de contribuer à une meilleure description et compréhension des interactions existant dans un système ternaire Eu(III)/AH/Alumine, dans un contexte environnemental. L'alumine n'est pas très représentative des minéraux principaux des sols. Elle a cependant été choisie comme surface d'étude car ses sites de surfaces sont proches des sites aluminol des argiles, très répandus, et car elle permet une étude SLRT avec le solide en solution, de par sa couleur blanche, ce qui n'est pas le cas des oxydes de fer ou des argiles. Pour l'acide humique, le choix s'est porté sur un acide humique commercial Aldrich (AHA), qui peut être considéré comme un analogue de certains acides humiques naturels de sols ou de tourbe (Vermeer 1996, Chapitre 3). Pour étudier les interactions dans ce système ternaire, la répartition de l'europium(III) dans les différents compartiments du système a été étudiée par expériences en flacons fermés dites « en batch ». La répartition et le fractionnement de l'acide humique ont également été quantifiés. La spéciation de l'europium(III) a été étudiée par SLRT, qui permet une étude à l'état de trace.

L'objectif étant de décrire ce système dans un contexte naturel, l'influence de plusieurs conditions physico-chimiques de la solution a été étudiée – pH, force ionique, concentration en matière organique – tous ayant une influence sur le comportement du métal en solution. Le

rôle de la force ionique n'est pourtant pas souvent étudié car considéré comme secondaire. Il pourrait cependant être important dans le cas d'écosystèmes côtiers, ou dans le cas des stockages de déchets dans des dômes de sel, concernant les fluides à l'interface entre le colis et la géobiosphère. Dans chacun des cas, les systèmes binaires correspondant Eu(III)/AHA, Eu(III)/alumine et AHA/alumine ont été étudiés également.

Le principal problème vis-à-vis de la modélisation de ce système est dû au fractionnement de la matière organique lors de son adsorption sur les surfaces minérales. Afin de caractériser de fractionnement en terme de réactivité des AH et de modification de la protonation, il a fallu dans un premier temps mettre au point une méthode permettant d'étudier la réactivité des SH à concentration environnementale, mais aussi à la faible concentration résiduelle en AH après une expérience d'adsorption (**Chapitre 2**). De cette manière, il a été possible d'étudier et de quantifier l'influence des interactions AHA/α-Al_2O_3 sur la réactivité des fractions adsorbées et dissoutes d'AH (**Chapitre 3**). Les interactions entre Eu(III), AHA et α-Al_2O_3 ont été étudiées à différents pH, par expériences en batch (macroscopique) et SLRT (spectroscopique) (**Chapitre 4**), ainsi qu'à différentes forces ioniques et concentrations en AHA (**Chapitre 5**). Enfin, la spéciation de l'Eu(III) dans ce système ternaire a été décrite numériquement en utilisant les modèles NICA-Donnan, pour l'AHA, et CD-MUSIC, pour la description de la surface d'alumine (**Chapitre 6**). Les chapitres suivants ont été rédigés en anglais, sous la forme d'articles de revue. Deux d'entre eux ont été acceptés pour publication dans *Environmental Science & Technology*.

RÉFÉRENCES

Ali, M. A. and Dzombak D. A. (1996). "Competitive sorption of simple organic acids and sulfate on goethite." *Environmental Science & Technology* **30**(4): 1061-1071.

Avena, M. J. and Koopal L. K. (1998). "Desorption of humic acids from an iron oxide surface." *Environmental Science & Technology* **32**(17): 2572-2577.

Avena, M. J., Koopal L. K., et al. (1999). "Proton binding to humic acids: Electrostatic and intrinsic interactions." *Journal of Colloid and Interface Science* **217**(1): 37-48.

Baalousha, M. and Lead J. R. (2007). "Characterization of natural aquatic colloids (< 5 nm) by flow-field flow fractionation and atomic force microscopy." *Environmental Science & Technology* **41**(4): 1111-1117.

Benedetti, M. F., Milne C. J., et al. (1995). "Metal ion binding to humic substances: application of the Non-Ideal Competitive Adsorption Model." *Environmental Science & Technology* **29**: 446-457.

Benedetti, M. F., vanRiemsdik W. H., et al. (1996). "Humic substances considered as a heterogeneous donnan gel phase." *Environmental Science & Technology* **30**(6): 1805-1813.

Berthoud, T., Decambox P., et al. (1989). "Direct determination of traces of lanthanide ions in aqueous solutions by laser-induced time-resolved spectrofluorimetry." *Analytica Chimica Acta* **220**: 235-241.

Boily, J. F. and Fein J. B. (2000). "Proton binding to humic acids and sorption of Pb(II) and humic acid to the corundum surface." *Chemical Geology* **168**(3-4): 239-253.

Bouby, M., Manh T. N., et al. (2002). "Characterization of aquatic colloids by a combination of LIBD and ICP-MS following the size fractionation." *Radiochimica Acta* **90**(9-11): 727-732.

Brevet, J., Claret F., et al. (2009). "Spectral and temporal luminescent properties of Eu(III) in humic substance solutions from different origins." *Spectrochimica Acta Part a-Molecular and Biomolecular Spectroscopy* **74**(2): 446-453.

Bünzli, J.-C. G. (1989). Luminescent probes. *Lanthanides probe in life , chemical and earth sciences - Theory and practice*. J.-C. G. Bünzli and G. R. Choppin. Amsterdam, Elsevier.

Buleva, M. and Petkanchin I. (1999). "Interaction of humic substances with silica and alumina colloids: adsorption and stability - Electro-optical study." *Colloids and Surfaces a-Physicochemical and Engineering Aspects* **151**(1-2): 225-231.

Caceci, M. and Moulin V. (1991). Investigation of humic acid samples of different sources by photon correlation spectroscopy. *Humic substances in the aquatic and terrestrial environment: Proceedings of an International Symposium Linköping, Sweden, August 21–23, 1989.* B. Allard, H. Boren and A. Grimvall. Berlin, Springer. **33:** 97-104.

Caceci, M. S. (1985). "The interaction of Humic-Acid with Europium(III) - Complexation strength as a function of load and pH." *Radiochimica Acta* **39**(1): 51-56.

Chorover, J. and Amistadi M. K. (2001). "Reaction of forest floor organic matter at goethite, birnessite and smectite surfaces." *Geochimica Et Cosmochimica Acta* **65**(1): 95-109.

Christl, I. and Kretzschmar R. (2001). "Interaction of copper and fulvic acid at the hematite-water interface." *Geochimica Et Cosmochimica Acta* **65**(20): 3435-3442.

Chung, K. H., Lee W., et al. (2005). "Comparison of synchronous and laser-induced fluorescence spectroscopy applied to the Eu(III)-fulvate complexation." *Talanta* **65**(2): 389-395.

Claret, F., Schafer T., et al. (2008). "Fractionation of Suwannee River fulvic acid and Aldrich humic acid on alpha-Al_2O_3: Spectroscopic evidence." *Environmental Science & Technology* **42**(23): 8809-8815.

Conte, P. and Piccolo A. (1999). "Conformational arrangement of dissolved humic substances. Influence of solution composition on association of humic molecules." *Environmental Science & Technology* **33**(10): 1682-1690.

Crançon, P. (2001). Migration de l'uranium dans un podzol. Le rôle des colloïdes dans la zone non saturée et la nappe : application aux Landes de Gascogne. Grenoble, France, Université de Grenoble 1, Saint-Martin-d'Hères, France. http://inisdb.iaea.org/inis/php/download.php?s=p&rn=32062144. **PhD:** 284.

Crançon, P., Pili E., et al. (2010). "Uranium facilitated transport by water-dispersible colloids in field and soil columns." *Science of the Total Environment* **408**(9): 2118.

Crançon, P. and van der Lee J. (2003). "Speciation and mobility of uranium(VI) in humic-containing soils." *Radiochimica Acta* **91**(11): 673-679.

d'Orlyé, F. and Reiller P. E. (soumise). "Potential of capillary electrophoresis for estimation of humic substances physico-chemical properties."

de Levie, R. (2005). *Advanced Excel for Scientific Data Analysis.*, Oxford University Press.

Dobbs, J. C., Susetyo W., et al. (1989a). "Characterization of metal-binding sites in fulvic-acids by lanthanide ion probe spectroscopy." *Analytical Chemistry* **61**(5): 483-488.

Dobbs, J. C., Susetyo W., et al. (1989b). "A novel-approach to metal-humic complexation studies by lanthanide ion probe spectroscopy." *International Journal of Environmental Analytical Chemistry* **37**(1): 1-17.

Dryer, D. J., Korshin G. V., et al. (2008). "In situ examination of the protonation behavior of fulvic acids using differential absorbance spectroscopy." *Environmental Science & Technology* **42**(17): 6644-6649.

Fairhurst, A. J. and Warwick P. (1998). "The influence of humic acid on europium-mineral interactions." *Colloids and Surfaces a-Physicochemical and Engineering Aspects* **145**(1-3): 229-234.

Fairhurst, A. J., Warwick P., et al. (1995a). "The effect of pH on Europium-mineral interactions in the presence of humic acid." *Radiochimica Acta* **69**(2): 103-111.

Fairhurst, A. J., Warwick P., et al. (1995b). "The influence of humic acid on the adsorption of Europium onto inorganic colloids as a function of pH." *Colloids and Surfaces a-Physicochemical and Engineering Aspects* **99**(2-3): 187-199.

Filius, J. D., Lumsdon D. G., et al. (2000). "Adsorption of fulvic acid on goethite." *Geochimica Et Cosmochimica Acta* **64**(1): 51-60.

Filius, J. D., Meeussen J. C. L., et al. (2001). "Modeling the binding of benzenecarboxylates by goethite: The ligand and charge distribution model." *Journal of Colloid and Interface Science* **244**(1): 31-42.

Freyer, M., Walther C., et al. (2009). "Formation of Cm humate complexes in aqueous solution at pH(c) 3 to 5.5: The role of fast interchange." *Radiochimica Acta* **97**(10): 547-558.

Ghosh, S., Mashayekhi H., et al. (2010). "Colloidal Stability of Al2O3 Nanoparticles as Affected by Coating of Structurally Different Humic Acids." *Langmuir* **26**(2): 873-879.

Ghosh, S., Wang Z. Y., et al. (2009). "Sorption and Fractionation of a Peat Derived Humic Acid by Kaolinite, Montmorillonite, and Goethite." *Pedosphere* **19**(1): 21-30.

Gu, B. H., Mehlhorn T. L., et al. (1996). "Competitive adsorption, displacement, and transport of organic matter on iron oxide .1. Competitive adsorption." *Geochimica Et Cosmochimica Acta* **60**(11): 1943-1950.

Gu, B. H., Schmitt J., et al. (1995). "Adsorption and desorption of different organic-matter fractions on iron-oxide." *Geochimica Et Cosmochimica Acta* **59**(2): 219-229.

Gu, B. H., Schmitt J., et al. (1994). "Adsorption and desorption of natural organic-matter on iron-oxide - Mechanisms and models." *Environmental Science & Technology* **28**(1): 38-46.

Heidmann, I., Christl I., et al. (2005). "Sorption of Cu and Pb to kaolinite-fulvic acid colloids: Assessment of sorbent interactions." *Geochimica Et Cosmochimica Acta* **69**(7): 1675-1686.

Hiemstra, T. and van Riemsdijk W. H. (1996). "A surface structural approach to ion adsorption: The charge distribution (CD) model." *Journal of Colloid and Interface Science* **179**(2): 488-508.

Hiemstra, T., Yong H., et al. (1999). "Interfacial charging phenomena of aluminum (hydr)oxides." *Langmuir* **15**(18): 5942-5955.

Horrocks, W. D., Jr. and Sudnick D. R. (1979). "Lanthanide ion probes of structure in biology. Laser-induced luminescence decay constants provide a direct measure of the number of metal-coordinated water-molecules." *Journal of the American Chemical Society* **101**(2): 334-340.

Hummel, W., Berner U., et al. (2002). "Nagra/PSI chemical thermodynamic data base 01/01." *Radiochimica Acta* **90**(9-11): 805-813.

Hur, J. and Schlautman M. A. (2003). "Molecular weight fractionation of humic substances by adsorption onto minerals." *Journal of Colloid and Interface Science* **264**(2): 313-321.

Hur, J. and Schlautman M. A. (2004). "Effects of pH and phosphate on the adsorptive fractionation of purified Aldrich humic acid on kaolinite and hematite." *Journal of Colloid and Interface Science* **277**(2): 264-270.

IUPAC Compendium of Chemical Terminology, 2nd ed. (the "Gold Book"). Compiled by A. D. McNaught and A. Wilkinson. Blackwell Scientific Publications, Oxford (1997). XML on-line corrected version: http://goldbook.iupac.org (2006-) created by M. Nic, J. Jirat, B. Kosata; updates compiled by A. Jenkins. ISBN 0-9678550-9-8.

Jain, A., Yadav K., et al. (2009). "Spectroscopic investigation on europium complexation with humic acid and its model compounds." *Spectrochimica Acta Part a-Molecular and Biomolecular Spectroscopy* **72**(5): 1122-1126.

Jorgensen, C. K. and Judd B. R. (1964). "Hypersensitive pseudoquadrupole transitions in lanthanides." *Molecular Physics* **8**(3): 281-290.

Judd, B. R. (1962). "Optical absorption intensities of rare-earth ions." *Physical Review* **127**(3): 750-761.

Kang, S. H. and Xing B. S. (2008). "Humic acid fractionation upon sequential adsorption onto goethite." *Langmuir* **24**(6): 2525-2531.

Kaplan, D. I., Serkiz S. M., et al. (2010). "Europium sorption to sediments in the presence of natural organic matter: A laboratory and modeling study." *Applied Geochemistry* **25**(2): 224-232.

Kar, A. S., Kumar S., et al. (2011). "Sorption of curium by silica colloids: Effect of humic acid." *Journal of Hazardous Materials* **186**(2-3): 1961-1965.

Keizer, M. G. and van Riemsdijk W. H. (1994). A computer program for the calculation of chemical speciation and transport in soil-water systems (ECOSAT 4.7). Agricultural University of Wageningen. Wageningen, Agricultural University of Wageningen.

Kimura, T. and Choppin G. R. (1994). "Luminescence study on determination of the hydration number of Cm(III)." *Journal of Alloys and Compounds* **213**: 313-317.

Kimura, T., Kato Y., et al. (1998). "Comparative study on the hydration states of Cm(III) and Eu(III) in solution and in cation exchange resin." *Journal of Alloys and Compounds*: 719-722.

Kinniburgh, D. G., Milne C. J., et al. (1996). "Metal ion binding by humic acid: Application of the NICA-Donnan model." *Environmental Science & Technology* **30**(5): 1687-1698.

Kumke, M. U., Eidner S., et al. (2005). "Fluorescence quenching and luminescence sensitization in complexes of Tb3+ and Eu3+ with humic substances." *Environmental Science & Technology* **39**(24): 9528-9533.

Lead, J. R., Hamilton-Taylor J., et al. (1998). "Europium binding by fulvic acids." *Analytica Chimica Acta* **369**(1-2): 171-180.

Manning, T. J. and Bennett D. M. (2000). "Aggregation studies of humic acid using multiangle laser light scattering." *The Science of the Total Environment* **257**: 171-176.

Marang, L. (2007). Influence de la matière organique naturelle sur la spéciation des radionucléides en contexte géochimique. Géochimie Fondamentale et Appliquée. Paris, France, Université Denis Diderot (Paris VII), and CEA-R-6187 Report. http://tel.archives-ouvertes.fr/docs/00/41/87/23/PDF/These_laura_marang_final.pdf.: 178.

Marang, L., Eidner S., et al. (2009). "Spectroscopic characterization of the competitive binding of Eu(III), Ca(II), and Cu(II) to a sedimentary originated humic acid." *Chemical Geology* **264**(1-4): 154-161.

Marang, L., Reiller P. E., et al. (2008). "Combining spectroscopic and potentiometric approaches to characterize competitive binding to humic substances." *Environmental Science & Technology* **42**(14): 5094-5098.

Marmodée, B., de Klerk J. S., et al. (2009). "High-resolution steady-state and time-resolved luminescence studies on the complexes of Eu(III) with aromatic or aliphatic carboxylic acids." *Analytica Chimica Acta* **652**(1-2): 285-294.

McCarthy, J. F., Sanford W. E., et al. (1998). "Lanthanide field tracers demonstrate enhanced transport of transuranic radionuclides by natural organic matter." *Environmental Science & Technology* **32**(24): 3901-3906.

Meier, M., Namjesnik-Dejanovic K., et al. (1999). "Fractionation of aquatic natural organic matter upon sorption to goethite and kaolinite." *Chemical Geology* **157**(3-4): 275-284.

Milne, C. J., Kinniburgh D. G., et al. (2001). "Generic NICA-Donnan model parameters for proton binding by humic substances." *Environmental Science & Technology* **35**(10): 2049-2059.

Milne, C. J., Kinniburgh D. G., et al. (2003). "Generic NICA-Donnan model parameters for metal-ion binding by humic substances." *Environmental Science & Technology* **37**(5): 958-971.

Morgenstern, M., Klenze R., et al. (2000). "The formation of mixed-hydroxo complexes of Cm(III) and Am(III) with humic acid in the neutral pH range." *Radiochimica Acta* **88**(1): 7-16.

Moulin, C., Wei J., et al. (1999). "Europium complexes investigations in natural waters by time-resolved laser-induced fluorescence." *Analytica Chimica Acta* **396**(2-3): 253-261.

Moulin, V., Reiller P., et al. (2001). "Direct characterization of iodine covalently bound to fulvic acids by electrospray mass spectrometry." *Rapid Communications in Mass Spectrometry* **15**(24): 2488-2496.

Naber, A., Plaschke M., et al. (2006). "Scanning transmission X-ray and laser scanning luminescence microscopy of the carboxyl group and Eu(III) distribution in humic acid aggregates." *Journal of Electron Spectroscopy and Related Phenomena* **153**(3): 71-74.

Ochs, M., Cosovic B., et al. (1994). "Coordinative and hydrophobic interaction of humic substances with hydrophilic Al2O3 and hydrophobic mercury surfaces." *Geochimica Et Cosmochimica Acta* **58**(2): 639-650.

Ofelt, G. S. (1962). "Intensities of crystal spectra of rare-earth ions." *Journal of Chemical Physics* **37**(3): 511-&.

Österberg, R., Mortensen K., et al. (1995). "Direct observation of humic-acid clusters, a nonequilibrium system with a fractal structure." *Naturwissenschaften* **82**(3): 137-139.

Panak, P., Klenze R., et al. (1996). "A study of ternary complexes of Cm(III) with humic acid and hydroxide or carbonate in neutral pH range by time-resolved laser fluorescence spectroscopy." *Radiochimica Acta* **74**: 141-146.

Pauling, L. (1929). "The principles determining the structure of complex ionic crystals." *Journal of the American Chemical Society* **51**: 1010-1026.

Piccolo, A. (2001). "The supramolecular structure of humic substances." *Soil Science* **166**(11): 810-832.

Pinheiro, J. P., Mota A. M., et al. (1996). "Dynamic properties of humic matter by dynamic light scattering and voltammetry." *Analytica Chimica Acta* **329**(1-2): 15-24.

Plancque, G., Moulin V., et al. (2003). "Europium speciation by time-resolved laser-induced fluorescence." *Analytica Chimica Acta* **478**(1): 11-22.

Plaschke, M., Rothe J., et al. (2009). STXM and LSLM investigation of Eu(III) induced humic acid colloid aggregation. *9th International Conference on X-Ray Microscopy*. C. David, F. Nolting, C. Quitmann, M. Stampanoni and F. Pfeiffer. Bristol, Iop Publishing Ltd. **186**.

Rabung, T., Stumpf T., et al. (2000). "Sorption of Am(III) and Eu(III) onto gamma-alumina: experiment and modelling." *Radiochimica Acta* **88**: 711-716.

Ranville, J. F. and Schmiermund R. L. (1999). General Aspects of Aquatic Colloids in Environmental Geochemistry. *The Environmental Geochemistry of Mineral Deposits: Part A: Processes, techniques, and health issues*, Society of Economic Geologists. **Reviews in Economic Geology, Vol 6A.:** 183-199.

Reid, P. M., Wilkinson A. E., et al. (1990). "Determination of molecular weights of humic substances by analytical (UV scanning) ultracentrifugation." *Geochimica et Cosmochimica Acta* **54**: 131-138.

Reid, P. M., Wilkinson A. E., et al. (1991). "Aggregation of humic substances in aqueous media as determined by light-scattering methods." *Journal of Soil Science* **42**(2): 259-270.

Reiller, P. (2010). Analyse critique des données de complexation des lanthanides et actinides par la matière organique naturelle : Cas des substances humiques. Gif-sur-Yvette, France, CEA**:** 184.

Reiller, P., Amekraz B., et al. (2006). "Sorption of Aldrich humic acid onto hematite: Insights into fractionation phenomena by electrospray ionization with quadrupole time-of-flight mass spectrometry." *Environmental Science & Technology* **40**(7): 2235-2241.

Reiller, P., Moulin V., et al. (2002). "Retention behaviour of humic substances onto mineral surfaces and consequences upon thorium (IV) mobility: case of iron oxides." *Applied Geochemistry* **17**(12): 1551-1562.

Reiller, P. E. and Brevet J. (2010). "Bi-exponential decay of Eu(III) complexed by Suwannee River humic substances: Spectroscopic evidence of two different excited species." *Spectrochimica Acta Part a-Molecular and Biomolecular Spectroscopy* **75**(2): 629-636.

Reiller, P. E., Testard F., et al. (en écriture). "Aggregation Properties of Concentrated Humic Substances by Atomic Force Microscopy and Small Angle Neutron Scattering." *Langmuir*.

Rice, J. A. and Maccarthy P. (1991). "Statistical evaluation of the elemental composition of humic substances." *Organic Geochemistry* **17**(5): 635-648.

Rice, J. A., Tombacz E., et al. (1999). "Applications of light and X-ray scattering to characterize the fractal properties of soil organic matter." *Geoderma* **88**(3-4): 251-264.

Saito, T., Koopal L. K., et al. (2004). "Adsorption of humic acid on goethite: Isotherms, charge adjustments, and potential profiles." *Langmuir* **20**(3): 689-700.

Saito, T., Nagasaki S., et al. (2005). "Electrostatic interaction models for ion binding to humic substances." *Colloids and Surfaces a-Physicochemical and Engineering Aspects* **265**(1-3): 104-113.

Sakuragi, T., Sato S., et al. (2004). "Am(III) and Eu(III) uptake on hematite in the presence of humic acid." *Radiochimica Acta* **92**(9-11): 697-702.

Samadfam, M., Sato S., et al. (1998). "Effects of humic acid on the sorption of Eu(III) onto kaolinite." *Radiochimica Acta* **82**: 361-365.

Santschi, P. H., Roberts K. A., et al. (2002). "Organic nature of colloidal actinides transported in surface water environments." *Environmental Science & Technology* **36**(17): 3711-3719.

Schlautman, M. A. and Morgan J. J. (1994). "Adsorption of aquatic humic substances on colloidal-size aluminum-oxide particles - Influence of solution chemistry." *Geochimica Et Cosmochimica Acta* **58**(20): 4293-4303.

Simpson, A. J., Kingery W. L., et al. (2002). "Molecular structures and associations of humic substances in the terrestrial environment." *Naturwissenschaften* **89**(2): 84-88.

Stumm, W. and Morgan J. J. (1996). *Aquatic Chemistry - Chemical Equilibria and Rates in Natural Waters, 3rd Edition*, John Wiley & Sons, Inc.

Supkowski, R. M. and Horrocks W. D. (2002). "On the determination of the number of water molecules, q, coordinated to europium(III) ions in solution from luminescence decay lifetimes." *Inorganica Chimica Acta* **340**: 44-48.

Suteerapataranon, S., Bouby M., et al. (2006). "Interaction of trace elements in acid mine drainage solution with humic acid." *Water Research* **40**(10): 2044-2054.

Takahashi, Y., Minai Y., et al. (1999). "Comparison of adsorption behavior of multiple inorganic ions on kaolinite and silica in the presence of humic acid using the multitracer technique." *Geochimica Et Cosmochimica Acta* **63**(6): 815-836.

Takahashi, Y., Tada A., et al. (2000). "Formation of Outer- and Inner-Sphere Complexes of Lanthanide Elements at Montmorillonite-Water Interface." *Chemistry Letters*(6): 700-701.

Tan, X. L., Fang M., et al. (2009). "Adsorption of Eu(III) onto TiO2: Effect of pH, concentration, ionic strength and soil fulvic acid." *Journal of Hazardous Materials* **168**(1): 458-465.

Tan, X. L., Wang X. K., et al. (2008). "Sorption of Eu(III) on humic acid or fulvic acid bound to hydrous alumina studied by SEM-EDS, XPS, TRLFS, and batch techniques." *Environmental Science & Technology* **42**(17): 6532-6537.

These, A., Winkler M., et al. (2004). "Determination of molecular formulas and structural regularities of low molecular weight fulvic acids by size-exclusion chromatography with electrospray ionization quadrupole time-of-flight mass spectrometry." *Rapid Communications in Mass Spectrometry* **18**(16): 1777-1786.

Thurman, E. (1985). *Organic Chemistry of Natural Waters*. The Hague.

Thurman, E. M., Wershaw R. L., et al. (1982). "Molecular size of aquatic humic substances." *Organic Geochemistry* **4**(1): 27-35.

Tipping, E. (2002). *Cation binding by humic substances*. Cambridge, U.K., Cambridge University Press.

Tombacz, E., Dobos A., et al. (2000). "Effect of pH and ionic strength on the interaction of humic acid with aluminium oxide." *Colloid and Polymer Science* **278**(4): 337-345.

Vekshin, N. L. (1999). "Screening hypochromism in molecular aggregates and biopolymers." *Journal of Biological Physics* **25**(4): 339-354.

Vermeer, A. W. P. (1996). Interaction between humic acid and hematite and their effects upon metal speciation. Wageningen, The Netherlands, Landbouwuniversiteit Wageningen**:** 199.

Vermeer, A. W. P., McCulloch J. K., et al. (1999). "Metal ion adsorption to complexes of humic acid and metal oxides: Deviations from the additivity rule." *Environmental Science & Technology* **33**(21): 3892-3897.

Wang, X., Xu D., et al. (2006). "Sorption and complexation of Eu(III) on alumina: Effects of pH, Ionic strength, humic acid and chelating resin on kinetic dissociation study." *Applied Radiation and Isotopes* **64**(4): 414-421.

Weerasooriya, R., Aluthpatabendi D., et al. (2001). "Charge distribution multi-site complexation (CD-MUSIC) modeling of Pb(II) adsorption on gibbsite." *Colloids and Surfaces a-Physicochemical and Engineering Aspects* **189**(1-3): 131-144.

Weng, L. P., van Riemsdijk W. H., et al. (2007). "Adsorption of humic acids onto goethite: Effects of molar mass, pH and ionic strength." *Journal of Colloid and Interface Science* **314**(1): 107-118.

Weng, L. P., van Riemsdijk W. H., et al. (2008a). "Cu2+ and Ca2+ adsorption to goethite in the presence of fulvic acids." *Geochimica Et Cosmochimica Acta* **72**(24): 5857-5870.

Weng, L. P., van Riemsdijk W. H., et al. (2008b). "Humic nanoparticles at the oxide-water interface: Interactions with phosphate oon adsorption." *Environmental Science & Technology* **42**(23): 8747-8752.

Weng, L. P., van Riemsdijk W. H., et al. (2009). "Effects of fulvic and humic acids on arsenate adsorption to goethite: experiments and modeling." *Environmental Science & Technology* **43**(19): 7198-204.

Weng, L. P., Van Riemsdijk W. H., et al. (2006a). "Adsorption of humic substances on goethite: Comparison between humic acids and fulvic acids." *Environmental Science & Technology* **40**(24): 7494-7500.

Weng, L. P., van Riemsdijk W. H., et al. (2006b). "Ligand and Charge Distribution (LCD) model for the description of fulvic acid adsorption to goethite." *Journal of Colloid and Interface Science* **302**(2): 442-457.

Wershaw, R. L. (1993). "Model for humus." *Environmental Science & Technology* **27**(5): 814-816.

Wershaw, R. L. (1999). "Molecular aggregation of humic substances." *Soil Science* **164**(11): 803-813.

Zhou, Q. H., Maurice P. A., et al. (2001). "Size fractionation upon adsorption of fulvic acid on goethite: Equilibrium and kinetic studies." *Geochimica Et Cosmochimica Acta* **65**(5): 803-812.

CHAPITRE 2

USING SPECTROPHOTOMETRIC TITRATIONS TO CHARACTERIZE HUMIC ACID REACTIVITY AT ENVIRONMENTAL CONCENTRATIONS

Noémie Janot[1,2], Pascal E. Reiller[2], Gregory V. Korshin[3], Marc F. Benedetti[1]

[1] Laboratoire de Géochimie des Eaux, Université Paris Diderot, IPGP, UMR CNRS 7154, Case Postale 7052, 75025 Paris, Cedex 13, France.

[2] CEA Saclay, CEA/DEN/DANS/DPC/SECR, Laboratoire de Spéciation des Radionucléides et des Molécules, Bâtiment 391 PC 33, F-91191 Gif-sur-Yvette CEDEX, France.

[3] Department of Civil and Environmental Engineering, University of Washington, Seattle, Washington 98195-2700, United States.

Environmental Science & Technology **2010,** *44*, (17), 6782-6788.

RÉSUMÉ

La réactivité de la matière organique dissoute est généralement caractérisée par titrages potentiométriques. Cependant, du fait de la sensibilité des électrodes pH, cette méthode nécessite l'utilisation de solutions concentrées en matière organique (>1 g/L), soit des conditions non représentatives de celles des eaux naturelles (de 0.1 à 100 mg/L). Afin d'obtenir des données de protonation de matière organique à des concentrations plus proches des valeurs environnementales, les titrages spectrophotométriques (Dryer *et al.*, Environ. Sci. Technol., 42, 6644, 2008) semblent une alternative intéressante aux titrages potentiométriques traditionnels.

Des titrages spectrophotométriques basés sur les spectres UV-Visible de solutions diluées d'acide humique Aldrich purifié (5 mg_{DOC}/L) ont été effectués. Après calcul des variations d'absorbance différentielle en fonction du pH, les changements de réactivité des groupes fonctionnels de l'acide humique vis-à-vis des protons ont été estimés. L'influence de la force ionique a également été étudiée. Après correction électrostatique des données spectrophotométriques, une corrélation linéaire est obtenue entre les données spectrophotométriques et potentiométriques, corrélation valable pour cet échantillon, dans la gamme de force ionique étudiée dans cette étude. Cette relation opérationnelle peut être utilisée comme une fonction de transfert entre les deux propriétés. Les titrages spectrophotométriques sont alors utilisés pour déterminer les variations de protonation de l'acide humique Aldrich après adsorption sur un oxyde d'aluminium α-Al_2O_3.

ABSTRACT

Potentiometric titration is a common method to characterize dissolved organic matter (DOM) reactivity. Because of the sensitivity of pH electrodes, it is necessary to work with very high DOM (>1 g/L) concentrations that are unrealistic compared to those found in natural waters (0.1 to 100 mg/L). To obtain proton binding data for concentrations closer to environmental values, spectroscopic titration methodology is a viable alternative to traditional potentiometric titrations. Spectrophotometric titrations and UV-visible spectra of a diluted solution of purified Aldrich humic acid (5 mg_{DOC}/L) are used to estimate changes in proton binding moieties as function of pH and ionic strength after calculation of differential absorbance spectra variations. After electrostatic correction of spectrophotometric data, there is a linear operational correlation between spectrophotometric and potentiometric data which can be used as a transfer function between the two properties. Spectrophotometric titrations are then used to determine the changes of humic acid protonation after adsorption onto α-alumina.

1 Introduction

Speciation and migration of metals in the environment are partly controlled by their interactions with natural organic matter (NOM) and minerals in soils (McCarthy et al. 1998; McCarthy et al. 1998). In aquatic systems, whether an organic molecule partitions to mineral surfaces or remains dissolved determines in large part its potential transport and susceptibility to degradation (Aufdenkampe et al. 2001). For instance, in major rivers of the world 90% of transported organic matter is either adsorbed to fine minerals or remains dissolved (Meybeck 1982; Keil et al. 1997). A better description of ternary metal/NOM/surface systems is needed to improve the understanding of the behavior of metals.

Because of its heterogeneous nature, the composition and chemical properties of NOM are modified during adsorption onto mineral oxides (Gu et al. 1994; Hur and Schlautman 2003; Kaiser 2003; Hur and Schlautman 2004; Saito et al. 2004; Reiller et al. 2006; Claret et al. 2008). Previous investigations (Davis and Gloor 1981; Day et al. 1994) suggest that the NOM fractions of higher molecular weight, greater aromatic and carboxyl functional groups content, and more hydrophobicity show preferential adsorption onto mineral oxides. This leads to modeling difficulties of the ternary systems (Robertson and Leckie 1994; Vermeer et al. 1999). A better knowledge of NOM binding moieties modifications after partitioning on mineral surfaces is necessary to describe the behavior of metals in ternary systems.

Humic substances (HS), mainly composed of humic and fulvic acids, are a prominent part of NOM, and are often used as surrogates of NOM. One of the most accurate ways to quantify HS functional groups is potentiometric titration, generally performed at a high concentration, *i.e.*, c > 500 mg_{HA}/L, to obtain signals significantly different from those of background electrolyte titrations. These solution conditions are often unrealistic when compared to concentrations of dissolved organic carbon (DOC) in natural waters, *i.e.*, 0.1 to 50 mg_{DOC}/L, and much greater than those of HS in the supernatant of NOM adsorption experiments (Gu et al. 1994; Hur and Schlautman 2003; Kaiser 2003; Hur and Schlautman 2004; Saito et al. 2004; Reiller et al. 2006; Claret et al. 2008). It is necessary to consider an alternative technique to obtain proton binding data of NOM under realistic environmental concentrations.

HS solutions are colored and absorb UV and visible light. UV-Visible spectra of HS solutions, even though they tend to be rather featureless (MacCarthy and Rice 1985), may help to characterize HS sorption-fractionation processes (Korshin et al. 1997; Claret et al. 2008). Subtle changes in HS spectra induced by varying physico-chemical conditions have been used in differential absorbance spectroscopy to characterize HS (Ghosh and Schnitzer

1979; Korshin et al. 1999), and to interpret titration data of fulvic acids in dilute solution, *e.g.*, 5 mg_{DOC}/L (Dryer et al. 2008). These spectrophotometric titrations allow the examination of the evolution of absorbance spectra with changes in pH. HS light-absorbing functional groups, or chromophores, are deemed to typically contain conjugated double bonds and aromatic rings. The deprotonation of chromophores at increasing pH modifies the chromophores' absorbance spectra and/or forms new absorbing centers, which leads to a progressive modification of their absorbance properties. In contrast, potentiometric titrations determine the development of the sample charge within the pH range. So far, no attempt has been made to directly link the evolution of the NOM absorbance signal to the change in charge with changes in pH.

The aim of this study is to investigate the possible link between these two phenomena, even an operational one. The functional groups determined by potentiometry are composed of, bound to, or in close vicinity of the HS molecules chromophores. It seemed then possible to find a transfer function between variations of sample charge and solution absorbance. Previous studies have pointed to the importance of HS conformations that are affected by ionic strength on spectroscopic measurements (Conte and Piccolo 1999; Del Vecchio and Blough 2004). Variations of molar extinction coefficients and the chromism effect (Vekshin 1987) depend both on chemical parameters of the solution and the HS studied. These variations must be considered when relating potentiometric and spectrophotometric measurements.

Hereafter, spectrophotometric titrations at different ionic strengths were used to examine the deprotonation of purified Aldrich humic acid. The results were compared with those obtained from potentiometric titrations, in order to validate the spectroscopic method to characterize humic acid reactivity in solutions under environmental conditions and to determine a relationship between results of both methods for this humic acid. A spectrophotometric titration of a supernatant from a HS sorption experiment on α-alumina was also performed under environmentally realistic conditions to test the methodology and to probe the variation in acido-basic properties.

2 Materials and methods

2.1 Preparation of samples

Commercial Aldrich humic acid was purified (PAHA) according to Kim et al. (1990). Stock suspension at 2.5 g_{DOC}/L was prepared by diluting PAHA in NaOH (pH around 10) to completely dissolve the sample. In this work, concentrations of PAHA solutions, noted in g/L, always correspond to g_{DOC}/L. Alumina (α-Al_2O_3) was purchased from Interchim (pure 99.99%, size fraction 200–500 nm). The solid was washed thrice with carbonate-free NaOH and thrice with Millipore water before drying and storage at room temperature under N_2 atmosphere according to Alliot et al. (2005).

2.2 Potentiometric titrations

All titrations were performed using a computer-controlled system under N_2 atmosphere, in a thermostatted vessel (25 °C) equipped with a magnetic stirrer, at a HA concentration equal to 0.5 g/L. Ionic strength (I) was fixed using $NaClO_4$ (0.01, 0.1, and 0.5 mol/L). The quoted ionic strengths are the initial values before the addition of any titrant. In data analyses, actual I was calculated for every data point, accounting for both background electrolyte ions and free H^+ and OH^-. The pH values of the solutions were controlled during titrations by addition of 0.1 mol/L $HClO_4$ and NaOH solutions. Base titrant (titrisol for 0.1 mol/L solution) was prepared with degassed Millipore water. The pH values were recorded with two pH Metrohm 6.0133.100 glass electrodes and a single Metrohm 6.0733.100 reference electrode. The reference electrode was connected to the reaction vessel via an electrolyte bridge filled with NaCl at the background electrolyte concentration to prevent $KClO_4$ precipitation in the system. The pH electrodes were calibrated by performing a blank titration of the background electrolyte prior to the sample titration. The aqueous suspension was purged with N_2 at pH = 3 for 4 h. The suspension was then titrated by adding small volumes of titrant, and pH was recorded as a function of the titrant volume added to the suspension. After each addition, a drift criterion for pH was used (ΔmV/min < 0.05) and a maximum time of 15 min was set for acquiring each data point. A similar procedure was followed for the blank solution titration. Three forward and backward titrations were performed to eliminate the hysteresis effect (Milne et al. 1995).

2.3 Absorbance measurements

2.3.1 Absorbance titrations

After potentiometric titrations, solutions were diluted in background electrolyte to obtain 100 ml of solution at a concentration of 5 mg/L in a thermostated vessel at 25 °C. After acid addition (pH 3), the solution was N_2-purged for 1 h. The pH was increased by addition of NaOH at 0.01 or 0.1 mol/L.

Absorbance spectra were recorded in a 5 cm quartz cuvette at ca. 0.5 pH intervals between pH 3 and 11 using a Thermo Evolution 600 UV/Visible spectrophotometer between 190 and 600 nm. UV/Visible spectra were recorded at room temperature (25 ± 4 °C). Variations of temperature between 15 and 35 °C had no influence on solution absorption (data not shown). The final data were corrected for dilution effects due to acid or base additions.

2.3.2 Influence of ionic strength on solution absorbance

To study the influence of *I* on absorbance of the solution, 500 mL of a 5 mg/L PAHA solution at *I* = 5 mmol/L $NaClO_4$ was made and acidified with $HClO_4$ (0.1 mol/L) to pH 3. Aliquots (50 mL) from this solution were sampled and solid $NaClO_4$ was added to each sample to obtain solutions with electrolyte concentrations of 0.01, 0.05, 0.1, 0.2, 0.3, 0.4 and 0.5 mol/L $NaClO_4$. The pH values were adjusted if needed, and absorbance spectra were recorded.

2.4 Adsorption experiment

Three solutions of 10 g/L α-Al_2O_3 and 100 mg/L PAHA, *I* = 0.1 mol/L $NaClO_4$ and pH = 6, were made in 10.4 ml polycarbonate Beckman centrifugation tubes (355603). After 5 days of equilibration, the solutions were ultracentrifuged at 60 000 rpm for 2 h. The supernatants were mixed and the solution was diluted in 0.1 mol/L $NaClO_4$ to obtain a 100-mL solution of 5 mg/L, which was then titrated using the spectrophotometric method previously described. PAHA concentration in the supernatant was measured using Shimadzu TOC-VCSH analyzer and was 26.5% of the initial content of PAHA.

3 Results and Discussion

3.1 Potentiometric titrations

Results of PAHA titrations are shown in Figure 1, together with the fits obtained by the NICA-Donnan model (Kinniburgh et al. 1999).

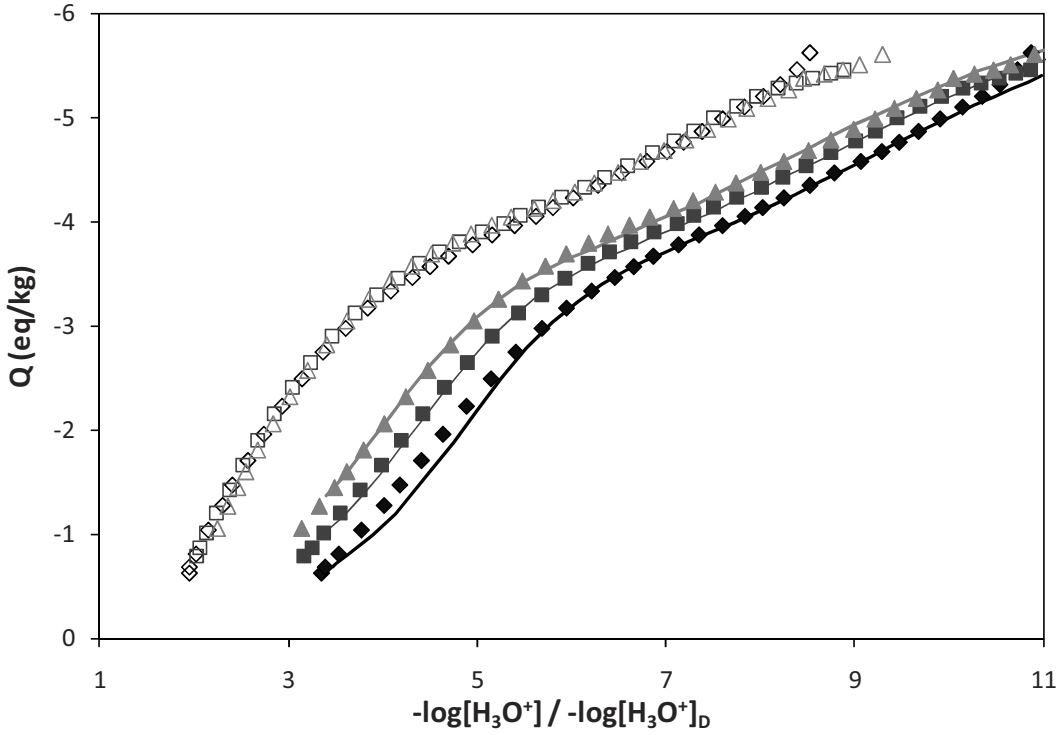

Figure 1. Potentiometric titration of the purified Aldrich humic acid at 0.01 (◆,◇) 0.1 (■,□) and 0.5 mol/L $NaClO_4$ (▲,△). The solid symbols are charge plotted against the concentration of H_3O^+ in the solution. The open symbols are charge plotted against the concentration of H_3O^+ in the Donnan phase, leading to a Master Curve. The best fit smooth lines through the data were obtained by NICA-Donnan parameters given in Table 1.

In this model, the median affinity constants (log $\widetilde{K}_i$), and the heterogeneity of distribution (m_i) for the two main types of binding sites of humic acid (low-affinity, or so-called carboxylic, and high-affinity of so called phenolic groups) are fitted. The electrostatic parameters are obtained using the Master Curve procedure (Milne et al. 1995), optimizing the Donnan parameter *b* in order to merge the original curves. The pH values were corrected for concentrations of protons using the Davies equation (Davies 1962).

The optimization of NICA-Donnan parameters for the titration curves was calculated using ECOSAT and FIT software (Kinniburgh 1993; Keizer and van Riemsdijk 1994). Modeling parameters are given in Table 1, together with the ones used by Vermeer et al. (1999) and Milne *et al.* (2001) for Aldrich humic acid.

Table 1. NICA-Donnan modeling parameters for PAHA potentiometric titration and calculated charge from absorbance measurements after retention experiment.

	$\log \tilde{K}_1$	m_1	Q_1	$\log \tilde{K}_2$	m_2	Q_2	Q_0	b
HH18 (Milne et al. 2001)	3.76	0.55	2.94	8.07	0.24	2.40		0.69
HH24 (Milne et al. 2001)	2.87	0.89	2.31	*8.00* (fixed)	0.14	5.34		0.25
PAHA (Vermeer 1996)	4.03	0.44	3.74	8.48	0.53	1.30		
this study	2.66	0.81	3.24	6.90	0.29	2.88	0.60	0.4
PAHA after fractionation onto α-Al_2O_3 (R=10mg/g)	2.90	0.85	1.61	8.00	0.25	2.37	0.29	0.4

Differences between modeling of the same humic acid used in several studies can be due to (i) range of *I* studied, (ii) differences of the background electrolyte used, and (iii) differences in the stock and purification procedure. Our parameters are, however, within the range of those obtained previously.

3.2 Spectrophotometric titrations

PAHA absorbance spectra (see insert in Figure 2) show a broad and featureless shape characteristic of HS absorbance spectra throughout the pH range (MacCarthy and Rice 1985). The absorbance is increasing with the solution pH due to the progressive deprotonation of the chromophores and change in structure (Dryer et al. 2008). The solution at pH ≈ 11 absorbs around 10% more than the same solution at pH ≈ 3. Differential absorbance spectra were calculated using the following equation

$$\Delta A_{pH}(\lambda) = \frac{1}{l_{cell}} \left[\frac{A_{pH}(\lambda)}{DOC} - \frac{A_{pH_{ref}}(\lambda)}{DOC_{ref}} \right] \quad (1)$$

where l_{cell} is the cell length (cm), DOC and DOC_{ref} (mg/L) are the dilution-corrected concentrations of DOC in the solution at the pH of interest and at the chosen reference pH, respectively. $A_{pH}(\lambda)$ and $A_{pH_{ref}}(\lambda)$ are the absorbance values measured at a given wavelength λ at the pH of interest and at the reference pH, respectively.

The spectrum recorded at the lowest pH value, i.e., $pH_{ref} \approx 3$, is used as a reference to examine the evolution of differential spectra throughout the entire pH range, according to Dryer et al (2008).

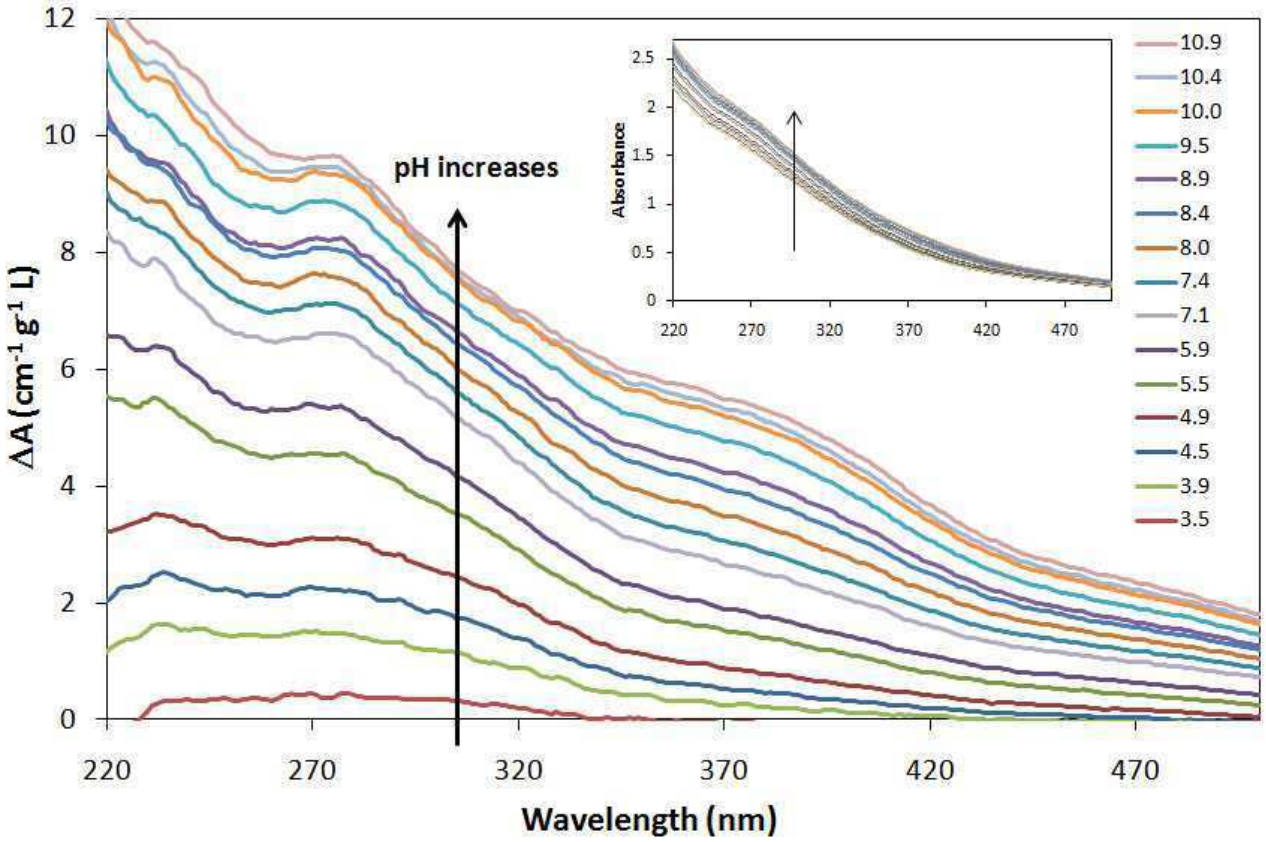

Figure 2. Differential absorbance spectra of PAHA in 0.1 mol/L $NaClO_4$ (pH_{ref} = 2.9). The original absorbance spectra are shown in the insert.

Specific features appear in the differential spectra when the solution pH is increased from 3.5 to 10.9 (see Figure 2), such as the large band centered at 370 nm and the peak centered at 270 nm. This latter peak corresponds to the UV region where the π-π* electron transition occurs, for example for phenolic substances and polycyclic aromatic hydrocarbons (Chin et al. 1994), and so become more important with the deprotonation of the aromatic moieties of PAHA. The broad band at 370 nm and higher wavelengths is similar to the feature observed in the pH-differential spectra of Suwannee River fulvic acid (Dryer et al. 2008). This feature appears to be specific to humic species and can be hypothesized to be associated with interchromophore interactions, in accord with observations made in prior publications (Del Vecchio and Blough 2004). However, its exact nature remains to be ascertained.

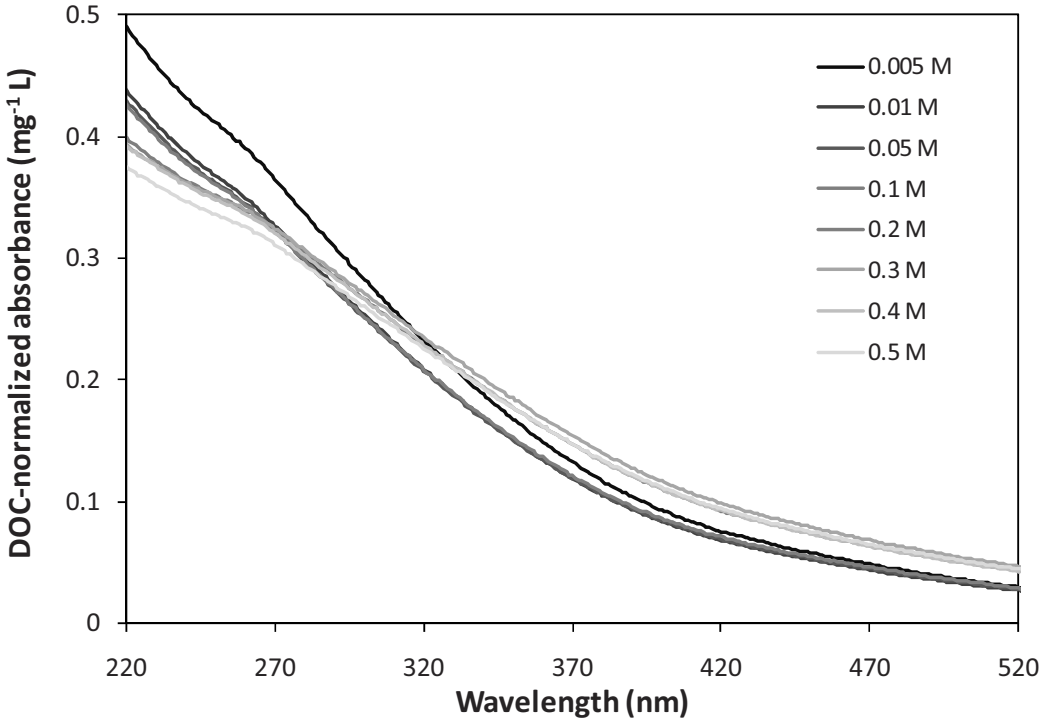

Figure 3. DOC-normalized absorbance spectra of PAHA solutions (~5 mg/L) at pH 3, *I* = 0.005 - 0.5 mol/L $NaClO_4$.

Figure 3 shows the DOC-normalized absorbance spectra of PAHA solutions at variable *I*, from 5×10^{-3} up to 0.5 mol/L $NaClO_4$, and pH = 3.0 ± 0.1. There are two main groups: one corresponding to curves with *I* ranging from 0.01 to 0.1 mol/L, and the second corresponding to *I* ranging from 0.2 to 0.5 mol/L $NaClO_4$. Except for the lowest *I*, a trend can be seen. For wavelengths below 270 nm, the signal decreases with increasing *I*, whereas for wavelengths above 270 nm, the signal increases with *I* but with no differences inside the two groups. Spectrophotometric titrations and modeling were then studied at this specific wavelength because (i) it was the wavelength for which the most important feature was observed, and (ii) ionic strength will have a minor influence on the signal at the reference pH. The fundamental reasons behind this behavior are surely hidden within the modifications of HS structure, but they are outside the scope of this study.

Titration curves were built using the values of differential absorbance at 270 nm versus proton concentration in the Donnan phase $[H^+]_D$. They showed the differential absorbance increase with pH and *I* (see Figure 4). Plotting those curves against $[H^+]_D$ did not result in a Master Curve in this case: there was still an effect of *I* on the absorbance of solution with pH.

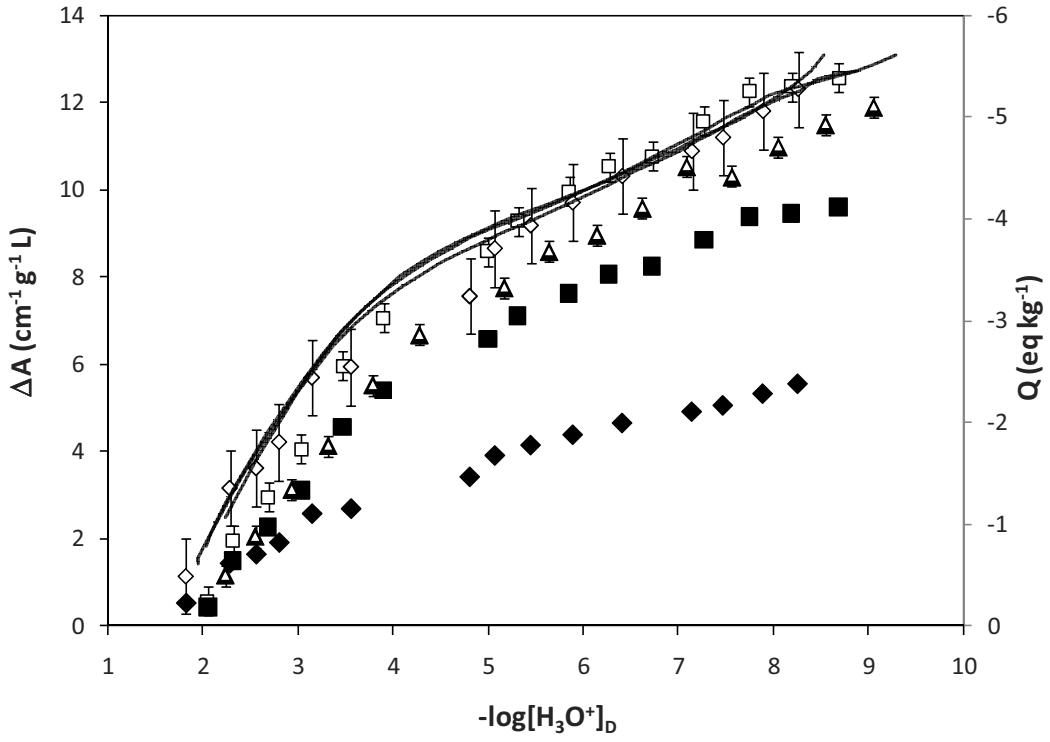

Figure 4. Original and corrected spectrophotometric titration curves of PAHA at I = 0.01 (◇), 0.1 (□), and 0.5 (△) mol/L $NaClO_4$. Results are plotted against the concentration of protons in the Donnan gel $[H_3O^+]_D$. The close symbols are the original data. The open symbols are the data corrected from electrostatic component (0.5 mol/L being the reference for correction, both curves are stacked). The lines are the Master Curve from the potentiometric titrations (on the right axis).

This suggests the presence of an additional effect of I on the conformation of PAHA that influenced the spectroscopic response of the solution, to which potentiometric titrations were not sensitive.

The results shown in Figure 4 suggest that PAHA mass absorptivity increases with electrolyte concentration. Nevertheless, the interactions between chromophores, leading to a modification of absorbance of the solution, or chromism, must be taken into account. Hyperchromism, *i.e.*, increase of molecular absorptivity, can be explained by interactions between neighboring or stacked chromophores, enhancing energy and electrons transfer between donors and acceptors (Vekshin 1987). This is consistent with previous observations that humic molecules tend to undergo aggregation at higher ionic strength, when the electrostatic double layer is more compressed (Conte and Piccolo 1999; Duval et al. 2005).

3.3 Modeling

To model the data, NICA parameters (m_i, $\log\tilde{K}_i$) of PAHA obtained by potentiometric titrations were used. The electrostatic effects were accounted for by the Donnan model, using the concentration of protons into the Donnan gel at a given pH $[H^+]_D$ and at the reference pH $[H^+]_{Dref}$. The absorbance titration curves were modeled using the following equation, derived from the NICA equation.

$$\Delta A_{pH}(\lambda) = \left| A_1(\lambda)\frac{\left(\tilde{K}_1\left[H^+\right]_D\right)^{m_1}}{1+\left(\tilde{K}_1\left[H^+\right]_D\right)^{m_1}} - A_1(\lambda)\frac{\left(\tilde{K}_1\left[H^+\right]_{D_{ref}}\right)^{m_1}}{1+\left(\tilde{K}_1\left[H^+\right]_{D_{ref}}\right)^{m_1}}\right| + \left| A_2(\lambda)\frac{\left(\tilde{K}_2\left[H^+\right]_D\right)^{m_2}}{1+\left(\tilde{K}_2\left[H^+\right]_D\right)^{m_2}} - A_2(\lambda)\frac{\left(\tilde{K}_2\left[H^+\right]_{D_{ref}}\right)^{m_2}}{1+\left(\tilde{K}_2\left[H^+\right]_{D_{ref}}\right)^{m_2}}\right| \quad (2)$$

The only optimized parameters are $A_1(\lambda)$, and $A_2(\lambda)$, which represent the maximum change of absorbance of two mains groups of chromophores of low and high affinity for protons. These values depend on the chosen wavelength for modeling, here 270 nm. For the sake of clarity, they will be henceforth denoted as A_1 and A_2 instead of A_1(270nm) and A_2(270nm). Figure 5 shows the titration curve with the respective influence of the two main groups of chromophores, and the result of modeling for the experiment at 0.1 mol/L $NaClO_4$.

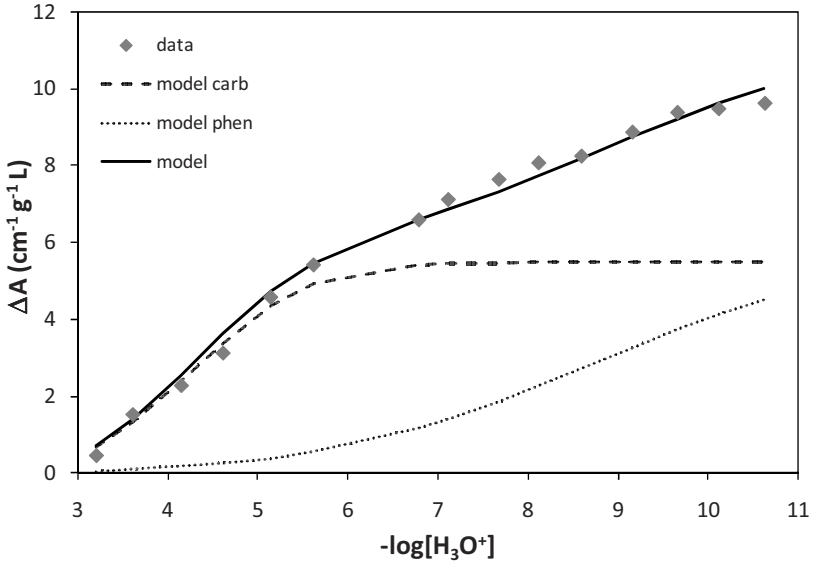

Figure 5. Titration curve and modeling of PAHA differential absorbance at *I* = 0.1 mol/L $NaClO_4$.

As shown in Figure 6, the overall maximum change of absorbance by the two main groups of chromophores increased linearly with log*I*, with parameters of linear regression being dependent on modeling wavelength.

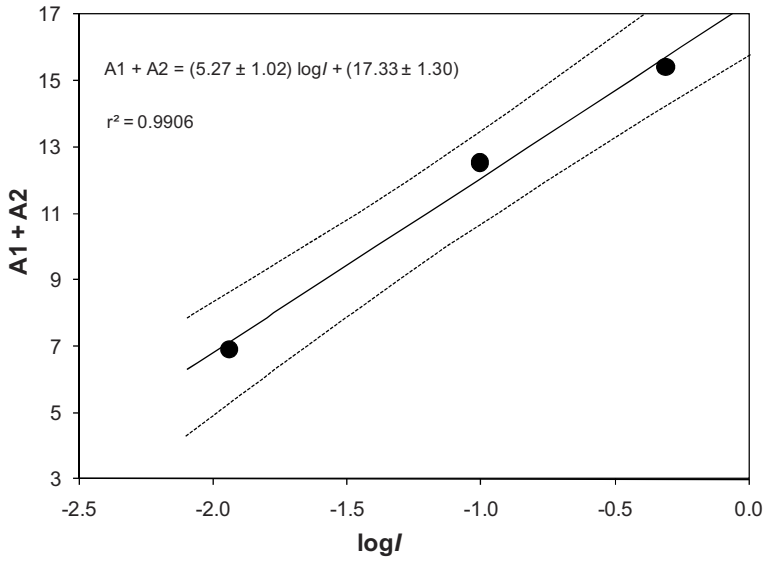

Figure 6. Comparison of the evolution of maximal absorbance A_1+A_2 as a function of log*I*. The continuous line is the result of the linear regression and the dotted ones the statistical envelope (A_1+A_2) ± σ(A_1+A_2).

The conformation of humic acid, which changes with the concentration of electrolyte ions, had an influence on the absorbance of these solutions. But the proportion of the two mains groups of chromophores did not change significantly: within uncertainties it remained the same for all of the ionic strength studied (Table 2).

Table 2. Maximal absorbances of the low affinity- (A_1) and high affinity- (A_2) type groups obtained for the three ionic strengths (*I*) studied and comparison with results of potentiometric titration.

I (mol/L)	A_1	A_2	A_1+A_2	$\frac{A1}{A1+A2}$
0.01	3.69 ± 0.16	3.22 ± 0.35	6.90 ± 0.38	0.53 ± 0.04
0.10	6.37 ± 0.19	6.16 ± 0.37	12.53 ± 0.42	0.51 ± 0.02
0.50	7.56 ± 0.25	7.85 ± 0.42	15.41 ± 0.49	0.49 ± 0.02
Potentiometry (Q) (eq/kg)	3.24 ± 0.21	2.88 ± 0.39	6.12 ± 0.44	0.53 ± 0.05

3.4 Comparison of methods

Modeling of potentiometric and spectrophotometric titration curves gave the same distribution of binding sites as seen in Table 2. In both cases, around 51% of the signal was due to low affinity-type groups, and 49% to high affinity-type groups.

An additional correction was needed to account for the effect of *I* on the spectroscopic signal in addition to the Donnan correction. Data at low *I* were corrected to include results at the higher electrolyte concentration (0.5 mol/L $NaClO_4$), for which the effects of counterions in the double layer were minimal and had less influence on the solution absorptivity.

In the range of *I* studied here (0.01 to 0.5 mol/L) there is a linear relationship between the sum of maximal change of absorbance of both types of groups (A_1+A_2) and log*I* as shown in Figure 6: $A_1+A_2 = c \log(I) + d$, with c = 5.27 ± 1.02 and d = 17.33 ± 1.30. The correction factor f_I was calculated from this linear regression.

$$f_I = \frac{c \log(0.5) + d}{c \log(I) + d} \quad (3)$$

This correction, suitable in the range of *I* studied in this study, was then applied to the differential absorbance values:

$$(\Delta A)_{I,\,corr} = f_I\,(\Delta A)_I \quad (4)$$

The corrected titration curves plotted against $[H^+]_D$ collapsed rather well into a single titration curve independent of ionic strength like for the Master Curve of potentiometric titrations, as shown in Figure 4.

Figure 7 shows charge versus electrostatic-corrected differential absorbance values at 270 nm for the same concentrations of protons and the three ionic strengths. There is a linear relationship between both properties. The linear regression of ΔQ *vs.* ΔA_{corr} gave a slope of -0.367 ± 0.003. This is the transfer function between spectrophotometric and potentiometric titrations for PAHA, at 270 nm. This proportionality is observed in the case of PAHA, for both titrations performed with the same stability constraints and under free-CO_2 conditions and should be established for other HS samples. Measurements should be made on purified samples only to avoid interferences with particles and inorganic species that absorb light in the UV range such as metals and nitrate ions.

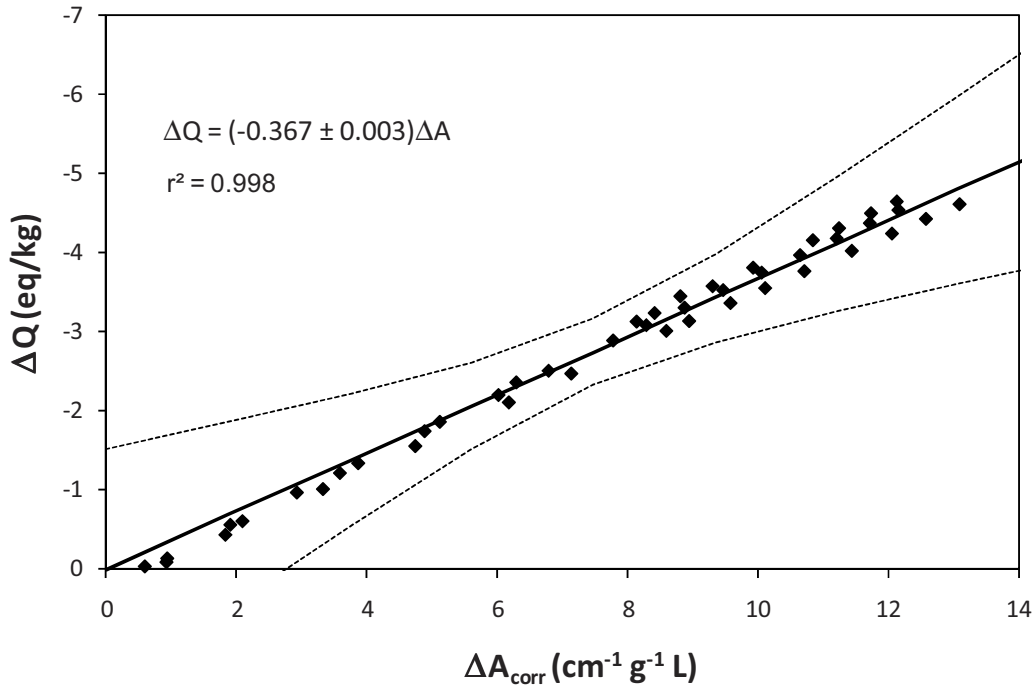

Figure 7. Comparison between charge and corrected differential absorbance for PAHA at same concentration of protons for the three studied *I*. The continuous line is the result of the linear regression and the dotted ones are the statistical envelope Q ± σQ.

Here again, the fundamental reasons behind this linear relationship remain unclear. Also one should note that the relative uncertainties of ΔQ from measured ΔA remain important. The modifications of the chemical environment of the chromophores absorbing around 270 nm with pH and ionic strength are clearly at stake. Nevertheless, this operational relationship could be used for this sample.

3.5 Application to PAHA after adsorption onto α-Al_2O_3

It seems possible, using spectrophotometric titrations, to study fractions of PAHA in the supernatant of retention experiments to quantify modifications of PAHA binding moieties due to the contact with the mineral surface. This exercise should be viewed as a test for the operational relationship under conditions outside its domain of calibration.

The results of differential absorbance spectra of the supernatant are shown in Figure 8. The loss of proton binding sites, as well as the modification of the different features of the differential absorbance spectra, are clearly visible, especially the loss of the broad range around 370 nm and the rising of the peak centered at 270 nm.

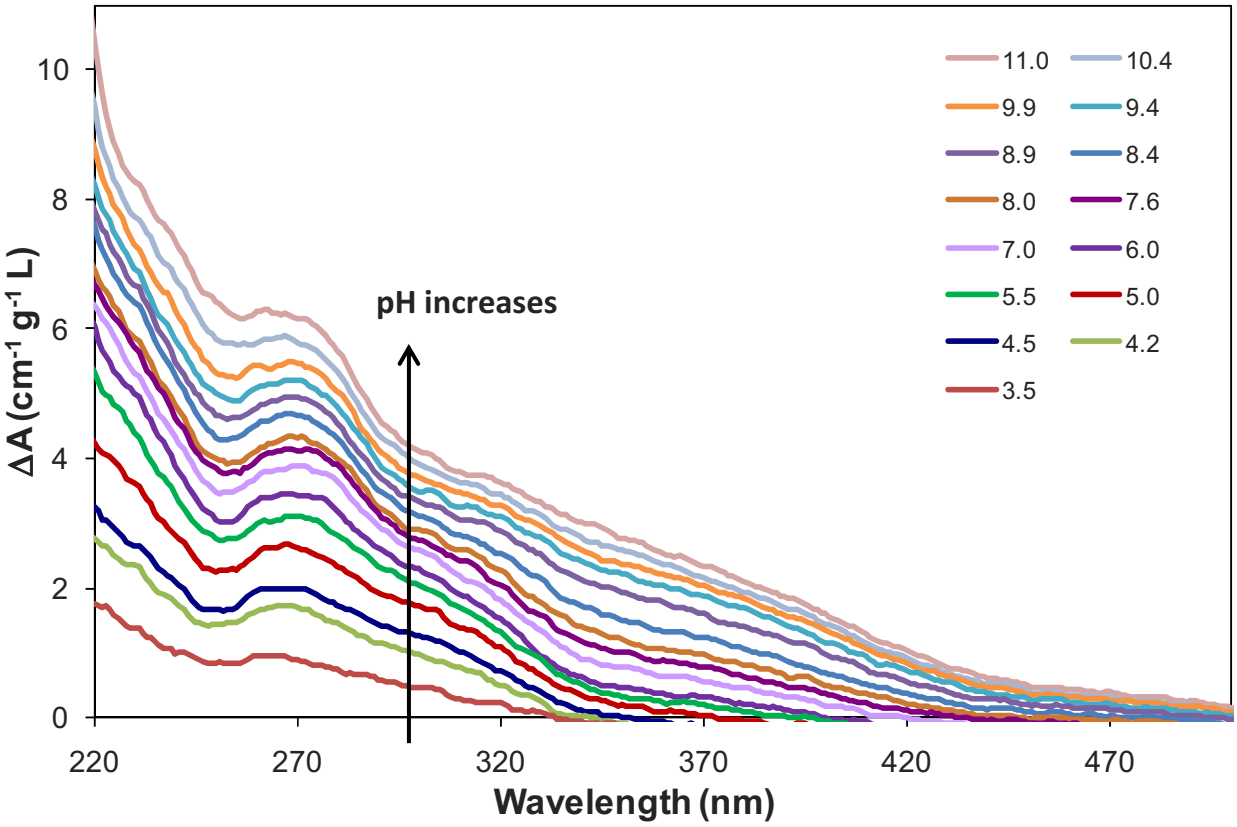

Figure 8. Differential absorbance spectra of PAHA in 0.1 mol/L $NaClO_4$ after fractionation onto α-Al_2O_3 (R=10mg/g).

A titration curve has been built and corrected from electrostatic effects using eqs (3) and (4) as described above (see Figure 9).

The charge of nonsorbed PAHA Q_{R10} was calculated from the corrected spectrophotometric titration curve using the linear ΔQ vs. ΔA_{corr} equation obtained previously. The NICA-Donnan parameters for PAHA fraction generated in the adsorption experiment were optimized using FIT and ECOSAT software (Kinniburgh 1993; Keizer and van Riemsdijk 1994) and given in Table 1.

With this approach, it appears that there is no need to greatly modify the heterogeneity parameters m_i before and after sorption, but a shift of the median affinity constants toward higher pH is required for the nonsorbed sample.

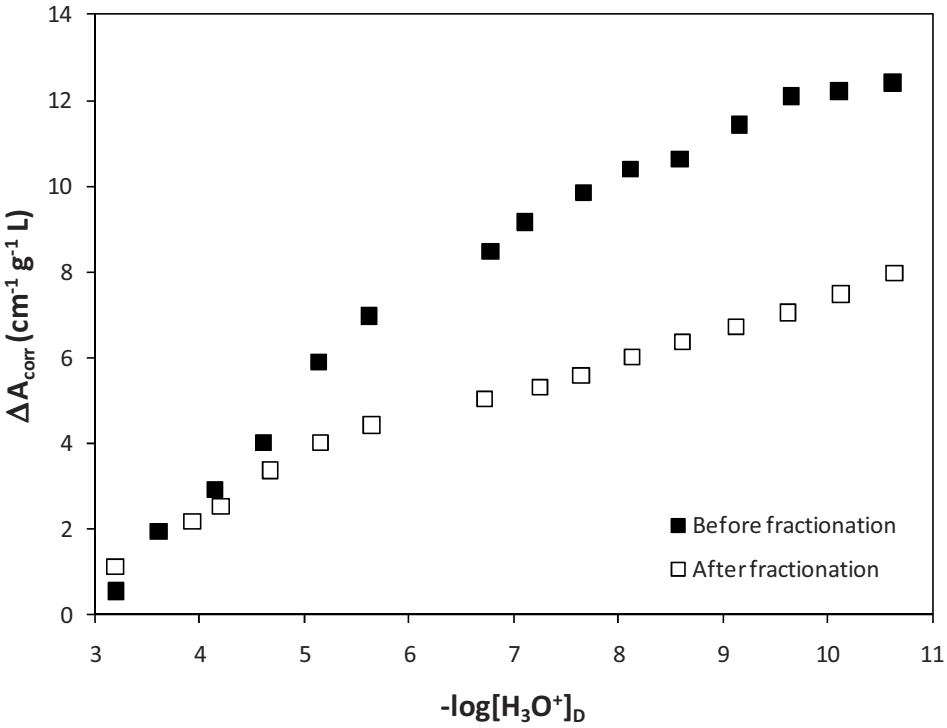

Figure 9. Spectrophotmetric titration curve of PAHA before and after contact with α-Al_2O_3. *I* = 0.1 mol/L $NaClO_4$.

During the retention experiment, carried out at pH 6, around 61% of the sites of nonsorbed PAHA are deprotonated: 52% are low affinity-type sites and 9% are high affinity-type sites. The former should have been more attracted by the surface than the latter. The modeling suggests a general loss of 50% of low-affinity-type sites and 17% of high-affinity-type sites after contact with the oxide. This suggests, within the validity limit of the transfer function, that fractions of PAHA molecules that have stayed on the surface contained almost all the ionized low affinity-type sites, and a greater proportion of high-affinity sites than their ionized proportion. Low affinity-type sites are not only composed of aliphatic but also of benzoic including hydroxybenzoic compounds (Moulin et al. 2001; These et al. 2004), and the sorption data of HS and of phthalic (Gu et al. 1995; Ali and Dzombak 1996) or hydroxybenzoic acids (Davis and Leckie 1978; Evanko and Dzombak 1998) on iron and aluminum (oxy)hydroxide extend largely after the pK of their first carboxylic function as it is the case for HS (Varadachari et al. 1997; Meier et al. 1999; Reiller et al. 2002). Thus, high-affinity-type sites are proportionally over-represented on the surface, as demonstrated by Claret *et al.* (2008).

REFERENCES

Ali, M. A. and D. A. Dzombak (1996). "Competitive sorption of simple organic acids and sulfate on goethite." *Environmental Science & Technology* **30**(4): 1061-1071.

Alliot, C., L. Bion, et al. (2005). "Sorption of aqueous carbonic, acetic, and oxalic acids onto α-alumina." *Journal of Colloid and Interface Science* **287**(2): 444-451.

Aufdenkampe, A. K., J. I. Hedges, et al. (2001). "Sorptive fractionation of dissolved organic nitrogen and amino acids onto fine sediments within the Amazon Basin." *Limnology and Oceanography* **46**(8): 1921-1935.

Chin, Y. P., G. Aiken, et al. (1994). "Molecular weight, polydispersity, and spectroscopic properties of aquatic humic substances." *Environmental Science & Technology* **28**(11): 1853-1858.

Claret, F., T. Schäfer, et al. (2008). "Fractionation of Suwannee River fulvic acid and Aldrich humic acids on α-Al_2O_3: spectroscopic evidence." *Environmental Science & Technology* **42**(23): 8809-8815.

Conte, P. and A. Piccolo (1999). "Conformational arrangement of dissolved humic substances. Influence of solution composition on association of humic molecules." *Environmental Science & Technology* **33**(10): 1682-1690.

Davies, C. W. (1962). *Ion Association*. London, Butterworth.

Davis, J. A. and R. Gloor (1981). "Adsorption of dissolved organics in lake water by Aluminum-oxide - Effect of molecular weight." *Environmental Science & Technology* **15**(10): 1223-1229.

Davis, J. A. and J. O. Leckie (1978). "Effect of adsorbed complexing ligands on trace-metal uptake by hydrous oxides." *Environmental Science & Technology* **12**(12): 1309-1315.

Day, G. M., B. T. Hart, et al. (1994). "Adsorption of natural organic matter onto goethite." *Colloids and Surfaces a-Physicochemical and Engineering Aspects* **89**(1): 1-13.

Del Vecchio, R. and N. V. Blough (2004). "On the origin of the optical properties of humic substances." *Environmental Science & Technology* **38**(14): 3885-3891.

Dryer, D. J., G. V. Korshin, et al. (2008). "In situ examination of the protonation behavior of fulvic acids using differential absorbance spectroscopy." *Environmental Science & Technology* **42**(17): 6644-6649.

Duval, J. F. L., K. J. Wilkinson, et al. (2005). "Humic substances are soft and permeable: evidence from their electrophoretic mobilities." *Environmental Science & Technology* **39**: 6435-6445.

Evanko, C. R. and D. A. Dzombak (1998). "Influence of structural features on sorption of NOM-analogue organic acids to goethite." *Environmental Science & Technology* **32**(19): 2846-2855.

Ghosh, K. and M. Schnitzer (1979). "UV and visible absorption spectroscopic inverstigations in relation to macromolecular characteristics of humic substances." *Journal of Soil Science* **30**(4): 735-745.

Gu, B., J. Schmitt, et al. (1994). "Adsorption and desorption of natural organic matter on iron oxide: Mechanisms and models." *Environmental Science & Technology* **28**: 38-46.

Gu, B. H., J. Schmitt, et al. (1995). "Adsorption and desorption of different organic-matter fractions on iron-oxide." *Geochimica Et Cosmochimica Acta* **59**(2): 219-229.

Hur, J. and M. A. Schlautman (2003). "Molecular weight fractionation of humic substances by adsorption onto minerals." *Journal of Colloid and Interface Science* **264**(2): 313-321.

Hur, J. and M. A. Schlautman (2004). "Effects of pH and phosphate on the adsorptive fractionation of purified Aldrich humic acid on kaolinite and hematite." *Journal of Colloid and Interface Science* **277**(2): 264-270.

Kaiser, K. (2003). "Sorption of natural organic matter fractions to goethite (α-FeOOH): Effect of chemical composition as revealed by liquid-state C-13 NMR and wet-chemical analysis." *Organic Geochemistry* **34**(11): 1569-1579.

Keil, R. G., L. M. Mayer, et al. (1997). "Loss of organic matter from riverine particles in deltas." *Geochimica Et Cosmochimica Acta* **61**(7): 1507-1511.

Keizer, M. G. and W. H. van Riemsdijk (1994). *A computer program for the Calculation of Chemical Speciation and Transport in Soil-Water Systems (ECOSAT 4.7).* . Wageningen, Agricultural University of Wageningen.

Kim, J. I., G. Buckau, et al. (1990). "Characterization of humic and fulvic acids from Gorleben groundwater." *Fresenius Journal of Analytical Chemistry* **338**: 245-252.

Kinniburgh, D. G. (1993). FIT Non-linear Optimization Algorithm and User Manual. Nottingham, UK, British Geological Survey.

Kinniburgh, D. G., W. H. van Riemsdijk, et al. (1999). "Ion binding to natural organic matter: Competition, heterogeneity, stoichiometry and thermodynamic consistency." *Colloids and Surfaces A* **151**: 147-166.

Korshin, G. V., M. M. Benjamin, et al. (1999). "Use of differential spectroscopy to evaluate the structure and reactivity of humics." *Water Science and Technology* **40**(9): 9-16.

Korshin, G. V., C.-W. Li, et al. (1997). "Monitoring the properties of natural organic matter through UV spectroscopy: A consistent theory." *Water Research* **31**(7): 1787-1795.

MacCarthy, P. and J. A. Rice (1985). Spectroscopic methods (other than NMR) for determining functionality in humic substances. *Humic Substances in soil, sediment and water. Geochemistry, isolation, and characterisation*. G. R. Aiken, D. M. McKnight, R. Wershaw and P. MacCarthy. New York, John Wiley and Sons**:** 527-559.

McCarthy, J. F., K. R. Czerwinski, et al. (1998). "Mobilization of transuranic radionuclides from disposal trenches by natural organic matter." *Journal of Contaminant Hydrology* **30**(1-2): 49-77.

McCarthy, J. F., W. E. Sanford, et al. (1998). "Lanthanide field tracers demonstrate enhanced transport of transuranic radionuclides by natural organic matter." *Environmental Science & Technology* **32**(24): 3901-3906.

Meier, M., K. Namjesnik-Dejanovic, et al. (1999). "Fractionation of aquatic natural organic matter upon sorption to goethite and kaolinite." *Chemical Geology* **157**(3-4): 275-284.

Meybeck, M. (1982). "Carbon, Nitrogen, and Phosphorus transport by world rivers." *American Journal of Science* **282**(4): 401-450.

Milne, C. C. J., D. G. Kinniburgh, et al. (1995). "Analysis of proton binding by peat humic acid using a simple electrostatic model." *Geochimica et Cosmochimica Acta* **59**: 1101-1112.

Milne, C. J., D. G. Kinniburgh, et al. (2001). "Generic NICA-Donnan model parameters for proton binding by humic substances." *Environmental Science & Technology* **35**(10): 2049-2059.

Moulin, V., P. Reiller, et al. (2001). "Direct characterization of iodine covalently bound to fulvic acids by electrospray mass spectrometry." *Rapid Communications in Mass Spectrometry* **15**(24): 2488-2496.

Reiller, P., B. Amekraz, et al. (2006). "Sorption of Aldrich humic acid onto hematite: Insights into fractionation phenomena by electrospray ionization with quadrupole time-of-flight mass spectrometry." *Environmental Science & Technology* **40**(7): 2235-2241.

Reiller, P., V. Moulin, et al. (2002). "Retention behaviour of humic substances onto mineral surfaces and consequences upon thorium (IV) mobility: case of iron oxides." *Applied Geochemistry* **17**(12): 1551-1562.

Robertson, A. P. and J. O. Leckie (1994). Humic acid/goethite interactions and their effect on copper binding. *Humic substances in the global environment and implication on human health*. N. Senesi and T. M. Miano, Elsevier**:** 487-492.

Saito, T., L. K. Koopal, et al. (2004). "Adsorption of humic acid on goethite: Isotherms, charge adjustments, and potential profiles." *Langmuir* **20**(3): 689-700.

These, A., M. Winkler, et al. (2004). "Determination of molecular formulas and structural regularities of low molecular weight fulvic acids by size-exclusion chromatography with electrospray ionization quadrupole time-of-flight mass spectrometry." *Rapid Communications in Mass Spectrometry* **18**(16): 1777-1786.

Varadachari, C., T. Chattopadhyay, et al. (1997). "Complexation of humic substances with oxides of iron and aluminum." *Soil Science* **162**(1): 28-34.

Vekshin, N. L. (1987). "Screening hypochromism in chromophore stacks." *Optics and Spectroscopy* **63**: 517-519.

Vermeer, A. W. P. (1996). Interaction between humic acid and hematite and their effects upon metal speciation. PhD Thesis. Wageningen, The Netherlands, Landbouwuniversiteit Wageningen**:** 199.

Vermeer, A. W. P., J. K. McCulloch, et al. (1999). "Metal ion adsorption to complexes of humic acid and metal oxides: Deviation from the additivity rule." *Environmental Science & Technology* **33**(21): 3892-3897.

CHAPITRE 3

CHARACTERIZATION OF HUMIC ACID REACTIVITY MODIFICATIONS DUE TO ADSORPTION ONTO α-Al_2O_3

Noémie Janot, Pascal E. Reiller, Marc F. Benedetti

RÉSUMÉ

L'influence du pH, de la force ionique, et du taux de couverture R (exprimé en mg de matière organique par g ou m² de matière minérale) sur l'adsorption de PAHA sur l'alumine α-Al_2O_3 est étudiée par expériences en flacons fermés dites « en batch ». Après un temps d'équilibre fixé du système, les échantillons sont centrifugés et la quantité de PAHA dans le surnageant est mesurée par analyse du carbone organique dissous. La quantité d'acide humique adsorbée par m² de surface diminue lorsque le pH augmente. A pH constant, la quantité de PAHA adsorbée augmente avec la concentration initiale de matière organique jusqu'à atteindre un seuil de saturation dont la valeur dépend du pH.

Les paramètres caractéristiques des spectres UV-Visible tels que l'absorbance spécifique $SUVA_{254}$, les ratios d'absorbances E_2/E_3, la largeur de bande Δ_{ET} renseignent sur l'aromaticité des fractions de PAHA se trouvant dans les surnageants. Aucune modification significative n'est observée au dessus de R = 20 mg/g pour une étude à pH 6,8. Pour des taux de couverture inférieurs, une diminution de l'aromaticité des fractions non adsorbées est observée, indiquant une adsorption préférentielle des fractions plus aromatiques. Des analyses LC-OCD sur les mêmes surnageants montrent une adsorption préférentielle des fractions de plus grande taille à cette valeur de pH d'équilibre.

Des titrages spectrophotométriques ont été effectués sur les surnageants d'expériences de sorption PAHA/α-Al_2O_3 à pH 6,8, pour différentes concentrations en acide humique. Les évolutions de spectres UV-Visible sont traitées comme dans le chapitre précédent et transformées en courbes de titrages. Ces courbes sont modélisées en utilisant le modèle NICA-Donnan. Les paramètres de protonation des fractions solubles de PAHA sont comparés à ceux du PAHA avant adsorption. À partir de la concentration de PAHA dans le surnageant, par bilan de matière, des « courbes de titrage » sont également calculées pour les fractions de PAHA adsorbées sur la surface minérale et modélisées. Pour la fraction en solution, les résultats montrent une modification des paramètres de protonation pour les taux de fractionnement les plus importants, soit $R < 20\ mg_{PAHA}/g_{\alpha\text{-}Al_2O_3}$, essentiellement sur les sites de basse affinité (sites dits carboxyliques) : les résultats de la modélisation montrent une diminution du nombre de ces sites et de leur constante d'affinité pour les protons. Il est en revanche difficile de voir une évolution des paramètres de protonation des sites de haute affinité (sites dits phénoliques) du fait du pH expérimental choisi.

ABSTRACT

Adsorption of PAHA onto α-Al_2O_3 is studied by batch experiments at different pH, ionic strength and coverage ratios R (mg of PAHA by g or m² of mineral surface). After equilibration, samples are centrifuged and the concentration of PAHA in the supernatants is measured by DOC analysis. The amount of adsorbed PAHA per m² of mineral surface is decreasing with increasing pH. At constant pH value, the amount of adsorbed PAHA increases with initial PAHA concentration until a plateau is reached, this last value being pH-dependent.

UV/Visible specific parameters such as specific absorbance $SUVA_{254}$, ratio of absorbance values E_2/E_3 and width of the electron-transfer absorbance band Δ_{ET} are calculated for supernatant PAHA fractions of adsorption experiments at pH 6.8, to have an insight on the evolution of PAHA characteristics with varying coverage ratio. No modification is observed compared to original compound for $R \geq 20$ $mg_{PAHA}/g_{\alpha\text{-}Al_2O_3}$. Below this ratio, aromaticity decreases with initial PAHA concentration. LC-OCD measurements on these supernantants also show a preferential adsorption of higher size fractions.

Spectrophotometric titrations were done on supernatants corresponding to adsorption experiments at $pH \approx 6.8$ and different PAHA concentrations. Evolutions of UV/Visible spectra with varying pH were treated as explained in a previous work (Janot *et al.*, Environ. Sci. Technol., 44, 6782, 2010) to obtain titration curves described with the NICA-Donnan model. Protonation parameters of non-sorbed PAHA fractions are compared to those obtained for the PAHA before contact with the oxide, ~~and~~ a decrease of amount of low-affinity type sites after adsorption, as well as of their affinity constant is obtained. From PAHA concentration in the supernatant and mass balance, "titration curves" are calculated and fitted for the adsorbed fractions. Due to experimental pH, it is difficult to see any significant evolution of proton-binding parameters for the high affinity-type sites of both fractions.

1 Introduction

The interactions between humic substances (HS) and mineral surfaces modify their behavior toward contaminants in the environment. Due to HS heterogeneous nature, their composition and binding properties are modified during adsorption onto minerals (Davis and Gloor 1981; Hur and Schlautman 2003; Saito et al. 2004; Reiller et al. 2006; Claret et al. 2008; Janot et al. 2010). Interactions between HS and mineral surfaces are known to be controlled by different processes: electrostatic and hydrophobic interactions, ligand-exchange between phenolic and carboxylic groups of humic substances and oxide surface sites. The adsorption of humic substances onto mineral surfaces varies with pH, ionic strength, and concentration ratios between organic and inorganic compounds (Schlautman and Morgan 1994; Vermeer et al. 1998; Saito et al. 2004; Weng et al. 2007), but also with humic substances origin and mineral surface (Hur and Schlautman 2003).

During adsorption, fractionation of HS aggregates occurs, leading to two pools of organic matter, a dissolved one and an adsorbed one, each one with different properties. Previous studies have shown the influence of this fractionation on the modification of structures and moieties on humic molecules. Generally, these studies analyze the dissolved organic fraction, which stays in the supernatant after centrifugation of the mixture. The modification of UV/Visible parameters (such as SUVA, E_2/E_3, or ε_{280}) gives information on aromaticity of molecules: all studies show a preferential adsorption of molecules with higher aromaticity (Gu et al. 1995; Meier et al. 1999; Chorover and Amistadi 2001; Zhou et al. 2001; Reiller et al. 2006; Claret et al. 2008). The apparent molecular weight (MW) of non-sorbed fraction has also been studied, using size-exclusion chromatography (SEC). Majority of studies have shown a preferential adsorption of higher MW fractions of various NOM extracts on goethite at pH between 4 and 7.5 (Meier et al. 1999; Chorover and Amistadi 2001; Zhou et al. 2001). However, Hur and Schlautman (2004) have shown that the apparent MW of non-sorbed fractions of purified Aldrich humic acid onto hematite was dependent on pH: below the point of zero charge (pH 8), the authors noted an enrichment of high MW fractions in the solution, and an apparent lower MW at higher pH. This is consistent with the work of Reiller et al. (2006) which observed a preferential adsorption of low molecular weight (m/z) fraction using ESI-MS with the same system at pH 7. Kang et al. (2008) showed a preferential adsorption of low MW fractions of soil humic acid onto goethite at pH 5 by SEC. The proposition of a general trend for size modification of HS molecules after adsorption onto oxides is not straightforward. The influence of pH, which seems of great importance, has not been well

established yet. Fractionation of HS aggregates structure after adsorption onto a mineral oxide has already been evidenced. However, to our knowledge, no study has yet looked at the modification of reactivity of the produced organic fractions, which could explain the difficulty to model the behavior of ternary systems composed of metal/HS/mineral since additivity is often not respected (Robertson and Leckie 1994; Vermeer et al. 1999). It is actually difficult to access to the binding properties of the dissolved fraction of HS, due to the low concentration in solution after the adsorption experiments.

Previous works (Dryer et al. 2008; Janot et al. 2010) have described spectrophotometric titrations, which allow accessing the reactivity of HS in solution at relevant environmental concentration (< 10 mg_{HS}/L). The aim of this study is to use these spectrophotometric titrations to study dissolved fractions of HS after adsorption experiment, in order to quantify modifications of their binding moieties due to the contact with the mineral surface.

In this work the modifications of reactivity of Purified Aldrich Humic Acid (PAHA) fraction left in solution after adsorption onto α-Al_2O_3 at different organic/mineral ratios are qualitatively characterized. HS adsorption onto oxides have mostly been studied on Fe oxides, but aluminol surface sites of Al oxides are part of clays reactive sites, which are very abundant in the environment. An attempt to access reactivity of adsorbed PAHA fraction is also proposed. The quantification of PAHA adsorption onto α-Al_2O_3 depending on pH and initial PAHA concentration has also been studied by batch experiments.

2 Materials and methods

2.1 Preparation of samples

Commercial Aldrich humic acid was purified (PAHA) according to Kim et al. (1990). A stock suspension at 5 g_{HA}/L was prepared by diluting PAHA in NaOH (pH around 10) to promote complete PAHA dissolution. In this work, concentrations of PAHA solutions, noted in mg/L, always correspond to mg_{PAHA}/L.

Alumina (α-Al_2O_3) was purchased from Interchim (pure 99.99%, size fraction 200–500 nm). The solid was washed thrice with carbonate-free NaOH and thrice with freshly produced milli-Q water before drying and storage at room temperature under N_2 atmosphere according to Alliot et al. (2005). Specific area has been found at 15 m^2/g using N_2-BET method, and the pH_{PZC} has been measured at 9.6 by potentiometric titration (presented in Chapter 6) and verified by zeta potential measurements (pH_{IEP} found at 9.5)

2.2 Adsorption experiments

Suspensions of 1 g/L α-Al_2O_3 with varying PAHA concentration, ionic strength *I* ($NaClO_4$) and pH were made in 10.4 ml Beckman centrifugation tubes (355603). After 3 days of equilibration, final pH was measured and solutions were ultracentrifuged (60 000 rpm for 2 h).

PAHA concentrations in the supernatant were measured using a Shimadzu TOC-VCSH analyzer for data at 0.1 M $NaClO_4$ and for the adsorption isotherm at pH 4, using PAHA as a standard between 0 and 50 mg/L; standard deviation is 0.6 mg/L. For other data sets (at 0.01 M and isotherms at pH 6.2 and 7.4) a carbon contamination was observed in the storage tubes. PAHA concentrations in the supernatants were then determined by UV measurements, with PAHA calibration. UV measurements are known to induce a bias on adsorbed HS quantification, due to the modification of chromophores with fractionation, especially at low humic concentration (Gu et al. 1996; Claret et al. 2008). A non-contaminated set of supernatant solution has then been used as reference to choose the wavelengths of calibration in order to minimize the difference between UV and DOC measurements. For each wavelength between 220 and 600 nm, calibration curves were determined. Best results were found when using the mean of values obtained from wavelengths between 290 and 320 nm

2.3 LC-OCD measurements

Size-exclusion chromatography with organic carbon detector was used to determine structural modifications of PAHA aggregates after adsorption onto α-Al_2O_3. The detailed experimental procedure has been described elsewhere (Huber et al. 2011). Mobile phase was a phosphate buffer of pH of 6.85. The acidification solution was prepared by adding 4 mL o-phosphoric acid (85%) and 0.5 g potassium peroxodisulfate to 1 L of demineralised water. OC detector was calibrated using phthalate solution. Calibration being different from the one used for adsorption quantification, results can then not be compared directly.

2.4 Titration experiments

A series of retention experiments at 10 g/L α-Al_2O_3 and various initial PAHA concentrations (600, 300, 200, 120 and 70 mg/L), I = 0.1 mol/L ($NaClO_4$), pH = 6.8 ± 0.3, and 5 days of equilibration was also done. For each PAHA concentration, at least three replicates were made. The supernatants were mixed and the solution was diluted in 0.1 mol/L ($NaClO_4$) to obtain a 100-mL solution of 10 mg/L, which was then titrated between pH 3 and pH 11 using

the spectrophotometric method described in Janot et al. (2010). PAHA concentrations in the supernatant were measured using Shimadzu TOC-VCSH analyzer.

3 Results and Discussion

3.1 Influence of solution parameters on PAHA adsorption

Quantification of PAHA adsorption onto α-Al_2O_3 was made at different pH, for a coverage ratio R = 25 $mg_{PAHA}/g_{\alpha\text{-}Al_2O_3}$. Humic acid adsorption onto oxides reported in the literature show a surface concentration up to 4.5 mg_{HA}/m^2, depending on mineral, ionic strength, pH and initial coverage ratio (Schlautman and Morgan 1994; Fairhurst and Warwick 1998; Murphy et al. 1999; Boily and Fein 2000; Reiller et al. 2002; Hur and Schlautman 2004; Weng et al. 2007). Our results showed a typical decrease of PAHA retention onto α-Al_2O_3 with increasing pH (see Figure 1), from 1.24 mg/m² at pH 4.0 (i.e., 76% of initial amount of PAHA) to 0.61 mg/m² at pH 8.8 (i.e., 37%).

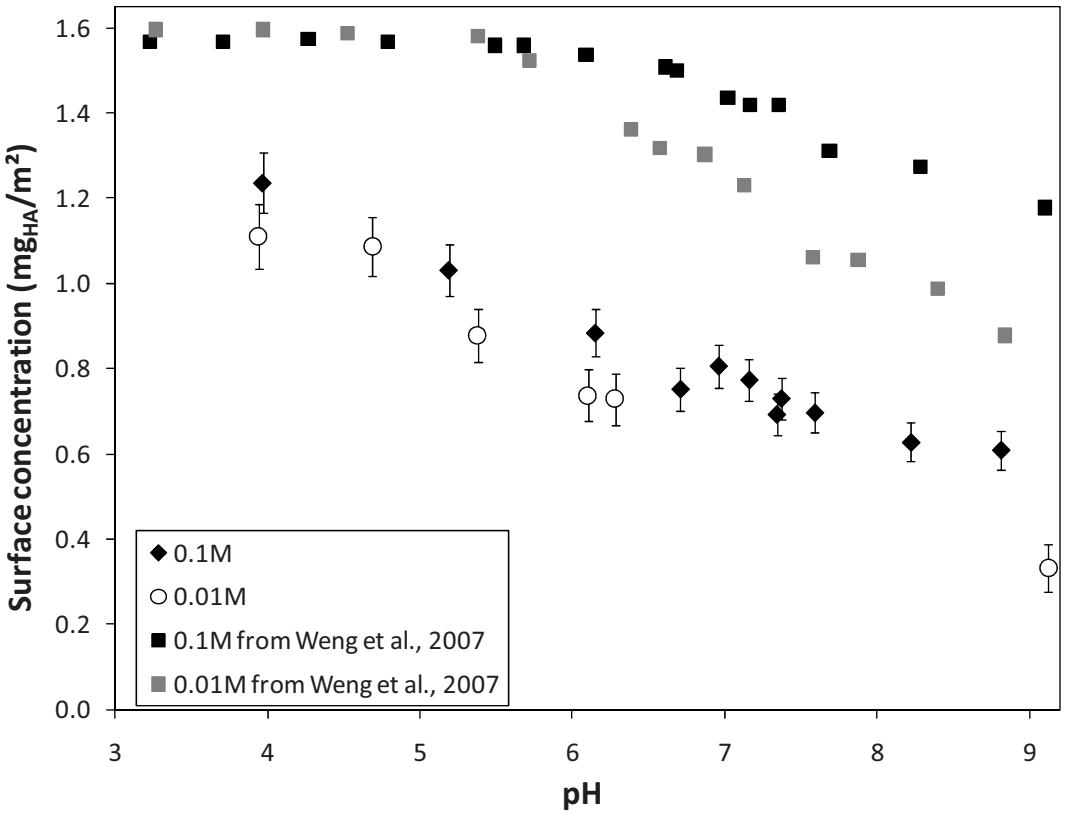

Figure 1. Influence of pH and ionic strength on PAHA adsorption onto α-Al_2O_3. Re-calculated data from Weng et al. (2007) for HA adsorption onto goethite have been plotted for comparison.

As previously observed for simple organic acids, the sorption of acid anions is linked to their protonation constant (Evanko and Dzombak 1998). From potentiometric titrations data of PAHA, the median intrinsic affinity parameters were found at $\log\tilde{K}_1 = 2.66$ and $\log\tilde{K}_2 = 6.90$ (Janot et al. 2010), which gives maximum of affinity distribution around 5.0 and 9.2 at 0.01 M and 4.5 and 9.7 at 0.1 M, respectively. This induces a monotonous decrease of the sorption. At low pH, inner-sphere complexation occurs between deprotonated carboxylic ligands of PAHA and positively charged surface groups of the oxide. When pH increases, the net positive charge of alumina surface is decreasing and the more negatively charged PAHA is less attracted to it. The high point of zero charge of the surface, i.e. 9.6, also explains the significant amount of PAHA bound throughout the pH range studied.

Despite the too few data at 0.01 M, adsorption of PAHA also seems to slightly depend on ionic strength (see Figure 1), with amount of PAHA adsorbed decreasing with ionic strength above pH 5. Weng et al.(2007) have made the same observations for a HA/goethite system, in the same surface coverage conditions: 150 mg_{HA}/L with 1 g/L of goethite with a 94 m^2/g specific area, i.e. 1.60 mg_{HA}/m^2 when we used 1.66 mg_{HA}/m^2 in our experiment. The authors also noticed no difference in HA surface concentration between 0.1 M and 0.01 M $NaNO_3$ below pH 5.7, but a lower adsorption of HA at lower ionic strength for higher pH values. Their results have been plotted on Figure 1 for comparison. Sakuragi et al. (2004) reported the same behavior for humic acid adsorption onto hematite between 0.05 and 0.5 M. When ionic strength increases, the Donnan volume and the electrostatic repulsion between charges decrease, allowing molecules to move closer and leading to an increase of adsorbed PAHA amount. Filius et al. (2000) and Reiller et al. (2002) did not evidence any effect of salt concentration on fulvic acid adsorption on goethite. This influence of electrostatic effects is ~~explained by the larger size of humic acid molecules, which conformation~~ is more dependent on ionic strength than fulvic acids (Saito et al. 2004).

The influence of PAHA initial amount (10 g/L of α-Al_2O_3, 5 days of equilibration) was studied at pH 6.8 ± 0.3. Results are shown in Figure 2, together with the results from Claret et al. (2008) obtained for the same system (same concentration of α-Al_2O_3, pH = 6.1 ± 0.1 and 24 h of contact). The two data sets are consistent, which shows that equilibration time has almost no influence on PAHA adsorption between 1 and 5 days. This isotherm is also compared with three other experiments performed at 1 g/L α-Al_2O_3 and pH = 4.2 ± 0.2,

6.2 ± 0.1, 7.2 ± 0.2 (see Figure 2). The three points at R = 25 $mg_{PAHA}/g_{\alpha\text{-}Al_2O_3}$ are taken from the pH-isotherm shown in Figure 1.

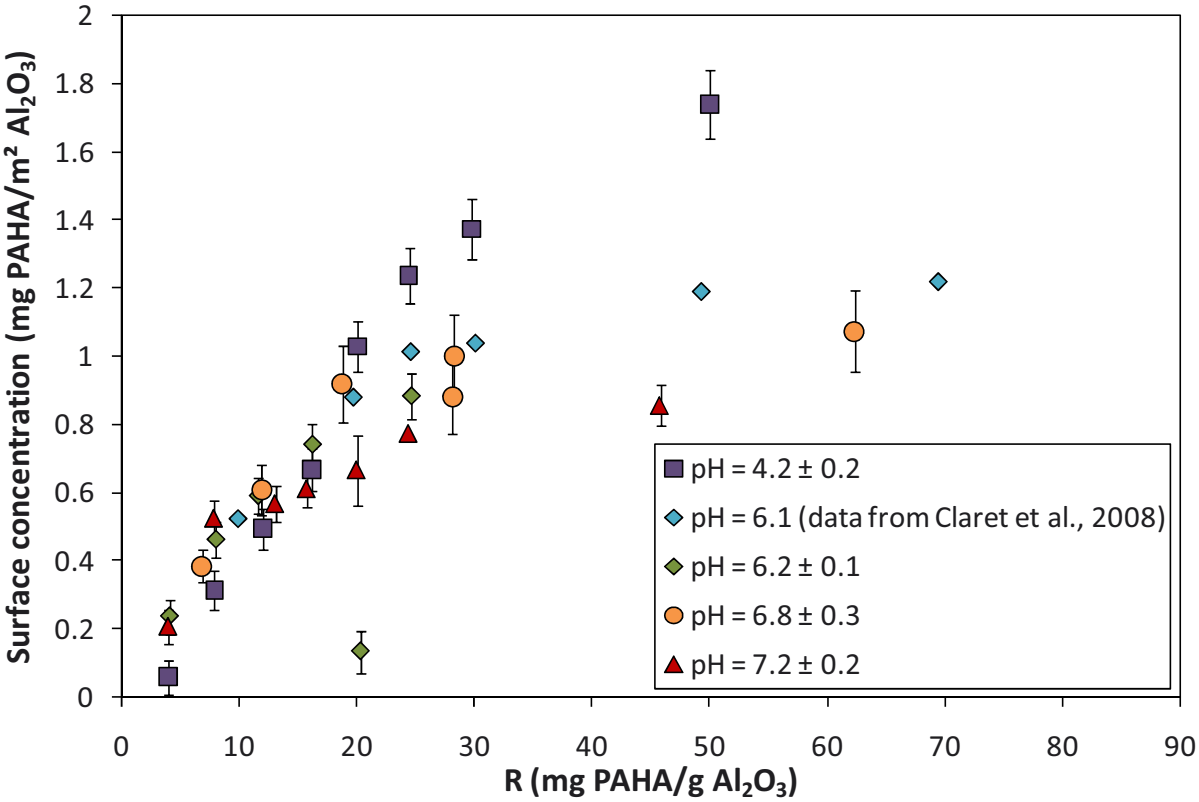

Figure 2. PAHA surface concentration depending on pH and initial concentration. Error bars correspond to σ.

Except for one data point at pH 6.2 and 20 $mg_{PAHA}/g_{\alpha\text{-}Al_2O_3}$, PAHA adsorption onto α-Al_2O_3 at different pH follows the same trend. The adsorption isotherms show an increase with increasing initial quantity, until a plateau is reached. This saturation threshold decreases with increasing pH, which is commonly found in the case of HS adsorption onto metal (hydr)oxides (Schlautman and Morgan 1994; Vermeer et al. 1998; Filius et al. 2000; Saito et al. 2004; Kang and Xing 2008). Saturation is reached for a lower R value at higher pH.

3.2 Characterization of supernatants

UV/Visible measurements were made on the supernatants from adsorption isotherm at pH 6.8 and 10 g/L α-Al_2O_3. UV/Visible spectra of NOM samples can provide some structural information. $SUVA_{254}$ (Specific UV Absorbance at 254 nm) values are summarized in Table

1, together with the ratio of absorbance values at 254 and 365 nm (E_2/E_3) and the half-width of the electron-transfer band (Δ_{ET}, in electron-volt) as described by Korshin et al. (1999):

$$\Delta_{ET} = 2.18 \left(\ln \left(\frac{A_{280}}{A_{350}} \right) \right)^{-1/2}$$

These values have been measured for the original PAHA solution as well as for the different supernatants.

Table 1. Parameters of UV absorbance spectra of the different samples (at pH = 6).

	$SUVA_{254}$ (mg^{-1} L m^{-1})	Δ_{ET} (eV)	E_2/E_3
PAHA	5.0	2.5	3.0
R = 60 mg/g	5.5	2.4	3.3
R = 30 mg/g	6.2	2.5	3.1
R = 20 mg/g	5.4	2.4	3.3
R = 12 mg/g	3.9	2.0	5.8
R = 7 mg/g	2.3	1.9	6.5

The three parameters shown in Table 1 are almost constant for $20 \leq R \leq 60$ $mg_{PAHA}/g_{\alpha\text{-}Al_2O_3}$ and comparable to the values of original PAHA at the same pH and ionic strength. For $R < 20$ $mg_{PAHA}/g_{\alpha\text{-}Al_2O_3}$, i.e. highest fractionation rates, $SUVA_{254}$ is decreasing. Previous studies have shown that aromaticity is correlated to $SUVA_{254}$ as well as Δ_{ET} (Chin et al. 1994; Korshin et al. 1999; Weishaar et al. 2003) and anti-correlated to E_2/E_3 (Peuravuori and Pihlaja 1997). In our case, it means that PAHA fractions in solution for concentration ratios below 20 $mg_{PAHA}/g_{\alpha\text{-}Al_2O_3}$ show a loss of aromaticity regarding to original PAHA. The same observation was made by Claret et al. (2008) for the same system after adsorption at pH = 6.1, with a decrease observed for $R < 10$ $mg_{PAHA}/g_{\alpha\text{-}Al_2O_3}$ (see Figure 3); the difference in initial $SUVA_{254}$ value between the two experiments may be due to the use of different batch of PAHA. The preferential adsorption of more aromatic HA fractions is in agreement with literature data (Gu et al. 1995; Meier et al. 1999; Chorover and Amistadi 2001; Zhou et al. 2001; Reiller et al. 2006; Claret et al. 2008).

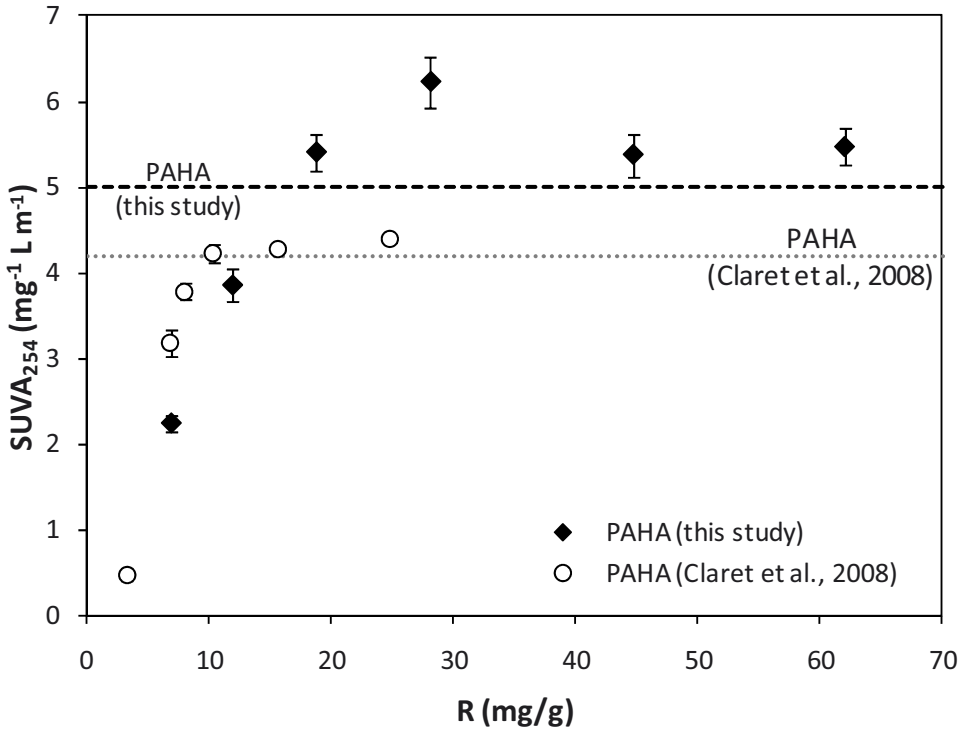

Figure 3. $SUVA_{254}$ values (at pH = 6) for PAHA and supernatants from retention experiments and comparison with results from Claret et al., 2008.

LC-OCD measurements were performed on the same samples. Figure 4 shows the chromatograms obtained, with the organic carbon signal depending on elution time, larger aggregates being eluted faster. A preferential adsorption of larger molecules is occuring: when coverage ratio decreases, the peak observed around 43 min is delayed, indicating a loss of larger molecules in solution after centrifugation of the samples. This peak is decreasing with R value. This observation is in agreement with spectroscopic measurements and decrease of Δ_{ET} value with R: Korshin et al. (1999) noted a correlation between Δ_{ET} value and gyration radii of humic molecules obtained by low-angle X-ray diffraction.

For R < 15 mg/g, we observe an increase of a peak located around 53 min, which was not seen for higher PAHA concentrations. However, there is no change in elution time of the peak located around 60 min: its intensity is changing with R value, but no shift is observed: the size of those smaller molecules is not affected by adsorption onto alumina surface for this contact time.

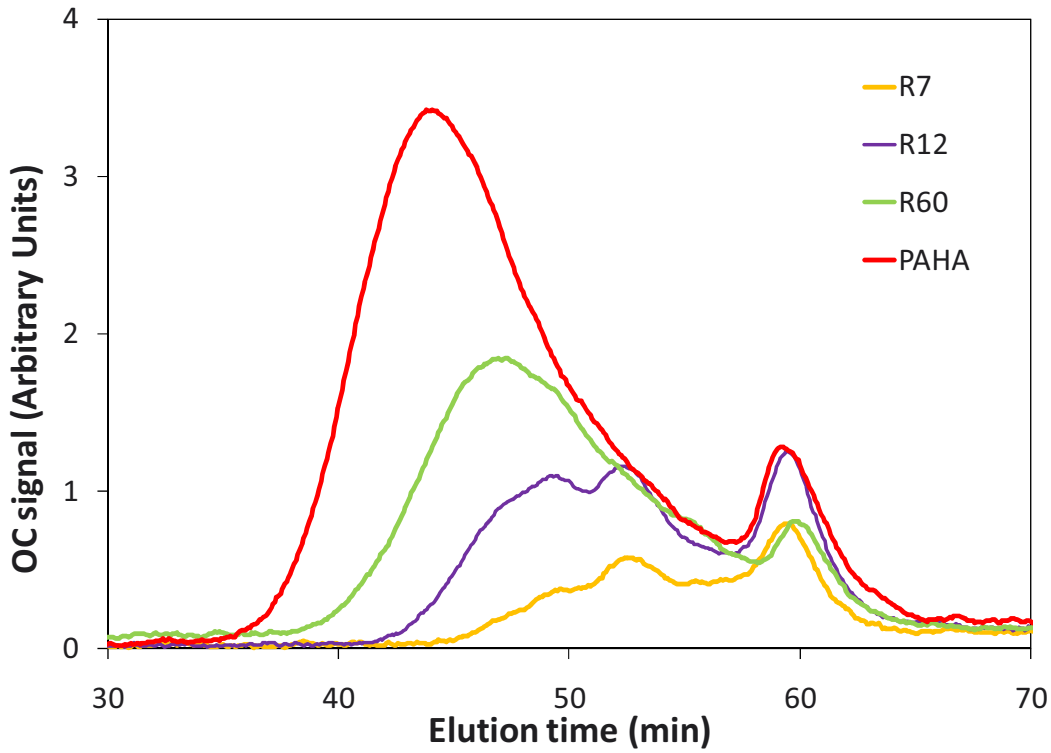

Figure 4. LC-OCD chromatograms of PAHA and of supernatants from adsorption experiments at pH ≈ 6.8 (R in $mg_{PAHA}/g_{\alpha\text{-}Al_2O_3}$).

3.3 Spectrophotometric titrations

The differential absorbance spectra of all the supernatants were calculated as described by Janot et al. (2010). The results of differential absorbance spectra of the supernatants for different initial coverage rates are shown in Figure 5. The main evolution is the decrease of differential absorbance values with decreasing R value, at all the wavelength studied. Deprotonation induces less change in the UV/Visible spectra for PAHA fractions compared to the original PAHA. This can be related to the loss of proton binding sites. The modification of the different features on the differential absorbance spectra are clearly visible too, especially the loss of the broad range around 370 nm, leading to the apparition of a 330 nm-centered feature for the two lowest R values.

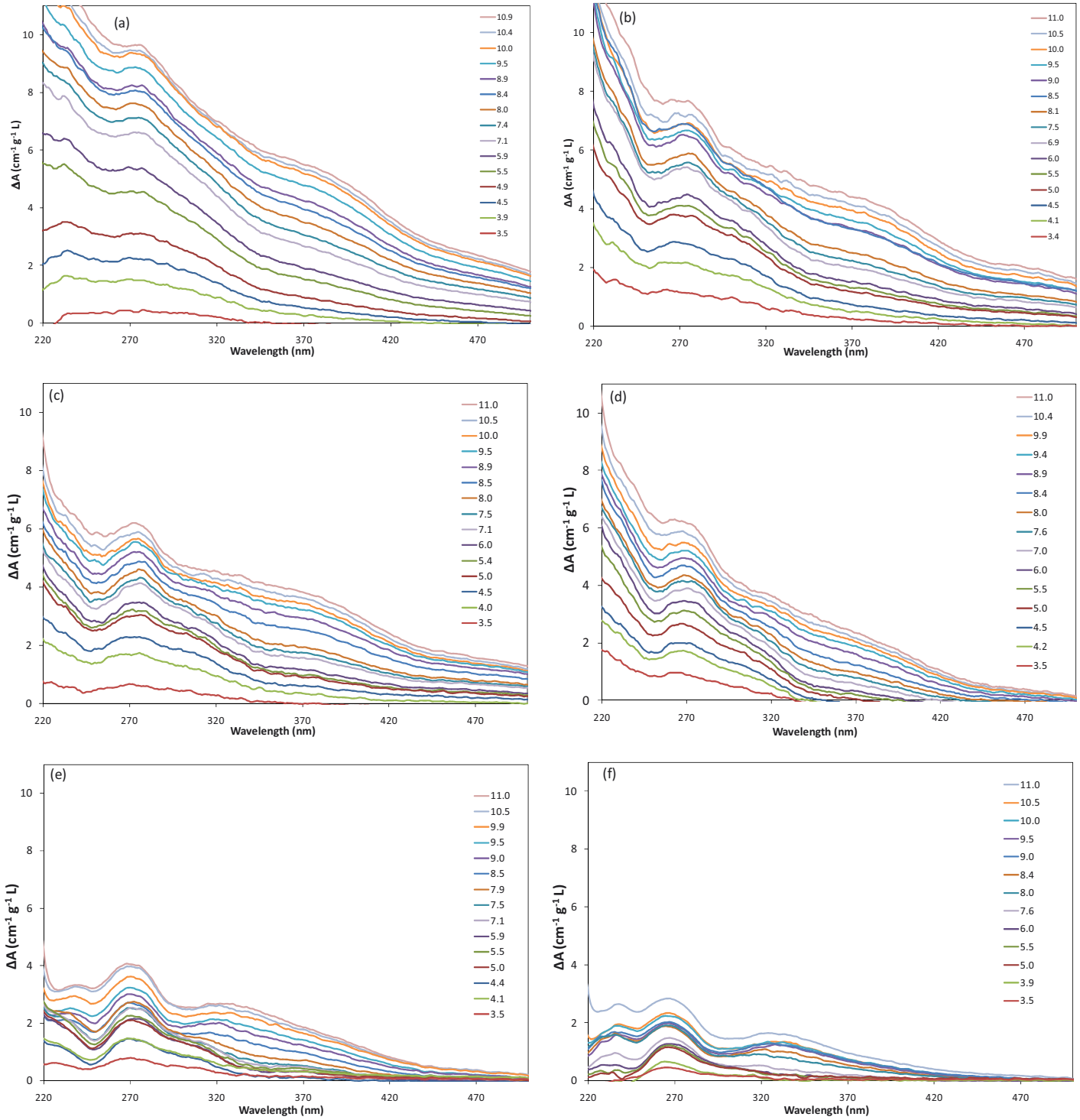

Figure 5. Differential absorbance spectra of supernatants from retention experiments ($pH_{ref} \approx 3.0$) for (a) original PAHA and different organic/mineral ratios (b) R = 60 mg/g (c) R = 30 mg/g (d) R = 20 mg/g (e) R = 12 mg/g (f) R = 7 mg/g.

Titration curves were built using the values of differential absorbance at 270 nm versus pH. This value is increasing with pH and decreasing with R. The transformation from spectrophotometric data to titration curves may be found elsewhere (Janot et al. 2010). The electrostatic correction previously determined has been applied to these titration curves, and the corresponding charges have been calculated using the transfer function obtained for un-fractioned PAHA (Janot et al. 2010). This function may be used as we are in the same conditions of ionic strength and working with the same HA. However it should be emphasized that fractionation may induce modifications to this transfer function, which we are not able to characterize. Results of charge calculations in function of pH and coverage ratio are shown in Figure 6.

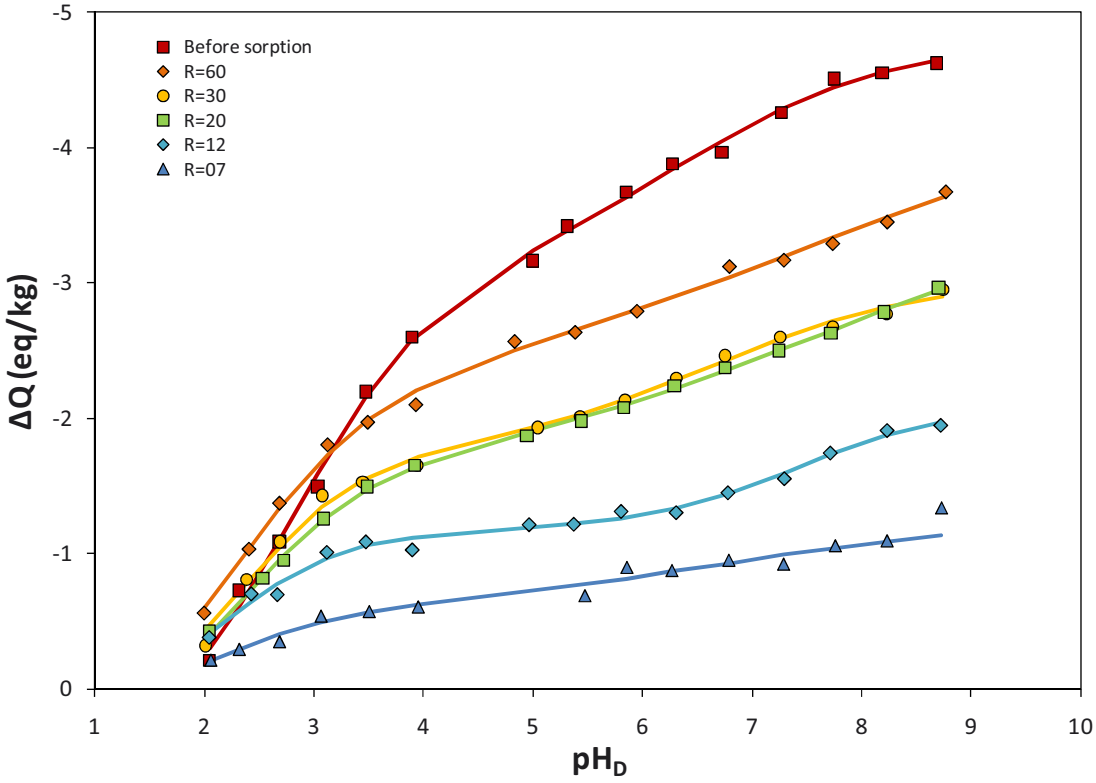

Figure 6. Calculated charge curves for the different supernatant titrations (data plots), depending on pH in the Donnan gel, and the corresponding fits (lines).

3.4 Modeling

Data modeling has been done in the NICA-Donnan formalism (Kinniburgh et al. 1999), optimizing the parameters with the software FIT (Kinniburgh 1993). The number of data points in the spectrophotometric titration curves is much lower than in the potentiometric ones. The parameters describing the charge vs. pH_{Donnan} curve for the original sample (before

adsorption) were re-calculated using spectrophotometric data, for the sake of comparison with data from adsorption experiments. To constrain the calculation, first, Q_0 for the original sample as been set equal to the value found in potentiometric modeling, i.e., 0.6 eq/kg. This corresponds to 13% of ΔQ_{max}. The assumption made is that the proportion of Q_0 / ΔQ_{max} was specific of PAHA, and for the other samples Q_0 values have been fixed at 13% of the corresponding ΔQ_{max}.

The fitting obtained are satisfactory for all samples ($r^2 > 0.98$), but for 60 and 30 $mg_{PAHA}/g_{\alpha\text{-}Al_2O_3}$ the best fit was obtained for m_1 values larger than 1, which is difficult to explain within the framework of the model and regarding titrations data of various humic substances from the litterature (Milne et al. 2001). Except for these two values, m_1 is increasing with decreasing R value. Values of m_1 below 1 for these two ratios were optimized between surrounding values. The obtained parameters are shown in Table 2 and the corresponding fits are displayed on Figure 6.

Table 2. NICA-Donnan parameters for calculated charge from absorbance measurements after retention experiment (The fixed values are in italic).

	$\log\tilde{K}_1$	m_1	Q_1	$\log\tilde{K}_2$	m_2	Q_2	Q_0	Q_1+Q_2
Before sorption	2.80 ± 0.15	0.66 ± 0.09	3.63 ± 0.59	6.41 ± 0.50	0.45 ± 0.23	1.77 ± 0.79	*0.60*	5.40 ± 0.99
R=60	2.33 ± 0.07	*0.68*	2.56 ± 0.33	7.52 ± 1.37	0.23 ± 0.13	2.36 ± 1.32	*0.48*	4.92 ± 1.36
R=30	2.31 ± 0.07	*0.74*	2.16 ± 0.10	6.64 ± 0.23	0.47 ± 0.13	1.23 ± 0.21	*0.38*	3.39 ± 0.23
R=20	2.37 ± 0.03	0.74 ± 0.09	1.93 ± 0.27	7.72 ± 0.70	0.25 ± 0.10	2.19 ± 0.92	*0.38*	4.12 ± 0.96
R=12	2.14 ± 0.08	0.78 ± 0.16	1.42 ± 0.07	7.44 ± 0.33	0.60 ± 0.24	0.94 ± 0.25	*0.25*	2.36 ± 0.26
R=07	2.10 ± 0.20	0.78 ± 0.80	0.69 ± 0.78	6.63 ± 2.10	0.27 ± 0.67	0.79 ± 1.74	*0.17*	1.48 ± 1.91

The overall charge $Q_1 + Q_2$ decreases with the initial quantity of PAHA in the system, most of the reactive molecules being retained onto the mineral surface, their functional sites being either directly fixed to the surface via ligand exchange or via lateral interactions such as hydrophobic interactions (Ochs et al. 1994).

For the sake of clarity, the evolution of NICA-Donnan parameters with R and comparison to initial PAHA are plotted in Figure 7 (blue symbols). The progressive decrease of Q_1 with R shows a preferential adsorption of the molecules bearing the most reactive moieties. At experimental pH, i.e., 6.8 ± 0.3, around 96 % of low affinity-type (so-called carboxylic) sites

are deprotonated and more easily retained onto the positively-charged alumina surface, which results in a non-sorbed PAHA fraction depleted in these moieties. There is no apparent evolution of the number of high affinity-type (so-called phenolic) sites Q_2, which seems to be constant above R = 20 $mg_{PAHA}/g_{\alpha\text{-}Al_2O_3}$ and not significantly different from the original PAHA. However, it is lower for remaining PAHA fraction in solution at the two lowest ratios. This is consistent with the loss of aromaticity observed from the UV/Visible spectra for these supernatants (see Figure 3).

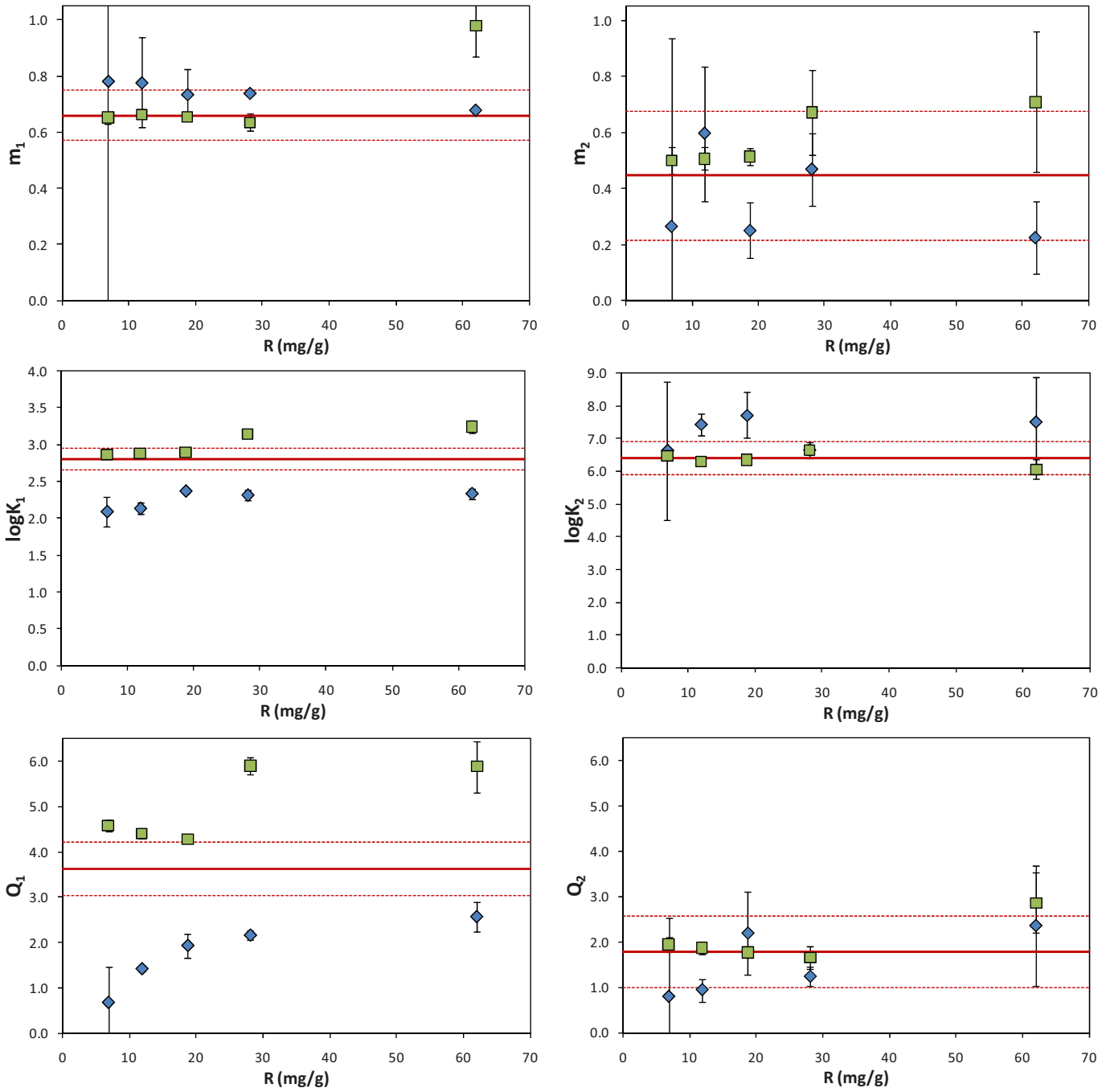

Figure 7. NICA-Donnan parameters for the dissolved (blue) and adsorbed (green) fractions of PAHA, compared to the initial value (red line). Errors bars are equal to σ.

The heterogeneity parameter m_1 increases with decreasing ratio. This would mean that low affinity-type sites of PAHA fraction in solution are more homogeneous than initial PAHA. When fractionation is more important, the apparent homogeneity of low affinity-type sites increases too. We can not conclude regarding the evolution of m_2, which is variable but not significantly different from the original value. This is due to experimental pH, i.e., 6.8 ± 0.3, under which the majority of phenolic-type sites are not deprotonated ($\log\tilde{K}_2$ = 8.7 at I = 0.1 M). Results would have been different if experiments have been done at another equilibrium pH value. However, at higher pH, lower adsorption is expected (see Figure 1), which would induce little modifications in the non-sorbed fractions reactivity.

The $\log\tilde{K}_1$ values of supernatant fractions seem to slightly decrease with coverage ratio, which would mean a higher affinity for proton and a greater tendency for deprotonation. Previous works on adsorption of simple organic acids onto mineral oxides have shown that adsorption is maximal at the pH corresponding to the pK_a of the acid (Schulthess and McCarthy 1990; Gu et al. 1995). Some of these molecules, often considered as analogs of humic substances, show a maximum of adsorption below pH 4: it is the case of benzoic acid onto goethite (Evanko and Dzombak 1998), phtalic acid onto hematite (Gu et al. 1995) or salicylic acid onto δ-alumina (Kraemer et al. 1998). For these molecules, there is almost no more adsorption at pH higher than 6. By analogy, at the pH of our experiment (6.8) , those molecules would be very weakly sorbed. The lower value of $\log\tilde{K}_1$ for the humic molecules found in the supernatants regarding the original value may be related to the presence in these molecules of such organic moieties with very low pK_a (3.0 for salicylic acid, 4.2 for benzoic acid and 2.9 for the first pK_a of phtalic acid).

It is difficult to conclude regarding the evolution of $\log\tilde{K}_2$, which values seem higher in the non-sorbed PAHA molecules than in the original bulk PAHA. This would mean that organic molecules with lowest $\log\tilde{K}_2$, i.e. moieties first ionized when pH increases, are preferentially adsorbed onto the surface.

However, it must be highlighted that these parameters are fitted from 15-points data sets, and that the correlation matrices show a strong correlation between Q_1, m_2 and Q_2, as shown in Table 3. Precautions must then be taken when discussing them.

Table 3. Correlation matrices from NICA-Donnan parameters optimization of non-sorbed PAHA fractions.

R = 60 mg/g	log K1	Q1	log K2	m2	Q2
log K1	1				
Q1	-0.423	1			
log K2	0.759	-0.620	1		
m2	-0.666	**0.928**	-0.855	1	
Q2	0.670	-0.884	0.914	**-0.986**	1

R = 30 mg/g	log K1	Q1	log K2	m2	Q2
log K1	1				
Q1	0.819	1			
log K2	0.247	0.138	1		
m2	0.546	0.815	-0.343	1	
Q2	-0.618	-0.855	0.364	**-0.950**	1

R = 20 mg/g	log K1	m1	Q1	log K2	m2	Q2
log K1	1					
m1	-0.469	1				
Q1	0.458	**-0.932**	1			
log K2	0.004	0.624	-0.780	1		
m2	0.306	-0.865	**0.975**	-0.895	1	
Q2	-0.273	0.844	**-0.957**	**0.927**	**-0.995**	1

R = 12 mg/g	log K1	m1	Q1	log K2	m2	Q2
log K1	1					
m1	-0.035	1				
Q1	0.503	-0.763	1			
log K2	-0.148	0.139	-0.266	1		
m2	0.424	-0.559	0.810	-0.685	1	
Q2	-0.404	0.547	-0.778	0.788	**-0.944**	1

R = 7 mg/g	log K1	m1	Q1	log K2	m2	Q2
log K1	1					
m1	-0.179	1				
Q1	0.091	-0.900	1			
log K2	0.572	0.017	-0.291	1		
m2	-0.096	-0.785	**0.964**	-0.520	1	
Q2	0.074	0.803	**-0.967**	0.524	**-0.997**	1

In order to study the modifications of PAHA reactivity in the two fractions due to adsorption, the charging behavior of adsorbed PAHA fraction is still missing. From DOC measurements, the proportion of dissolved and adsorbed fractions can be calculated for each coverage ratio. It seems then possible from mass balance to calculate the charge of the adsorbed PAHA fraction. Results are plotted in Figure 8.

Site densities of adsorbed fractions seem higher than the one of original PAHA: most reactive fractions seem to preferentially adsorb onto the oxide surface. Before saturation of the surface is reached, i.e. $R < 30\ mg_{PAHA}/g_{\alpha\text{-}Al_2O_3}$ (see Figure 2), there is almost no difference between charging behavior of adsorbed fractions. But once saturation is reached, it seems that charge is increasing with R.

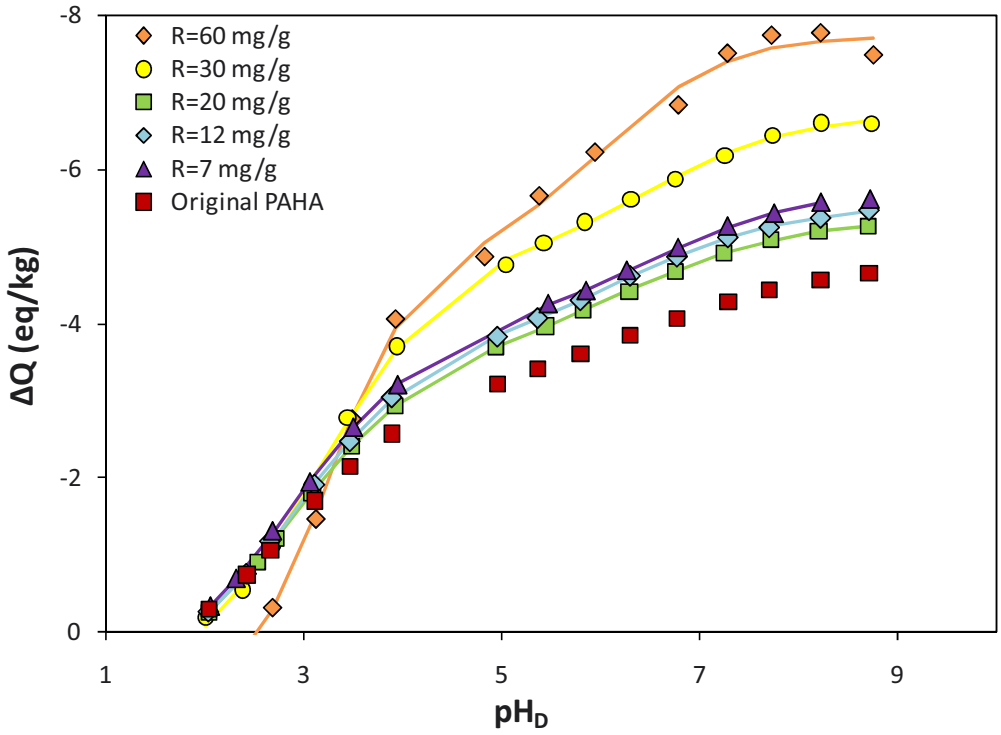

Figure 8. Calculated charge curves for adsorbed fractions of PAHA.

The modeling of the charging curves of adsorbed fractions is then done as previously for the fraction in solution, to characterize an evolution of the NICA-Donnan parameters with adsorption. The hypothesis of a constant Q_0 / ΔQ_{max} was applied in this case too. The evolutions of the different parameters with initial coverage ratio R, compared to the results for dissolved fraction and original material, are shown in Figure 7 (green symbols). The $\log\tilde{K}_1$ values of PAHA adsorbed fractions are similar to the ones of original PAHA for $R < 30\ mg_{PAHA}/g_{\alpha\text{-}Al_2O_3}$. For the highest R values, when saturation of the surface is reached,

the $\log\tilde{K}_1$ values slightly increase, while the apparent homogeneity of the low-affinity sites distribution m_1 increases too. It is difficult to conclude about m_1 value at $R = 60\ mg_{PAHA}/g_{\alpha\text{-}Al_2O_3}$, which is most likely due to the steep slope of the charging curve at low pH (see Figure 8), which is itself due to the slightly higher charge obtained for the corresponding non-sorbed fraction compared to the original sample. The charge is always higher in the adsorbed fraction than in the original material. The quantity of low affinity-type sites seems to be always significantly higher in the sorbed fraction than in the dissolved one, due to the preferential adsorption of fractions bearing the most reactive moieties. The saturation seems to be reached for $Q_1 = 6$ eq/kg.

As a consequence of the non-sorbed fraction parameters, there is no apparent evolution of both the $\log\tilde{K}_2$ and m_2 values, comparable to the value of original PAHA. They are inside the statistical envelope $m_2 \pm \sigma(m_2)$ of the original PAHA, even if the values obtained for $R \geq 30\ mg_{PAHA}/g_{\alpha\text{-}Al_2O_3}$ are slightly higher. This would mean that the functional sites in the adsorbed fraction are more homogeneous when saturation is reached. Except for the fraction at $R = 60\ mg_{PAHA}/g_{\alpha\text{-}Al_2O_3}$, Q_2 value of adsorbed PAHA fraction are the same as original material. For the highest concentration, Q_2 is slightly higher.

From these measurements it appears that fractionation due to adsorption of PAHA onto $\alpha\text{-}Al_2O_3$ mostly impact the low affinity type sites, which are almost totally ionized at the experimental pH $\approx$ 6.8. The difficulty to find any trend for high affinity type sites behavior may be due to the slight variations of pH value between the different batch solutions, which have a large impact on the ionization of these functional sites at the chosen experimental pH.

Spectrophotometric measurements are a useful technique to study variations of PAHA protonation behavior due to adsorption onto a mineral surface. However, it seems essential to have titration curves with more data, in order to have better constrained fits. This would require setting up a coupled titrator – UV/Visible spectrophotometer set-up, to let the experiment run continuously long enough, and would avoid carbonation of the solutions as well as material loss during samplings. It would also be important to do the same study at different experimental pH, in order to characterize PAHA reactivity modifications due to adsorption throughout a large pH range.

REFERENCES

Alliot, C., Bion L., et al. (2005). "Sorption of aqueous carbonic, acetic, and oxalic acids onto alpha-alumina." *Journal of Colloid and Interface Science* **287**(2): 444-451.

Boily, J. F. and Fein J. B. (2000). "Proton binding to humic acids and sorption of Pb(II) and humic acid to the corundum surface." *Chemical Geology* **168**(3-4): 239-253.

Chin, Y. P., Aiken G., et al. (1994). "Molecular weight, polydispersity, and spectroscopic properties of aquatic humic substances." *Environmental Science & Technology* **28**(11): 1853-1858.

Chorover, J. and Amistadi M. K. (2001). "Reaction of forest floor organic matter at goethite, birnessite and smectite surfaces." *Geochimica Et Cosmochimica Acta* **65**(1): 95-109.

Claret, F., Schafer T., et al. (2008). "Fractionation of Suwannee River Fulvic Acid and Aldrich Humic Acid on alpha-Al2O3: Spectroscopic Evidence." *Environmental Science & Technology* **42**(23): 8809-8815.

Davis, J. A. and Gloor R. (1981). "Adsorption of dissolved organics in lake water by aluminum-oxide - effect of molecular weight." *Environmental Science & Technology* **15**(10): 1223-1229.

Dryer, D. J., Korshin G. V., et al. (2008). "In situ examination of the protonation behavior of fulvic acids using differential absorbance spectroscopy." *Environmental Science & Technology* **42**(17): 6644-6649.

Evanko, C. R. and Dzombak D. A. (1998). "Influence of structural features on sorption of NOM-analogue organic acids to goethite." *Environmental Science & Technology* **32**(19): 2846-2855.

Fairhurst, A. J. and Warwick P. (1998). "The influence of humic acid on europium-mineral interactions." *Colloids and Surfaces a-Physicochemical and Engineering Aspects* **145**(1-3): 229-234.

Filius, J. D., Lumsdon D. G., et al. (2000). "Adsorption of fulvic acid on goethite." *Geochimica Et Cosmochimica Acta* **64**(1): 51-60.

Gu, B. H., Mehlhorn T. L., et al. (1996). "Competitive adsorption, displacement, and transport of organic matter on iron oxide .1. Competitive adsorption." *Geochimica Et Cosmochimica Acta* **60**(11): 1943-1950.

Gu, B. H., Schmitt J., et al. (1995). "Adsorption and desorption of different organic-matter fractions on iron-oxide." *Geochimica Et Cosmochimica Acta* **59**(2): 219-229.

Huber, S. A., Balz A., et al. (2011). "Characterisation of aquatic humic and non-humic matter with size-exclusion chromatography - organic carbon detection - organic nitrogen detection (LC-OCD-OND)." *Water Research* **45**(2): 879-885.

Hur, J. and Schlautman M. A. (2003). "Molecular weight fractionation of humic substances by adsorption onto minerals." *Journal of Colloid and Interface Science* **264**(2): 313-321.

Hur, J. and Schlautman M. A. (2004). "Effects of pH and phosphate on the adsorptive fractionation of purified Aldrich humic acid on kaolinite and hematite." *Journal of Colloid and Interface Science* **277**(2): 264-270.

Janot, N., Reiller P. E., et al. (2010). "Using Spectrophotometric Titrations To Characterize Humic Acid Reactivity at Environmental Concentrations." *Environmental Science & Technology* **44**(17): 6782-6788.

Kang, S. H. and Xing B. S. (2008). "Humic acid fractionation upon sequential adsorption onto goethite." *Langmuir* **24**(6): 2525-2531.

Kim, J. I., Buckau G., et al. (1990). "Characterization of humic and fulvic-acids from Gorleben groundwater." *Fresenius Journal of Analytical Chemistry* **338**(3): 245-252.

Kinniburgh, D. G. (1993). FIT Non-linear Optimization Algorithm and User Manual. Nottingham, UK, British Geological Survey.

Kinniburgh, D. G., van Riemsdijk W. H., et al. (1999). "Ion binding to natural organic matter: competition, heterogeneity, stoichiometry and thermodynamic consistency." *Colloids and Surfaces a-Physicochemical and Engineering Aspects* **151**(1-2): 147-166.

Korshin, G. V., Kumke M. U., et al. (1999). "Influence of chlorination on chromophores and fluorophores in humic substances." *Environmental Science & Technology* **33**(8): 1207-1212.

Kraemer, S. M., Chiu V. Q., et al. (1998). "Influence of pH and competitive adsorption on the kinetics of ligand-promoted dissolution of aluminum oxide." *Environmental Science & Technology* **32**(19): 2876-2882.

Meier, M., Namjesnik-Dejanovic K., et al. (1999). "Fractionation of aquatic natural organic matter upon sorption to goethite and kaolinite." *Chemical Geology* **157**(3-4): 275-284.

Milne, C. J., Kinniburgh D. G., et al. (2001). "Generic NICA-Donnan model parameters for proton binding by humic substances." *Environmental Science & Technology* **35**(10): 2049-2059.

Murphy, R. J., Lenhart J. J., et al. (1999). "The sorption of thorium (IV) and uranium (VI) to hematite in the presence of natural organic matter." *Colloids and Surfaces a-Physicochemical and Engineering Aspects* **157**(1-3): 47-62.

Ochs, M., Cosovic B., et al. (1994). "Coordinative and hydrophobic interaction of humic substances with hydrophilic Al2O3 and hydrophobic mercury surfaces." *Geochimica Et Cosmochimica Acta* **58**(2): 639-650.

Peuravuori, J. and Pihlaja K. (1997). "Molecular size distribution and spectroscopic properties of aquatic humic substances." *Analytica Chimica Acta* **337**(2): 133-149.

Reiller, P., Amekraz B., et al. (2006). "Sorption of Aldrich humic acid onto hematite: Insights into fractionation phenomena by electrospray ionization with quadrupole time-of-flight mass spectrometry." *Environmental Science & Technology* **40**(7): 2235-2241.

Reiller, P., Moulin V., et al. (2002). "Retention behaviour of humic substances onto mineral surfaces and consequences upon thorium (IV) mobility: case of iron oxides." *Applied Geochemistry* **17**(12): 1551-1562.

Robertson, A. P. and Leckie J. O. (1994). Humic acid/goethite interactions and their effect on copper binding. *Humic substances in the global environment and implication on human health*. N. Senesi and T. M. Miano, Elsevier**:** 487-492.

Saito, T., Koopal L. K., et al. (2004). "Adsorption of humic acid on goethite: Isotherms, charge adjustments, and potential profiles." *Langmuir* **20**(3): 689-700.

Sakuragi, T., Sato S., et al. (2004). "Am(III) and Eu(III) uptake on hematite in the presence of humic acid." *Radiochimica Acta* **92**(9-11): 697-702.

Schlautman, M. A. and Morgan J. J. (1994). "Adsorption of aquatic humic substances on colloidal-size aluminum-oxide particles - Influence of solution chemistry." *Geochimica Et Cosmochimica Acta* **58**(20): 4293-4303.

Schulthess, C. P. and McCarthy J. F. (1990). "Competitive adsorption of aqueous carbonic and acetic-acids by an Aluminum-oxide." *Soil Science Society of America Journal* **54**(3): 688-694.

Vermeer, A. W. P., McCulloch J. K., et al. (1999). "Metal ion adsorption to complexes of humic acid and metal oxides: Deviations from the additivity rule." *Environmental Science & Technology* **33**(21): 3892-3897.

Vermeer, A. W. P., van Riemsdijk W. H., et al. (1998). "Adsorption of humic acid to mineral particles. 1. Specific and electrostatic interactions." *Langmuir* **14**(10): 2810-2819.

Weishaar, J. L., Aiken G. R., et al. (2003). "Evaluation of specific ultraviolet absorbance as an indicator of the chemical composition and reactivity of dissolved organic carbon." *Environmental Science & Technology* **37**(20): 4702-4708.

Weng, L. P., Van Riemsdijk W. H., et al. (2007). "Adsorption of humic acids onto goethite: Effects of molar mass, pH and ionic strength." *Journal of Colloid and Interface Science* **314**(1): 107-118.

Zhou, Q. H., Maurice P. A., et al. (2001). "Size fractionation upon adsorption of fulvic acid on goethite: Equilibrium and kinetic studies." *Geochimica Et Cosmochimica Acta* **65**(5): 803-812.

CHAPITRE 4

COLLOIDAL α-Al_2O_3, EUROPIUM(III) AND HUMIC SUBSTANCES INTERACTIONS: A MACROSCOPIC AND SPECTROSCOPIC STUDY

Noémie Janot[1,2], Marc F. Benedetti[1], Pascal E. Reiller[2]

[1] Laboratoire de Géochimie des Eaux, Université Paris Diderot, IPGP, UMR CNRS 7154, Case Postale 7052, 75025 Paris, Cedex 13, France.

[2] CEA Saclay, CEA/DEN/DANS/DPC/SECR, Laboratoire de Spéciation des Radionucléides et des Molécules, Bâtiment 391 PC 33, F-91191 Gif-sur-Yvette CEDEX, France.

Accepted in *Environmental Science & Technology*.

Part of the Nanoscale Metal-Organic Matter Interactions Special Issue.

RÉSUMÉ

Dans cette partie, l'adsorption de Eu(III) sur α-Al_2O_3 en présence d'acide humique Aldrich purifié (PAHA) est étudiée au moyen d'expériences en batch et de spectrofluorimétrie laser à résolution temporelle (SLRT). Ces expériences ont été réalisées à différents pH, à force ionique constante (0.1 mol/L $NaClO_4$), 10^{-6} mol/L Eu(III), 1 g/L α-Al_2O_3 et 28 mg/L PAHA, ce qui assure une complexation totale Eu(III)/PAHA.

L'adsorption de Eu(III) sur l'alumine présente un front de sorption attendu à pH 7, modifié en présence de PAHA : à pH < 6,5, la présence de PAHA augmente fortement la rétention de l'europium(III) sur la surface, alors qu'elle la diminue à pH intermédiaire (6.5 < pH < 8). La présence d'Eu(III) augmente légèrement l'adsorption de PAHA sur α-Al_2O_3 sur toute la gamme de pH étudiée (4-10).

Les évolutions des spectres de luminescence et les temps de décroissance des systèmes binaires (Eu(III)/α-Al_2O_3 et Eu(III)/PAHA) indiquent une augmentation de la complexation surfacique et humique lorsque le pH augmente. La décroissance de luminescence bi-exponentielle est observée à tous les pH pour le système Eu(III)/PAHA, la composante la plus rapide étant indépendante du pH de la solution. Dans le système ternaire Eu(III)/PAHA/α-Al_2O_3, l'existence de cette décroissance bi-exponentielle observée à toutes les valeurs de pH signifie que l'Eu(III) se trouve toujours au voisinage direct de la substance humique. En dessous de pH 7, les spectres de l'Eu(III) dans le système ternaire ne sont pas différents de ceux de l'Eu(III) en contact avec uniquement PAHA, ce qui implique un complexe de symétrie identique. Cependant, l'augmentation du temps de décroissance de la luminescence dans le cas du système ternaire indique un changement de la conformation de PAHA sur la surface minérale. A pH élevé, en revanche, l'influence de la surface minérale sur la spéciation de l'Eu(III) dans le système ternaire est remarquable sur les spectres de luminescence : décalage de la longueur d'onde maximale pour la transition $^5D_0 \rightarrow {}^7F_2$, élargissement de la transition $^5D_0 \rightarrow {}^7F_1$.

ABSTRACT

Eu(III) sorption onto α-Al_2O_3 in the presence of purified Aldrich humic acid (PAHA) is studied by batch experiments and time-resolved laser-induced luminescence spectroscopy of Eu(III). Experiments are conducted at varying pH, at 0.1 mol/L $NaClO_4$, 10^{-6} mol/L Eu(III), 1 g/L α-Al_2O_3 and 28 mg/L PAHA, which assured a complete Eu(III)-PAHA complexation. Adsorption of Eu(III) presents the expected pH-edge at 7, which is modified by addition of PAHA. Presence of Eu(III) slightly increases PAHA sorption throughout the pH range. The evolutions of luminescence spectra and decay times of the binary systems, that is, Eu(III)/α-Al_2O_3 and Eu(III)/PAHA, indicate a progressive surface- and humic-complexation with increasing pH. The typical biexponential luminescence decay in Eu(III)/PAHA system is also recorded, the fastest deactivation depending barely on pH. In ternary Eu(III)/PAHA/α-Al_2O_3 system, the existence of a luminescence biexponential decay for all pH means that Eu(III) is always in the direct neighborhood of the humic substance. Below pH 7, the spectra of the ternary system (Eu(III)/PAHA/α-Al_2O_3) are not different from the ones of Eu(III)/PAHA system, implying the same complex symmetry. Nevertheless, the increase of luminescence decay time points to a change in PAHA conformation onto the surface.

1 Introduction

Natural organic matter (NOM) interactions with mineral colloids in soils partly control the speciation and migration of heavy metals as well as nanoparticles in the environment, and notably of lanthanides and actinides (McCarthy et al. 1998; McCarthy et al. 1998). The modeling of ternary systems consisting of metal/NOM/mineral surface has often led to discrepancies. Particularly, the additivity of the binary systems was not fulfilled (Vermeer et al. 1999; Christl and Kretzschmar 2001). In some examples, successful modeling exercises were proposed for fulvic acids (Heidmann et al. 2005; Weng et al. 2008). These samples can be assumed to be more or less similar to simple organic molecules (Schulthess and McCarthy 1990). Fulvic acids (FA) sorption is stable or decreases with increasing ionic strength (Schlautman and Morgan 1994; Filius et al. 2000; Weng et al. 2006), whereas sorption of humic acids (HA) onto oxides increases with ionic strength (Murphy et al. 1994; Schlautman and Morgan 1994; Weng et al. 2006). Hence, it is still difficult to propose interpretations of HA effects on the modeling of ternary systems in a wide parametric space (Vermeer et al. 1999; Lippold and Lippmann-Pipke 2009). Moreover, heterogeneous composition and nature of HA (Rice and Lin 1993; MacCarthy 2001), and constant modification of HA aggregates with physicochemical conditions of the solution (Conte and Piccolo 1999) or due to sorption (Hur and Schlautman 2003; Claret et al. 2008) do not ease the modeling of these systems. The accurate understanding and description of the HA-containing systems are still under discussion. A better description of these systems is still needed to improve the understanding of the behavior of metals and nanoparticles in the environment.

One way to obtain both macroscopic and spectroscopic information on Ln/An(III) sorption onto mineral surfaces is through time-resolved laser-induced luminescence spectroscopy (TRLS). Due to their luminescence properties, one can have a direct insight on speciation of the ions in solution, in contact with humic substances (Thomason et al. 1996; Kumke et al. 2005; Marang et al. 2008; Brevet et al. 2009; Marang et al. 2009; Reiller and Brevet 2010) as well as sorbed onto mineral surfaces (Rabung et al. 2005; Huittinen et al. 2009) or in ternary systems (Tan et al. 2008). Measurements can be made at low metal ion concentration, to get as close as possible to environmental concentrations. TRLS has been used in either combination of the ternary systems, but up to now no direct comparison has been done between the two binary systems and the corresponding ternary system in a whole range of pH.

The aim of this study was to investigate the influence of Aldrich humic acid on the behavior and the speciation of a lanthanide, europium(III), as a chemical analog of An(III), in presence

or absence of α-Al_2O_3. Aluminum oxides are not the more frequent mineral surfaces found in the environment, but their aluminol surface sites are part of aluminosilicates reactive sites, very abundant in natural systems. Besides, its transparency for light allows spectroscopic measurements with mineral in solution, contrary to iron oxides (Huittinen et al. 2009). Macroscopic and spectroscopic experiments have been carried out to see the influence of pH on the evolution of the different systems.

2 Experimental section

2.1 Materials

Commercial Aldrich humic acid was purified (PAHA) according to Kim et al. (1990). Stock suspension at 1 g/L has been prepared by diluting PAHA in NaOH (pH around 10) in order to completely dissolve the sample. The solution was then stored in the dark under N_2. Proton exchange capacity was determined by potentiometry and found at 6.12 eq/kg (Janot et al. 2010). Alumina (α-Al_2O_3) was purchased from Interchim (pure 99.99%, size fraction 200–500 nm). The solid was washed thrice with carbonate-free NaOH and thrice with Millipore water before drying and storage at room temperature under N_2 atmosphere according to Alliot et al. (2005). The specific surface area measured by N_2-BET method was 15 m^2/g. Point of zero charge was determined by acid-base titrations and found at pH = 9.4 (data not shown). Europium(III) stock solution (10^{-3} mol/L) was obtained from the dissolution of Eu_2O_3 (Johnson Matthey, 99.99%) in $HClO_4$. All solutions were prepared using freshly boiled milli-Q water.

2.2 Methods

Batch contact experiments were conducted in 10.4 mL Beckman centrifugation tubes (355603). The different concentrations of compounds were 1 g/L of α-Al_2O_3, 10^{-6} mol/L of Eu(III) and 28 mg/L of PAHA, which assured a complete complexation of Eu(III) by PAHA (see Milne et al. (2003) and Marang et al. (2008), confirmed by Figure 1).

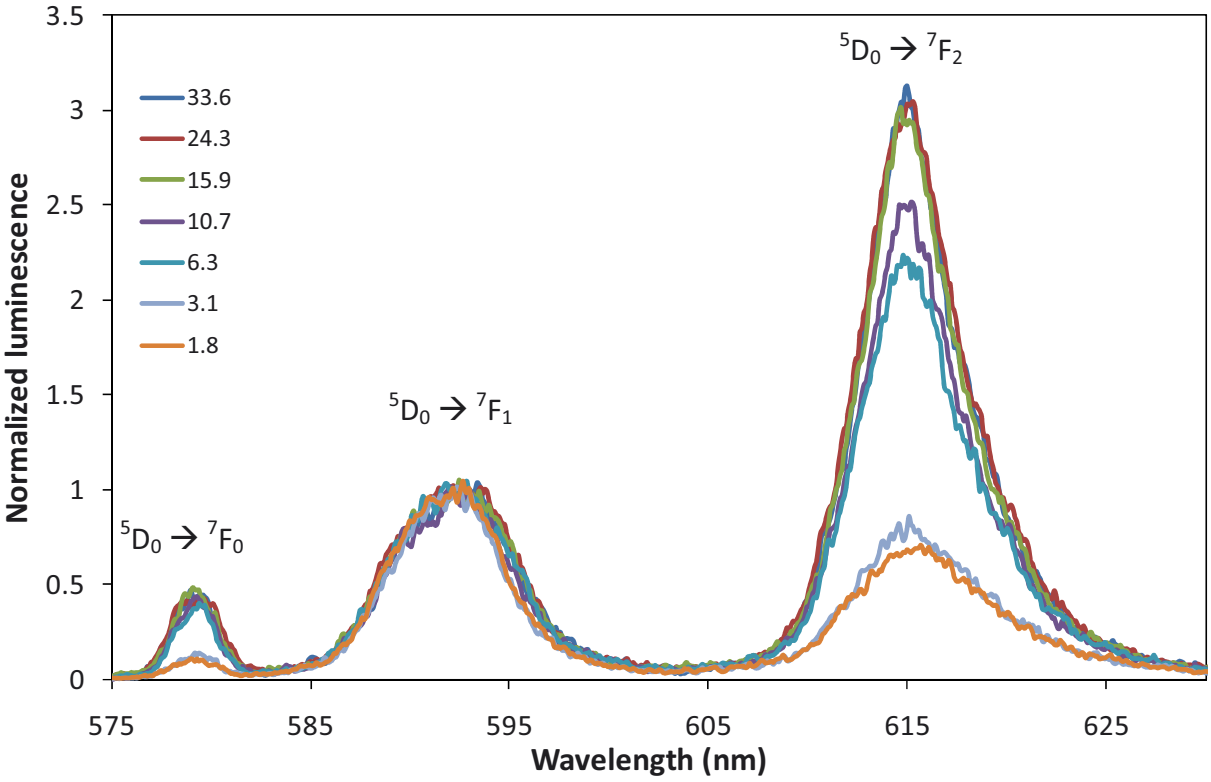

Figure 1. TRLS spectra of europium(III) complexed by PAHA at varying concentration (mg/L) at pH 4; [Eu(III)] = 10^{-6} mol/L, *I* = 0.1 mol/L $NaClO_4$. Spectra are normalized to the mean of five points around the maximum value of the $^5D_0 \rightarrow {}^7F_1$ transition.

First solid α-Al_2O_3, then PAHA and Eu(III) stock solutions and finally freshly degassed electrolyte solutions were weighed, with no specific contact time applied between additions. To minimize carbonation of the systems, nitrogen was swept on the top of the solution before closing the tubes. Ionic strength was fixed at 0.1 mol/L $NaClO_4$. The pH values of the solutions were adjusted by addition of fresh 0.1 mol/L $HClO_4$ and NaOH solutions. They were measured using one combined glass electrode (Radiometer Analytical) connected to a Radiometer Analytical pH Meter. To prevent $KClO_4$ precipitation in the electrode frit, the electrode filling solution was modified with NaCl at 0.1 mol/L. The pH electrode was calibrated using buffer solutions (pH 4.01, 7.01, and 10.00). The solutions were applied to three-dimensional stirring for 3 days of equilibration at room temperature before pH measurements and analyses.

After equilibration, subsamples (2.4 mL) were taken from the centrifugation tubes and analyzed in quartz cuvettes (10 mm). Preliminary experiments showed no significant differences between aliquots taken from one same tube. Eu(III) laser-induced properties were studied in contact with either PAHA, or α-Al_2O_3, or both components using TRLS. The

excitation laser beam was generated by a 355 nm tripled output of a Continuum Nd:YAG laser, coupled to an optical parametric oscillator system (Panther II, Continuum, Santa Clara, CA). The time-resolved luminescence signal is collected at 90° and focused into an Acton spectrometer (slit 1 mm) equipped with 600 lines/mm grating. For the time-resolved detection, the luminescence signal was collected during a gate width L = 300 µs, at an initial gate delay D = 10 µs after the excitation by a laser flash. To increase the signal to noise ratio, 1000 accumulations were performed for each spectrum. To avoid the aggregation and settling of the samples occurring in α-Al_2O_3-containing systems, these samples were manually shaken between two measurements. All luminescence measurements were performed at ambient temperature (21 °C ± 2). The excitation wavelength was set at λ_{exc} = 393.8 nm. The observed luminescence corresponds to the transitions of the $^5D_0$ excited state to the ground ^7F_j manifold (Bünzli 1989). They are the $^5D_0 \rightarrow {}^7F_0$ transition, forbidden for magnetic and electric reasons ($\lambda_{max} \approx$ 580 nm), the $^5D_0 \rightarrow {}^7F_1$ magnetic dipole transition ($\lambda_{max} \approx$ 593 nm), and the $^5D_0 \rightarrow {}^7F_2$ "hypersensitive" transition ($\lambda_{max} \approx$ 615 nm) (Judd 1962; Ofelt 1962) (see Figure 1).

To characterize adsorbed amounts of PAHA and Eu(III) onto α-Al_2O_3, after equilibration the solutions were ultracentrifuged at 60000 rpm during 2 h. Concentration of PAHA in the supernatant was measured by a Shimadzu TOC-VCSH analyzer, calibrated in concentration of PAHA between 0 and 50 mg_{HA}/L. The quantification of nonsorbed Eu(III) was made using TRLS using the standard addition method (Berthoud et al. 1989), diluting an aliquot of the supernatant in K_2CO_3 3 mol/L. This method allows determination of Eu(III) concentration down to 10^{-9} mol/L.

3 Results and Discussion

3.1 Macroscopic Adsorption Experiments

Figure 2 shows the influences of pH and Eu(III) on PAHA adsorption onto α-Al_2O_3. The humic acid sorption is typically decreasing when pH increases and α-Al_2O_3 surface becomes less positively charged, as for other oxides (Schlautman and Morgan 1994; Varadachari et al. 1997; Reiller et al. 2002). Adsorption is nevertheless significant throughout the pH range, going from 1.24 mg_{HA}/m^2 at pH 4.0 (i.e., 76% of initial amount of PAHA) to 0.61 mg_{HA}/m^2 at pH 8.8 (i.e., 37%). The presence of Eu(III) seems to homogeneously increase the retention of the humic substance onto α-Al_2O_3 surface throughout the pH range studied. For the ternary system, PAHA sorption goes from 1.60 mg_{HA}/m^2 at pH 3.9 (i.e., 88%) to 0.69 mg_{HA}/m^2 at pH 9.6 (i.e., 38%).

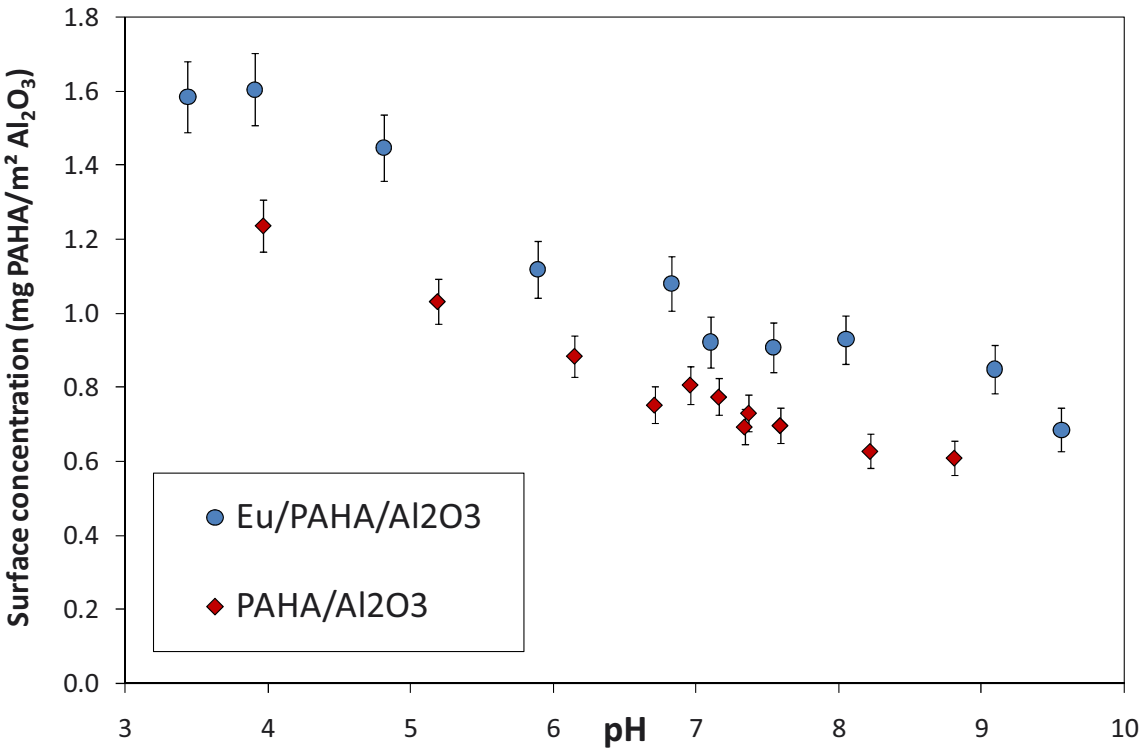

Figure 2. Surface concentration of PAHA on α-Al_2O_3 depending on pH, with (●) or without (◇) Eu(III). [α-Al_2O_3] = 1 g/L, $[PAHA]_{initial}$ = 26.5 ± 2 mg/L, $[Eu(III)]_{initial}$ = 10^{-6} mol/L, *I* = 0.1 mol/L $NaClO_4$. Error bars correspond to 2σ.

Schlautman and Morgan (1994) reported an increase of HA sorption onto γ-Al_2O_3 in presence of Ca^{2+} between pH 4 and 10 for different coverage rates (from 0.1 to 5.6 mg_{HA}/m^2) in 0.1 mol/L NaCl, but did not observe this increase in their Ca/FA/alumina system. Krepelova et al. (2006) also noticed this increase in sorption of HA in a U(VI)/HA/kaolinite system (initial ratio of 0.32 mg_{HA}/m^2), but only at 0.01 mol/L and not at 0.1 mol/L $NaClO_4$. The same trend was reported by Christl and Kretzschmar (2001) when studying fulvic acid sorption in a Cu/FA/hematite system in 0.01 $NaNO_3$ media (initial ratio of 0.68 mg_{FA}/m^2), but not at 0.03 and 0.1 mol/L. Weng et al. (2008) observed an increase of FA sorption in a Cu/FA/goethite system at 0.1 mol/L $NaNO_3$ for two initial FA concentrations, that is, 0.13 and 0.80 mg_{FA}/m^2. This latter value is closer to our organic matter-to-mineral ratio, that is, 1.86 mg_{HA}/m^2. However, the direct comparison between HA and FA may not be straightforward regarding the influence of ionic strength on FA and HA sorption (Murphy et al. 1994; Schlautman and Morgan 1994; Filius et al. 2000; Weng et al. 2006).

This increase of HS adsorption in ternary systems is often interpreted as the formation of a metal bridge between the negatively charge surface and humic binding sites, which is unlikely at pH 4, that is, before the sorption edge of Eu(III). Schlautman and Morgan (1994) attribute

this increase at low to neutral pH to hydrophobic bonding, polyvalent ions screening the repulsive charges of the humic molecule at the mineral surface and thus enhancing HA adsorption. One could also propose the variation of humic conformation induced by ionic strength (Avena et al. 1999; Rice et al. 1999) or agglomeration induced by complexation of Ln(III) (Caceci and Moulin 1991; Plaschke et al. 2002). The ratios between the different components, as well as the metal charge, may also play a major role.

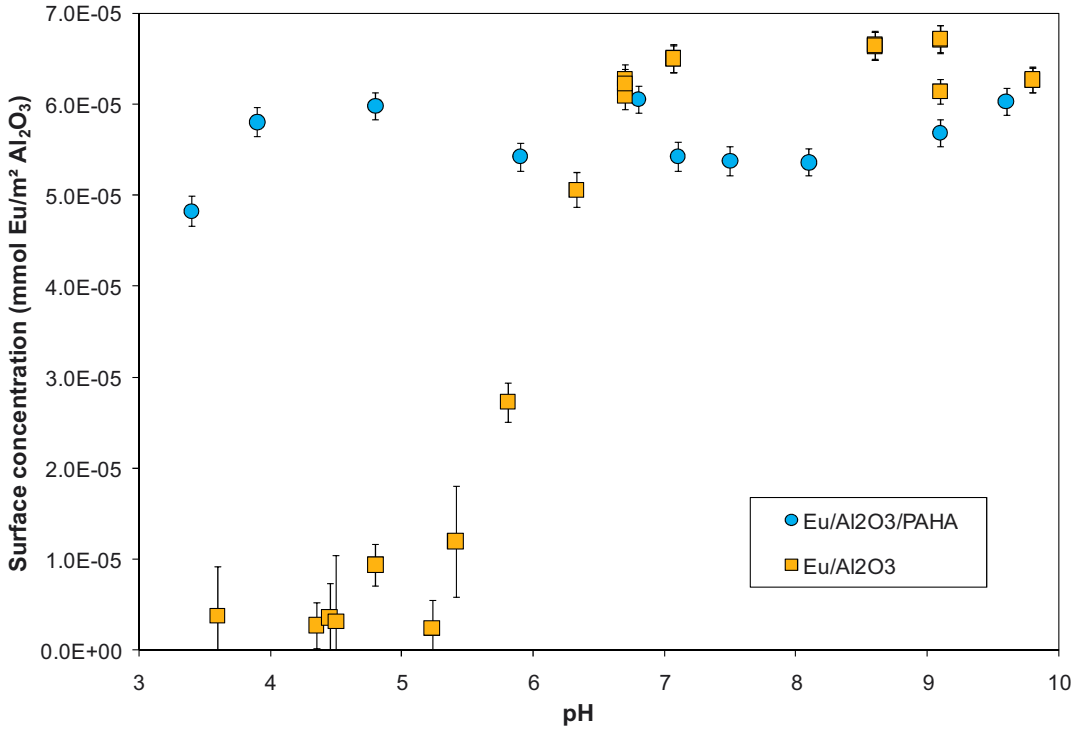

Figure 3. Surface concentration of Eu(III) on α-Al_2O_3 depending on pH, with (●) or without (□) PAHA. [α-Al_2O_3] = 1 g/L, $[PAHA]_{initial}$ = 28 mg/L, $[Eu(III)]_{initial}$ = 10^{-6} mol/L, *I* = 0.1 mol/L $NaClO_4$. Error bars correspond to 2σ.

Figure 3 shows the influence of pH and PAHA on Eu(III) adsorption onto α-Al_2O_3. In the binary Eu(III)/α-Al_2O_3 system, the adsorption curve shows the expected sorption-edge around pH 7 for Ln/An(III) (Righetto et al. 1991; Fairhurst et al. 1995; Fairhurst and Warwick 1998; Alliot et al. 2005), increasing from 3.5 × 10^{-6} mmol Eu/m² retained at pH 4.4, that is, 5% of initial amount of Eu(III), to 6.4 × 10^{-6} mmol Eu/m² at pH 9.8 (i.e., ≈100%). Inorganic speciation of Eu(III) using data from Hummel et al. (2002) is shown in Figure 4a.

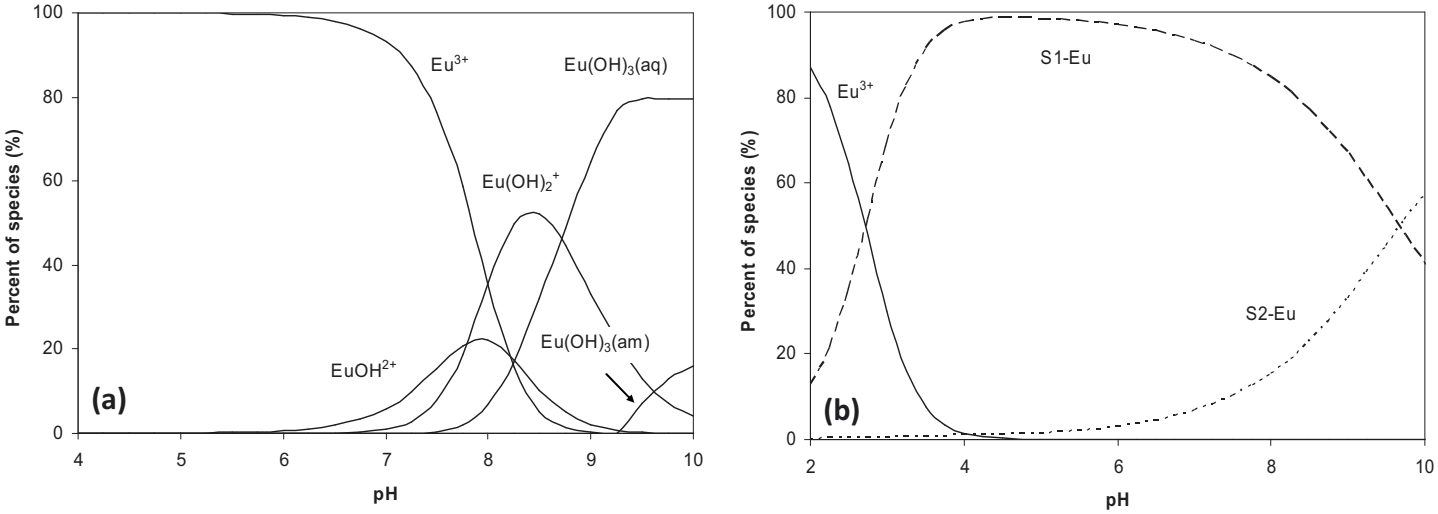

Figure 4. Inorganic (a) and humic (b) Eu(III) speciation in solution as a function of pH determined by ECOSAT, assuming no carbonation of the system. [PAHA] = 28 mg/L, [Eu(III)] = 10^{-6} mol/L, *I* = 0.1 mol/L $NaClO_4$.

Eu^{3+} is predominant up to pH 7, and then hydrolyzed species become the predominant ones. Eu(III) adsorption increases just before its first hydrolysis, as previously observed by Bradbury and Baeyens (2009) onto Illite. They have shown that surface complexation of metals is closely related to their first hydrolysis constants (Bradbury and Baeyens 2009).

As expected, presence of HA changes Eu(III) behavior: at pH < 6, PAHA enhances Eu(III) retention onto the surface (Fairhurst et al. 1995; Fairhurst and Warwick 1998). Around their first acidity constants, PAHA molecules, negatively charged, adsorb onto the positively charged oxide surface at low pH values, and Eu(III)-PAHA complexes adsorb onto the surface. The Eu(III)-PAHA speciation under our experimental conditions determined by ECOSAT software (Keizer and van Riemsdijk 1994) and generic data from Milne (2003) is shown in Figure 4b. At pH greater than 7, the presence of PAHA is slightly decreasing Eu(III) adsorption compared to the binary system, as previously observed in other metal-oxide systems (Fairhurst et al. 1995; Fairhurst and Warwick 1998; Reiller et al. 2002; Reiller et al. 2005; Tan et al. 2008). This is commonly thought to be due to the progressive decrease of HA sorption with increasing pH and the resulting competition for Eu(III) between adsorbed HA and HA in solution. At pH ≥ 8, the adsorption of Eu(III) onto the surface increases slightly again, resulting from the competition of Eu(III) between α-Al_2O_3 surface, surface-adsorbed PAHA, and dissolved PAHA.

3.2 Eu(III) Luminescence Analysis

Eu(III) luminescence spectra and decay times in the different systems were analyzed by TRLS at different pH. The peak shapes and asymmetry ratios, that is, $^5D_0 \rightarrow {}^7F_2$ to $^5D_0 \rightarrow {}^7F_1$ ($^7F_2/^7F_1$), provide information on Eu(III) speciation (Bünzli 1989). The calculation of ratios avoids us the necessity to take into account light attenuation for comparing the different systems, as this information is independent from the total luminescence recorded. The evolution of these ratios depending on pH is shown in Figure 5 for the different systems.

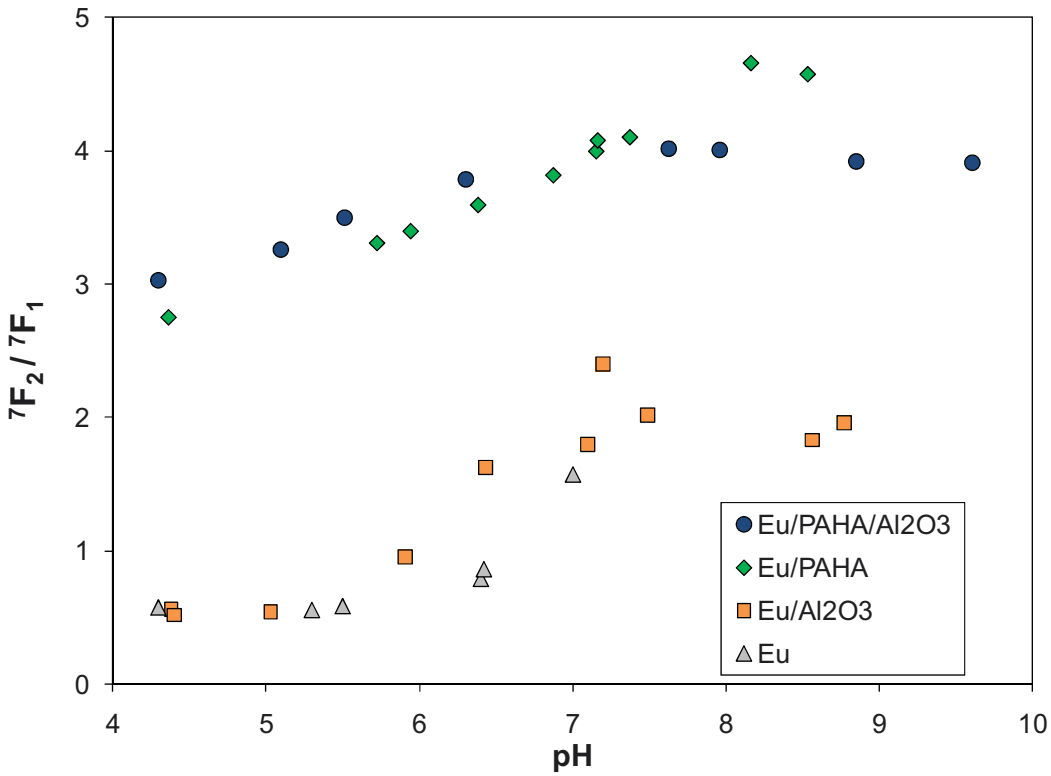

Figure 5. Evolution of $^5D_0 \rightarrow {}^7F_2/^5D_0 \rightarrow {}^7F_1$ ratio depending on pH; [α-Al_2O_3] = 1 g/L, $[PAHA]_{initial}$ = 28 mg/L, $[Eu(III)]_{initial}$ = 10^{-6} mol/L, *I* = 0.1 mol/L $NaClO_4$.

Luminescence decay times have been measured with delay steps of 10 to 25 µs. They are plotted against pH for the different systems in Figure 6. They have been adjusted to the decay of $^5D_0 \rightarrow {}^7F_1$ transition area (between 585 and 600 nm) (Kumke et al. 2005; Brevet et al. 2009; Reiller and Brevet 2010), as it is less sensitive to solution conditions (Judd 1962; Ofelt 1962).

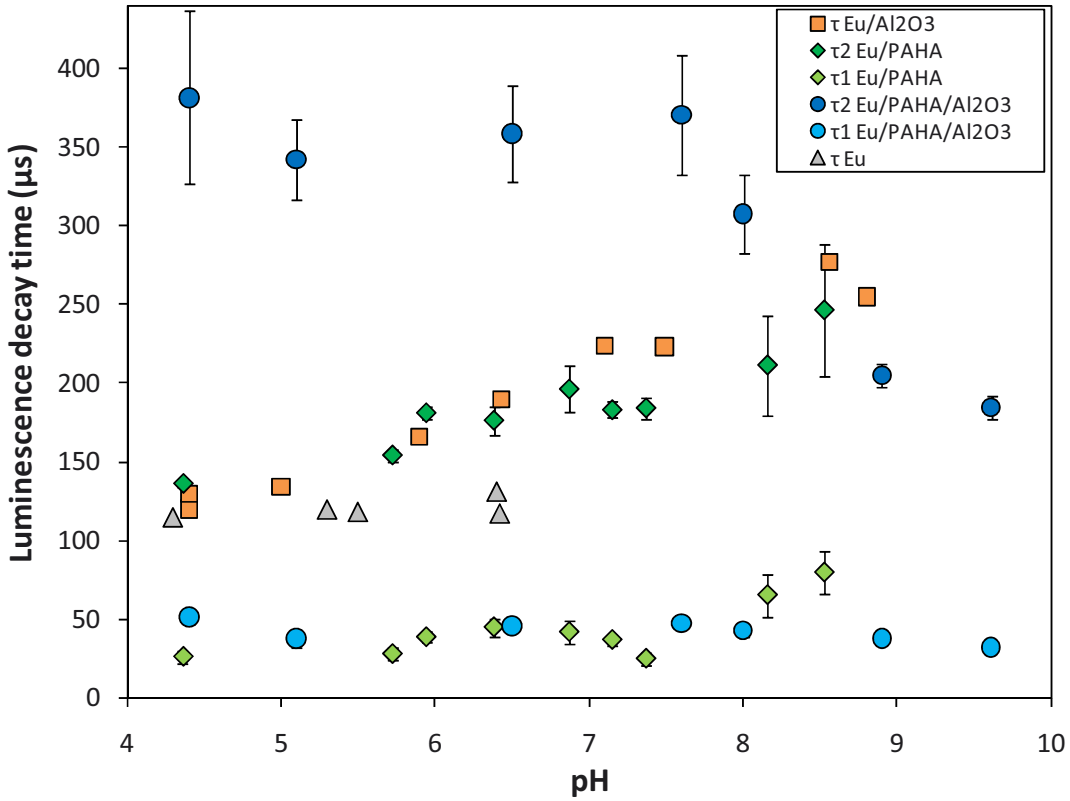

Figure 6. Evolution of Eu(III) luminescence decay times in contact with PAHA, α-Al_2O_3 or both compounds depending on pH; [α-Al_2O_3] = 1 g/L, $[PAHA]_{initial}$ = 28 mg/L, $[Eu(III)]_{initial}$ = 10^{-6} mol/L, *I* = 0.1 mol/L $NaClO_4$; Error bars correspond to 2σ.

3.2.1 Binary systems

As seen in Figure 5, the $^7F_2/^7F_1$ ratio in Eu(III)/α-Al_2O_3 system increases from 0.6 at pH 4.4 to 2.0 at pH 8.8. When pH increases, the possibility for Eu(III) to form surface complexes on α-Al_2O_3 is also increasing, as seen in macroscopic data. The $^5D_0 \rightarrow {}^7F_0$ transition appears for pH > 5.5, indicating a loss of symmetry in the ion environment above this pH value, which corresponds to the beginning of Eu(III) adsorption (Figure 3).

Monoexponential luminescence decay time (τ) of Eu(III) ions in binary Eu(III)/α-Al2O3 system increases with pH, from τ = 120 ± 3 µs at pH 4.4 to τ = 277 ± 5 µs at pH 8.8 (Figure 6). A greater luminescence decay time means that there is a higher probability for an excited Eu(III) ion to emit a photon than to lose energy through other nonradiative pathways, that is, quenching by water molecules, OH groups, and NH groups. The increase of τ is interpreted as the substitution of water molecules in the first coordination sphere of the luminescent ion (Horrocks and Sudnick 1979; Supkowski and Horrocks 2002). Here, the increase of τ from 120 µs to 277 µs would correspond to the loss of five water molecules according to Kimura et

al. (1998). Water molecules are supposed to be excluded from the first coordination sphere of Eu(III) when surface complexes are formed onto α-Al_2O_3. Nevertheless, this number must be taken carefully, as previous studies have shown that the relationship between luminescence decay time and the number of surrounding water molecules may depend on the system studied (Takahashi et al. 2000). One should better consider the more complete relationship determined otherwise (Horrocks and Sudnick 1979; Supkowski and Horrocks 2002), which requires the measure of the decay time in D_2O in all the three systems, which was out of the scope of this study.

In Eu(III)/PAHA systems, $^7F_2/^7F_1$ increases from 2.6 at pH 4.1 to 4.6 at pH 8.5 (Figure 5). There is apparently a continuous evolution of the chemical environment of Eu(III) throughout the pH range. This could be linked to the evolution of the type of bonding of Eu(III) within the humic structure (Morgenstern et al. 2000). The evolution parallels the Eu(III)/α-Al_2O_3 system at a different magnitude, with $^7F_2/^7F_1 > 1$ at all pH. In presence of PAHA, the $^5D_0 \rightarrow ^7F_0$ transition is always present (as in Figure 7 at pH 4.1). Together with the fact that the $^5D_0 \rightarrow ^7F_2$ transition is the most prominent one at all pH, this means that Eu(III) is always bound to the humic acid.

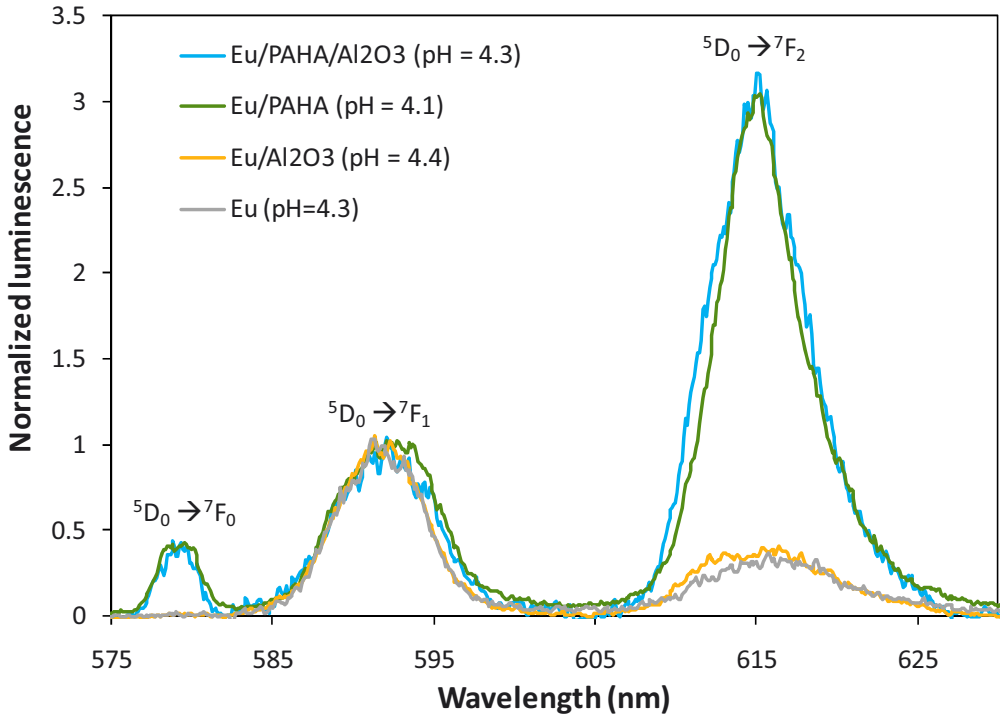

Figure 7. TRLS spectra of Eu(III) in contact with PAHA, α-Al_2O_3, both compounds or background electrolyte only, at pH = 4.2 ± 0.2. Spectra are normalized to the mean of five points around the maximum value of the $^5D_0 \rightarrow ^7F_1$ transition.

A typical biexponential luminescence decay is recorded throughout the pH range, with a short luminescence decay time ($\tau_1 < 70$ µs) and a longer one ($120 < \tau_2 < 250$ µs), as previously seen (Kumke et al. 2005; Brevet et al. 2009; Marang et al. 2009; Reiller and Brevet 2010) (Figure 6). The first decay time is shorter than free aqueous Eu^{3+} ($\tau \approx 114$ µs) (Horrocks and Sudnick 1979) and independent of pH, which suggests that this phenomenon barely depends on the chemical environment of Eu(III) and may be due to a fast exchange between Eu(III) and humic acid (Freyer et al. 2009; Reiller and Brevet 2010). Conversely, τ_2 continuously increases with pH from 137 ± 2 µs at pH 4.4 to 246 ± 42 µs at pH 8.5, which means that water molecules are progressively excluded from the coordination sphere of Eu(III) when pH increases.

3.2.2 Ternary system

A comparable ternary system was studied by Tan et al. by TRLS at pH 6.3 on hydrous alumina (mixture of bayerite, boehmite, and diaspore) and Chinese soil HA/FA (Tan et al. 2008). The direct comparison of the $^7F_2/^7F_1$ ratios may not be done (Brevet et al. 2009), but the trends can be compared. Recalculated $^7F_2/^7F_1$ from Tan et al. (2008) are equal to 2.0 in their Eu/hydrous alumina system and 5.0 in their Eu/HA system. In their ternary system Eu/HA/alumina, this value is equal to 4.8, which is similar to the Eu/HA binary system. Therefore, no, or only minor, changes in Eu(III) environment are expected between the HA-containing systems.

Here this behavior is probed for a wider pH range. The $^7F_2/^7F_1$ ratios of ternary Eu(III)/PAHA/α-Al_2O_3 system are much more important than in Eu(III)/α-Al_2O_3 system, and are slightly increasing from 3.0 at pH 4.3 to 4.0 at pH 7.6 (Figure 5). Above pH 7.6, the peak ratio is constant, but there is a shift from 615 to 617 nm of $^5D_0 \rightarrow {}^7F_2$ maxima accompanied with a change in peak shape (Figure 8), indicating a further change in Eu(III) chemical environment.

At pH < 7, the $^7F_2/^7F_1$ ratios of binary Eu(III)/PAHA or ternary Eu(III)/PAHA/α-Al_2O_3 systems are very close, as it was for Tan et al. at pH 6.3 (Tan et al. 2008). It seems that Eu(III) has a very similar environment in both systems, whether it is in binary system Eu(III)/PAHA or sorbed with PAHA onto α-Al_2O_3 in ternary system. This would suggest that throughout this pH range Eu(III) is directly linked to sorbed humic aggregates and has a limited access to the aluminol surface sites. Conversely, Tan et al. (2008) reported based on XPS that Eu(III) was

fixed to both components in the ternary system. This is not apparent here, as it was not in their TRLS spectra.

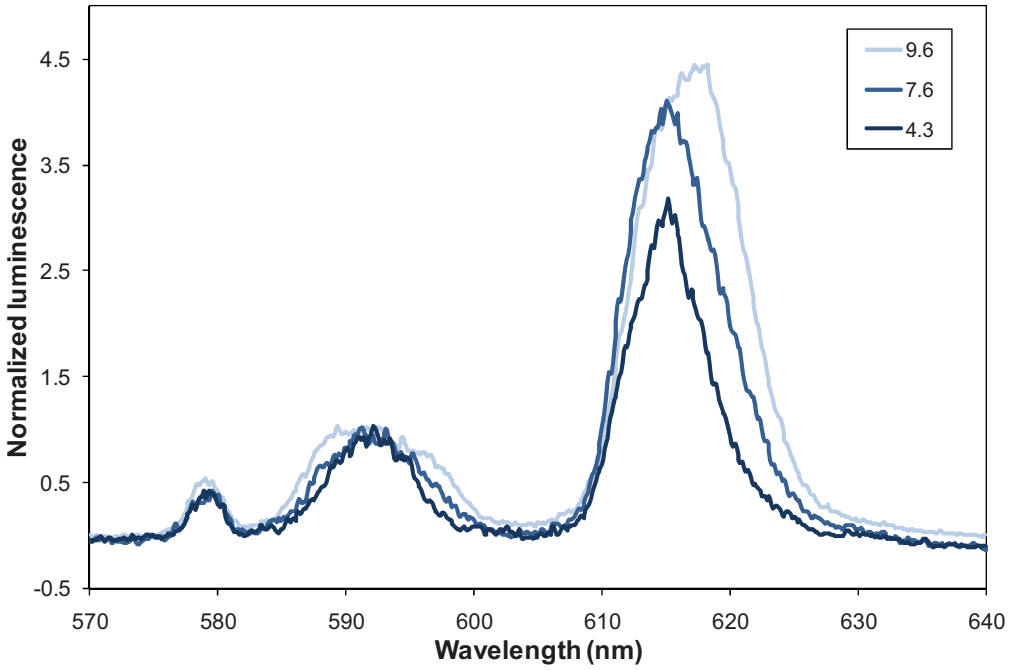

Figure 8. Evolution of Eu(III) luminescence spectra in the ternary system at pH = 4.3, 7.6, and 9.6. Spectra are normalized to the mean of five points around the maximum value of the $^5D_0 \rightarrow {}^7F_1$ transition.

As shown in Figure 6, there is a biexponential decay in the ternary system (see Figure 9), which first decay time is directly comparable to the one in Eu(III)/PAHA system. This fast de-excitation is another direct indication that Eu(III) is strongly linked to sorbed humic aggregates. These results also suggest that sorbed Eu(III) in the ternary system is always bound to the sorbed humic acid entities, even at high pH when humic acid sorption is the lowest (Figure 2).

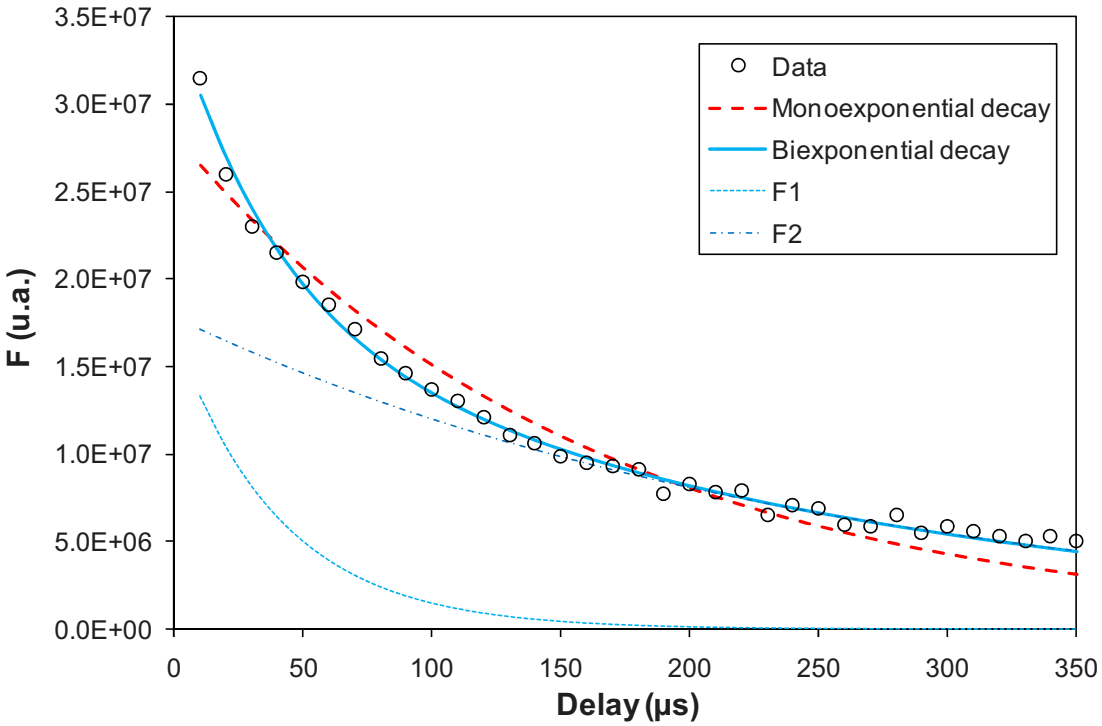

Figure 9. Luminescence decay times of Eu(III) in the ternary system at pH = 4.3. The bi-exponential decay is clearly seen.

Assuming that τ_1 is due to a fast exchange mechanism and τ_2 is due to complexation environment, according to Kimura et al. (1998) it would mean that there are only two water molecules remaining in the first coordination sphere of Eu(III) in Eu(III)/PAHA/α-Al_2O_3 system at pH 4.4, when there would be seven in the Eu(III)/PAHA system at the very same pH. These values are also doubtful as mentioned earlier.

At low pH, the spectrum in the ternary system is almost the same as the spectrum of Eu-PAHA complex, and very different from the one of Eu(III) in contact with α-Al_2O_3 (Figure 7). The spectroscopic and macroscopic data lead us to think that, at pH < 7, Eu-PAHA complexes are sorbed onto α-Al_2O_3 surface. The increase in τ_2 may then be due to a more constrained environment of Eu(III), but of the same symmetry, in the sorbed humic structure, which may decrease the probability of the Eu(III) ions to lose energy through quenching moieties.

When pH is increasing, the slower decay time τ_2 decreases from 382 µs at pH 4.4 to 185 µs at pH 9.6, which means that there is a greater probability of Eu(III) to be submitted to quenching process when PAHA is less sorbed onto the surface, or that Eu is progressively more exposed to quenching groups. One can also consider the fractionation of humic acid during sorption. After the pH-edge there is a small decrease in Eu(III) sorption in the ternary system (Figure 3). This is in fact reflecting the progressive change in the structure of Eu(III)/PAHA sorbed

onto the surface and the competition of Eu(III) with dissolved PAHA. At pH greater than 8.5, the $^5D_0 \rightarrow ^7F_1$ transitions of the binary Eu(III)/α-Al_2O_3 and the ternary systems are the same (Figure 10), giving indication that alumina has a direct influence on Eu(III) environment. Above pH 8, influence of the mineral surface and possible ternary complexes should be taken into account when trying to model such a system.

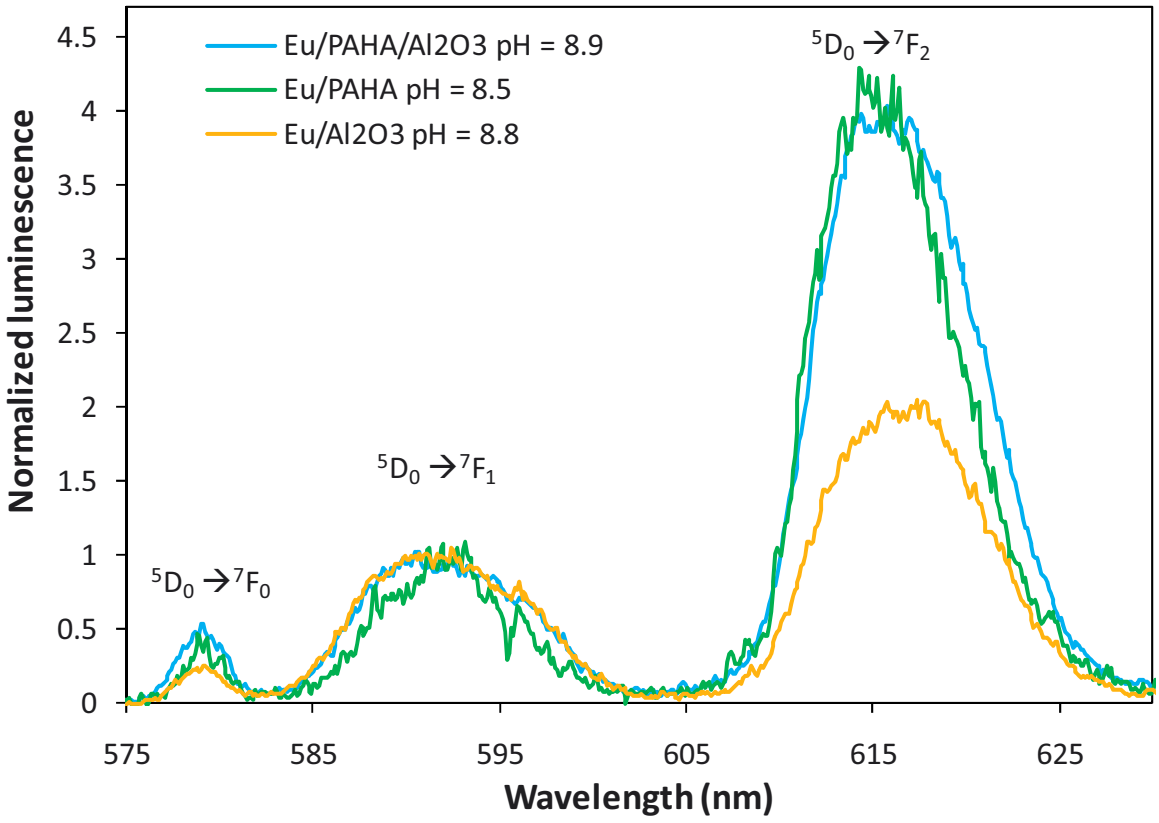

Figure 10. TRLS spectra of Eu(III) in contact with PAHA, α-Al_2O_3, both compounds or background electrolyte only, at pH = 8.7 ± 0.2. Spectra are normalized to the mean of five points around the maximum value of the $^5D_0 \rightarrow ^7F_1$ transition.

REFERENCES

Alliot, C., L. Bion, et al. (2005). "Effect of aqueous acetic, oxalic and carbonic acids on the adsorption of americium onto α-alumina." *Radiochimica Acta* **93**(8): 435-442.

Avena, M. J., A. W. P. Vermeer, et al. (1999). "Volume and structure of humic acids studied by viscometry pH and electrolyte concentration effects." *Colloids and Surfaces A* **151**(1-2): 213-224.

Berthoud, T., P. Decambox, et al. (1989). "Direct determination of traces of lanthanide ions in aqueous solutions by laser-induced time-resolved spectrofluorimetry." *Analytica Chimica Acta* **220**: 235-241.

Bradbury, M. H. and B. Baeyens (2009). "Sorption modelling on illite Part I: Titration measurements and the sorption of Ni, Co, Eu and Sn." *Geochimica Et Cosmochimica Acta* **73**(4): 990-1003.

Bradbury, M. H. and B. Baeyens (2009). "Sorption modelling on illite. Part II: Actinide sorption and linear free energy relationships." *Geochimica et Cosmochimica Acta* **73**(4): 1004-1013.

Brevet, J., F. Claret, et al. (2009). "Spectral and temporal luminescent properties of Eu(III) in humic substances solutions from different origins." *Spectrochimica Acta A* **74**(2): 446-453.

Bünzli, J.-C. G. (1989). Luminescent probes. *Lanthanides probe in life , chemical and earth sciences - Theory and practice*. J.-C. G. Bünzli and G. R. Choppin. Amsterdam, Elsevier.

Caceci, M. and V. Moulin (1991). Investigation of humic acid samples of different sources by photon correlation spectroscopy. *Humic substances in the aquatic and terrestrial environment: Proceedings of an International Symposium Linköping, Sweden, August 21–23, 1989*. B. Allard, H. Boren and A. Grimvall. Berlin, Springer. **33:** 97-104.

Christl, I. and R. Kretzschmar (2001). "Interaction of copper and fulvic acid at the hematite-water interface." *Geochimica et Cosmochimica Acta* **65**(20): 3435-3442.

Claret, F., T. Schäfer, et al. (2008). "Fractionation of Suwannee River fulvic acid and Aldrich humic acids on α-Al_2O_3: spectroscopic evidence." *Environmental Science & Technology* **42**(23): 8809-8815.

Conte, P. and A. Piccolo (1999). "Conformational arrangement of dissolved humic substances. Influence of solution composition on association of humic molecules." *Environmental Science & Technology* **33**(10): 1682-1690.

Fairhurst, A. J. and P. Warwick (1998). "The influence of humic acid on europium-mineral interactions." *Colloids and Surfaces A: Physicochemical and Engineering Aspects* **145**(1-3): 229-234.

Fairhurst, A. J., P. Warwick, et al. (1995). "The influence of humic acid on the adsorption of europium onto inorganic colloids as a function of pH." *Colloids and Surfaces A: Physicochemical and Engineering Aspects* **99**(2-3): 187-199.

Filius, J. D., D. G. Lumsdon, et al. (2000). "Adsorption of fulvic acid on goethite." *Geochimica et Cosmochimica Acta* **64**: 51-60.

Freyer, M., C. Walther, et al. (2009). "Formation of Cm humate complexes in aqueous solution at pH_c 3 to 5.5: The role of fast interchange." *Radiochimica Acta* **97**(10): 547-558.

Heidmann, I., I. Christl, et al. (2005). "Sorption of Cu and Pb to kaolinite-fulvic acid colloids: Assessment of sorbent interactions." *Geochimica et Cosmochimica Acta* **69**(7): 1675-1686.

Horrocks, W. D., Jr. and D. R. Sudnick (1979). "Lanthanide ion probes of structure in biology - Laser-induced luminescence decay constants provide a direct measure of the number of metal-coordinated water-molecules." *Journal of the American Chemical Society* **101**(2): 334-340.

Huittinen, N., T. Rabung, et al. (2009). "Sorption of Cm(III) and Gd(III) onto gibbsite, α-$Al(OH)_3$: A batch and TRLFS study." *Journal of Colloid and Interface Science* **332**(1): 158-164.

Hummel, W., U. Berner, et al. (2002). "Nagra/PSI chemical thermodynamic data base 01/01." *Radiochimica Acta* **90**(9-11): 805-813.

Hur, J. and M. A. Schlautman (2003). "Molecular weight fractionation of humic substances by adsorption onto minerals." *Journal of Colloid and Interface Science* **264**(2): 313-321.

Janot, N., P. E. Reiller, et al. (2010). "Using spectrophotometric titrations to characterize humic acid reactivity at environmental concentrations." *Environmental Science & Technology* **44**(17): 6782-6788.

Judd, B. R. (1962). "Optical absorption intensities of rare-earth ions." *Physical Review* **127**(3): 750-761.

Keizer, M. G. and W. H. van Riemsdijk (1994). *A computer program for the calculation of chemical speciation and transport in soil-water systems (ECOSAT 4.7).* . Wageningen, The Netherlands, Agricultural University of Wageningen.

Kim, J. I., G. Buckau, et al. (1990). "Characterization of humic and fulvic acids from Gorleben groundwater." *Fresenius Journal of Analytical Chemistry* **338**: 245-252.

Kimura, T., Y. Kato, et al. (1998). "Comparative study on the hydration states of Cm(III) and Eu(III) in solution and in cation exchange resin." *Journal of Alloys and Compounds* **271/273**: 719-722.

Krepelova, A., S. Sachs, et al. (2006). "Uranium(VI) sorption onto kaolinite in the presence and absence of humic acid." *Radiochimica Acta* **94**(12): 825-833.

Kumke, M. U., S. Eidner, et al. (2005). "Fluorescence quenching and luminescence sensitization in complexes of Tb^{3+} and Eu^{3+} with humic substances." *Environmental Science & Technology* **39**(24): 9528-9533.

Lippold, H. and J. Lippmann-Pipke (2009). "Effect of humic matter on metal adsorption onto clay materials: Testing the linear additive model." *Journal of Contaminant Hydrology* **109**(1-4): 40-48.

MacCarthy, P. (2001). "The principles of humic substances." *Soil Science* **166**(11): 738-751.

Marang, L., S. Eidner, et al. (2009). "Spectroscopic characterization of the competitive binding of Eu(III), Ca(II), and Cu(II) to a sedimentary originated humic acid." *Chemical Geology* **264**(1-4): 154-161.

Marang, L., P. E. Reiller, et al. (2008). "Combining spectroscopic and potentiometric approaches to characterize competitive binding to humic substances." *Environmental Science & Technology* **42**(14): 5094-5098.

McCarthy, J. F., K. R. Czerwinski, et al. (1998). "Mobilization of transuranic radionuclides from disposal trenches by natural organic matter." *Journal of Contaminant Hydrology* **30**(1-2): 49-77.

McCarthy, J. F., W. E. Sanford, et al. (1998). "Lanthanide field tracers demonstrate enhanced transport of transuranic radionuclides by natural organic matter." *Environmental Science & Technology* **32**(24): 3901-3906.

Milne, C. J., D. G. Kinniburgh, et al. (2003). "Generic NICA-Donnan model parameters for metal-ion binding by humic substances." *Environmental Science & Technology* **37**(5): 958-971.

Morgenstern, M., R. Klenze, et al. (2000). "The formation of mixed-hydroxo complexes of Cm(III) and Am(III) with humic acid in the neutral pH range." *Radiochimica Acta* **88**: 7-16.

Murphy, E. M., J. M. Zachara, et al. (1994). "Interaction of hydrophobic organic compounds with mineral bound humic substances." *Environmental Science & Technology* **28**(7): 1291-1299.

Ofelt, G. S. (1962). "Intensities of crystal spectra of rare-earth ions." *The Journal of Chemical Physics* **37**(3): 511-520.

Plancque, G., V. Moulin, et al. (2003). "Europium speciation by time-resolved laser-induced fluorescence." *Analytica Chimica Acta* **478**(1): 11-22.

Plaschke, M., J. Rothe, et al. (2002). "Combined AFM and STXM in situ study of the influence of Eu(III) on the agglomeration of humic acid." *Colloids and Surfaces A* **197**(1-3): 245-256.

Rabung, T., M. C. Pierret, et al. (2005). "Sorption of Eu(III)/Cm(III) on Ca-montmorillonite and Na-illite. Part 1: Batch sorption and time-resolved laser fluorescence spectroscopy experiments." *Geochimica Et Cosmochimica Acta* **69**(23): 5393-5402.

Reiller, P., F. Casanova, et al. (2005). "Influence of addition order and contact time on thorium(IV) retention by hematite in the presence of humic acids." *Environmental Science & Technology* **39**(6): 1641-1648.

Reiller, P., V. Moulin, et al. (2002). "Retention behaviour of humic substances onto mineral surfaces and consequences upon thorium (IV) mobility: case of iron oxides." *Applied Geochemistry* **17**(12): 1551-1562.

Reiller, P. E. and J. Brevet (2010). "Bi-exponential decay of Eu(III) complexed by Suwannee River humic substances: Spectroscopic evidence of two different excited species." *Spectrochimica Acta Part A: Molecular and Biomolecular Spectroscopy* **75**(2): 629-636.

Rice, J. A. and J. S. Lin (1993). "Fractal nature of humic materials." *Environmental Science & Technology* **27**(2): 413-414.

Rice, J. A., E. Tombácz, et al. (1999). "Application of light and X-ray scattering to characterize the fractal properties of soil organic matter." *Geoderma* **88**: 251-264.

Righetto, L., G. Bidoglio, et al. (1991). "Competitive actinide interactions in colloidal humic acid-mineral oxide systems." *Environmental Science & Technology* **25**: 1913-1919.

Schlautman, M. A. and J. J. Morgan (1994). "Adsorption of aquatic humic substances on colloidal-size aluminum oxide particles: Influence of solution chemistry." *Geochimica et Cosmochimica Acta* **58**(20): 4293-4303.

Schulthess, C. P. and J. F. McCarthy (1990). "Competitive adsorption of aqueous carbonic and acetic acids by an aluminium oxide." *Soil Science* **54**: 688-694.

Supkowski, R. M. and W. D. Horrocks, Jr. (2002). "On the determination of the number of water molecules, q, coordinated to europium(III) ions in solution from luminescence decay lifetimes." *Inorganica Chimica Acta* **340**: 44-48.

Takahashi, Y., A. Tada, et al. (2000). "Formation of outer- and inner-sphere complexes of lanthanide elements at montmorillonite-water Interface." *Chemistry Letters*(6): 700-701.

Tan, X. L., X. K. Wang, et al. (2008). "Sorption of Eu(III) on humic acid or fulvic acid bound to hydrous alumina studied by SEM-EDS, XPS, TRLFS, and batch techniques." *Environmental Science & Technology* **42**(17): 6532-6537.

Thomason, J. W., W. Susetyo, et al. (1996). "Fluorescence studies of metal humic complexes with the use of lanthanide ion probe spectroscopy." *Applied Spectroscopy* **50**(3): 401-408.

Varadachari, C., T. Chattopadhyay, et al. (1997). "Complexation of humic substances with oxides of iron and aluminum." *Soil Science* **162**(1): 28-34.

Vermeer, A. W. P., J. K. McCulloch, et al. (1999). "Metal ion adsorption to complexes of humic acid and metal oxides: Deviation from the additivity rule." *Environmental Science & Technology* **33**(21): 3892-3897.

Weng, L. P., W. H. van Riemsdijk, et al. (2008). "Cu^{2+} and Ca^{2+} adsorption to goethite in the presence of fulvic acids." *Geochimica et Cosmochimica Acta* **72**(24): 5857.

Weng, L. P., W. H. van Riemsdijk, et al. (2006). "Adsorption of humic substances on goethite: Comparison between humic acids and fulvic acids." *Environmental Science & Technology* **40**(24): 7494-7500.

CHAPITRE 5

INFLUENCE OF IONIC STRENGTH AND HUMIC CONCENTRATION ON EUROPIUM(III), α-Al_2O_3 AND HUMIC ACID INTERACTIONS

Noémie Janot, Marc F. Benedetti, Pascal E. Reiller

RÉSUMÉ

Comme dans le chapitre précédent, la spéciation de l'europium(III) en présence d'acide humique purifié (PAHA) et/ou de α-Al_2O_3 est étudiée par spectrofluorimétrie laser à résolution temporelle, à partir d'expériences en batch. Les concentrations en PAHA et Eu(III) retenues à la surface ont également été mesurées en fonction des conditions de la solution. Dans un premier temps, l'influence de la force ionique sur ce système est caractérisée. Les résultats montrent que celle-ci a peu d'influence sur le système binaire Eu(III)/α-Al_2O_3, macroscopiquement comme à l'échelle moléculaire. En revanche, on observe une modification de la symétrie de l'environnement de Eu(III) au-delà de pH 7 dans le système binaire Eu(III)/PAHA, bien qu'aucune différence ne soit observée au niveau des temps de décroissance de la luminescence de Eu(III) entre les deux forces ioniques étudiées. Dans le système ternaire, le temps de décroissance de luminescence de Eu(III) est beaucoup plus court à plus faible force ionique, lorsque l'environnement de l'ion est moins contraint, probablement du fait de plus faibles concentrations en PAHA et en Eu(III) sur la surface.

Dans la seconde partie, l'influence de la concentration en PAHA dans le système est étudiée de la même manière. La complexation Eu(III)/PAHA est complète qu'à partir de 16 mg/L à pH 4 dans le système binaire. A pH plus élevé, les spectres évoluent moins et la décroissance bi-exponentielle est observée dès l'ajout de PAHA dans le système ; il n'y a pas d'évolution significative du temps de décroissance avec la concentration en PAHA. Dans le système ternaire, on observe une augmentation de la concentration de surface en PAHA avec la concentration initiale, jusqu'à saturation de la surface à pH > 6. À pH 4 et R = 70 $mg_{PAHA}/g_{\alpha\text{-}Al_2O_3}$, la saturation ne semble pas encore atteinte. Comme pour le système binaire, dans le système ternaire, on observe la complexation progressive de Eu(III) lorsque la concentration en PAHA augmente. A pH 4, la présence d'acide humique augmente l'adsorption de l'europium(III) sur la surface. En revanche, aux valeurs de pH plus élevées, en fonction de la concentration en PAHA, l'adsorption est favorisée ou non par rapport au système binaire Eu(III)/α-Al_2O_3. Aux différents pH étudiés, on observe une augmentation du temps de décroissance de la luminescence avec la concentration en PAHA dans le système ternaire, à des valeurs bien plus élevée que dans le système binaire Eu(III)/PAHA (dans lequel aucune variation significative n'est observée). L'environnement de Eu(III) est plus contraint au sein des molécules humiques adsorbées, ce qui est en accord avec les observations précédentes.

ABSTRACT

Speciation of Eu(III) in the presence of purified Aldrich humic acid (PAHA) and/or aluminum oxide α-Al_2O_3 has been studied by time-resolved luminescence spectroscopy at different pH, ionic strengths and PAHA concentrations. As expected, results show a weak influence of ionic strength on Eu(III) adsorption onto α-Al_2O_3. However, in the binary Eu(III)/PAHA system, variations of electrolyte concentration, which modify PAHA conformation, influence humic-bound Eu(III) environment symmetry at high pH. In the ternary system Eu(III)/PAHA/α-Al_2O_3, adsorption of both Eu(III) and PAHA onto the surface decrease with ionic strength. Luminescence spectra are different at high pH. Eu(III) luminescence decay is much faster at 0.01 M than at 0.1 M $NaClO_4$, most likely due to the lower surface concentration of PAHA leading to a lesser constrained environment for Eu(III) ions.

Concerning the PAHA concentration influence, spectroscopic results show that complete complexation of 10^{-6} mol/L Eu(III) at pH 4 in the binary Eu(III)/PAHA system is reached for 16 mg/L PAHA, and for lower PAHA concentrations at higher pH. At higher pH, there is less influence of PAHA concentration on Eu(III) luminescence spectra and decay times. There is no difference in asymmetry ratios between binary Eu(III)/PAHA and ternary systems between pH 4 and 7.7 and same PAHA concentration, meaning that the presence of mineral surface has almost no influence on Eu(III) environment symmetry below pH 8. In the ternary system, at different pH, decay times of Eu(III) luminescence increase with PAHA concentration. They are much higher in the ternary system than in the binary Eu(III)/PAHA system, which would mean that Eu(III) environment in PAHA-bound molecules is more constrained, as previously seen. Macroscopic results show that the presence of PAHA increases or not Eu(III) adsorption onto α-Al_2O_3 depending on pH: at low pH, Eu(III) retention is always higher in the ternary system, whereas at higher pH it depends on PAHA concentration.

1 Introduction

Natural organic matter (NOM) interactions with mineral colloids in soils are known to partly control the speciation and migration of heavy metals and nanoparticles in the environment, and notably of lanthanides and actinides (McCarthy and Zachara 1989). Previous works have studied the influence of pH on metal ions speciation in a ternary metal/NOM/mineral (Fairhurst and Warwick 1998; Lenhart and Honeyman 1999; Christl and Kretzschmar 2001; Reiller et al. 2002; Takahashi et al. 2002; Reiller et al. 2005; Weng et al. 2007). However, despite the fact that electrostatics has a great influence on humic acids conformation in solution (Rice et al. 1999; Duval et al. 2005) and on its adsorption onto mineral surfaces (Reiller et al. 2002; Sakuragi et al. 2004; Weng et al. 2007), to our knowledge, only a few studies on ionic strength influence on such ternary system have been conducted (Christl and Kretzschmar 2001). In literature, no or weak influence of ionic strength on metal binding onto oxides has been seen (Rabung et al. 2000; Christl and Kretzschmar 2001; Sakuragi et al. 2004; Xu et al. 2005; Wang et al. 2006; Chen et al. 2007; Tan et al. 2009). However, due to varying humic substances adsorption with ionic strength (Christl and Kretzschmar 2001; Weng et al. 2007), decrease of ionic strength may modify the fate of contaminants in the environment.

Previous studies on such ternary systems also showed the influence of humic substances concentration on the adsorption behavior of contaminants (Fairhurst et al. 1995; Fairhurst and Warwick 1998). Thus, this parameter has also to be taken into account when characterizing the speciation of a metal ion in a various range of environmental conditions.

Investigations have then been made to determine ionic strength and humic acid concentration influences on Eu(III) speciation in a ternary Eu(III)/humic acid/α-Al_2O_3 system, using purified Aldrich humic acid (PAHA) as a proxy for NOM. Aluminum oxides are not the more frequent mineral surfaces found in the environment, but their aluminol surface sites are part of aluminosilicates reactive sites, very abundant in natural systems. Besides, Eu(III) speciation in the different binary and ternary systems has been studied by time-resolved luminescence spectroscopy (TRLS). This method allows working at trace metal concentrations, and alumina white color allows spectroscopic measurements with mineral in solution, contrary to iron oxides. Results obtained for the ternary system have been compared with those of the corresponding Eu(III)/α-Al_2O_3 and Eu(III)/PAHA binary systems. Electrolyte concentration influence on surface concentration of Eu(III) and PAHA in the different systems has also been quantified.

2 Experimental section

2.1 Materials

Commercial Aldrich humic acid was purified (PAHA) according to Kim et al. (1990). Stock suspension at 1 g/L has been prepared by diluting PAHA in NaOH (pH around 10) in order to completely dissolve the sample. The solution was then stored in the dark under N_2. Proton exchange capacity was determined by potentiometry and found at 6.12 eq/kg (Janot et al. 2010). Alumina (α-Al_2O_3) was purchased from Interchim (pure 99.99%, size fraction 200–500 nm). The solid was washed thrice with carbonate-free NaOH and thrice with milli-Q water before drying and storage at room temperature under N_2 atmosphere according to Alliot et al. (2005). The specific surface area measured by N_2-BET method was 15 m²/g. Point of zero charge was determined by acid-base titrations and found at pH = 9.6 (data shown in Chapter 6). Europium(III) stock solution (10^{-3} mol/L) was obtained from the dissolution of Eu_2O_3 (Johnson Matthey, 99.99%) in $HClO_4$. All solutions were prepared using freshly boiled milli-Q water.

2.2 Methods

Batch contact experiments were conducted in 10.4 mL Beckman centrifugation tubes (355603), using 1 g/L of α-Al_2O_3, 10^{-6} mol/L of Eu(III) and various concentrations of PAHA. First solid α-Al_2O_3, then PAHA and Eu(III) stock solutions and finally freshly degassed electrolyte solution were weighed, with no specific contact time applied between additions. To minimize carbonation of the systems, nitrogen was swept on the top of the solution before closing the tubes. Ionic strength *I* was fixed at 0.01 or 0.1 mol/L $NaClO_4$. The pH values of the solutions were adjusted by addition of fresh 0.01 or 0.1 mol/L $HClO_4$ and NaOH solutions. They were measured using one combined glass electrode (Radiometer Analytical) connected to a Radiometer Analytical pH Meter. To prevent $KClO_4$ precipitation in the electrode frit, the electrode filling solution was modified with NaCl at 0.1 mol/L. The pH electrode was calibrated using buffer solutions (pH 4.01, 7.01, and 10.00). The solutions were applied to three-dimensional stirring for 3 days of equilibration at room temperature before pH measurements and analyses.

After equilibration, 2.4 mL aliquots were taken from the centrifugation tubes and analyzed in TRLS in quartz cuvettes (10 mm). Preliminary experiments showed no significant differences between aliquots taken from one same tube. Eu(III) laser-induced properties were studied in contact with either PAHA, or α-Al_2O_3, or both components, using TRLS. The excitation laser

beam was generated by a 355 nm tripled output of a Continuum Nd:YAG laser, coupled to an optical parametric oscillator system (Panther II, Continuum, Santa Clara, CA). The time-resolved luminescence signal is collected at 90° and focused into an Acton spectrometer (slit 1 mm) equipped with 600 lines/mm grating. For the time-resolved detection, the luminescence signal was collected during a gate width W = 300 µs, at an initial gate delay D = 10 µs after the excitation by a laser flash. To increase the signal to noise ratio, 1000 accumulations were performed for each spectrum. To avoid the aggregation and settling of the samples occurring in α-Al_2O_3-containing systems, these samples were manually shaken between two measurements. All luminescence measurements were performed at ambient temperature (21 °C ± 2). The excitation wavelength was set at λ_{exc} = 393.8 nm. The observed luminescence corresponds to the transitions of the $^5D_0$ excited state to the ground ^7F_j manifold (Bünzli 1989). They are the $^5D_0 \rightarrow {}^7F_0$ transition, forbidden for magnetic and electric reasons ($\lambda_{max} \approx$ 580 nm), the $^5D_0 \rightarrow {}^7F_1$ magnetic dipole transition ($\lambda_{max} \approx$ 593 nm), and the $^5D_0 \rightarrow {}^7F_2$ "hypersensitive" transition ($\lambda_{max} \approx$ 615 nm) (Judd 1962; Ofelt 1962; Jorgensen and Judd 1964).

To characterize adsorbed amounts of PAHA and Eu(III) onto α-Al_2O_3, after equilibration the solutions were ultracentrifuged at 60000 rpm during 2 h. Concentration of PAHA in the supernatant was measured by a Shimadzu TOC-VCSH analyzer or UV-Visible measurements, calibrated in concentration of PAHA. The quantification of non adsorbed Eu(III) was made using ICP-AES or TRLS using the standard addition method (Berthoud et al. 1989), diluting an aliquot of the supernatant in K_2CO_3 3 mol/L.

3 Influence of ionic strength on Eu(III) speciation

3.1 Binary Eu(III)/α-Al_2O_3 system

Figure 1 shows the influence of pH and ionic strength on Eu(III) sorption onto α-Al_2O_3. Concentration of Eu(III) in the supernatant has been measured by ICP-AES in the case of 0.01 M. Data from Chapter 4 at 0.1 M are reported for comparison. As expected, adsorption of Eu(III) onto α-Al_2O_3 seems to be weakly dependant on ionic strength, with a pH-edge slightly lower at lower ionic strength.

Our results are in agreement with previous studies made between pH 5 and 7 which have reported no or only weak influence of I between 10^{-3} and 2 mol/L on Eu(III) adsorption onto alumina (Xu et al. 2005; Wang et al. 2006), γ-Al_2O_3 (Rabung et al. 2000), red earth (Chen et al. 2007) or hematite (Sakuragi et al. 2004).

Eu(III) adsorption onto oxides is strongly pH-dependent, and weakly dependent from ionic strength, which indicate surface complexation with mainly formation of inner-sphere complexes.

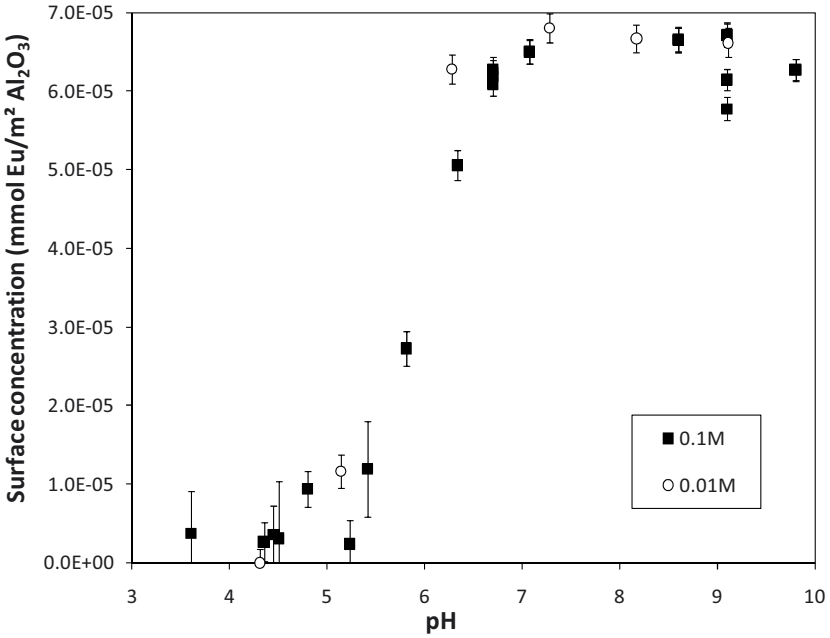

Figure 1. Surface concentration of Eu(III) onto α-Al_2O_3 depending on pH and *I*. [α-Al_2O_3] = 1 g/L, [Eu(III)] = 10^{-6} mol/L. Error bars correspond to 2σ.

Surface complexation of Eu(III) with aluminol sites from α-Al_2O_3 has been studied using TRLS at different pH and ionic strengths. The corresponding spectra, normalized to the maximum of $^5D_0 \rightarrow {}^7F_1$ transition, are displayed in Figure 2. The spectra seem similar at corresponding pH for the two ionic strengths studied. Below pH 6, Eu(III) is only weakly bound to the surface (see Figure 1), and the $^5D_0 \rightarrow {}^7F_0$ transition does not appear on the spectra. The relative importance of the $^5D_0 \rightarrow {}^7F_2$ transition increases with pH when Eu(III) forms complexes with the surface groups. There is a broadening of the $^5D_0 \rightarrow {}^7F_1$ transition with increasing pH, due to the degeneracy lift of the $^5D_0 \rightarrow {}^7F_1$ transition with increasing pH and symmetry loss due to surface complexation. The dissymmetric $^5D_0 \rightarrow {}^7F_2$ transition at pH = 4.3 at 0.01 M is due to the alumina signal (at $\lambda = 611.5$ nm) appearing when the Eu(III) luminescence signal is too low.

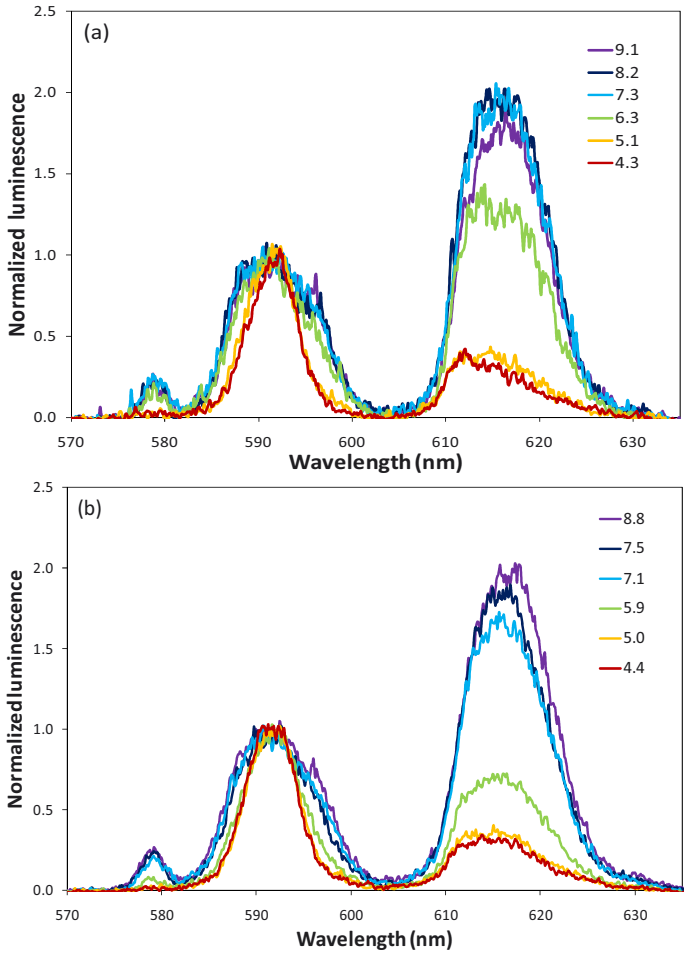

Figure 2. Comparison of Eu(III) luminescence spectra at different pH at 0.01 (a) and 0.1 M (b) $NaClO_4$ in the Eu(III)/α-Al_2O_3 system.

The evolutions of asymmetry area ratios $^5D_0 \rightarrow {}^7F_2$ / $^5D_0 \rightarrow {}^7F_1$ (noted $^7F_2/^7F_1$) are shown in Figure 3, together with the luminescence decay times. Luminescence decay times are calculated on the $^5D_0 \rightarrow {}^7F_1$ transition, to avoid the bias induced by the signal due to alumina. The maximum delay taken into account was 450 µs for all data points. Data from Rabung et al. (2000), for a Eu(III)/γ-Al_2O_3 system at 0.1 M $NaClO_4$ are shown for comparison. Even if the concentrations ratios between compounds are not directly comparable (we used 10^{-6} mol/L of Eu(III) for 15 m² of α-Al_2O_3 in our system, when Rabung et al. used $3.2 \cdot 10^{-6}$ mol/L of Eu(III) for 68 m² of γ-Al_2O_3), results are in good agreement. Rabung et al. (2000) found a higher asymmetry ratio at pH > 7, but they took into account only luminescence values at two maxima wavelengths (594 and 619 nm) when we used the area below peaks. Moreover, in their study, these authors present their results expressing the $^7F_1/^7F_2$ ratio, with one significant figure only. The small differences between values at high pH become high when we recalculate the $^7F_2/^7F_1$ ratio values.

There is no difference in evolution of asymmetry ratio with pH between the two ionic strengths studied, which confirms that there is no change in Eu(III) environment symmetry with varying electrolyte concentration. However, the luminescence decay times seem slightly higher between pH 5.5 and 7.5 for the lower ionic strength studied, which is in perfect agreement with macroscopic observations: the adsorption of Eu(III) begins at slightly lower pH at lower ionic strength. At both salt concentrations, Eu(III) luminescence decay time increases with pH: water molecules are excluded from Eu(III) coordination sphere when it forms complexes with surface sites (see Figure 1).

From these macroscopic and spectroscopic results, we see weak influence of ionic strength on Eu(III) binding to α-Al_2O_3, with no influence on Eu(III) environment symmetry.

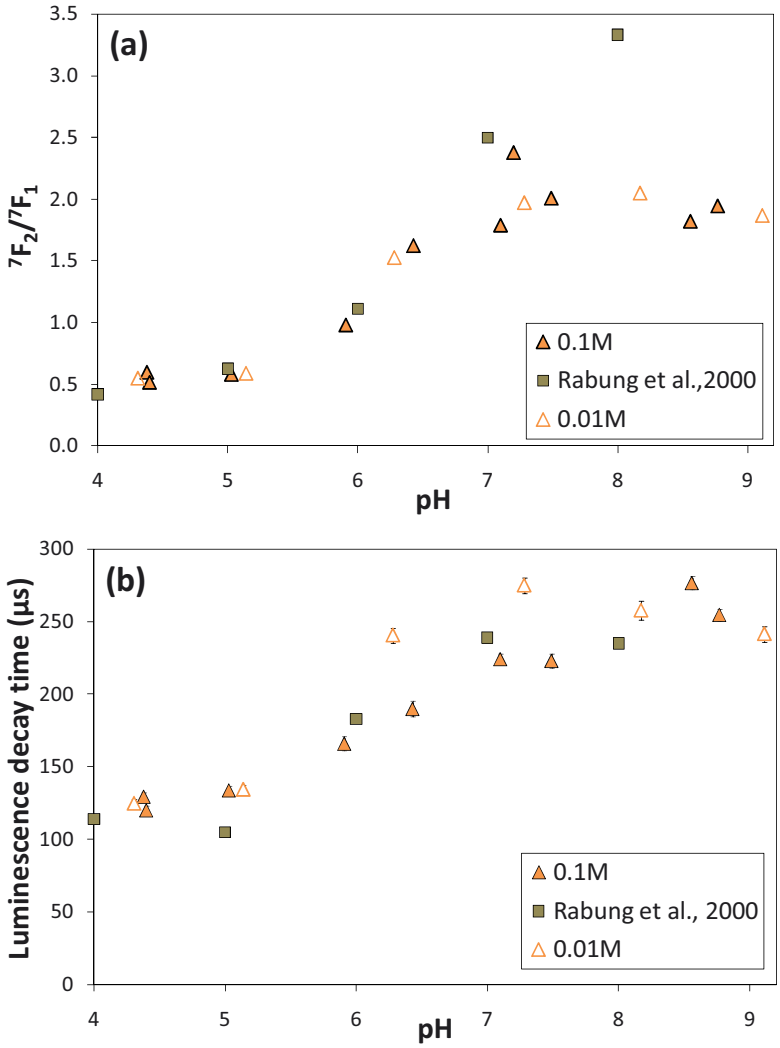

Figure 3. Evolution of asymmetry area ratios (a) and luminescence decay times (b) depending on pH and ionic strength. [α-Al_2O_3] = 1 g/L, [Eu(III)] = 10^{-6} mol/L. Data from Rabung et al. (2000) for Eu(III)/γ-Al_2O_3 system (at 0.1 M) are shown for comparison.

3.2 Binary Eu(III)/PAHA system

The evolution of Eu(III) binding to PAHA as a function of pH and *I* has been studied by TRLS. The evolution of Eu(III) luminescence spectra with ionic strength and pH is shown in Figure 4. With increasing pH, there is no evolution of the transition shapes: the $^5D_0 \rightarrow ^7F_0$ is seen at all pH values, indicating a loss of centro-symmetry compared to $Eu(H_2O)_n^{3+}$; the $^5D_0 \rightarrow ^7F_1$ does not change with varying pH as awaited; only the relative importance of the $^5D_0 \rightarrow ^7F_2$ transition compared to the $^5D_0 \rightarrow ^7F_1$ one is increasing with increasing pH showing the continuous change of symmetry and the increasing strength of complexation.

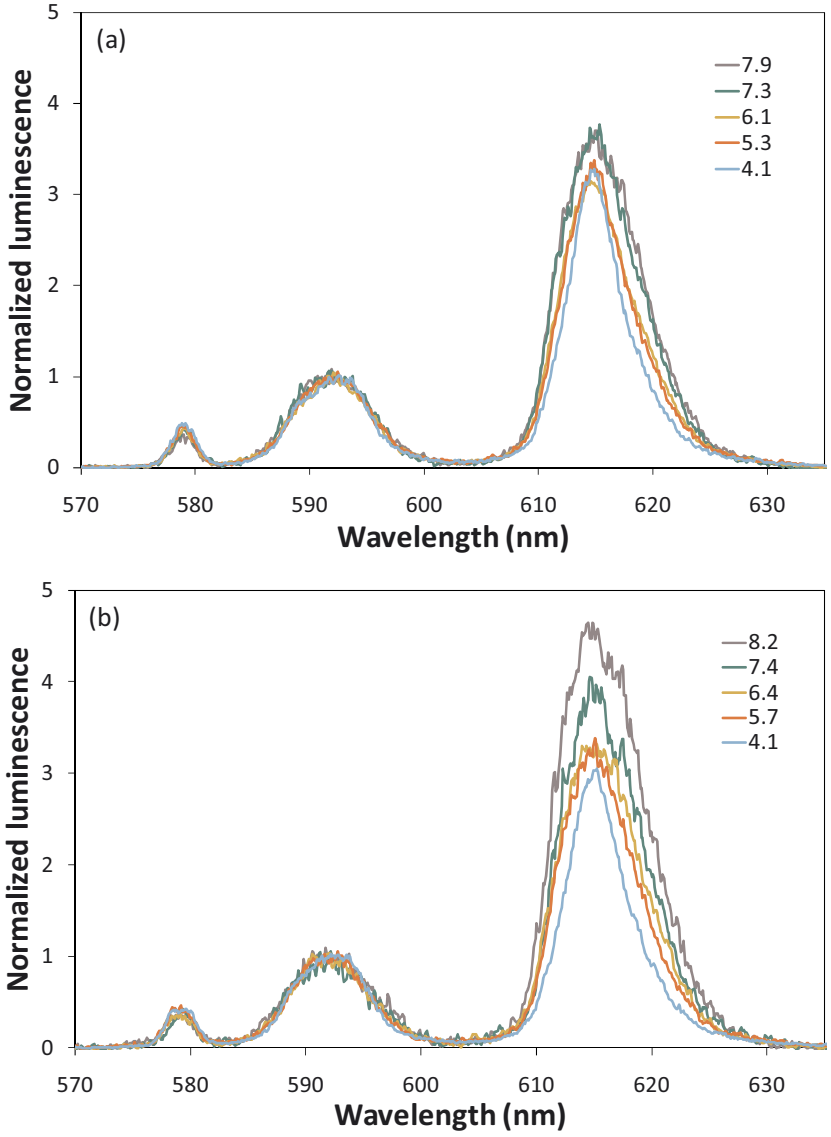

Figure 4. Eu(III) luminescence spectra at different pH in Eu(III)/PAHA system at 0.01 M (a) and 0.1 M (b) $NaClO_4$. [Eu(III)] = 10^{-6} mol/L, [PAHA] = 25 mg/L.

From these spectra, the asymmetry area ratios depending on pH and *I* are shown in Figure 5a. At pH < 5.5, there is no difference between the symmetry of Eu(III) environment at the two different ionic strengths studied. However, at higher pH, the asymmetry ratios are significantly higher at 0.1 M than at 0.01 M $NaClO_4$, as seen on the spectra in Figure 4. These variations of Eu(III) symmetry with ionic strength may be explained by electrostatic-influenced PAHA conformation (see Chapter 2). At higher ionic strength, the repulsion between charges is less important and the Donnan volume is smaller. Humic molecules may aggregate more easily, which can influence the symmetry of Eu(III) environment. This electrostatic influence will be more pronounced at higher pH, when more functional sites of PAHA are ionized.

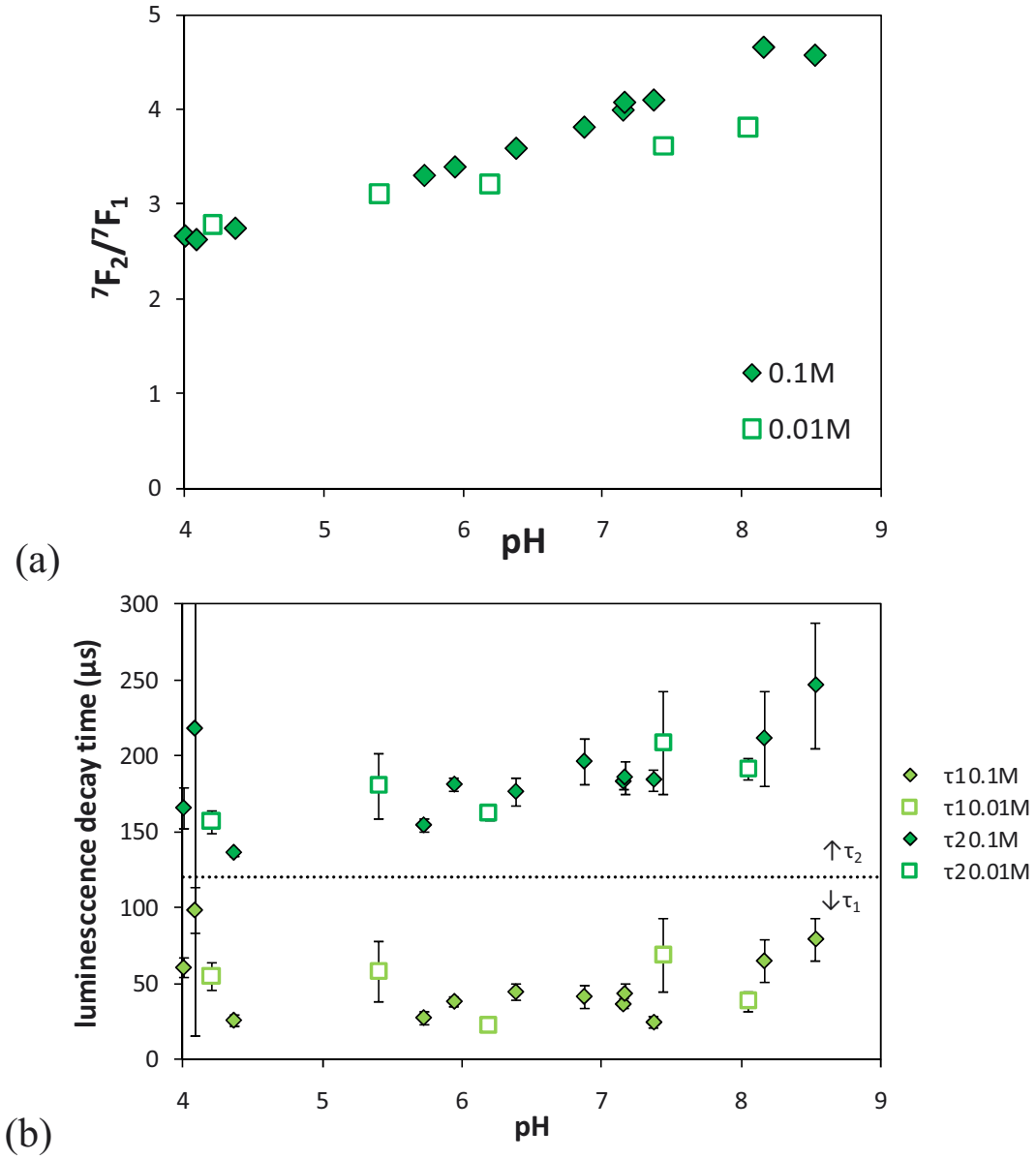

Figure 5. Asymmetry area ratios (a) and luminescence decay times (b) in Eu(III)/PAHA system, depending on pH and *I*. [Eu(III)] = 10^{-6} mol/L; [PAHA] = 25 mg/L.

However, this difference is not found in the evolution of Eu(III) luminescence decay times (see Figure 5b): at all pH studied, the luminescence decay time of Eu(III) is similar in 0.01 M or 0.1 M $NaClO_4$. This means that variation of electrolyte concentration has no impact on the probability of deexcitation, and thus on the number of quenching molecules in the first coordination sphere of Eu(III)-HA complexes. At all pH and ionic strengths values, the luminescence decay of Eu(III) is bi-exponential, with the first decay time τ_1 being shorter than luminescence decay time of $Eu(H_2O)_9^{3+}$, i.e., 100-110 µs . However, at pH around 4, luminescence decay times of Eu(III) seem peculiar, with high values of τ_1, but those fittings are characterized by great uncertainties. This should be due to a part of the signal coming from a low but significant proportion of Eu(III) not bound to PAHA molecules at this low pH.

In the binary Eu(III)/PAHA system, the influence of electrostatics seems to influence the symmetry of Eu(III) environment at high pH, but not the strength of complexation as there is the same amount of quenching molecules in Eu(III) coordination sphere at both ionic strength studied.

3.3 Ternary Eu(III)/PAHA/α-Al_2O_3 system

As Eu(III) adsorption is related to PAHA adsorption in the ternary system, PAHA concentrations in the supernatants of ternary systems at two ionic strengths were measured. Figure 6 show a decrease of PAHA adsorption onto α-Al_2O_3 with ionic strength, uniformly throughout the pH range studied. When ionic strength increases, hydrophobic bonding becomes more important as negative charges are more efficiently screened by electrolyte ions. Data from the binary PAHA/α-Al_2O_3 system previously shown (see Chapter 3) are plotted for comparison. Surprisingly, we see an effect of Eu(III) addition on PAHA adsorption at 0.1 M $NaClO_4$, but not at 0.01 M below pH 8. At lower ionic strength, PAHA concentration onto the surface is the same in the binary and ternary systems. The effect of Eu(III) on PAHA charge being negligible at both ionic strength studied under these conditions of concentrations (NICA-Donnan modeling, data not shown), is may be due to the difference of PAHA conformation between 0.01 and 0.1 M.

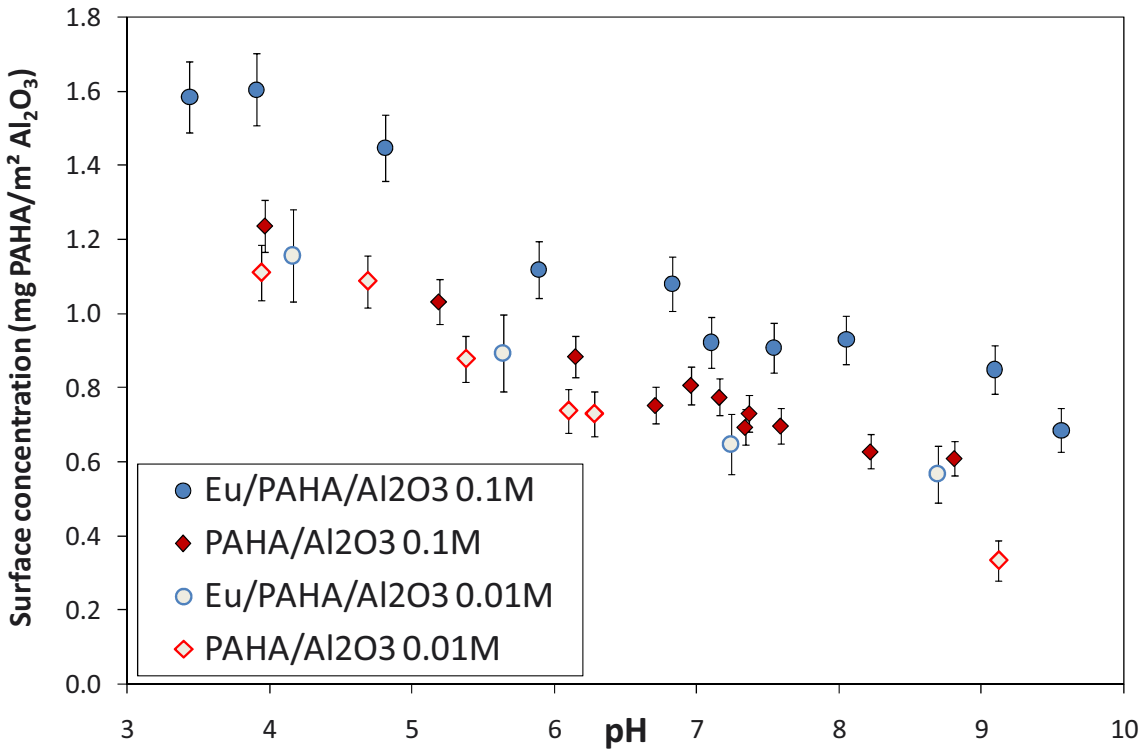

Figure 6. PAHA surface concentration in binary and ternary systems as a function of pH and ionic strength (R = 26.5 ± 0.5 $mg_{PAHA}/g_{\alpha\text{-}Al_2O_3}$).

Influence of ionic strength on the amount of Eu(III) adsorbed onto the mineral surface in the ternary Eu(III)/PAHA/α-Al_2O_3 system has been quantified. The surface concentration of Eu(III) measured by ICP-AES for data at 0.01 M are shown in Figure 7, together with data at 0.1 M from Chapter 4. The amount of adsorbed Eu(III) increases with ionic strength. These observations are in agreement with the Cu^{2+}/fulvic acid/hematite system described by Christl & Kretzschmar (2001). This can be related to the increase of PAHA adsorption with ionic strength, PAHA-bound Eu(III) being more adsorbed at higher electrolyte concentration. Even if, at 0.01 M, there is too few data to conclude clearly on the influence of pH, it seems that it may be comparable for the two ionic strengths studied. When pH increases, PAHA adsorption decreases, and Eu(III) ions may have easier access to surface sites, ~~to~~ which they can complex under these conditions, with only a weak effect of ionic strength (see Figure 1): at high pH, differences in Eu(III) surface concentration in the ternary system at different ionic strengths decrease.

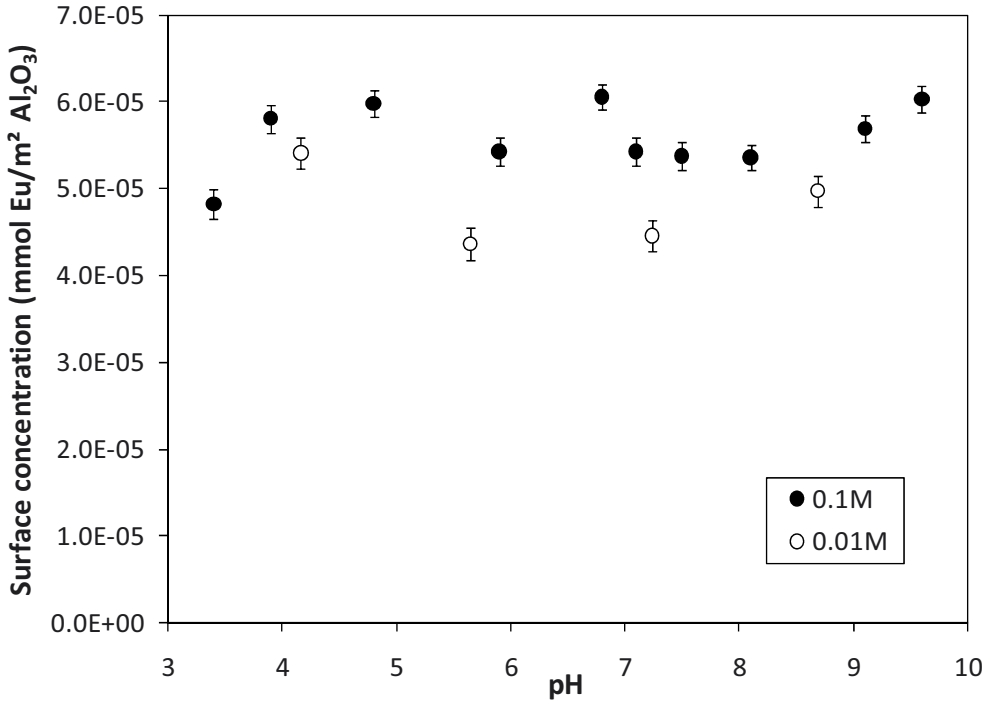

Figure 7. Surface concentration of Eu(III) onto α-Al_2O_3 in the ternary system depending on pH and ionic strength (R = 26.5 ± 0.5 $mg_{PAHA}/g_{α\text{-}Al_2O_3}$).

The time-resolved luminescence spectra of Eu(III) in the ternary system at 0.01 M and 0.1 M $NaClO_4$ and similar pH values are shown in Figure 8. The $^5D_0 \rightarrow {}^7F_0$ transition is always apparent, outlining the loss of centro-symmetry of Eu(III) environment in the ternary system. At 0.1 M, when pH increases, there is a broadening of both $^5D_0 \rightarrow {}^7F_1$ and $^5D_0 \rightarrow {}^7F_2$ transitions. The apparent maximum of the $^5D_0 \rightarrow {}^7F_2$ transition seems to be shifted toward higher wavelengths. Those are features appearing in the binary Eu(III)/α-Al_2O_3 system and not in the Eu(III)/PAHA one. They are less apparent at 0.01M. These observations are in agreement with macroscopic results which show a lower adsorption of Eu(III) onto the surface at lower ionic strength (see Figure 7).

The influence of α-Al_2O_3 on Eu(III) speciation at high pH in the ternary system at 0.1 M is confirmed by plotting the apparent maximum wavelengths of the $^5D_0 \rightarrow {}^7F_2$ transition vs. pH for the different systems (see Figure 9). The maximum of this transition is seen at higher wavelength in the binary Eu(III)/α-Al_2O_3 system than in the Eu(III)/PAHA system. In the ternary system, the maximum is shifting towards higher wavelengths when pH increasing at 0.1 M. However, at 0.01 M, this evolution is not apparent.

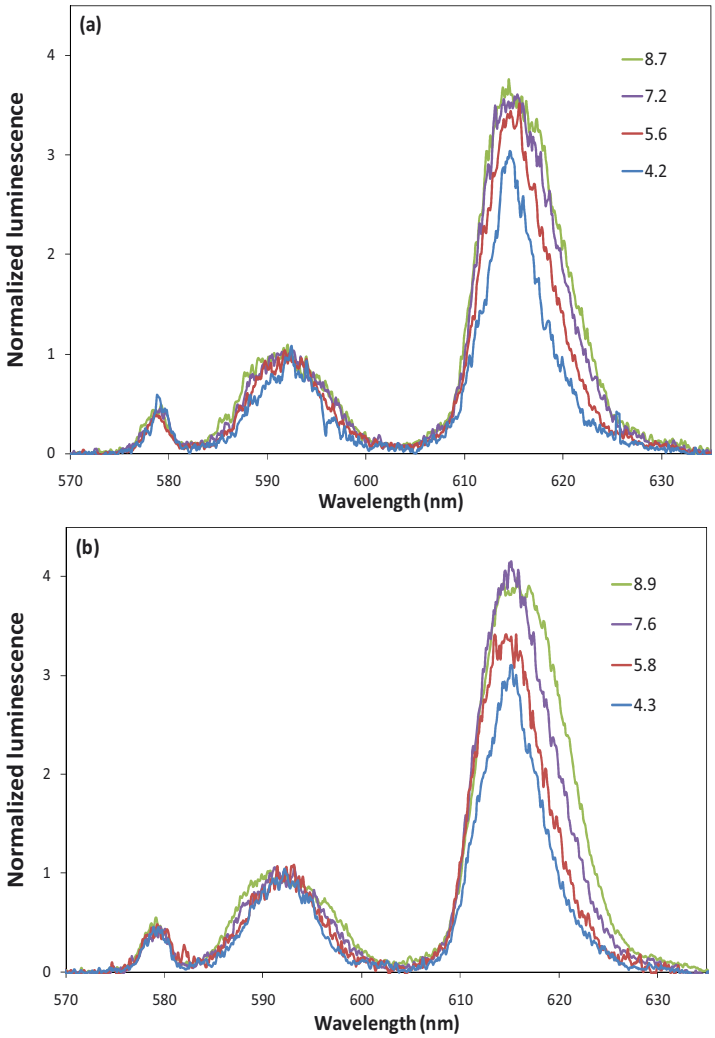

Figure 8. Eu(III) luminescence spectra in the ternary system at different pH at 0.01 M (a) and 0.1 M (b) $NaClO_4$ (R = 27.4 ± 0.5 $mg_{PAHA}/g_{\alpha\text{-}Al_2O_3}$).

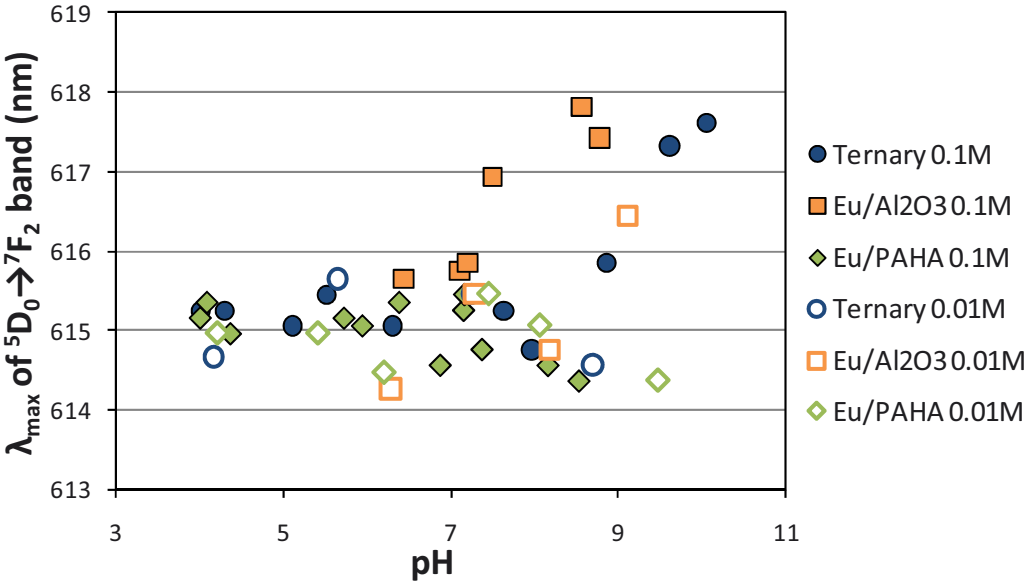

Figure 9. Wavelength of $^5D_0 \rightarrow {}^7F_2$ transition maxima depending on pH in the different systems studied.

At low pH, there is only slight difference in the asymmetry area ratios of Eu(III) spectra in the ternary systems at 0.01 and 0.1 M $NaClO_4$, as shown in Figure 10a. Above pH 7, the ratios at 0.01 M are slightly lower than the ratios at 0.1 M, as observed in the binary Eu(III)/PAHA system. This means that Eu(III) symmetry in these systems is very much alike.

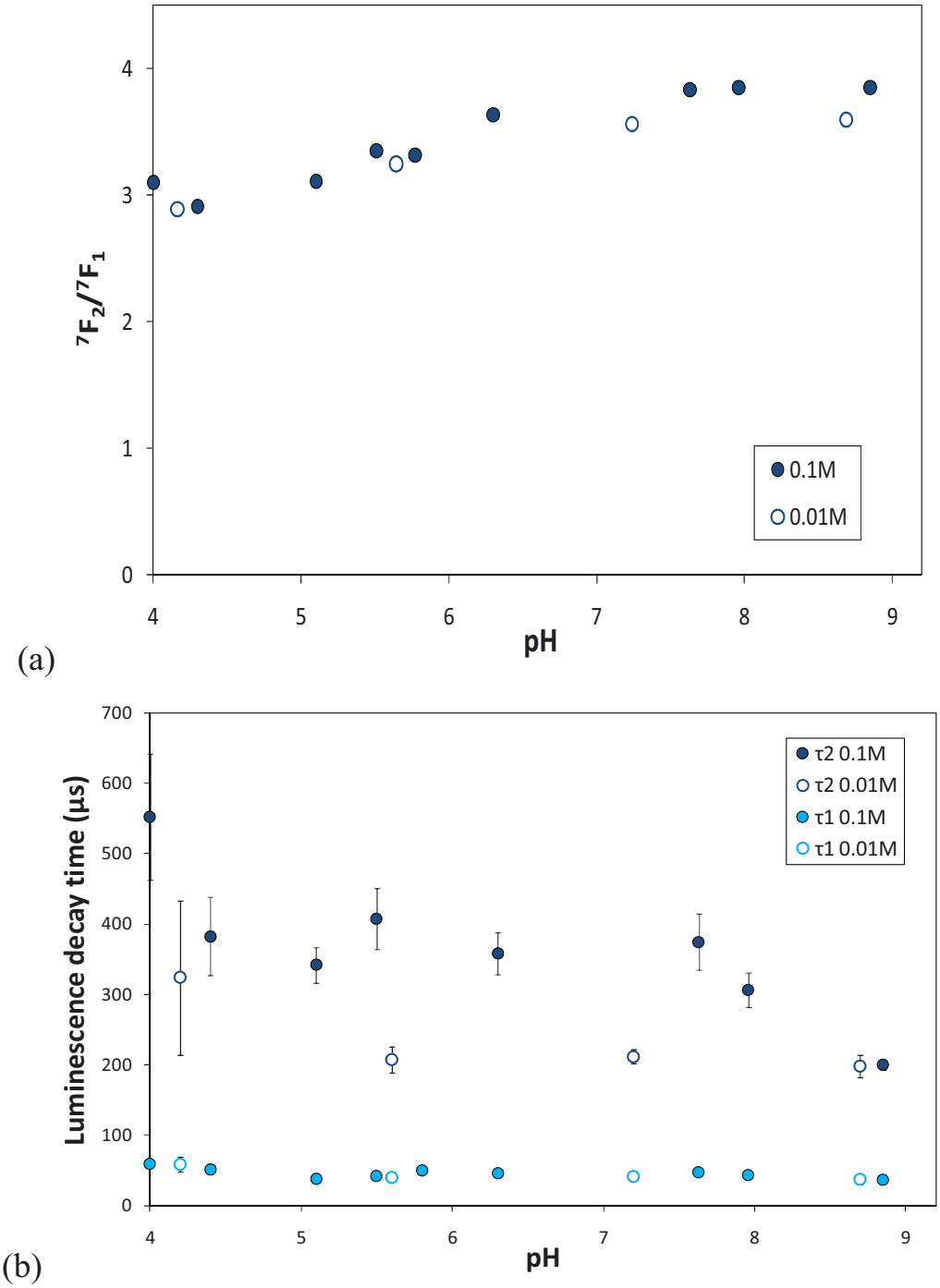

Figure 10. Asymmetry area ratios of Eu(III) luminescence spectra (a) and luminescence decay times of Eu(III) (b) in the ternary system at 0.01 and 0.1 M $NaClO_4$ depending on pH (R = 27.4 ± 0.5 $mg_{PAHA}/g_{\alpha\text{-}Al_2O_3}$).

For the determination of Eu(III) luminescence decay times shown in Figure 10b, the highest delay taken into account was 360 µs. The bi-exponential luminescence decay is observed in both cases, with the fastest τ_1 being independent from pH and ionic strength. This observation supports the hypothesis of a fast exchange of energy between humic molecules and excited Eu(III)* ions, independent from solution conditions.

The second decay time τ_2 is faster at lower ionic strength: $\tau_2 = 202 \pm 20$ µs, except at pH = 4.2 ($\tau_2 = 324 \pm 110$ µs) but uncertainties of this fitting are very high. This difference can be interpreted as a higher probability for Eu(III) to lose energy at 0.01 M than at 0.1 M in the ternary system. One can remind that it did not occur in the binary Eu(III)/PAHA system. However, at 0.01 M, the decay times of Eu(III) in the ternary system are comparable to the ones in the binary Eu(III)/PAHA system. This could be related to the lower surface concentration of both PAHA and Eu(III) at 0.01 M, Eu(III) environment being less constrained. This can be supported by the fact that at high pH, when there is less PAHA adsorbed onto the surface, τ_2 is the same at the two ionic strengths studied.

3.4 Conclusion

The influence of ionic strength on Eu(III) adsorption onto α-Al_2O_3 is weak, as expected. However, modifications of PAHA conformation due to ionic strength variations seem to impact Eu(III)/PAHA complexes symmetry. In the ternary system, decrease of ionic strength decreases Eu(III) and PAHA adsorption onto the surface. Consequently, Eu(III) environment seems less constrained at lower ionic strength, as shown by faster luminescence decay times throughout the pH range.

We have evidenced an influence of humic acid conformation on Eu(III) behavior, but the role of humic acid concentration is still to be characterized.

4 PAHA concentration effect on Eu(III) speciation

4.1 Binary Eu(III)/PAHA system

The influence of PAHA concentration on Eu(III) speciation has been studied by TRLS at three different pH values: 4.0 ± 0.1, 5.9 ± 0.2, 7.7 ± 0.3. Final concentrations of PAHA in the different samples are not always comparable due to pH adjustments, which modify the final volume of solutions.

At pH 4, from 16 mg/L of PAHA, ~~the totality~~ of Eu(III) (10^{-6} mol/L) is complexed by the humic molecules (see Figure 11a) : above this concentration, there is no evolution of Eu(III) luminescence spectra. When Eu(III) forms complexes with PAHA the $^5D_0 \rightarrow {}^7F_1$ transition is slightly broadened, and its apparent maximum is shifted towards higher wavelengths. This is also occurring at pH ≈ 6, as shown in Figure 11b. At this pH value, there is a continuous increase of the $^5D_0 \rightarrow {}^7F_2$ transition until 50 mg/L PAHA, with no plateau observed. The binding is observed at a lower humic concentration at pH 6 than at pH 4: at higher pH there is less competition with protons and PAHA moieties may form complexes with Eu(III) more easily. At pH ≈ 7.7, hydrolyzed species of Eu(III) are present in solution when there is no PAHA in the system, hence the observation of the $^5D_0 \rightarrow {}^7F_0$ transition and the relative importance of the $^5D_0 \rightarrow {}^7F_2$ transition seen in Figure 11c in the corresponding spectra. At this pH, the signal is weaker and the spectra are noisier, but the spectra seem comparable between 10 and 25 mg/L of PAHA.

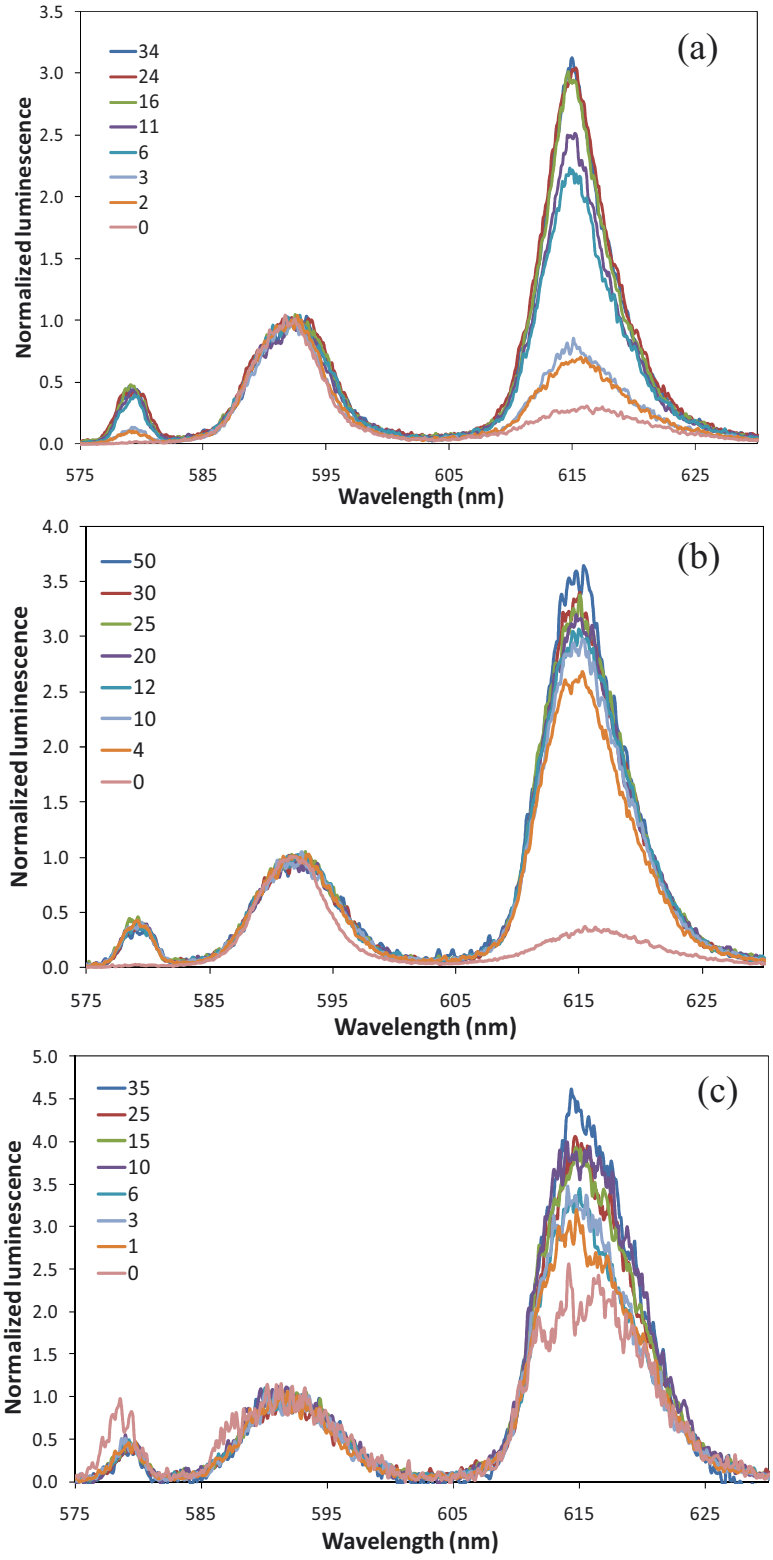

Figure 11. Eu(III) luminescence spectra at different PAHA concentrations (in mg/L) in the binary Eu(III)/PAHA system, at pH = 4.0 ± 0.1 (a); pH = 5.9 ± 0.2 (except the spectra of Eu(III) alone, pH = 5.5) (b); pH = 7.7 ± 0.3 (c). [Eu(III)]=10^{-6} mol/L.

At all pH values, the asymmetry area ratios increase with pH, until a plateau is reached, the value of this plateau increasing with pH (see Figure 12a). This saturation seems to be reached around 20 mg/L of PAHA at all pH, even if the low signal recorded at pH ≈ 8 leads to noisy spectra and evolution. Data values at 0 mg/L of PAHA correspond to the values obtained for Eu(III) alone in solution.

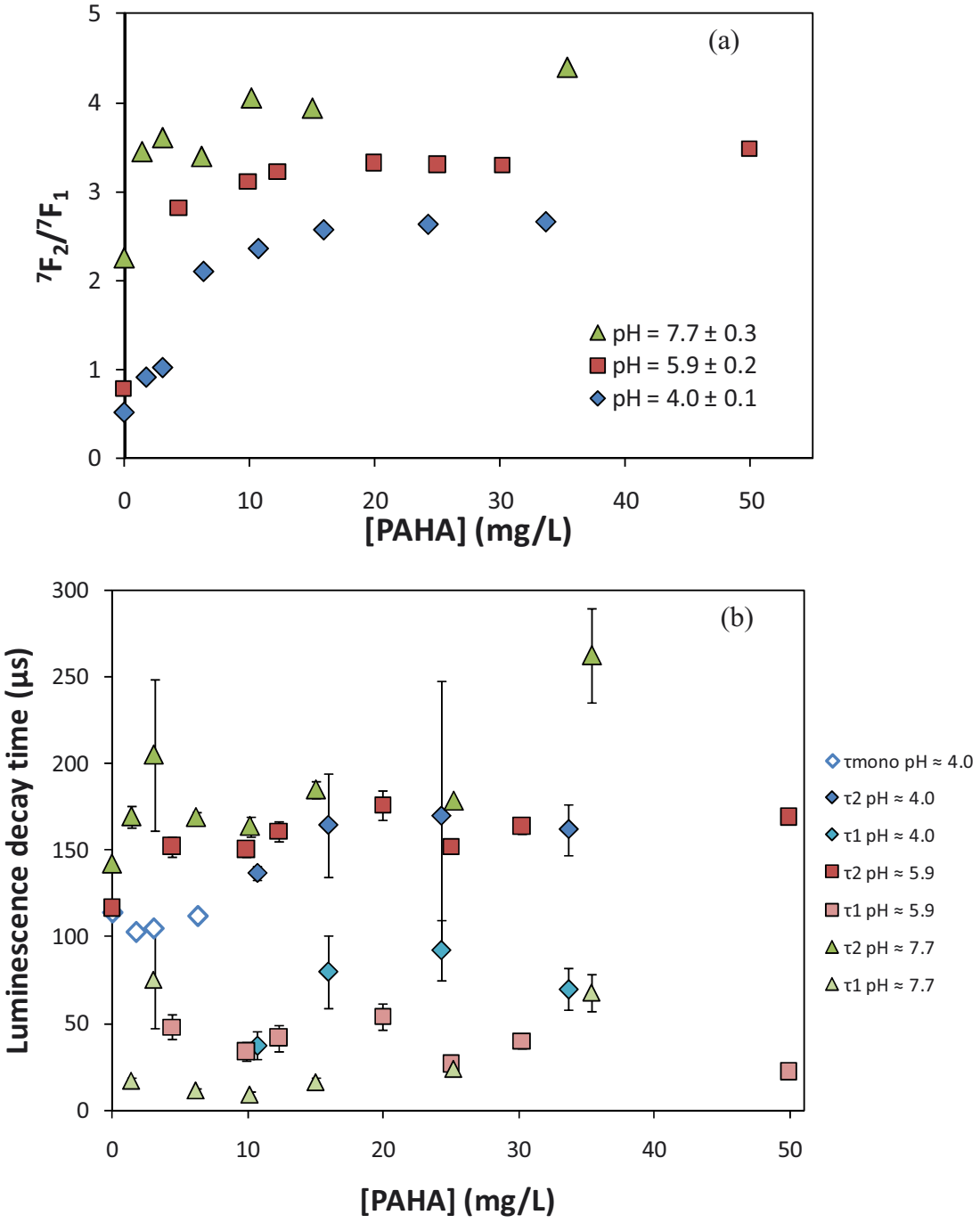

Figure 12. Evolution of asymmetry area ratios (a) and Eu(III) luminescence decay times (b) depending on pH and PAHA concentration in the binary Eu(III)/PAHA system.

Figure 12b shows the corresponding Eu(III) luminescence decay times. At pH 4 and PAHA < 10 mg/L, only one luminescence decay time is seen, which value is close to the one of free Eu^{3+}, meaning that the humic complexation is not apparent. Above 10 $mg_{PAHA}/g_{\alpha\text{-}Al_2O_3}$, the decay of luminescence is bi-exponential, with no significant influence of PAHA concentration on τ_2. At pH 6, whatever the PAHA concentration in the system, two luminescence decay times are needed for fitting the luminescence decay. PAHA concentration does not have an influence on Eu(III) luminescence decay times. At pH 7.7, the bi-exponential decay is also seen at all humic concentrations. There is a greater variation of τ_1 and τ_2 values, which may be due partially to the low and noisy signal.

Above 15 mg/L, at low pH, there is no influence of PAHA concentration on Eu(III) speciation (for 10^{-6} mol/L Eu(III)). At lower concentration, not all Eu(III) ions are complexed and the luminescence signal recorded is due to both free and PAHA-bound species. Above pH 5.5, even 5 mg/L of PAHA are enough to totally complex Eu(III) present.

4.2 Ternary Eu(III)/PAHA/α-Al_2O_3 system

First, PAHA and Eu(III) concentrations onto the surface at different coverage ratios and pH values were quantified. Figure 13 show the increase of PAHA surface concentration the ternary system with increasing coverage ratio and decreasing pH, as seen in the binary PAHA/α-Al_2O_3 system (see Chapter 3). At high pH, we observe a saturation of the mineral surface for R > 20 $mg_{PAHA}/g_{\alpha\text{-}Al_2O_3}$, which is not seen at pH 3.9. The presence of Eu(III) seems to increase PAHA adsorption at low and intermediate pH, for sufficient initial PAHA concentrations (above 20 $mg_{PAHA}/g_{\alpha\text{-}Al_2O_3}$).

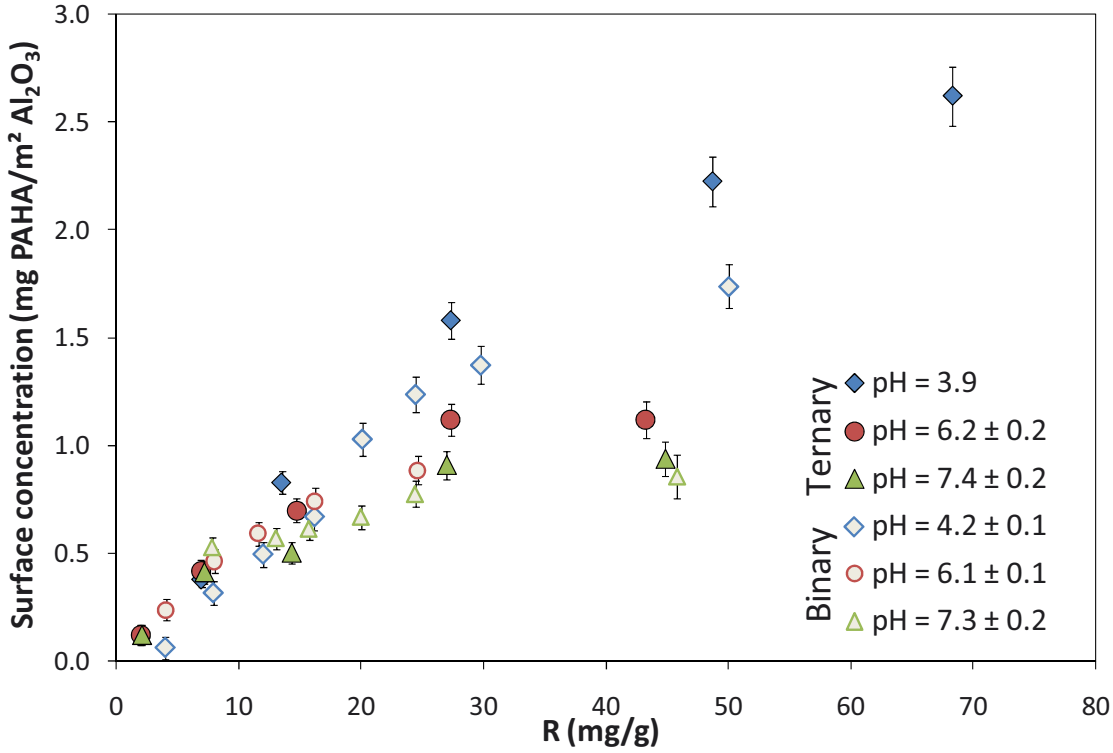

Figure 13. PAHA Surface concentration depending on PAHA initial concentration and pH, in presence (ternary) or absence (binary) of europium(III).

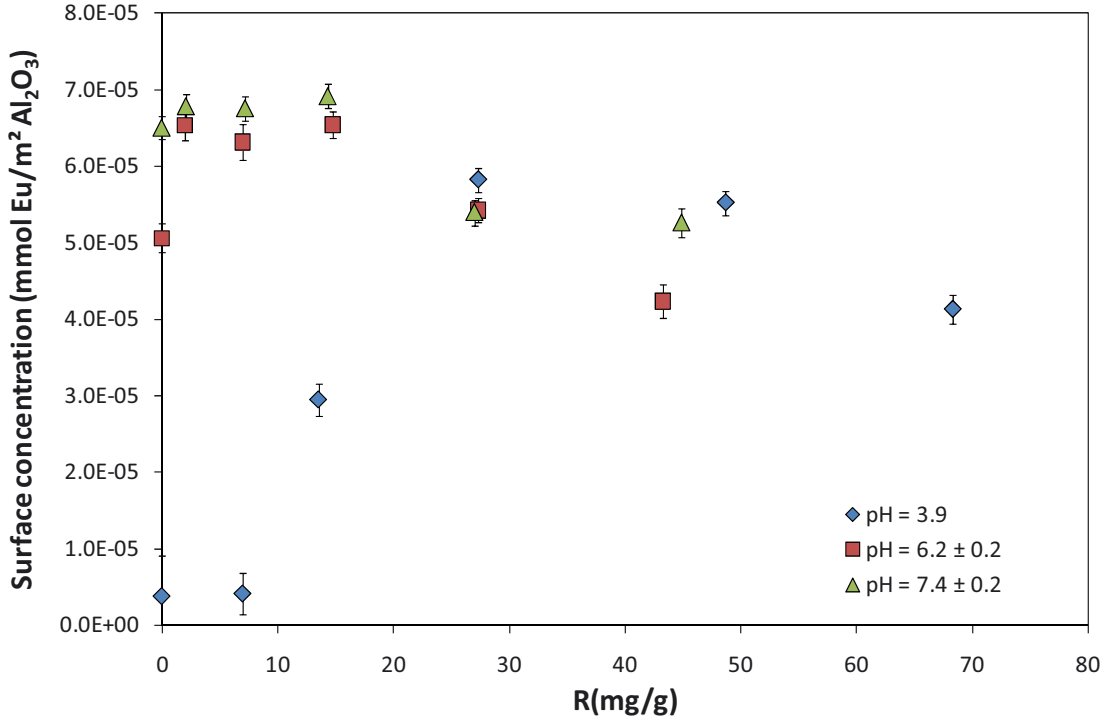

Figure 14. Influence of PAHA initial concentration and pH on the adsorption of Eu(III) onto α-Al_2O_3 in the ternary system.

The influence of PAHA initial concentration on the adsorption of Eu(III) onto α-Al_2O_3 at different pH is shown in Figure 14. In this case, data at R = 0 $mg_{PAHA}/g_{\alpha\text{-}Al_2O_3}$ correspond to values in the binary Eu(III)/α-Al_2O_3 system.

At pH 4 and low PAHA concentration, Eu(III) adsorption is minimal, as seen in the binary Eu(III)/α-Al_2O_3 system. When PAHA concentration increases and adsorbs onto the surface, the humic-bound Eu(III) is adsorbed too. When coverage ratio increases, PAHA concentration in solution does too. There is then competition of Eu(III) for both humic fractions, which leads to the decrease of Eu(III) concentration onto the surface at high R values (above 50 $mg_{PAHA}/g_{\alpha\text{-}Al_2O_3}$).

At higher pH, almost all Eu(III) is adsorbed at low humic concentration. When saturation of the surface is reached, there is a competition of Eu(III) between adsorbed and dissolved humic fractions, and adsorbed amount of Eu(III) decreases with increasing PAHA concentration. At pH ≈ 7.5, Eu(III) seems to stay preferentially adsorbed onto the surface.

The influence of PAHA concentration on time-resolved Eu(III) luminescence spectra has been studied at different pH: results are shown in Figure 15. At low pH, i.e., 4.3 ± 0.1, there is an evolution of the $^5D_0 \rightarrow {}^7F_0$ transition from its absence when there is no PAHA in the system to its maximum development for R > 15 $mg_{PAHA}/g_{\alpha\text{-}Al_2O_3}$, as seen in the binary Eu(III)/PAHA system.

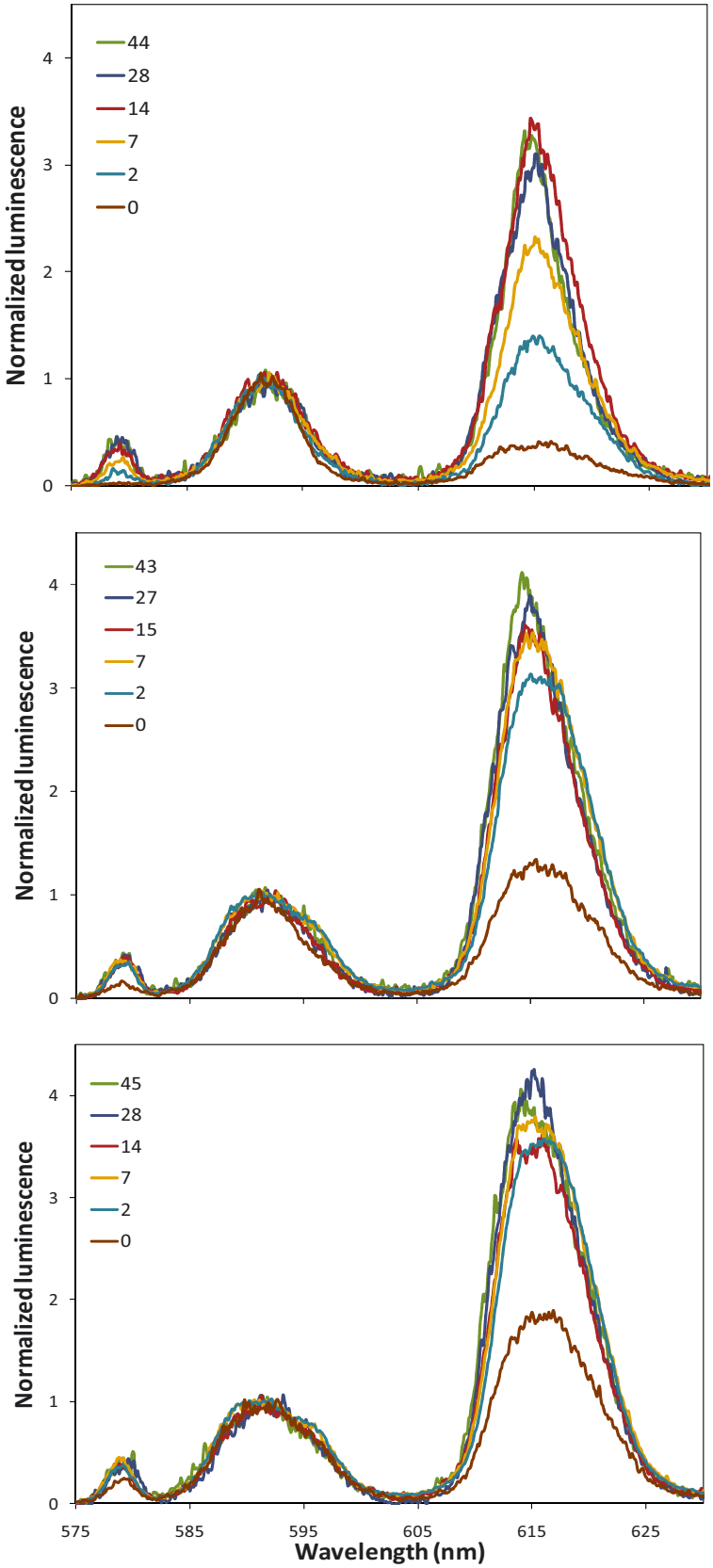

Figure 15. Eu(III) luminescence spectra in the ternary system for different coverage ratios (in $mg_{PAHA}/g_{\alpha\text{-}Al_2O_3}$), at pH = 4.3 ± 0.1; 6.3 ± 0.1; 7.4 ± 0.2. [Eu(III)] = 10^{-6} mol/L.

The asymmetry area ratio is increasing with coverage ratio, at all pH, until a plateau is reached, which value is increasing with pH (see Figure 16). Above R = 15 $mg_{PAHA}/g_{\alpha\text{-}Al_2O_3}$, the increase of PAHA concentration does not seem to have a great influence on Eu(III) environment symmetry. Results of the binary Eu(III)/PAHA system are plotted for comparison. There is no significant difference in the evolution of the asymmetry ratios between the binary and ternary systems, for these values of pH. This means that the presence or absence of mineral surface does not have any influence of Eu(III) environment symmetry between pH 4 and pH 7.6.

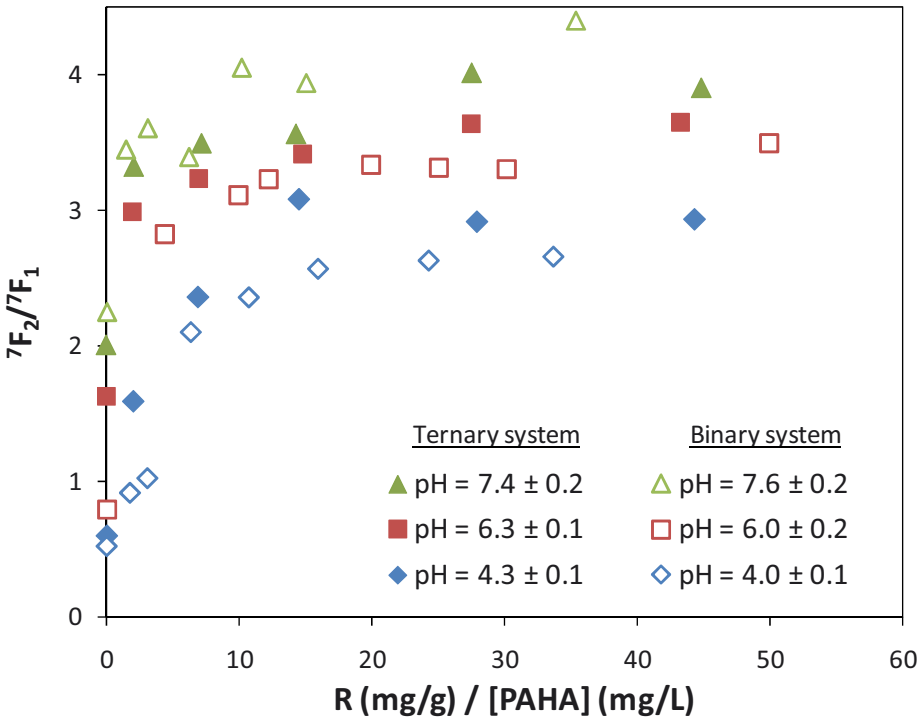

Figure 16. Evolution of asymmetry area ratios depending on pH and PAHA amount in the ternary (in $mg_{PAHA}/g_{\alpha\text{-}Al_2O_3}$) and binary (in mg_{PAHA}/L) systems. [Eu(III)]=10^{-6} mol/L, [α-Al_2O_3] = 1 g/L.

In the absence of PAHA, the luminescence decay of Eu(III) is always monoexponential : see the plots at 0 $mg_{PAHA}/g_{\alpha\text{-}Al_2O_3}$ on Figure 17. However, when there is organic matter in the system, even at low concentration, i.e. 2 $mg_{PAHA}/g_{\alpha\text{-}Al_2O_3}$, a bi-exponential decay of Eu(III) luminescence is occuring (see Figure 17). As for the binary Eu(III)/PAHA system, the fastest decay time τ_1 is always independent from PAHA concentration and pH. At pH = 4.3, except for data point at 2 $mg_{PAHA}/g_{\alpha\text{-}Al_2O_3}$ which is characterized by great uncertainties, the luminescence decay time τ_2 is increasing with coverage ratio. The progressive complexation of Eu(III) by PAHA excludes quenching molecules from the first coordination sphere of the

ion. At pH 6.3, presence of PAHA in the system increases τ_2 from 190 ± 5 µs to 235 ± 22 µs when $R \leq 15$ $mg_{PAHA}/g_{\alpha\text{-}Al_2O_3}$. Above this coverage ratio, τ_2 increases with PAHA concentration: at $R > 25$ $mg_{PAHA}/g_{\alpha\text{-}Al_2O_3}$, τ_2 = 340 ± 50 µs at pH 6.3, which is comparable to the values obtained at pH 4.3. At pH 7.4, the presence of PAHA in the system decreases luminescence decay time until $R = 7$ $mg_{PAHA}/g_{\alpha\text{-}Al_2O_3}$. Above this value, τ_2 increases with PAHA concentration: at $R > 25$ $mg_{PAHA}/g_{\alpha\text{-}Al_2O_3}$, $\tau_2 = 256 \pm 43$ µs. Above 15 $mg_{PAHA}/g_{\alpha\text{-}Al_2O_3}$, at 0.1 M, luminescence decay time decreases with increasing pH, which is in agreement with observations made in Chapter 4.

In the ternary system, luminescence decay time of Eu(III) is higher than in the binary systems. This may again be due to a more constrained Eu(III) environment within PAHA molecules when they are adsorbed onto the mineral surface, which would decrease the probability to lose energy through quenching moieties. This is in agreement with previous observations made at different pH and ionic strength values.

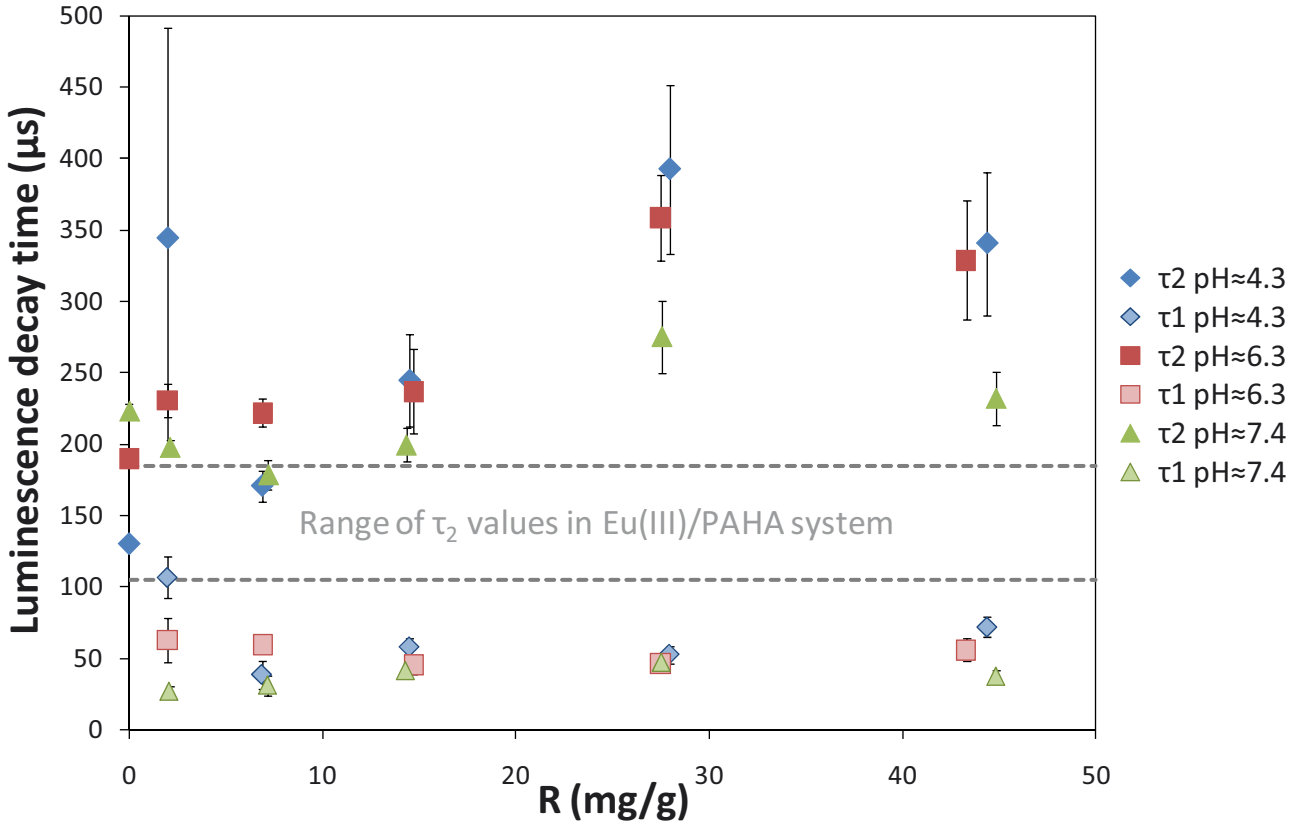

Figure 17. Influence of PAHA/α-Al_2O_3 ratio on Eu(III) luminescence decay times in the ternary system for different pH values. The range of values observed in the binary Eu(III)/PAHA system is indicated for comparison.
[Eu(III)]=10^{-6} mol/L, [α-Al_2O_3] = 1 g/L.

4.3 Conclusion

Natural organic matter concentration does have an influence on Eu(III) behavior in a ternary system. Eu(III) seems always in the direct neighborhood of humic molecules, as the bi-exponential decay of Eu(III) luminescence is always apparent. Moreover, Eu(III) symmetry does not seem to be different between binary Eu(III)/PAHA and ternary system between pH 4.0 and 7.6. And yet, the presence of α-Al_2O_3 in solution leads to higher Eu(III) luminescence decay times, which are interpreted as the result of a more constrained environment of Eu(III) when it is bound to adsorbed PAHA moieties.

Depending on pH, the presence of humic molecules may increase of decrease the contaminant adsorption or its transport in the environment. At low pH, i.e. below pH-edge of Eu(III) adsorption onto α-Al_2O_3, the presence of humic acid, whatever its concentration, increases Eu(III) retention compared to the binary Eu(III)/α-Al_2O_3 system. However, at intermediate pH, between 6.0 and 7.6, Eu(III) adsorption increases at low HA concentration, but once the saturation of the mineral surface is reached, Eu(III) adsorption may be decreased due to the competition with non-adsorbed humic fractions. One must then take into account a whole range of parameters (and not only pH) when studying the speciation of a pollutant in a natural system.

REFERENCES

Alliot, C., Bion L., et al. (2005). "Sorption of aqueous carbonic, acetic, and oxalic acids onto alpha-alumina." *Journal of Colloid and Interface Science* **287**(2): 444-451.

Berthoud, T., Decambox P., et al. (1989). "Direct determination of traces of lanthanide ions in aqueous solutions by laser-induced time-resolved spectrofluorimetry." *Analytica Chimica Acta* **220**: 235-241.

Bünzli, J.-C. G. (1989). Luminescent probes. *Lanthanides probe in life , chemical and earth sciences - Theory and practice*. J.-C. G. Bünzli and G. R. Choppin. Amsterdam, Elsevier.

Chen, L., Yu X. J., et al. (2007). "Effect of humic acid, pH and ionic strength on the sorption of Eu(III) on red earth and its solid component." *Journal of Radioanalytical and Nuclear Chemistry* **274**(1): 187-193.

Christl, I. and Kretzschmar R. (2001). "Interaction of copper and fulvic acid at the hematite-water interface." *Geochimica Et Cosmochimica Acta* **65**(20): 3435-3442.

Duval, J. F. L., Wilkinson K. J., et al. (2005). "Humic substances are soft and permeable: Evidence from their electrophoretic mobilities." *Environmental Science & Technology* **39**(17): 6435-6445.

Fairhurst, A. J. and Warwick P. (1998). "The influence of humic acid on europium-mineral interactions." *Colloids and Surfaces a-Physicochemical and Engineering Aspects* **145**(1-3): 229-234.

Fairhurst, A. J., Warwick P., et al. (1995). "The influence of humic acid on the adsorption of Europium onto inorganic colloids as a function of pH." *Colloids and Surfaces a-Physicochemical and Engineering Aspects* **99**(2-3): 187-199.

Janot, N., Reiller P. E., et al. (2010). "Using spectrophotometric titrations to characterize humic acid reactivity at environmental concentration." *Environmental Science & Technology* **44**(17): 6782-6788.

Jorgensen, C. K. and Judd B. R. (1964). "Hypersensitive pseudoquadrupole transitions in lanthanides." *Molecular Physics* **8**(3): 281-290.

Judd, B. R. (1962). "Optical absorption intensities of rare-earth ions." *Physical Review* **127**(3): 750-761.

Kim, J. I., Buckau G., et al. (1990). "Characterization of humic and fulvic-acids from Gorleben groundwater." *Fresenius Journal of Analytical Chemistry* **338**(3): 245-252.

Lenhart, J. J. and Honeyman B. D. (1999). "Uranium(VI) sorption to hematite in the presence of humic acid." *Geochimica Et Cosmochimica Acta* **63**(19-20): 2891-2901.

McCarthy, J. F. and Zachara J. M. (1989). "Subsurface transport of contaminants - Mobile colloids in the subsurface environment may alter the transport of contaminants." *Environmental Science & Technology* **23**(5): 496-502.

Ofelt, G. S. (1962). "Intensities of crystal spectra of rare-earth ions." *Journal of Chemical Physics* **37**(3): 511-&.

Rabung, T., Stumpf T., et al. (2000). "Sorption of Am(III) and Eu(III) onto gamma-alumina: experiment and modelling." *Radiochimica Acta* **88**: 711-716.

Reiller, P., Casanova F., et al. (2005). "Influence of addition order and contact time on thorium(IV) retention by hematite in the presence of humic acids." *Environmental Science & Technology* **39**(6): 1641-1648.

Reiller, P., Moulin V., et al. (2002). "Retention behaviour of humic substances onto mineral surfaces and consequences upon thorium (IV) mobility: case of iron oxides." *Applied Geochemistry* **17**(12): 1551-1562.

Rice, J. A., Tombacz E., et al. (1999). "Applications of light and X-ray scattering to characterize the fractal properties of soil organic matter." *Geoderma* **88**(3-4): 251-264.

Sakuragi, T., Sato S., et al. (2004). "Am(III) and Eu(III) uptake on hematite in the presence of humic acid." *Radiochimica Acta* **92**(9-11): 697-702.

Takahashi, Y., Kimura T., et al. (2002). "Direct observation of Cm(III)-fulvate species on fulvic acid-montmorillonite hybrid by laser-induced fluorescence spectroscopy." *Geochimica Et Cosmochimica Acta* **66**(1): 1-12.

Tan, X. L., Fang M., et al. (2009). "Adsorption of Eu(III) onto TiO2: Effect of pH, concentration, ionic strength and soil fulvic acid." *Journal of Hazardous Materials* **168**(1): 458-465.

Wang, X., Xu D., et al. (2006). "Sorption and complexation of Eu(III) on alumina: Effects of pH, Ionic strength, humic acid and chelating resin on kinetic dissociation study." *Applied Radiation and Isotopes* **64**(4): 414-421.

Weng, L. P., van Riemsdijk W. H., et al. (2007). "Adsorption of humic acids onto goethite: Effects of molar mass, pH and ionic strength." *Journal of Colloid and Interface Science* **314**(1): 107-118.

Xu, D., Ning Q. L., et al. (2005). "Sorption and desorption of Eu(III) on alumina." *Journal of Radioanalytical and Nuclear Chemistry* **266**(3): 419-424.

CHAPITRE 6

MODELING Eu(III) SPECIATION IN A Eu(III)/PAHA/α-Al_2O_3 TERNARY SYSTEM

Noémie Janot, Pascal E. Reiller, Marc F. Benedetti

RÉSUMÉ

Ce chapitre concerne la modélisation de la spéciation de Eu(III) dans un système ternaire comportant un acide humique (PAHA) et un oxyde d'aluminium (α-Al_2O_3). Dans un premier temps, des titrages potentiométriques de suspensions d'α-Al_2O_3 ont été effectués. La charge de surface de l'oxyde est décrite dans le cadre du modèle CD-MUSIC (Hiemstra and van Riemsdijk 1996). L'adsorption d'Eu(III) sur la surface α-Al_2O_3 a été étudiée à différents pH, forces ioniques et concentrations en solide, de manière à déterminer des paramètres de complexation de Eu(III) sur cette surface. Ensuite, les analyses SLRT du système Eu(III)/PAHA à pH 4 présentées précédemment (cf. Chapitre 5) ont servi à déterminer une « courbe de titrage » spectroscopique, afin d'ajuster les paramètres génériques NICA-Donnan de complexation de l'europium avec cet acide humique. La complexation de Eu(III) dans les deux systèmes binaires (organique et minéral) est ainsi décrite numériquement.

Afin de calculer la spéciation de l'ion dans le système ternaire, le fractionnement de l'acide humique dû à l'adsorption sur la surface, et la modification de la réactivité des deux compartiments organiques ainsi créés sont pris en compte. Les paramètres de protonation tirés des titrages spectrophotométriques des surnageants d'expériences d'adsorption (cf. Chapitre 3) sont utilisés pour modifier les paramètres NICA-Donnan des deux fractions organiques. La concentration de surface de l'europium(III) dans le système ternaire Eu(III)/PAHA/α-Al_2O_3 est calculée en fonction du pH, de la force ionique et de la concentration en matière organique. Cette approche propose des résultats convaincants, mais nécessiterait des ajustements, notamment aux conditions où le fractionnement organique est le plus important – et donc les modifications de réactivité également. Les résultats montrent la prédominance de la complexation organique : sur une large gamme de pH, Eu(III) est essentiellement lié à la fraction adsorbée. La complexation minérale n'intervient qu'au-delà de pH 8, ce qui est en accord avec les résultats de l'étude SLRT (cf. Chapitres 4 et 5).

ABSTRACT

The aim of this study is to achieve modeling Eu(III) speciation in a ternary system, i.e., in presence of purified Aldrich humic acid (PAHA) and α-Al_2O_3. First, potentiometric titrations of α-Al_2O_3 are performed and the surface charge is described through the CD-MUSIC model. Eu(III) binding to this α-Al_2O_3 surface is defined using this model with data from adsorption experiments at different pH, ionic strengths and mineral concentrations. Then, time-resolved luminescence spectra of Eu(III) in presence of PAHA are obtained at pH 4 and different humic concentrations. They are used to calculate a spectroscopic "titration curve", allowing to determine Eu(III)/PAHA binding parameters of the NICA-Donnan model. These information are then used to describe Eu(III) interactions in the ternary system.

The proposed modeling is based upon the definition of two PAHA fractions, one in solution and one onto the surface, each one with different proton and europium(III) binding parameters. The modifications of protonation behavior of both fractions are taken from spectrophotometric titrations of non-adsorbed PAHA fraction at different organic loadings (see Chapter 3).

Eu(III) repartition in the ternary system is calculated for different pH, ionic strengths and PAHA concentrations, and results are compared to experimental observations. Results of modeling are in quite good agreement with experiments, even if it would need adjustments, especially at high HA fractionation rates. Results show the dominance of organic complexation through a large pH range, with predominance of the surface-bound fraction. Above pH 8, Eu(III) seems to be mostly complexed to the mineral surface, which is in agreement with spectroscopic observations.

1 Introduction

Interactions between humic substances (HS) and mineral surfaces have a great influence on contaminant behavior in the environment. Presence of humic substances greatly modifies the adsorption of metals onto minerals, and may enhance their solubility and potential transport (McCarthy et al. 1998a; McCarthy et al. 1998b). There are several models achieving to describe the different binary systems: Model VI (Tipping 1998) or NICA-Donnan (Kinniburgh et al. 1999) for metal complexation to humic substances, CD-MUSIC for metal adsorption onto surfaces (Hiemstra et al. 1989; Hiemstra and van Riemsdijk 1996), Ligand and Charge Distribution (LCD) model for humic substances retention onto oxides (Filius et al. 2001; Filius et al. 2003). However, due to the fractionation of humic molecules with adsorption onto surfaces (Meier et al. 1999; Hur and Schlautman 2003; Reiller et al. 2006; Claret et al. 2008), the additivity is often not respected in ternary systems (Vermeer et al. 1999; Christl and Kretzschmar 2001). Due to the modification of surface behavior of organic and inorganic colloids, the modeling of metal speciation through the different compartments of a ternary metal/HS/surface is still difficult. Some studies have managed to describe such ternary systems containing fulvic acids (Heidmann et al. 2005; Weng et al. 2008), but the large size of humic acid molecules makes it more difficult to describe. Actually, humic acids adsorption onto minerals increases with ionic strength, which is not observed for fulvic acids (Reiller et al. 2002; Weng et al. 2007), and different from the behavior of small organic molecules (Ali and Dzombak 1996). Recently, Weng et al. (2009) achieved to describe a ternary system with arsenate as contaminant, which has not the same behavior towards colloids than metallic ions.

The first step to successfully describe a metal/HA/surface system is to characterize the reactivity of HA fractions created upon adsorption. However, this is difficult due to the low concentrations of HA in the supernatant from adsorption experiments. Recently, spectrophotometric titrations have been described (Dryer et al. 2008; Janot et al. 2010). This method allows working at environmental relevant humic concentrations, i.e. less than 10 mg_{HS}/L. In a previous work we showed the possibility to use this method to determine the modifications of proton-binding behavior of HA fractions after adsorption onto a mineral surface (see Chapter 3).

In this work, Eu(III) speciation is studied in presence of purified Aldrich humic acid (PAHA) and α-Al_2O_3. Aluminum oxides are not the most common mineral in the environment, but

their surface sites might be used as analogs of the aluminol surface sites of clays, which are ubiquitous in natural systems. The Eu(III) repartition between the different compartments of the system, i.e., solution, surface, adsorbed-PAHA, and dissolved-PAHA is determined in the framework of CD-MUSIC and NICA-Donnan models.

2 Material and methods

2.1 Materials

Alumina (α-Al_2O_3) was purchased from Interchim (pure 99.99%, size fraction 200–500 nm). The solid was washed thrice with carbonate-free NaOH and thrice with milli-Q water before drying and storage at room temperature under N_2 atmosphere according to Alliot et al. (2005). Specific area was measured by N_2-BET method and found to be 15 m^2/g.

Europium(III) stock solution (10^{-3} mol/L) was obtained from the dissolution of Eu_2O_3 (Johnson Matthey, 99.99%) in $HClO_4$. All solutions were prepared using freshly boiled milli-Q water.

Commercial Aldrich humic acid was purified (PAHA) according to Kim et al. (1990). Stock suspension at 5 g_{PAHA}/L was prepared by diluting PAHA in NaOH (pH around 10) to completely dissolve the sample.

2.2 Potentiometric titrations of α-Al_2O_3

Potentiometric titrations were performed in a computer-controlled system under N_2 atmosphere, in a thermostated vessel (25 °C) equipped with a stirrer on 50-mL solutions at 100 g/L α-Al_2O_3. Ionic strength *I* was fixed using KNO_3 (for 0.01 M and 1 M titrations) or $NaClO_4$ (0.1 M titration). The quoted ionic strengths are the initial values before the addition of any titrant. In data analyses, actual *I* was calculated for every data point, accounting for both background electrolyte ions and free H^+ and OH^-. The pH values of the solutions were controlled during titrations by addition of 0.1 mol/L acid and base solutions. Base titrant (titrisol for 0.1 mol/L solution) was prepared with degassed milli-Q water. The pH values were recorded with two pH Metrohm 6.0133.100 glass electrodes and a single Metrohm 6.0733.100 reference electrode. The pH electrodes were calibrated by performing a blank titration of the background electrolyte prior to the sample titration. The aqueous suspension was purged with N_2 at pH = 4 for 90 mn. The suspension was then titrated by adding small volumes of titrant, and pH was recorded as a function of the titrant volume added to the

suspension. After each addition, a drift criterion for pH was used (ΔmV/min < 0.1) and a maximum time of 60 min was set for acquiring each data point. Usually stabilization of pH took less than 2 min. A similar procedure was followed for the blank solution titration. Two forward and backward titrations were performed to eliminate the hysteresis effect.

2.3 Adsorption experiments

Batch experiments were carried out at ambient temperature with 10^{-6} mol/L Eu(III) concentration at different pH, ionic strengths (0.01 M and 0.1 M $NaClO_4$) and various concentrations of organic and/or inorganic compounds. To minimize carbonation of the systems, nitrogen was swept on the top of the solution before closing the tubes. The pH values of the solutions were adjusted by addition of fresh 0.01 or 0.1 mol/L $HClO_4$ and NaOH solutions. They were measured using one combined glass electrode (Radiometer Analytical) connected to a Radiometer Analytical pH Meter. To prevent $KClO_4$ precipitation in the electrode frit, electrode filling solution was modified with 0.1 mol/L NaCl. The pH electrode was calibrated using buffer solutions (pH 4.01, 7.01, and 10.00). After 3 days of equilibration, the final pH was checked and samples were ~~ultracentrifuged~~ at 60000 rpm during 2 h. Eu(III) concentration in the supernatant was measured by ICP-AES or by standard addition method in Time-Resolved Luminescence Spectroscopy (TRLS), diluting an aliquot of the supernatant in K_2CO_3 3 mol/L

2.4 Spectroscopic measurements

Eu(III) speciation in binary and ternary systems has been studied by TRLS. The excitation laser beam was generated by a 355 nm tripled output of a Continuum Nd:YAG laser, coupled to an optical parametric oscillator system (Panther II, Continuum, Santa Clara, CA). The time-resolved luminescence signal is collected at 90° and focused into an Acton spectrometer (slit 1 mm) equipped with 600 lines/mm grating. For the time-resolved detection, the luminescence signal was collected during a gate width $W = 300$ µs, at an initial gate delay $D = 10$ µs after the excitation by a laser flash. To increase the signal to noise ratio, 1000 accumulations were performed for each spectrum. To avoid the aggregation and settling of the samples occurring in α-Al_2O_3-containing systems, these samples were manually shaken between two measurements. All luminescence measurements were performed at ambient temperature (21 °C ± 2). The excitation wavelength was set at $\lambda_{exc} = 393.8$ nm, which

corresponds to the $^7F_0 \rightarrow {}^5L_6$ transition of Eu(III). The observed luminescence corresponds to the transitions from the $^5D_0$ excited state to the ground ^7F_j manifold (Bünzli 1989).

3 Results and Discussion

3.1 Surface charge of α-Al_2O_3

The experimental charging curves are presented in Figure 1, together with the results of the fits obtained using CD-MUSIC model (Hiemstra et al. 1989; Hiemstra and van Riemsdijk 1996). Calculations were done using the ECOSAT software (Keizer and van Riemsdijk 1994). The pH_{PZC} was found at 9.6, meaning that the storage procedure managed to avoid carbonation of the surface. The oxide surface is positively charged below pH_{PZC}, with charge increasing with ionic strength.

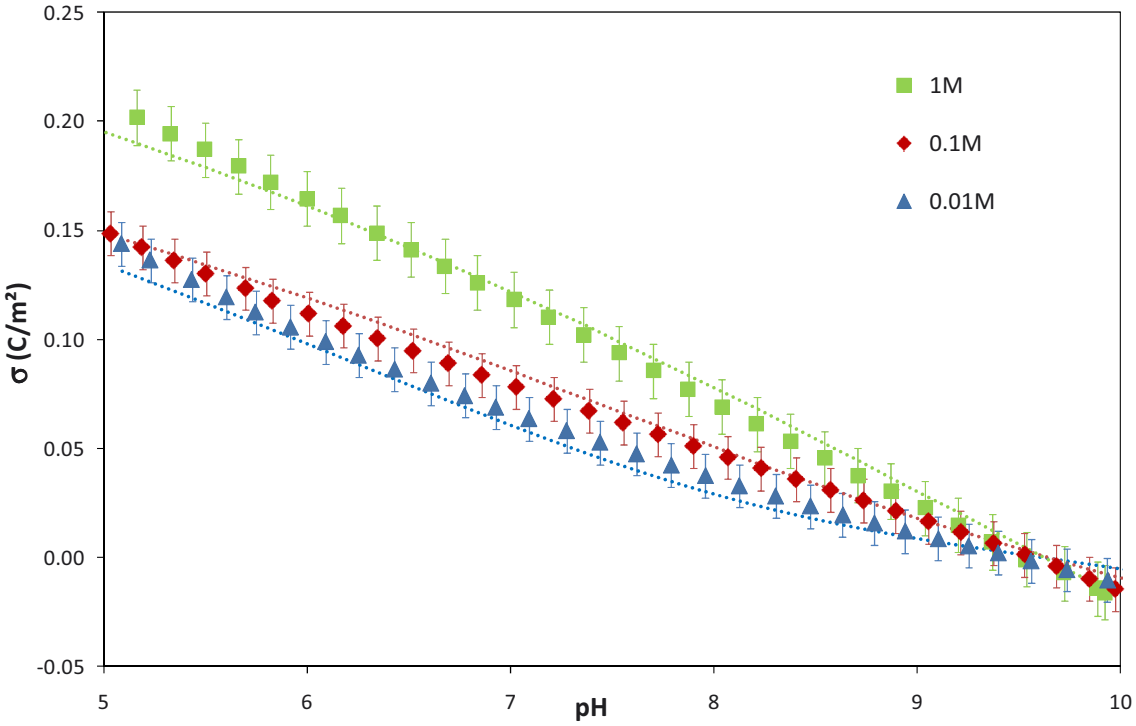

Figure 1. α-Al_2O_3 surface charge at different ionic strengths. The dotted lines are the results of modeling.

The application of Pauling valence rules to Al_2O_3 structure, in which the Al ions distribute their charge to the six surrounding O atoms, results in a charge of -0.5 per ≡AlOH site. Those singly coordinated surface groups can be protonated following the reaction

$$\equiv AlOH^{-1/2} + H^+ \leftrightarrows \equiv AlOH_2^{+1/2} \qquad K_H$$

in which K_H is the protonation constant.

In alumina structure, doubly coordinated surface sites $\equiv Al_2OH$ also exist, but they are uncharged in the studied pH range and will not be taken into account for the description of surface charging behavior (Hiemstra et al. 1999). The fitted parameters are summarized in Table 1.

The Basic Stern Model was used to describe the electrostatic double layer of the oxide interface (Westall and Hohl 1980). Ion pair formation of surface groups with electrolyte ions is taken into account, and described with the following equations

$\equiv AlOH^{-1/2} + C^+ \leftrightarrows \equiv AlOH^{-1/2} - C^+$ K_C

$\equiv AlOH_2^{+1/2} + A^- \leftrightarrows \equiv AlOH_2^{+1/2} - A^-$ K_A

where C^+ and A^- are the cation and the anion from the electrolyte, respectively. The electrolyte ions were all positioned in the outer plane of the Stern layer. Asymmetric binding of electrolyte ions on gibbsite has been previously evidenced (Hiemstra et al. 1999), so different affinity constants have been determined for the different electrolyte used. Their values were derived from those found for the charging of goethite (Rietra et al. 2000). The values obtained for cation pair formation are in accord with the ones of Rietra et al. (2000). However, NO_3^- ions were found to have very weak interaction with the alumina surface ($\log K_{NO3} = -1.6$), which is much lower than the observations made by Rietra et al. (2000) who found $\log K_{NO3} = -1$ for goethite. The affinity constants for ClO_4^- are coherent in the two studies: -1.4 in our case, -1.7 for Rietra et al. (2000).

The capacitance value found is quite high regarding the values proposed by Hiemstra and van Riemsdijk (2006) for metal (hydr)oxides surfaces. It is however similar to the value found by Rabung et al. (1998) in the case of hematite (2.24 F/m²).

Table 1. Fitted parameters used for describing the charging behavior of α-Al_2O_3 surface

Specific area	15 m²/g
Site density	8 sites/nm²
Stern layer capacitance	2.2 F/m²
$\log K_H$	9.6
$\log K_{Na}$	- 0.8
$\log K_K$	- 1.5
$\log K_{NO3}$	- 1.6
$\log K_{ClO4}$	- 1.4

A surface transformation of α-Al_2O_3 when hydrated was previously observed, which leads to a surface structure closer to $Al(OH)_3$ surface (Eng et al. 2000). After the 10 h long-titrations in solution, our sample of α-Al_2O_3 may develop gibbsite-like, or hydroxide-like, surface properties.

3.2 Eu(III) adsorption onto α-Al_2O_3

Eu(III) adsorption onto α-Al_2O_3 has been studied at different pH and two ionic strengths, 0.01 M and 0.1 M $NaClO_4$. Macroscopic results are shown in Figure 2**Erreur ! Source du renvoi introuvable.** (III) adsorption onto α-Al_2O_3 shows a great dependency to pH and a low dependency to ionic strength, which indicates inner-sphere complexation, as seen previously on various oxides (Rabung et al. 1998; Wang et al. 2006; Tan et al. 2009). The influence of metal/surface ratio has also been studied at pH = 6.17 ± 0.15 by changing α-Al_2O_3 concentration in the system. Results are shown in Figure 2. At high Eu(III)/α-Al_2O_3 ratio, with 0.5 g/L α-Al_2O_3, 58% of initial Eu(III) is retained onto the surface. The proportion of adsorbed Eu(III) increases with α-Al_2O_3 concentration, and reaches 100% around 5 g/L α-Al_2O_3.

Modeling has also been done using ECOSAT software and CD-MUSIC model. Data for Eu(III) speciation in solution have been taken from Hummel et al. (2002). Spectroscopic results showing the presence of one Eu(III) sorbed species, the formation of only one complex was taken into account. The best fit parameters ($r^2 \geq 0.90$) are displayed in Table 2. The results are shown in Figure 2.

Table 2. Fitted CD-MUSIC parameters obtained for Eu(III) complexation to α-Al_2O_3.

	Δz_0	Δz_1	logK
$\equiv AlOH^{-1/2} + Eu^{3+} \leftrightarrows \equiv AlOHEu^{+5/2}$	1.93	1.07	13.5

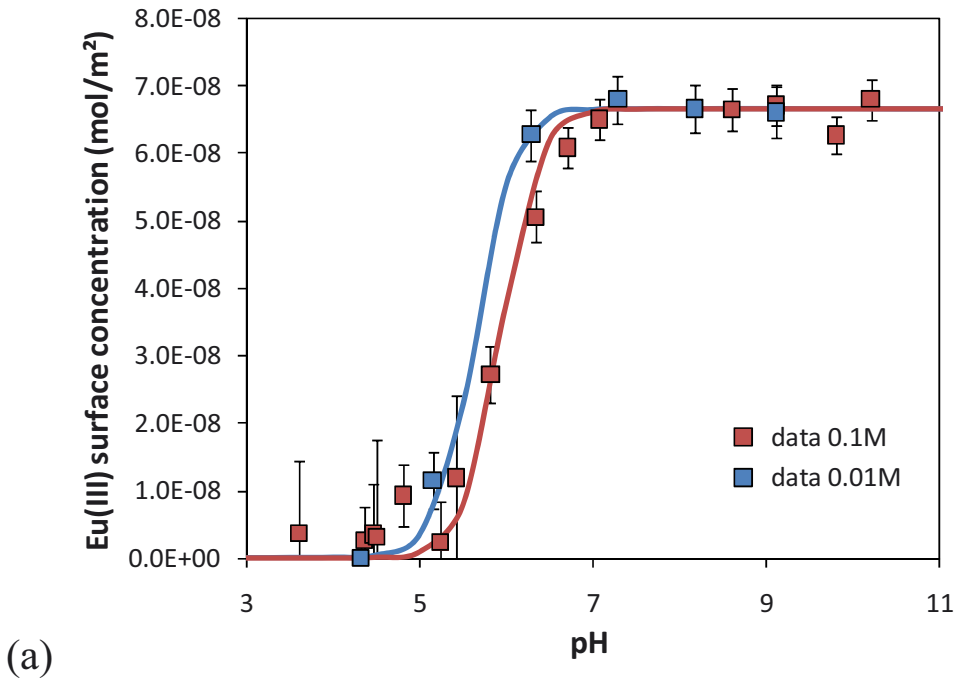

(a)

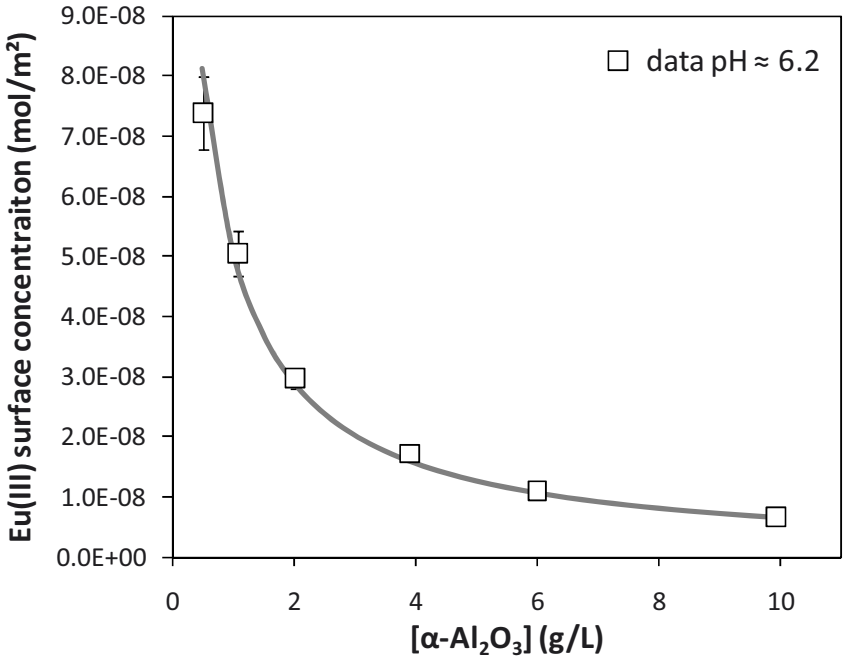

(b)

Figure 2. Surface concentration of Eu(III) in the binary Eu(III)/α-Al_2O_3 system depending on pH (a) and α-Al_2O_3 concentration (b). The lines are the results of modeling. [Eu(III)] = 10^{-6} mol/L; Error bars correspond to 2σ. (a) [α-Al_2O_3] = 1 g/L ; (b) *I* = 0.1 M $NaClO_4$ and pH = 6.2 ± 0.1.

These parameters were then used to model data sets from literature of Eu(III) binding to hydrous alumina (Tan et al. 2008) and γ-Al_2O_3 (Rabung et al. 2000), in order to check its efficiency. Results are shown in Figure 3.

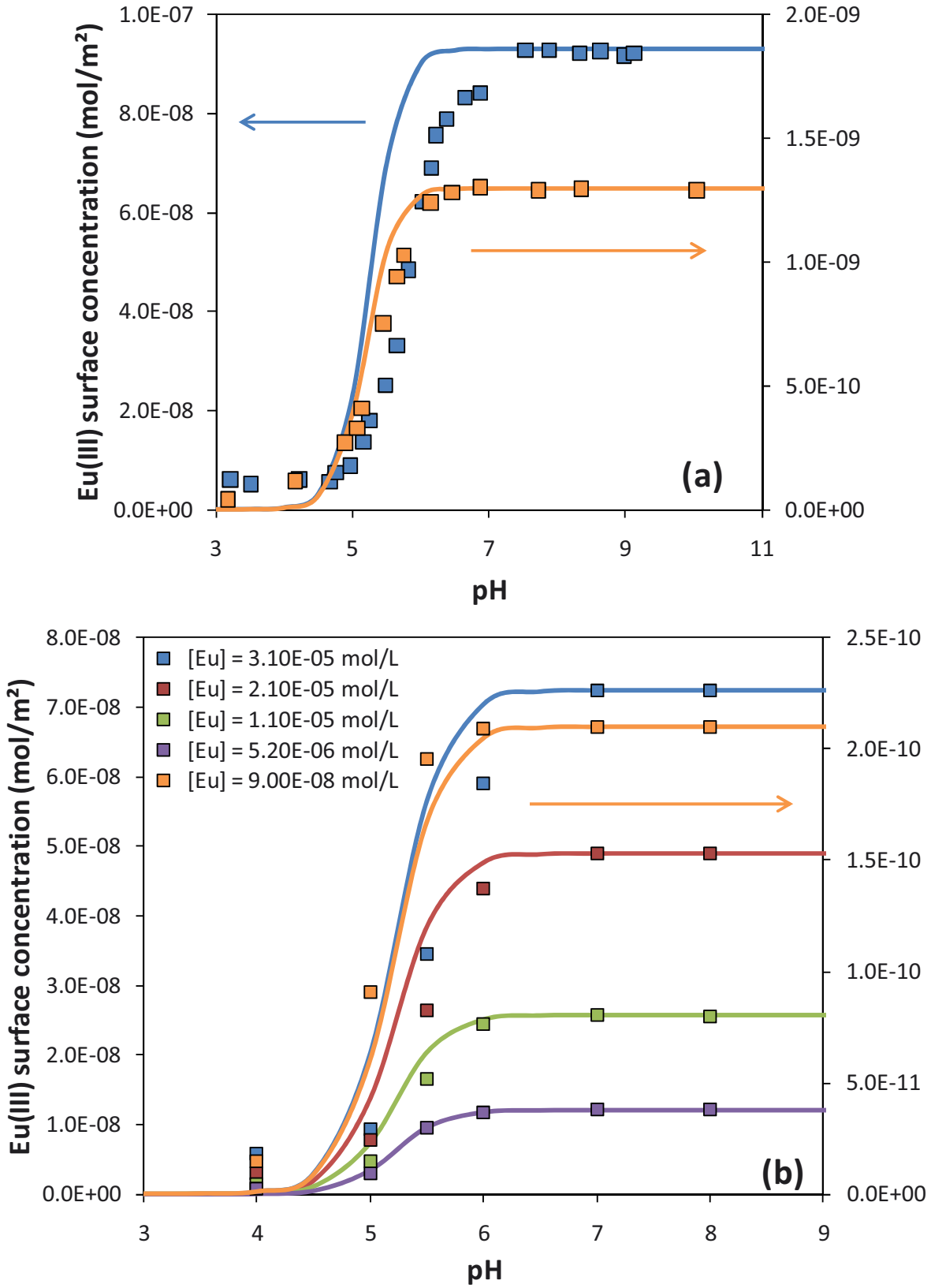

Figure 3. Eu(III) surface concentration on (a) 4.4 g/L hydrous alumina (105 m²/g), for I = 0.1 M KNO_3 and [Eu(III)] = 4.3 10^{-5} mol/L (blue) and 0.1 M $NaClO_4$ and [Eu(III)] = 6.0 10^{-7} mol/L (orange) (Tan et al. 2008) ; (b) 3.6 g/L γ-Al_2O_3 (119 m²/g) for I = 0.1 M $NaClO_4$ and various Eu(III) concentrations (Rabung et al. 2000). Symbols are the data from literature, and lines are the results of the modeling presented in this study.

The mineral surfaces used by these authors were not the same than the one used in this study, especially with higher specific area (above 100 m^2/g) than our surface (15 m^2/g). Results of modeling are yet quite good for Eu(III) concentrations close to the one used in our experiment, i.e. between $6 \cdot 10^{-6}$ and $6 \cdot 10^{-7}$ mol/L. For highest concentrations of Eu(III) (above 10^{-5} mol/L), modeling is overestimating Eu(III) adsorption, with pH-edges found at lower pH values than in experiments (see blue line on Figure 3a and blue, red and green lines on Figure 3b). When initial Eu(III) concentration is much lower, i.e. $9 \cdot 10^{-8}$ mol/L, the modeling is underestimating the adsorption.

The comparison of our modeling to literature data then validates a range of concentrations in which this modeling can be used, even if best fits may be obtained by fitting CD-MUSIC parameters for each mineral surface.

3.3 Eu(III) binding to humic acid

Eu(III) binding to PAHA has been studied by TRLS at pH 4 and different PAHA concentrations. Eu(III) luminescence spectra present an hypersensitive transition, $^5D_0 \rightarrow {}^7F_2$, ~~which intensity~~ is enhanced in the metal-ligand complex relative to its intensity for the aquo ion (Jorgensen and Judd 1964). Consequently, the change of relative intensities of $^5D_0 \rightarrow {}^7F_2$ and $^5D_0 \rightarrow {}^7F_1$ transitions indicates a change in Eu(III) environment symmetry. It evolves with the relative concentration of metal and humic acid as shown in Figure 4. Above 20 mg/l of PAHA in the system, the asymmetry ratio $^5D_0 \rightarrow {}^7F_2/{}^5D_0 \rightarrow {}^7F_1$ (noted $^7F_2/{}^7F_1$) does not evolve, meaning that all the Eu(III) is complexed to humic molecules. When there is no PAHA in the system, the asymmetry ratio value is the one corresponding to no complexation. It is then possible to use this evolution as a spectral titration curve (Dobbs et al. 1989).

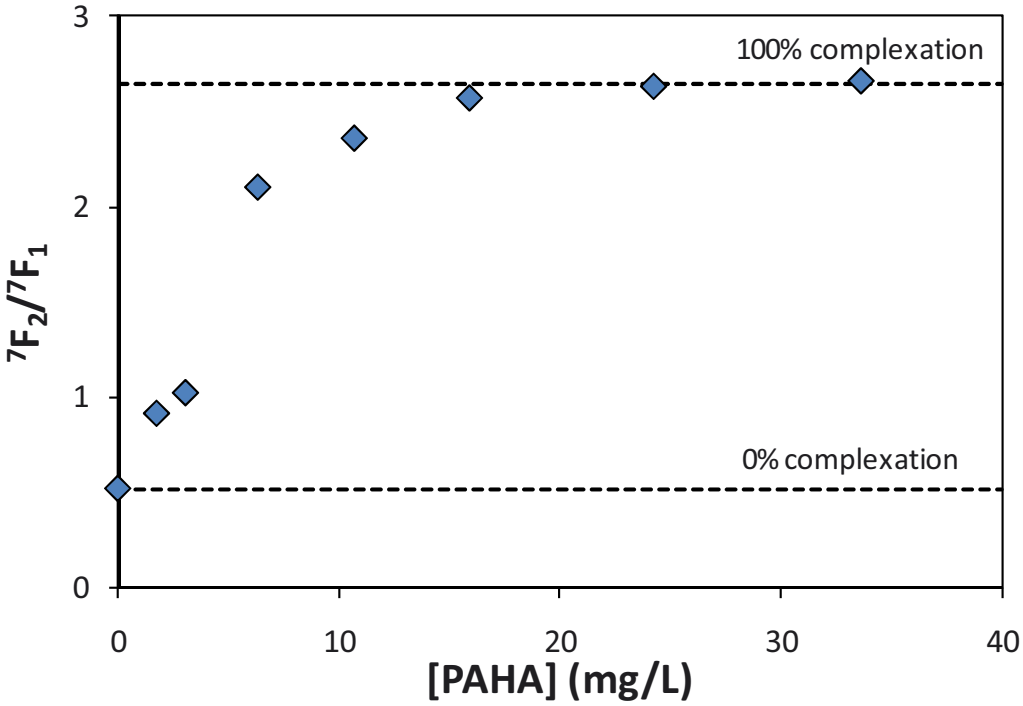

Figure 4. Evolution of asymmetry ratio of Eu(III)/PAHA spectra at pH 4 depending on humic concentration. [Eu(III)] = 10^{-6} mol/L, pH = 4, *I* = 0.1 M $NaClO_4$.

These asymmetry ratios have then been used as indicators of the proportion of Eu(III) complexed, in order to adjust the NICA-Donnan parameters for Eu(III)/humic acid binding (Milne et al. 2003; Marang et al. 2008), as shown in Figure 5. Modeling has been done using ECOSAT software

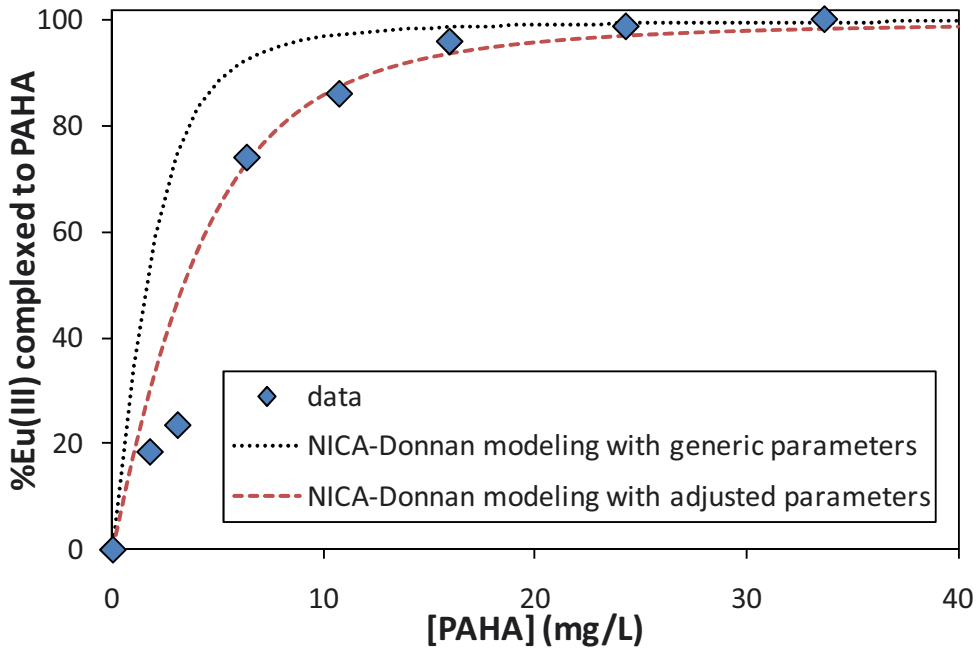

Figure 5. Results of adjustment of NICA-Donnan parameters for Eu(III)/PAHA binding.

This adjustment was done at pH 4 only, for at pH 6 100% complexation was immediately reached when PAHA was added in the system. At higher pH and in the absence of humic acid, due the presence of hydrolyzed species of Eu(III) in solution, it is not possible to have the asymmetry ratio value corresponding to the absence of complexation. Thus, only the parameters for the low affinity sites (S1) have been adjusted. Results are given in Table 3.

Table 3. NICA-Donnan parameters used for Eu(III)/PAHA binding.

	$\log\tilde{K}$	n
S1-Eu	1.05	0.50
S2-Eu	3.43[a]	0.36[a]

[a] Milne *et al.* (2003)

3.4 Eu(III) speciation in the ternary system

The difficulty to describe the ternary system is due to HA fractionation and modification of reactivity after adsorption onto the mineral surface. In this work, spectrophotometric titrations of PAHA supernatants presented in a previous study (Janot et al. 2010) are used to quantify proton-binding behavior of humic fractions. Two pools of PAHA are defined, one staying in solution after centrifugation of the suspension, noted $PAHA_{sol}$, and one adsorbed onto the mineral, noted $PAHA_{ads}$. Each one has different NICA-Donnan parameters. We have used parameters determined by spectrophotometric titrations of supernatant from adsorption experiments of binary PAHA/α-Al_2O_3 systems (Janot et al. 2010, and Chapter 3 of this thesis) to modify original PAHA proton binding parameters.

NICA-Donnan parameters obtained from spectrophotometric titrations of supernatants from adsorption experiments may not be used as it is: parameters for original PAHA – noted $PAHA_i$ – obtained from potentiometric and spectrophotometric titrations were not the same, due to the low number of data points recorded with the spectrophotometric method (Janot et al. 2010). Consequently, for the sake of comparison, the ratios obtained between potentiometric and spectrophotometric parameters for $PAHA_i$ have been applied to the spectrophotometric parameters obtained for PAHA fractions, in order to retrieve parameters

comparable to potentiometric results. Titrations of $PAHA_i$ and modeling of its charge before fractionation using the NICA-Donnan model are presented elsewhere (Janot et al. 2010).

In the ternary system, at 0.1 M $NaClO_4$ and an initial PAHA concentration of 28 mg/L, between 90 and 30 % of PAHA is adsorbed onto α-Al_2O_3, depending on pH (see Chapter 3 of this thesis). Except at pH < 4, fractionation is moderate, so we may use median proton-binding parameters determined from PAHA/α-Al_2O_3 supernatant titrations to describe protonation behavior of PAHA fractions in the ternary system.

From spectrophotometric titrations, we did not see any significant variation of Q_2, m_1 and m_2 for the dissolved fraction $PAHA_{sol}$, so these parameters were not changed. However, the values of Q_1 and $\log\tilde{K}_1$ were lowered, and $\log\tilde{K}_2$ increased compared to the original compound, as seen by spectrophotometric titrations of non-sorbed fractions (see Chapter 3).

The same calculation was performed for $PAHA_{ads}$. From spectrophotometric titrations and mass balance calculations, we observed an increase in Q_1 and $\log\tilde{K}_1$ values regarding the values fitted for non-fractionated PAHA (see Chapter 3).

The parameters for both fractions $PAHA_{sol}$ and $PAHA_{ads}$ – spectrophotometric parameters an recalculated "potentiometric-like" parameters – are reported in Table 4.

Table 4. NICA-Donnan proton-binding intrinsic parameters for original PAHA ($PAHA_i$), non-adsorbed PAHA fraction ($PAHA_{sol}$), and adsorbed PAHA fraction ($PAHA_{ads}$), determined from potentiometric and spectrophotometric titrations. In bold are the final parameters modified compared to $PAHA_i$.

	Q_1	$\log\tilde{K}_1$	m_1	Q_2	$\log\tilde{K}_2$	m_2
$PAHA_i$ (spectrophotometry)	3.63	2.80	0.66	1.77	6.41	0.45
$PAHA_i$ (potentiometry)	3.24	2.66	0.81	2.88	6.90	0.29
$PAHA_{sol}$ (spectrophotometry)	1.60	2.40	0.66	1.77	7.60	0.45
$PAHA_{sol}$ (used for modeling)	**1.80**	**2.25**	0.81	2.88	**8.15**	0.29
$PAHA_{ads}$ (spectrophotometry)	4.40	3.00	0.66	1.77	6.41	0.45
$PAHA_{ads}$ (used for modeling)	**3.90**	**2.85**	0.81	2.88	6.90	0.29

The $\log\tilde{K}_1$ values for protonation have varied for the two fractions regarding the original material. Consequently, the $\log\tilde{K}_1$ values for Eu(III)/PAHA binding determined previously (see Table 3) were modified in the same proportions. Following the same reasoning, the $\log\tilde{K}_2$ value for Eu(III) binding to non-sorbed PAHA fraction has been recalculated as well. The NICA-Donnan parameters taken into account for modeling Eu(III) binding to dissolved and adsorbed PAHA fractions are given in Table 5. For metal binding to humic acid, generic parameters for p_1 (0.62) and p_2 (0.41) value were used (Milne et al. 2001). m_i values for proton binding were the same in original PAHA and fractions, then n_i values for europium(III) binding were not changed.

Table 5. Modified NICA-Donnan intrinsic parameters for Eu(III) binding to PAHA fractions.

	$\log\tilde{K}_1$	$\log\tilde{K}_2$
Eu(III)/PAHA$_{sol}$	0.90	4.05
Eu(III)/PAHA$_{ads}$	1.12	3.43 (generic)

Using these parameters, the surface concentration of Eu(III) onto the solid has been calculated, using as inputs of the model the exact values of the different samples: pH, Eu(III) and α-Al_2O_3 concentrations, as well as amounts of both PAHA fractions. Eu(III) and α-Al_2O_3 concentrations may vary between two experiments due to modifications of solution volume when adjusting the pH value. These differences within a series explain the otherwise apparently peculiar variations of model for some data. Calculation was made for the experiments performed at different pH at 0.01 M and 0.1 M $NaClO_4$ as well as for the experiments performed at constant pH and various initial PAHA concentrations. Results are shown in Figure 6. They show theoretical and actual surface concentration of Eu(III), i.e. Eu(III) bound to the surface and to adsorbed PAHA.

With this modeling, the behavior of Eu(III) is rather well described in a ternary Eu(III)/PAHA/α-Al_2O_3 system depending on pH, especially at 0.1 M. This may be due to the use of NICA-Donnan parameters determined from 0.1 M adsorption experiments (Chapter 3). The trends of Eu(III) behavior depending on initial PAHA concentration are captured, but the values are not always accurate. The isotherm at pH 6.2 is well-described, whereas the Eu(III) adsorption at pH 7.4 seems underestimated. The behavior of Eu(III) at pH 4 is the lesser well described, even if the general trend is present. These conditions correspond to a very important fractionation rate, with a high percentage of PAHA being adsorbed and a great modification of PAHA reactivity (see Chapter 3). The disagreement between experimental and calculated concentrations under these conditions may be due to the values chosen for adapted protonation parameters of both PAHA fractions, which correspond to a median fractionation (around 70 %). This may be the reason for the difference at pH 4 and 0.01 M $NaClO_4$.

Moreover, the protonation parameters taken for the modeling were calculated from titrations made on supernatant from binary PAHA/α-Al_2O_3 system. Now, presence of Eu(III) may have an influence on the fractionation of humic moieties.

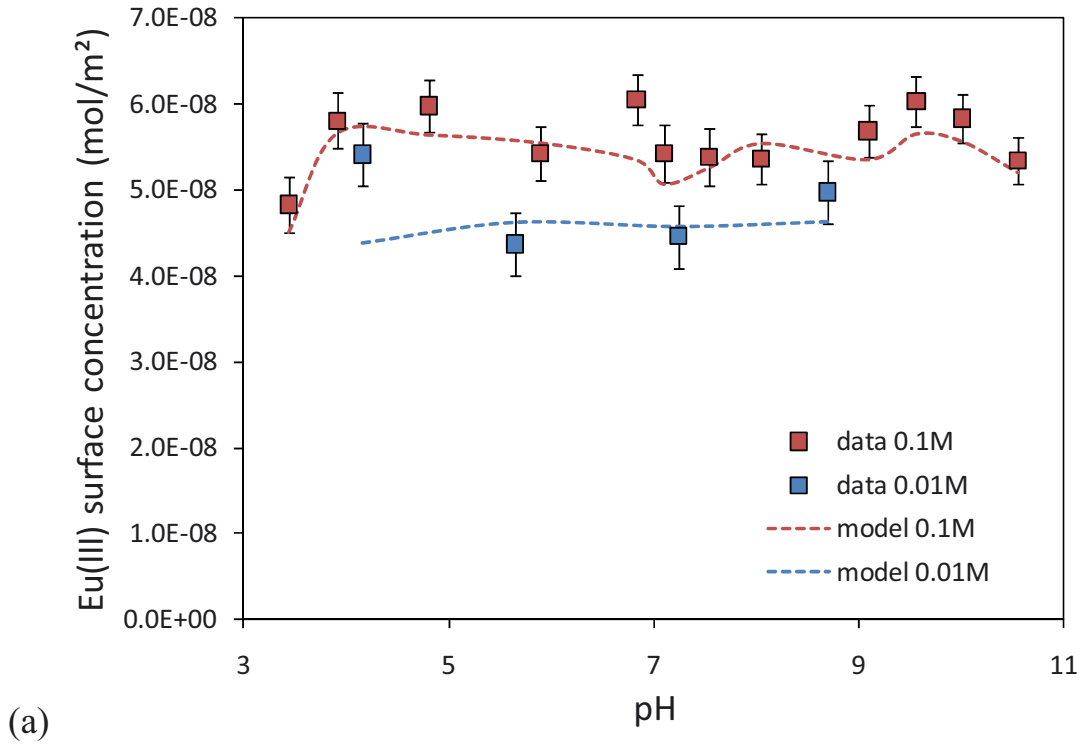

(a)

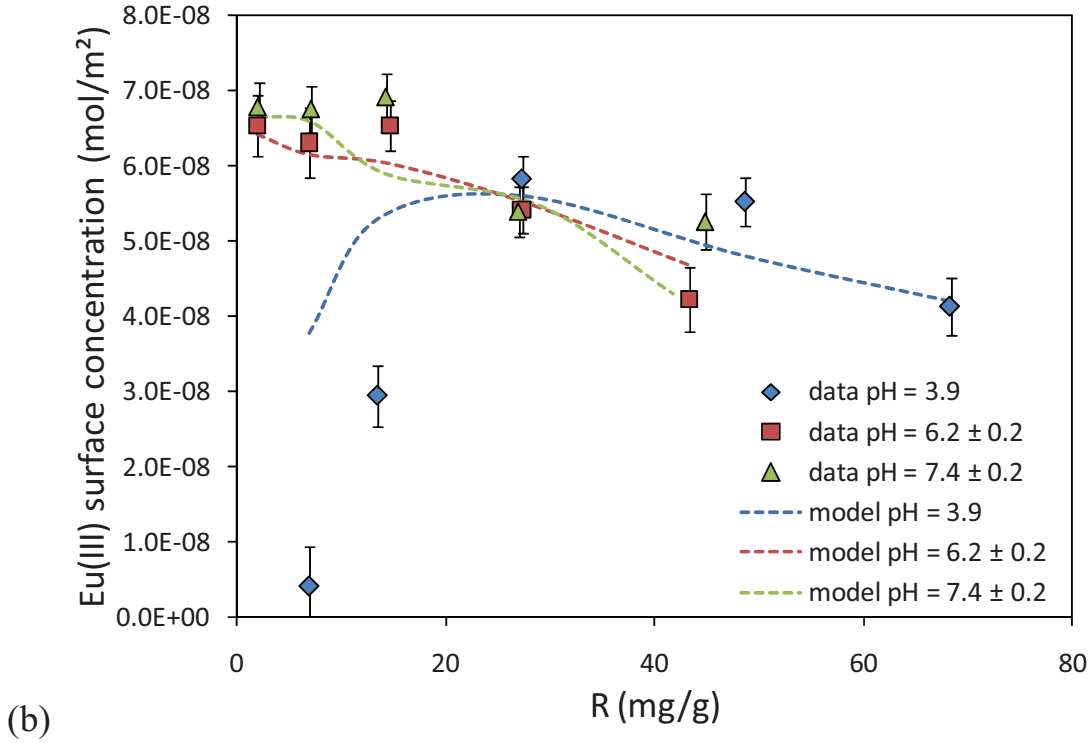

(b)

Figure 6. Eu(III) surface concentration in the ternary system depending on pH (a) and coverage ratio (b). Error bars correspond to 2σ.

Figure 7 shows the speciation of Eu(III) determined through this modeling depending on pH. One can see that between pH 4 and 8, Eu(III) is mainly bound to $PAHA_{ads}$. The influence of the mineral surface begins to be important only above pH 9, which is in agreement with spectroscopic observations (Janot et al. 2011). Actually, TRLS spectra of Eu(III) in the ternary system showed an apparition of surface-like features for pH values higher than 8: decrease of asymmetry ratio, broadening of $^5D_0 \rightarrow {}^7F_1$ transition, shifting of $^5D_0 \rightarrow {}^7F_2$ apparent maximum toward higher wavelengths (cf. Chapter 5).

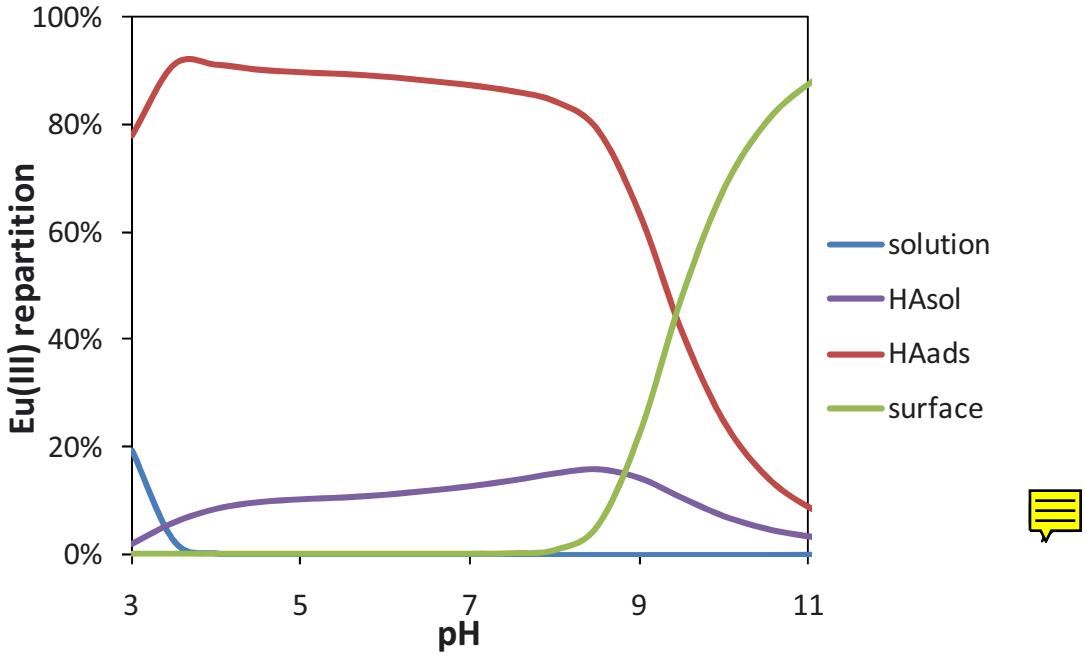

Figure 7. Eu(III) speciation in the ternary system depending on pH.
***I* = 0.1 M $NaClO_4$, [PAHA] = 28 mg/L, [α-Al_2O_3] = 1 g/L, [Eu(III)] = 10^{-6} mol/L.**

At 0.01 M $NaClO_4$, macroscopic observations showed less PAHA adsorbed onto the surface, so the surface concentration of Eu(III) is lower, but Eu(III) repartition is quite the same (data not shown).

Eu(III) repartition is also calculated for data at different coverage ratios, as shown in Figure 8. At pH 6.2 and 7.4, Eu(III) is partly complexed to the surface for coverage ratios below 10 $mg_{PAHA}/g_{\alpha\text{-}Al_2O_3}$. When PAHA concentration increases, Eu(III) is totally bound to PAHA, mostly to the adsorbed fraction. At pH 4, there is no influence of the surface, accordingly to binary Eu(III)/α-Al_2O_3 observations. Eu(III) surface concentration is only due to its complexation with $PAHA_{ads}$. Below 20 $mg_{PAHA}/g_{\alpha\text{-}Al_2O_3}$, there is a significant proportion of Eu(III) free in solution is mostly free, which is not seen at higher pH values.

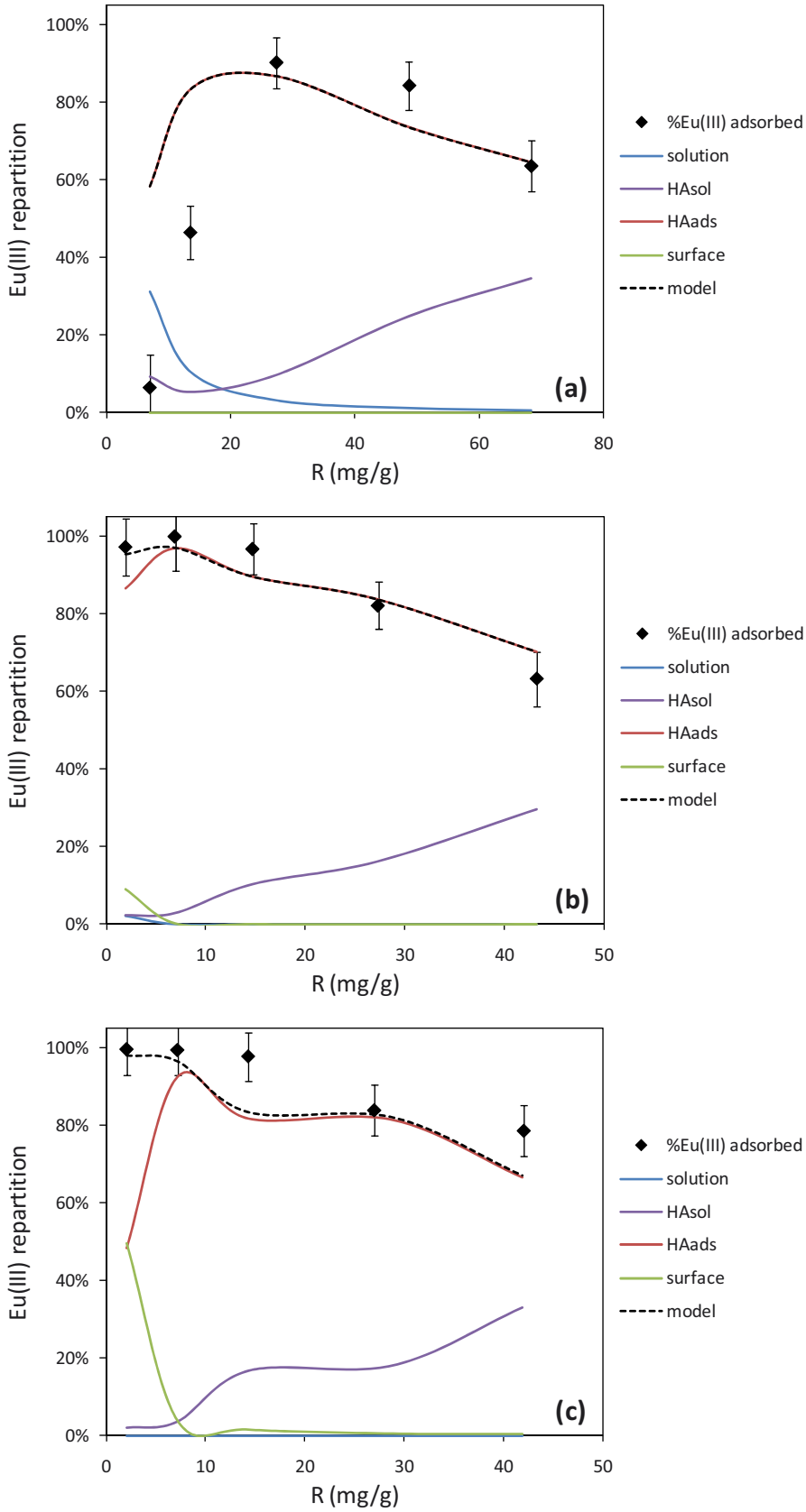

Figure 8. Eu(III) repartition in the ternary system depending on coverage ratio at (a) pH = 3.9 (b) pH = 6.2 ± 0.2 (c) pH = 7.4 ± 0.2. The dotted line "model" corresponds to the sum of HAads and surface results.

REFERENCES

Ali, M. A. and Dzombak D. A. (1996). "Competitive sorption of simple organic acids and sulfate on goethite." *Environmental Science & Technology* **30**(4): 1061-1071.

Alliot, C., Bion L., et al. (2005). "Sorption of aqueous carbonic, acetic, and oxalic acids onto alpha-alumina." *Journal of Colloid and Interface Science* **287**(2): 444-451.

Bünzli, J.-C. G. (1989). Luminescent probes. *Lanthanides probe in life , chemical and earth sciences - Theory and practice*. J.-C. G. Bünzli and G. R. Choppin. Amsterdam, Elsevier.

Christl, I. and Kretzschmar R. (2001). "Interaction of copper and fulvic acid at the hematite-water interface." *Geochimica Et Cosmochimica Acta* **65**(20): 3435-3442.

Claret, F., Schafer T., et al. (2008). "Fractionation of Suwannee River Fulvic Acid and Aldrich Humic Acid on alpha-Al2O3: Spectroscopic Evidence." *Environmental Science & Technology* **42**(23): 8809-8815.

Dobbs, J. C., Susetyo W., et al. (1989). "A novel-approach to metal-humic complexation studies by lanthanide ion probe spectroscopy." *International Journal of Environmental Analytical Chemistry* **37**(1): 1-17.

Dryer, D. J., Korshin G. V., et al. (2008). "In situ examination of the protonation behavior of fulvic acids using differential absorbance spectroscopy." *Environmental Science & Technology* **42**(17): 6644-6649.

Eng, P. J., Trainor T. P., et al. (2000). "Structure of the hydrated alpha-Al2O3 (0001) surface." *Science* **288**(5468): 1029-1033.

Filius, J. D., Meeussen J. C. L., et al. (2001). "Modeling the binding of benzenecarboxylates by goethite: The ligand and charge distribution model." *Journal of Colloid and Interface Science* **244**(1): 31-42.

Filius, J. D., Meeussen J. C. L., et al. (2003). "Modeling the binding of fulvic acid by goethite: The speciation of adsorbed FA molecules." *Geochimica Et Cosmochimica Acta* **67**(8): 1463-1474.

Heidmann, I., Christl I., et al. (2005). "Sorption of Cu and Pb to kaolinite-fulvic acid colloids: Assessment of sorbent interactions." *Geochimica Et Cosmochimica Acta* **69**(7): 1675-1686.

Hiemstra, T., Dewit J. C. M., et al. (1989). "Multisite proton adsorption modeling at the solid-solution interface of (hydr)oxides - A new approach. 2. Application to various important (hydr)oxides." *Journal of Colloid and Interface Science* **133**(1): 105-117.

Hiemstra, T. and van Riemsdijk W. H. (1996). "A surface structural approach to ion adsorption: The charge distribution (CD) model." *Journal of Colloid and Interface Science* **179**(2): 488-508.

Hiemstra, T. and van Riemsdijk W. H. (2006). "On the relationship between charge distribution, surface hydration, and the structure of the interface of metal hydroxides." *Journal of Colloid and Interface Science* **301**(1): 1-18.

Hiemstra, T., Yong H., et al. (1999). "Interfacial charging phenomena of aluminum (hydr)oxides." *Langmuir* **15**(18): 5942-5955.

Hummel, W., Berner U., et al. (2002). "Nagra/PSI chemical thermodynamic data base 01/01." *Radiochimica Acta* **90**(9-11): 805-813.

Hur, J. and Schlautman M. A. (2003). "Molecular weight fractionation of humic substances by adsorption onto minerals." *Journal of Colloid and Interface Science* **264**(2): 313-321.

Janot, N., Benedetti M. F., et al. (2011). "Colloidal a-Al2O3, Europium(III) and Humic Substances Interactions: A Macroscopic and Spectroscopic Study." *Environ Sci Technol*.

Janot, N., Reiller P. E., et al. (2010). "Using Spectrophotometric Titrations To Characterize Humic Acid Reactivity at Environmental Concentrations." *Environmental Science & Technology* **44**(17): 6782-6788.

Jorgensen, C. K. and Judd B. R. (1964). "Hypersensitive pseudoquadrupole transitions in lanthanides." *Molecular Physics* **8**(3): 281-290.

Keizer, M. G. and van Riemsdijk W. H. (1994). A computer program for the Calculation of Chemical Speciation and Transport in Soil-Water Systems (ECOSAT 4.7). Agricultural University of Wageningen. Wageningen, Agricultural University of Wageningen.

Kim, J. I., Buckau G., et al. (1990). "Characterization of humic and fulvic-acids from Gorleben groundwater." *Fresenius Journal of Analytical Chemistry* **338**(3): 245-252.

Kinniburgh, D. G., van Riemsdijk W. H., et al. (1999). "Ion binding to natural organic matter: competition, heterogeneity, stoichiometry and thermodynamic consistency." *Colloids and Surfaces a-Physicochemical and Engineering Aspects* **151**(1-2): 147-166.

Marang, L., Reiller P. E., et al. (2008). "Combining spectroscopic and potentiometric approaches to characterize competitive binding to humic substances." *Environmental Science & Technology* **42**(14): 5094-5098.

McCarthy, J. F., Czerwinski K. R., et al. (1998a). "Mobilization of transuranic radionuclides from disposal trenches by natural organic matter." *Journal of Contaminant Hydrology* **30**(1-2): 49-77.

McCarthy, J. F., Sanford W. E., et al. (1998b). "Lanthanide field tracers demonstrate enhanced transport of transuranic radionuclides by natural organic matter." *Environmental Science & Technology* **32**(24): 3901-3906.

Meier, M., Namjesnik-Dejanovic K., et al. (1999). "Fractionation of aquatic natural organic matter upon sorption to goethite and kaolinite." *Chemical Geology* **157**(3-4): 275-284.

Milne, C. J., Kinniburgh D. G., et al. (2001). "Generic NICA-Donnan model parameters for proton binding by humic substances." *Environmental Science & Technology* **35**(10): 2049-2059.

Milne, C. J., Kinniburgh D. G., et al. (2003). "Generic NICA-Donnan model parameters for metal-ion binding by humic substances." *Environmental Science & Technology* **37**(5): 958-971.

Rabung, T., Geckeis H., et al. (1998). "Sorption of Eu(III) on a natural hematite: Application of a surface complexation model." *Journal of Colloid and Interface Science* **208**(1): 153-161.

Rabung, T., Stumpf T., et al. (2000). "Sorption of Am(III) and Eu(III) onto gamma-alumina: experiment and modelling." *Radiochimica Acta* **88**: 711-716.

Reiller, P., Amekraz B., et al. (2006). "Sorption of Aldrich humic acid onto hematite: Insights into fractionation phenomena by electrospray ionization with quadrupole time-of-flight mass spectrometry." *Environmental Science & Technology* **40**(7): 2235-2241.

Reiller, P., Moulin V., et al. (2002). "Retention behaviour of humic substances onto mineral surfaces and consequences upon thorium (IV) mobility: case of iron oxides." *Applied Geochemistry* **17**(12): 1551-1562.

Rietra, R., Hiemstra T., et al. (2000). "Electrolyte anion affinity and its effect on oxyanion adsorption on goethite." *Journal of Colloid and Interface Science* **229**(1): 199-206.

Tan, X. L., Fang M., et al. (2009). "Adsorption of Eu(III) onto TiO2: Effect of pH, concentration, ionic strength and soil fulvic acid." *Journal of Hazardous Materials* **168**(1): 458-465.

Tan, X. L., Wang X. K., et al. (2008). "Sorption of Eu(III) on humic acid or fulvic acid bound to hydrous alumina studied by SEM-EDS, XPS, TRLFS, and batch techniques." *Environmental Science & Technology* **42**(17): 6532-6537.

Tipping, E. (1998). "Humic ion-binding model VI: An improved description of the interactions of protons and metal ions with humic substances." *Aquatic Geochemistry* **4**(1): 3-48.

Vermeer, A. W. P., McCulloch J. K., et al. (1999). "Metal ion adsorption to complexes of humic acid and metal oxides: Deviations from the additivity rule." *Environmental Science & Technology* **33**(21): 3892-3897.

Wang, X., Xu D., et al. (2006). "Sorption and complexation of Eu(III) on alumina: Effects of pH, Ionic strength, humic acid and chelating resin on kinetic dissociation study." *Applied Radiation and Isotopes* **64**(4): 414-421.

Weng, L., Van Riemsdiik W. H., et al. (2009). "Effects of fulvic and humic acids on arsenate adsorption to goethite: experiments and modeling." *Environ Sci Technol* **43**(19): 7198-204.

Weng, L. P., van Riemsdijk W. H., et al. (2007). "Adsorption of humic acids onto goethite: Effects of molar mass, pH and ionic strength." *Journal of Colloid and Interface Science* **314**(1): 107-118.

Weng, L. P., van Riemsdijk W. H., et al. (2008). "Cu2+ and Ca2+ adsorption to goethite in the presence of fulvic acids." *Geochimica Et Cosmochimica Acta* **72**(24): 5857-5870.

Westall, J. and Hohl H. (1980). "Comparison of electrostatic models for the oxide-solution interface." *Advances in Colloid and Interface Science* **12**(4): 265-294.

CONCLUSIONS ET PERSPECTIVES

Cette étude s'inscrit dans une problématique de compréhension du devenir des radionucléides dans un milieu naturel, dans lequel les contaminants se retrouvent en contact à la fois avec des surfaces minérales et de la matière organique naturelle. De nombreuses études portent sur ce type de systèmes ternaires, mais les composants utilisés (et leurs concentrations relatives) sont très diversifiés : divers oxydes métalliques ou argiles pour les surfaces, acides humiques, fulviques, ou acides organiques simples comme représentants de la matière organique naturelle, et contaminants cationiques ou anioniques variables. De ce fait, il est encore difficile d'avoir une compréhension claire des mécanismes en jeu. Dans ce contexte, ce travail réalisé en laboratoire s'est intéressé à l'influence d'un oxyde d'aluminium (α-Al_2O_3) et d'un acide humique (PAHA) sur le comportement de l'europium(III).

Afin de prédire le comportement d'un contaminant dans le milieu naturel, il est utile de parvenir à modéliser sa spéciation dans une large gamme de paramètres environnementaux (pH, force ionique, concentration en matière organique notamment). Or, s'il existe des modèles décrivant bien les interactions entre les différents composants deux à deux, la description des systèmes ternaires est toujours difficile, notamment du fait du fractionnement des agrégats humiques lors de leur adsorption sur des surfaces qui modifie leur composition et leur structure, et par là même leur réactivité.

Dans le cadre de ce travail, nous avons étudié la spéciation de l'europium(III) dans des conditions environnementales variées et, afin de modéliser les résultats obtenus, validé une méthode permettant d'étudier la réactivité des substances humiques à des concentrations représentatives de celles des milieux naturels.

Étude de la spéciation de l'europium(III) dans un système ternaire

La spéciation du radionucléide au sein du système ternaire Eu(III)/PAHA/α-Al_2O_3 a été étudiée dans une gamme variée de conditions environnementales, à différentes valeurs de pH, de force ionique et de concentration en matière organique. L'influence de ces paramètres a été étudiée au niveau macroscopique – sur les quantités d'europium(III) et/ou de PAHA adsorbées sur le minéral – ainsi qu'à l'échelle moléculaire – sur la spéciation de l'Eu(III) en solution, par

spectroscopie laser à résolution temporelle. Dans chaque cas, les différents systèmes binaires ont été étudiés de la même façon : Eu(III)/PAHA, Eu(III)/α-Al_2O_3, PAHA/α-Al_2O_3.

Les résultats montrent, comme attendu, que la présence de matière organique modifie l'adsorption de l'europium(III) sur la surface. Les résultats macroscopiques sont en accord avec ceux de la littérature. Ils montrent que la présence de matière organique augmente la fixation de Eu(III) à faible pH, mais qu'elle favorise présence en solution, et donc son transport éventuel, au-delà de pH 6-7 selon les concentrations respectives des différents composés. Une diminution de la force ionique provoque une diminution à la fois de l'adsorption de l'europium(III) mais aussi de l'acide humique. À pH donné, lorsque la concentration en acide humique augmente, la surface est saturée, et la concentration de la fraction organique dissoute augmente également, favorisant l'entraînement de Eu(III) en solution.

Les informations spectroscopiques – les spectres de luminescence, les ratios d'asymétrie, ainsi que les temps de décroissance de luminescence – montrent qu'à pH ≤ 8 dans le système ternaire, l'europium(III) est préférentiellement complexé à PAHA, sans réelle influence de la surface, excepté au niveau de temps de décroissance. En effet, les valeurs des temps de décroissance dans le système ternaire à 0.1 M sont bien plus importantes que dans les systèmes binaires. Ce phénomène est interprété comme dû à l'environnement plus contraint de Eu(III) lorsqu'il est lié à la matière organique naturelle adsorbée sur la surface : la concentration en PAHA est plus importante sur la surface, et la probabilité pour les ions Eu(III) complexés de perdre de l'énergie par l'intermédiaire des groupements fonctionnels environnants diminue. Cette conclusion est en accord avec les temps de décroissance plus faibles observés pour le système ternaire à plus faible force ionique, où les concentrations à la surface en Eu(III) et en PAHA sont plus faibles pour la même surface.

La décroissance bi-exponentielle de la luminescence de l'europium(III) est observée dès que PAHA est présent dans le système, sauf à pH 4 où elle n'est visible qu'au-delà d'une certaine concentration en acides humiques, lorsque tout l'europium(III) est complexé. La valeur du premier temps de décroissance est similaire quels que soient le pH, la force ionique et la concentration en matière organique dans le système, en présence de la phase minérale ou non. Il semble donc indépendant des conditions de la solution, et peut être interprété comme un échange rapide d'énergie entre l'Eu(III) excité et les molécules humiques auxquelles il est lié.

Pour améliorer encore la compréhension des mécanismes en jeu dans ce système, il pourrait être utile de travailler dans un plus grand espace paramétrique ; notamment de réaliser plus d'expériences à plus faible force ionique. Il semblerait également intéressant d'étudier ce système à différents rapports D_2O/H_2O, afin d'établir la relation entre temps de décroissance de luminescence et nombre de molécules d'eau dans la première sphère de coordination de l'europium(III) pour ce système.

Validation des titrages spectrophotométriques comme méthode d'étude de réactivité des substances humiques à faible concentration

L'étude de réactivité des substances humiques se fait généralement par l'intermédiaire des titrages potentiométriques. Or cette technique nécessite de travailler avec une forte concentration de colloïdes, dans des conditions qui ne sont pas représentatives des milieux naturels. Réussir à caractériser le comportement des SH à des concentrations plus réalistes permettrait également de pouvoir caractériser les modifications de réactivité de ces composés après adsorption sur une surface minérale, car la concentration en SH dans les surnageants des expériences de sorption est en général relativement faible. Nous avons donc utilisé une méthode de titrages spectrophotométriques, présentée par Dryer et al. (2008), qui permet de travailler à des faibles concentrations en SH (autour de 10 mg_{SH}/L). Afin de la valider comme méthode d'étude de la réactivité des SH, nous avons étudié les liens entre les résultats de titrages potentiométriques et spectrophotométriques de PAHA à différentes forces ioniques. Nous avons obtenu une fonction de transfert entre ces données, valables dans la gamme de force ionique étudiée (0.01 à 0.5 M), pour l'acide humique étudié.

Cette technique paraît prometteuse, cependant des études complémentaires sont nécessaires. En effet, il faudrait réaliser des titrages potentiométriques et spectrophotométriques d'une large gamme d'acides humiques et fulviques, afin de déterminer – si elles existent – des fonctions de transfert pour différents matériaux, ainsi que leur variabilité. La mise au point d'un couplage entre le titrateur et le spectrophotomètre, avec des mesures automatisées, permettrait également d'obtenir des courbes de titrage spectrophotométriques plus précises avec plus de points de mesures. De cette manière, les analyses se feraient en circuit fermé, sans risque de carbonatation du système et en éliminant les pertes d'échantillon lors du transfert entre les appareils de mesure.

Modélisation des interactions dans le système ternaire

Les titrages spectrophotométriques de surnageants d'expériences d'adsorption PAHA/α-Al_2O_3 ont mis en évidence la modification de la réactivité des fractions organiques après adsorption sur une surface minérale. Il paraît donc nécessaire de prendre en compte cette observation lors de la modélisation des interactions dans le système ternaire.

Pour la modélisation présentée dans ce travail, nous avons utilisé les résultats obtenus à partir de surnageants d'expériences d'adsorption à pH ≈ 7. La description du comportement de l'europium(III) est correcte, lorsque le taux de fractionnement de la matière organique n'est pas trop important. Or il paraît évident que les modifications de pH vont influer sur les groupes fonctionnels des substances humiques qui réagissent avec la surface minérale. Afin d'améliorer la modélisation proposée, il faudrait donc également réaliser des titrages spectrophotométriques de surnageants d'expériences d'adsorptions faites à d'autres valeurs de pH d'équilibre, afin de quantifier et qualifier les modifications de protonation de PAHA sur une large gamme de pH.

Il faut cependant souligner que ces titrages spectrophotométriques ont été réalisés à partir d'expériences d'adsorption d'un milieu binaire PAHA/α-Al_2O_3. Or la complexation de Eu(III) avec les groupes fonctionnels de PAHA modifie certainement leurs possibilités de complexation avec les groupes fonctionnels de la surface minérale, et influe probablement sur les modifications de protonation observées. Il n'est en revanche pas possible de réaliser ces titrages sur des surnageants de système ternaire, car la présence d'europium(III) modifie l'absorbance des solutions de PAHA, notamment à 270 nm, la longueur d'onde utilisée pour le calcul des courbes de titrage spectrophotométriques.

En outre, la modélisation proposée dans ce travail ne couvre pas la description numérique de l'adsorption de PAHA sur α-Al_2O_3, qu'il faudrait également réaliser, par exemple en adaptant le modèle LCD (Filius et al. 2001; Weng et al. 2007).

Références citées

Dryer, D. J., Korshin G. V., et al. (2008). "In situ examination of the protonation behavior of fulvic acids using differential absorbance spectroscopy." *Environmental Science & Technology* **42**(17): 6644-6649.

Filius, J. D., Meeussen J. C. L., et al. (2001). "Modeling the binding of benzenecarboxylates by goethite: The ligand and charge distribution model." *Journal of Colloid and Interface Science* **244**(1): 31-42.

Weng, L. P., van Riemsdijk W. H., et al. (2007). "Adsorption of humic acids onto goethite: Effects of molar mass, pH and ionic strength." *Journal of Colloid and Interface Science* **314**(1): 107-118.